The University of Nottingham

UNITED KINGDOM · CHINA · MALAYSIA

Department of Civil Engineering

Nottingham Transport Engineering Centre

Flexible Pavements and Climate Change

Impact of Climate Change on the Performance, Maintenance, and Life-cycle Costs of
Flexible Pavements

by

YANING QIAO, BSc, MSc.

Thesis submitted to the University of Nottingham

For the degree of Doctor of Philosophy

July 2015

TO MY FAMILY

ABSTRACT

Flexible pavements are environmentally sensitive elements of infrastructure and their performance can be influenced by climate. Climate change poses a challenge to design and management of flexible pavements in the future. Climate change can occur worldwide and thus all flexible pavements can be exposed to the impact. However, an assessment framework is not available to evaluate the impact of climate change on flexible pavements in terms of performance, maintenance decision-making and the subsequent life-cycle costs (LCC). This research has attempted to develop such a framework. Case studies on six flexible pavement sections from the United States were performed to demonstrate the application of the framework.

The framework started with the investigation of climate change using IPCC's (Inter-governmental Panel on Climate Change) climate change projections. Combinations of climate change projections and local historical climate were adopted as climatic inputs for the prediction of pavement performance. The Mechanistic-Empirical Pavement Design Guide (MEPDG) was used for prediction of pavement performance because it can provide reliable performance predictions with consideration of climatic factors. Pavement performance predictions were applied to schedule maintenance interventions. Maintenance effects of treatments were considered in maintenance decision-making. Maintenance effect models of International Roughness Index (IRI) and rutting were validated using pavement condition survey data from Virginia. With selected climate related LCC components, three maintenance interventions were optimised using a genetic algorithm to achieve the minimum LCC. Eventually the outputs of the system including pavement performance, intervention strategies, and LCC can be compared under various climate change and baseline scenarios. Hence, the differences in performance, decision-making, and LCC due to climate change can be derived.

The conclusions were drawn based on the scheme of maintenance decision-making. If flexible pavements are not maintained (Alternative 0), an increase in LCC will be incurred by climate change due to an increase in road roughness (IRI). For pavements maintained with strict thresholds (Alternative 1), climate change may lead to a significant reduction in the service life when the maintenance is triggered by climate sensitive distress. However, benefit can be gained from decreasing LCC as the earlier triggered maintenance may result in less average IRI. As a consequence, user costs, which can be associated with IRI, can be reduced. Hence, LCC can be reduced as user costs usually dominate LCC. However, the net present value (NPV) of agency costs can be increased due to the early intervention. For pavements with optimised maintenance (Alternative 2), the LCC is almost unaffected by climate change. However, the type or application time of interventions may need to be changed

in order to achieve this. Furthermore, the balance between agency and user costs did not seem to be influenced by climate change for Alternative 2.

Agencies should be aware that maintenance optimisation can significantly reduce the LCC and make the best use of treatments to mitigate the effects of climate change on flexible pavements. Pavement maintained with strict triggers may require earlier interventions as a result of climate change but can gain benefit in LCC. However, this indicates that a responsive maintenance regime may not take full advantage of interventions and that maintenance could be planned to be performed earlier in order to achieve minimised LCC. Due to climate change, road users may spend more on fuels, lubricants and tyre wear on flexible pavement sections that do not receive any maintenance treatments.

Key words: Flexible pavement, climate change, framework, pavement performance, maintenance effect, LCCA, MEPDG, maintenance optimisation.

PUBLICATIONS

During preparation of the thesis, the following papers have been published by or submitted to peer-reviewed journals/conferences:

Qiao, Y., Dawson, A., Parry, T., Flintsch, G., 2013. Quantifying the effect of climate change on the deterioration of a flexible pavement, Ninth International Conference on the Bearing Capacity of Roads, 25-27 Jun 2013, Trondheim, Norway, 555-563.

Qiao, Y., Flintsch, G.W., Dawson, A.R., Parry, T., 2013. Examining Effects of Climatic Factors on Flexible Pavement Performance and Service Life. Transportation Research Record, 2349(1), 100-107.

Qiao, Y., Dawson, A., Huvstig, A., Korkiala-Tanttu, L., 2014. Calculating rutting of some thin flexible pavements from repeated load triaxial test data. International Journal of Pavement Engineering, 1-10.

Qiao, Y., Dawson, A., Parry, T., Flintsch, G., 2015. Evaluating the effects of climate change on road maintenance intervention strategies and Life-cycle Costs. Transportation Research Part D: Transport and Environment (under review).

Cheng, Z., Qiao, Y., Guo, B., 2015. Imperfect Maintenance Model of Pavement Based On Markov Decision Process. The Ninth International Conference on Mathematical Methods in Reliability, 1-4 Jun 2015, Tokyo, Japan (paper accepted).

Qiao, Y., Dawson, A., Parry, T. Flintsch, G. 2015. Immediate Effects of Some Corrective Maintenance Interventions on Flexible Pavements, International Journal of Pavement Engineering (under review).

ACKNOWLEDGEMENT

DECLARATIONS

The research described in this thesis was conducted at the Nottingham Transport Engineering Centre, University of Nottingham between Jan 2011 and Feb 2015. I hereby declare that the work is my own and has not been submitted for a degree at another university.

Yaning Qiao

Feb 2015

x

CONTENTS

LIST OF FIGURES

LIST OF TABLES

LIST OF ACRONYMS

AADT	Annual Average Daily Traffic
AADTT	Annual Average Daily Truck Traffic
AASHTO	American Association of State Highway and Transportation Officials
AOGCM	Atmosphere/Ocean General Circulation Models
ARRB	Australian Road Research Board
ARS	Average Rectified Slope
BL	Baseline
CD	Cook's Distance
CRREL	Cold Regions Research and Engineering Laboratory
EICM	Enhanced Integrated Climatic Model
FHWA	Federal Highway Administration
GHG	Greenhouse Gas
GPS	Global Positioning System
GWP	Global Warming Potential
HMA	Hot Mix Asphalt Concrete
IPCC	Intergovernmental Panel on Climate Change
IRI	International Roughness Index
LCA	Life-cycle Assessment
LCC	Life-cycle Cost
LCCA	Life-cycle Cost Analysis
LTPP	Long-term Pavement Performance Program
MAGICC	Model for the Assessment of Greenhouse-gas Induced Climate Change
MEPDG	Mechanistic-empirical Pavement Design Guide

NCHRP	National Cooperative Highway Research Program (USA)
NPV	Net Present Value
PMS	Pavement Management System
PSI	Present Serviceability Index
PSR	Present Serviceability Rating
RTFOT	Rolling Thin Film Oven Test
SCENGEN	Scenario Generator
SRES	IPCC's Special Report on Emissions Scenarios
UGM	Unbound Granular Material
USD	United States Dollar
USGS	United States Geological Survey
VDOT	Virginia Department of Transportation
VOC	Vehicle Operating Costs
WMO	World Meteorological Organisation
WZ	Work Zone

CONVERSION OF UNITS

As case studies are performed for roads from the United States, U.S. customary units are used for substantial data and results, including historical climate measurements, the MEPDG prediction results, and pavement performance monitoring records. A list of unit conversions is presented below for comparisons of U.S. customary units and metric units.

1 inch = 25.4 mm

1 foot ≈ 304.8 mm

1 mile ≈ 1.61 km

1 in/mi ≈ 0.0158 m/km

1 ft/mi ≈ 0.19 m/km

1 ℉ = 1 ℃*9/5 − 32

1 psi ≈ 6.89 kPa

A figure is presented for easy comparisons of IRI under the two unit systems.

Conversion between in/mi and m/km

xxvi
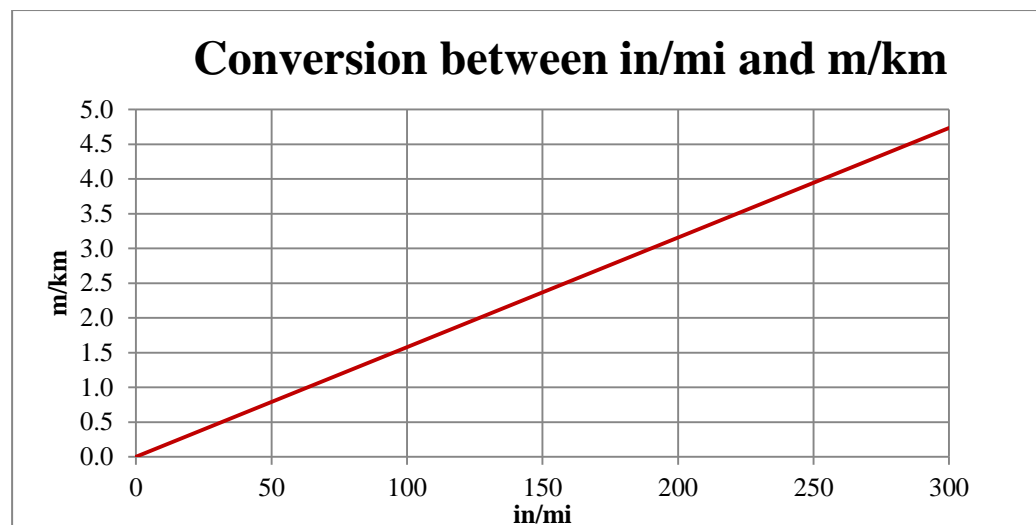
1. INTRODUCTION

1.1. Background

1.1.1. Problem statement

Flexible pavements can be impacted by their surrounding environment. The effects of temperature and moisture and their combination on pavement performance have been popular topics in pavement research for many decades. A typical flexible pavement may consist of asphalt layers, a bound base layer, an unbound base layer, subbase and subgrade. Temperature and moisture can affect the stress-strain response in the full depth of a pavement. Temperature can affect the bituminous layers (including asphalt layer and bound base layer) because these layers are viscous and can show elastic and plastic response to loadings. Moisture can impact the resilient response of unbound layers, subbase, and subgrade. Furthermore, moisture can do damage in asphalt layers and causes distress such as stripping (Aiery and Young-Kyu, 2002).

Climate change has been a popular topic in pavement research over the past decades. For years, meteorological surveys showed an increase in the global mean surface temperature but the reason of climate change has been under debate. However, it is not until recently that we can be almost certain that the warming trend in the past decades is man-made (IPCC, 2013). Furthermore, this trend does not seem likely to stop or even slow down in the near future.

For these reasons, the temperature and moisture patterns that flexible pavements are exposed to may be changed in the future. Consequently, climate change is likely to make an impact on flexible pavements (Dawson, 2014). The impact can be profound. Firstly, climate change occurs worldwide and so does its impact. Potentially, every flexible pavement may be influenced by climate change. Secondly, the life span of a flexible pavement (typically 20 – 40 years) is long enough to allow the impact of climate change to be revealed. The impact can accumulate and show its significance before or at the end of the service life. Therefore, it is necessary to quantify the impact and consider mitigation methods when appropriate.

1.1.2. Current literature on pavements under climate change

Attempts to systemically evaluate the impact of climate change on pavements have been focused on in the last decade. Qualitative studies were performed to investigate the potential effects of climate change on highways. These studies were usually based on risk assessment methods where the occurrence frequency and the consequence of various climate-related pavement distress

1. INTRODUCTION

types were discussed. In Europe, a trans-national joint research project named P2R2C2 (Pavement Performance and Remediation Requirements following Climate Change) was launched in 2008 to perform qualitative study on the effects of climate change on pavements, with an extensive literature review study of pavement material, structure, and hydrological performance, and to provide climate change adaptation recommendations for road owners. A summary report of the P2R2C2 project was given by Dawson and Carrera (2010). In the United States, a comprehensive NCHRP (the National Cooperative Highway Research Program) qualitative research on the impacts of climate change on highway systems was documented by Meyer et al. (2013), where recommendations on regions in which to investigate the impacts of climate change on highways in the United States were proposed. In this study, the projected climatic factors including temperature, precipitation, and the sea level rise in different climate zones of the U.S. were investigated. According to the representative future climate, three climate regions of concern were proposed, being the Northwest, Midwest, and Southeast. It was concluded that for different roads, the climatic factors of concern may differ. This indicated that the impacts of climate change on a specific road need to be evaluated individually. Furthermore, mitigation suggestions were proposed.

Quantitative studies were performed to determine the extent of the impact of climate change on performance of specific flexible pavements. Mills et al. (2009) investigated the impact of climate change on 17 selected sites in southern Canada by modelling pavement performance under various climate change scenarios using the MEPDG. It was found from simulation that the effects of climate change can accelerate pavement deterioration and maintenance and rehabilitation will be required earlier. Tighe et al. (2008) found that longitudinal cracking, alligator cracking, and rutting is likely to be exacerbated by climate change in Canada. A framework to quantify the effects of climate change (temperature, predication, and the sea level rise) on pavement performance was introduced by Li et al. (2011). Climate change projections on temperature and precipitation were used to generate future climate profiles, which were then adopted to predict future pavement performance using the MEPDG. Further considerations have been given to the subsequent service life of flexible pavements as a result of climate change. A reduction in predicted pavement service life due to climate change was reported in research (Mills et al., 2007, Qiao et al., 2013b, Tighe et al., 2008). Unfortunately, few investigations were performed to relate maintenance decision-making and life-cycle costs (LCC) to the additional deterioration and reduction in the service life due to climate change.

Research has been performed to estimate costs for road networks incurred by climate change. The Australian Road Research Board (ARRB) estimated a potential of 183.6 billion U.S. dollars (USD) to repair and maintain

road damage caused by temperature and precipitation changes related to climate change through 2100 on the African continent, using an opportunity cost approach (Chinowsky et al., 2011). The estimation can be used for African countries to claim budgets for mitigating the effect of climate change on road infrastructures. To achieve this, an analytical framework was developed to quantify the costs for adaptations of road infrastructure to climate change (World-Bank, 2009). Unfortunately, the framework did not consider pavement deterioration and cannot be applied for a specific road section or other road networks.

Houghton and Styles (2002) reviewed the ARRB research regarding the effects of climate change on the Australian national highway system. Based on future (2100) change in temperature, rainfall, and Thornthwaite Index, pavement deterioration and LCC were calculated using the ARRB Transport Research Pavement Life Cycle Costing model and Highway Development and Management Model (version 4, namely the HDM-4). By comparing to the road LCC estimated using baseline climate conditions, it was concluded that climate change could reduce the maintenance and rehabilitation costs nationally by 3% based on optimised agency costs. However, as an important and sometimes dominating LCC component, the user costs were neglected. The societal cost-benefit of highways needs to be achieved by the balance in benefit between road authorities and users. Therefore, user costs and the societal benefit of highways need to be taken into consideration.

1.2. Aims & objectives

The aim of this study is to develop a framework to assess the impact of climate change on the performance, maintenance decision-making, and LCC of flexible pavements. The framework should allow assessment of the impact of climate change on flexible pavements at either section or network level. Eventually, the framework is intended for road agencies and researchers to answer the following questions:

1. To what extent can climate change impact the deterioration of a particular flexible pavement?
2. How will maintenance decisions be made to adapt to climate change?
3. How will the consequent LCC be changed due to climate change?

An overall framework was conceived with four tasks to achieve the aim as follows:

1. INTRODUCTION
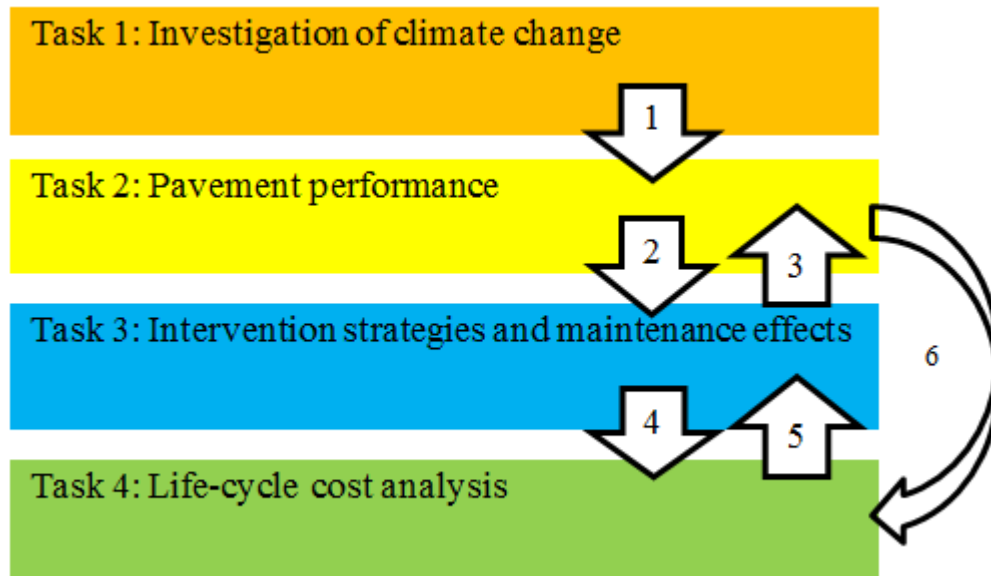
Figure 1-1 The overall framework

Task 1: The investigation of climate change is aimed for local prediction of climate change in terms of climatic factors that can have influences on flexible pavements. The climate change projections can be combined with historical climate measurements to create likely future climate profiles that can be input into pavement performance modelling. Climate change may have impact on a flexible pavement in both a direct and indirect way (represented by Arrow 1). The direct impact is from the change in the climatic environment of the pavement, including temperature and moisture. As an indirect impact, climate change may cause a demographic change, affecting traffic demand, and thus have an impact on pavement deterioration.

Task 2: Pavement performance under climate change and baseline scenarios can be predicted so that differences in deterioration due to climate change can be derived. Furthermore, pavement performance forms a basis for maintenance decision-making. Therefore, the impact of climate change on pavement deterioration is likely to have influences on maintenance planning (Arrow 2).

Task 3: Different interventions have different maintenance effects including functional and structural improvements on pavement performance. Thus the choice of intervention can provide feedback to performance (Arrow 3). The costs associated with different interventions are different (Arrow 4). For instance, compared to preventive maintenance, rehabilitation can have greater maintenance effects. However, the associated agency costs and user delay costs can be greater. In this study, maintenance is planned using pavement performance under climate change and baseline scenarios. As a consequence, differences in maintenance decision-making including change in

service life, intervention time and treatment choices due to climate change can be revealed.

Task 4: LCC components that are directly or indirectly related to climate change are selected. The LCC can have influences on maintenance planning (Arrow 5). Firstly, interventions need to be planned to reach minimum total LCC (agency costs + user costs + environmental costs) in order to maximise societal benefit. Secondly, maintenance budgets can limit the frequency and type of interventions. Arrow 6 indicates that pavement performance can have direct influence on the user costs.

Using this framework, questions asked in the first paragraph of this section can be answered. Question 1 can be answered with Task 1 and 2. Question 2 and 3 can be answered with the combination of all four Tasks. Furthermore, case studies of six road sections were performed to demonstrate the application of the framework (see later in the methodology).

The Objectives of this study are as follows:

(A) Investigation of climate change (Task 1).

(B) Sensitivity analysis of climatic factors on pavement performance (Task 2).

(C) MEPDG modelling of flexible pavement performance with combination of climate change projections and historical climatic data (Task 2).

(D) Validation of maintenance effect models (Task 3).

(F) Life-cycle costs analysis (LCCA) (Task 4).

(E) Optimisation of intervention strategies (Task 1, 2, 3 and 4).

1.3. Scope and limitations

The outputs of this research include an overall framework (Figure 1-1) and a detailed framework (see later in Figure 3-1). The overall framework can be further developed and is applicable for assessment on flexible pavements at network level. The detailed framework is designed for performing case studies at section scale. The scope of this research and the unavailability of desired information and technology leads to limitations. These limitations need to be addressed in further research to improve assessment accuracy and broaden the application of the framework. The scope and limitations of this study can be described as:

- Only the "long-term" impacts of climate change on flexible pavements will be considered. To be distinguished from the "long-term" impacts, the "short-term" impacts refer to extreme weather such as storm, flooding, and hurricanes. Climate is easier to predict than weather as weather can be random to some extent. For instance, accurate

prediction of weather for the next 40 years is impossible. Based on current knowledge, even prediction of the occurrence frequency of extreme weather events at local scale is not available. Therefore, the impact of climate change on flexible pavements excluded the effects of any particular hazardous weather events in this study.

- Demographic change is not going to be included in the study. As an indirect impact, environmental migrants may change the traffic demand of a specific location. Pavement performance, maintenance, and LCC can be affected by this change. Australian studies figured out that pavement maintenance and rehabilitation costs can be increased by approximately 30% due to climate-induced demographic change (Houghton and Styles, 2002). Unfortunately, prediction on the climate change induced demographic change at local scale is not available at present. This effect is still considered by the overall framework and could be integrated once necessary models are available. Only the direct impact of climate change on flexible pavements will be considered.

1.4. Contribution of this thesis

This study will contribute to current research as follows:

- Provide a framework for the assessment of the impact of climate change on the performance, maintenance decision-making, and LCC of flexible pavements. Based on predictions of pavement performance under climate change and baseline scenarios, this framework goes a step further to discuss the subsequent changes in pavement maintenance decision-making and LCC. Such a framework was not found elsewhere in the literature review.
- Consider the optimisation of maintenance allowing for the effects of climate change.
- Assess the sensitivity of MEPDG environmental factors on pavement performance. The seasonal variation of temperature is considered by a sine function and its sensitivity will be discussed and compared to other environmental factors.
- LCC components that are related to climate change are identified. The components are related to climate change by IRI.
- A data selection process is developed to extract pavement performance indices from a Pavement Management System (PMS) before and after a specific intervention. The process excluded possible invalid data to improve regression analysis.
- Integrate pavement performance prediction using MEPDG into pavement maintenance planning and optimisation. As is evidenced in the study, pavement maintenance can be significantly affected by

pavement performance predictions, so the integration can provide more reliable maintenance decision-making.

- Provide a possibility to evaluate the impact of climate change at a network level using the overall framework. The network can be extended to a district, a city, a state, or even a country.
- Provide a possibility to assess the cost-benefit of climate change adaptation measures, which is added agency costs components - for instance costs of stiffer asphalt layers or better drainage. The framework can be used to derive better design to achieve climate change resistance with high performance at low agency costs or total LCC.

1.5. Thesis outline

This thesis consists of six chapters. Chapter 1 forms an introduction to review current literature on flexible pavements and climate change. Problems to be solved by this study are formulated and introduced. Aims and objectives are defined with a proposed overall framework. The scope, limitations and contribution of the thesis are presented.

Chapter 2 reviews the theory of climate change and IPCC' (Intergovernmental Panel on Climate Change) projections on climate change and their climate change projection tools MAGICC/SCENGEN. Backgrounds, design principles, and distress prediction models of the MEPDG are introduced. Maintenance effect models and LCC components are also introduced. Most of the discussed models are used in the methodology in Chapter 3.

Chapter 3 demonstrates the application of the framework using six case studies. The advantages and disadvantages to apply the models for this study are discussed. Detailed information on how to utilise the framework is introduced. The basic information on the six studied cases can be found in this chapter. A method to combine the historical climate and climate change projections is presented. A sensitivity study on the environmental factors on pavement performance is described. Using this information, prediction of pavement performance under various climate change and baseline scenarios is performed, excluding the insignificant climatic factors. A maintenance data selection process and application of Cook's distance method is described to validate maintenance effect models. An algorithm is formulated and introduced to optimise maintenance interventions.

Chapter 4 presents the results of the case studies. The impact of climate change on the performance, maintenance decision-making, and LCC is presented and discussed.

1. INTRODUCTION

Chapter 5 summarises the results in Chapter 4 and makes conclusions about the general significance of this research. Furthermore, suggestions are provided on required information to apply the framework for other implementations.

Chapter 6 discusses the limitations of the research and offers methods by which the framework might be exploited more usefully in the future.

2. LITERATURE REVIEW

2.1. Climate change and projections

2.1.1. Theory on climate change

Paleoclimatologists studied the past climate by investigating climate proxies such as ice cores, sediments, tree rings and corals to reconstruct the past climate. For instance, ice in different layers of an ancient glacier contains water and trapped air bubbles over a long period. By analysing the proportion of isotopes of Hydrogen or Oxygen, the past climate change can be inferred based on the linear relation between the isotopic composition and temperature (Petit et al., 1999), validated from modern measurements. With this method, the past climate (temperature to be specific) can be reconstructed and temperature variations can be revealed. Another example to study the past climate is through tree rings, because the growth of a tree is affected by variations in climate, typically precipitation and sunlight.

The natural variations in the climate are evidenced by ice ages, which are extreme cold periods on the planet. During the ice ages, glaciers covered vast areas of the Earth, much more than the glacier areas today. When an ice age ends, glaciers melt and retreat. The giant ice covers left marks on rocks in the form of scratches and formed special geological phenomena such as till, eskers, and fjords, which are common in regions such as Scandinavian countries and Canada. The Earth is known to have gone through four major ice ages over the past 400,000 years, by studying reconstructed historical climate (see Figure 2-1). We are currently in an interglacial, which is the warm period between ice ages (Petit et al., 1999). The temperature has increased since the latest ice age to high temperature peaks and will drop again after that, according to the temperature pattern that has occurred during the past four major ice ages. Besides this long-term trend, short-term variations in temperature always exist.

2. LITERATURE REVIEW

The Vostok (Antarctica) Ice Core Record.
Carbon Dioxide versus Temperature for the last 420,000 years.
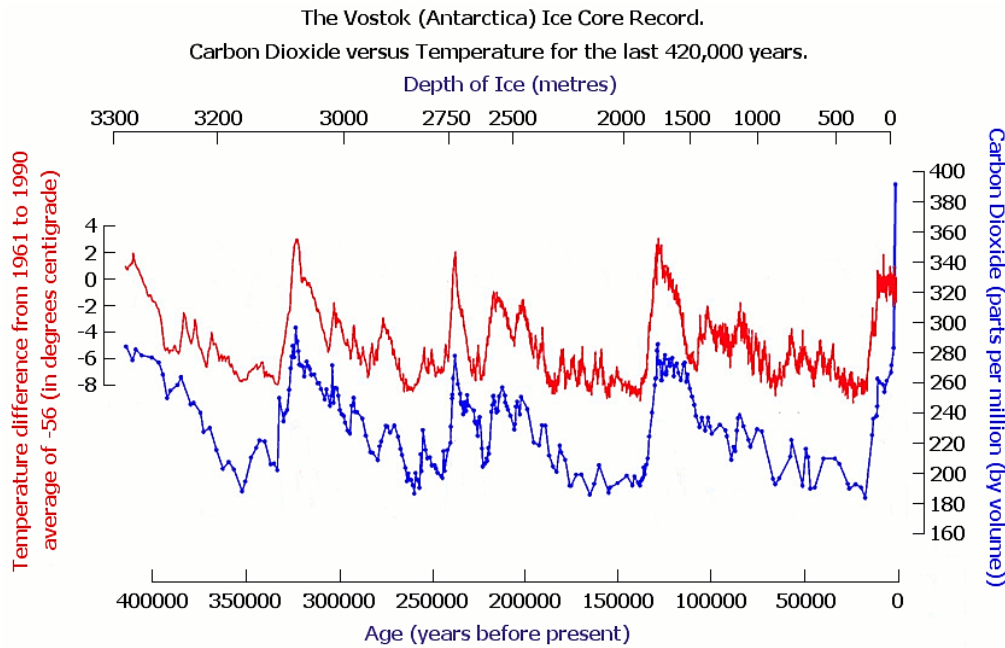
Figure 2-1 Atmospheric carbon dioxide concentration and estimated historical temperature (Petit et al., 1999)

The reason for the variations in the climate is not yet fully understood, although consensus has been reached regarding several influential factors. The impact of the orbit of the Earth on climate change (also known as Milankovitch cycles) is one of the clearly demonstrated factors (Imbrie and Imbrie, 1980, Croll, 1864, Paillard, 2001). Astronomical theory was developed as early as the 1860s by James Croll, who first attributed climate change to the changes in the orbit of the Earth (Croll, 1864). This theory was further supported by Imbrie and Imbrie (1980), who modelled the climatic response to the orbital parameters of the Earth. Other factors including variations in the solar output, changes in atmospheric compositions, and changes in the ocean current have been referred to in the literature.

As a system, the climate is balanced with solar radiation as input, through adsorption, and reflection of the rest of the energy into space. The balance can be disturbed by any interruption of these processes, especially on the adsorption and reflection. It was conventionally understood that the climate is affected by natural drivers, which alter the atmospheric energy budget (IPCC, 2013). The net budget is quantified by the radiative forcing, which is the difference of the insolation captivated by the Earth and radiated back to space.

The radiative forcing can be significantly affected by the concentration of Greenhouse Gas (GHG) in the atmosphere (Myhre et al., 1998, Charlson et al., 1992). The concentration of GHGs in the atmosphere has a great impact on the absorption process because GHGs are adept at absorbing solar radiation. The natural balance of GHGs will be disturbed, when the GHGs concentration in the atmosphere exceeds the removal capability by the earth. Higher

concentration of GHGs leads to more energy remaining in the earth, thus the globe is warmer. Evidence can be seen from past Paleoclimatology study by studying the trapped ancient air bubbles in the ice cores from Antarctica. It was found that the concentrations of carbon dioxide and methane in the air correlated well with the air temperature over the past 420,000 years (see Figure 2-1) (Petit et al., 1999).

It is almost certain that the observed climate change that has occurred in the past few decades is man-made (IPCC, 2013). As a significant source of GHGs, the GHGs emissions due to human activities have been increasing and increase the radiative forcing and thus increase the global temperature. The emissions of GHGs have increased by 75% between 1970 and 2004 and at an increasing rate. Therefore, the emissions and temperature do not seem likely to decrease in the near future. As a consequence of the warming, glaciers start to melt and the sea level will rise. Moreover, estuarine water circulation can be affected and thus precipitation is affected. Precipitation changes more because sea water becomes warmer so evaporates more easily.

2.1.2. Observations on climate change

Recent climate observations from various weather stations revealed that the global average temperature is increasing. Sea level measurements of the past several decades showed the rising of the sea level. These short-term observations support the presumption that the Earth's current climate is changing.

2.1.2.1. Temperature

It was found by observation (see Figure 2-2) that the global average surface temperature has increased approximately 0.74 ℃ since 1850, with eleven (1995 - 2006) years ranking among the eleven warmest years according to the record of global surface temperature (IPCC, 2007). The increase is greater at high northern latitudes, as average Arctic temperatures have increased at almost twice the global average rate in the past 100 years. It has also been discovered that the linear trend of temperature growth over the most recent 50 years is almost twice that of the past 100 years.
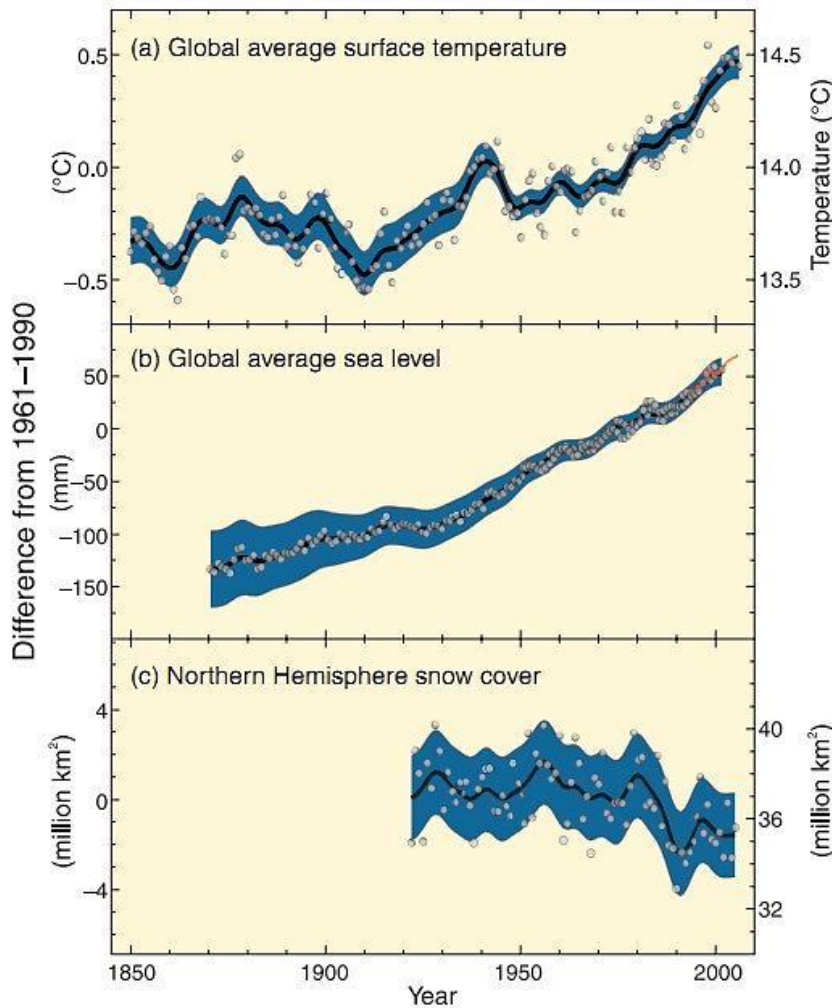
Figure 2-2 Observation of climate change on temperature, sea level and snow cover (IPCC, 2007)

2.1.2.2. Snow and ice

As temperature rises, snow and ice melts. For instance, a general retreating trend was observed for the snow cover in the Northern Hemisphere between 1920 and 2000, although coupled with insignificant increases occasionally (see Figure 2-2). The annual average speed of ice retreat is found to be 2.7% per decade in the Arctic Ocean, according to satellite inspection (IPCC, 2007). Observational evidence both from continents and oceans indicates high confidence that snow, ice and extent of frozen ground can be affected by climate change. Furthermore, snow and ice melting accelerates the rising of the sea level.

2.1.2.3. Precipitation

Over the period from 1900 to 2005, precipitation experienced a significant increase in eastern parts of North and South America, northern Europe and

northern and central Asia. Despite the increases, it has been found in other places that precipitation has decreased such as the Sahel, the Mediterranean, southern Africa and parts of southern Asia (IPCC, 2007).

2.1.2.4. Sea level

The average global ocean temperature has increased due to the fact that 80% of the heat added to the climate system has been absorbed by the ocean. Therefore, oceans play an important role for global temperature. It was found that the sea level rise can be related to the global surface temperature (Rahmstorf, 2007, Vermeer and Rahmstorf, 2009). The increase in sea level shows less fluctuation than temperature (see Figure 2-2). The increases of global sea level have risen from an average rate of approximately 1.8 mm/year (over period 1961 to 2003) to 3.1 mm/year (over period 1993 to 2003) (IPCC, 2007).

2.1.2.5. Extreme weather

Extreme weather in forms of heat waves, heavy precipitation, and extreme high sea level has occurred in some regions more frequently in the last 50 years. Judging by the observations at a global scale over the past 50 years, it is very likely that cold days/nights and frost have become less frequent. Hot days/nights have been more frequent, and heat waves have become more frequent in most land areas (IPCC, 2007). It is also very likely that heavy precipitation events have occurred more frequently in most areas (IPCC, 2007). Furthermore, the high sea level has increased globally in the past 40 years.

2.1.3. IPCC

IPCC is a subordinate organisation of the United Nations, which produces climate change reports by summarising research on the subject. IPCC was founded on 1988, as a combination of the World Meteorological Organisation (WMO) and United Nations Environment Programme (UNEP). In 2007, the Nobel Peace Prize was awarded to IPCC to recognise their efforts to build up and disseminate greater knowledge about man-made climate change.

IPCC has published five versions of the climate change assessment report, respectively in 1990, 1995, 2001, 2007 and 2013. The 5th assessment report (2013 version), named AR5, is one of the most up-to-date summaries of climate change worldwide, including knowledge on the scientific, technical and socio-economic aspects of climate change (IPCC, 2013). AR5 was updated from the 4th assessment report (AR4, 2007 version). In this research, the climate change observations and projections were principally based on AR4, which did not significantly differ from those in AR5.

Based on the knowledge of the physical science of climate change, AR4 presented the trend of global warming in the past centuries and provided projections. AR4 includes a synthesis report and three reports contributed from three working groups (WG) respectively, including:

- The Physical Science Basis (WG I)
- Impacts, Adaptation, and Vulnerability; Volume 1. Global and Sectoral Aspects (WG II)
- Mitigation of Climate Change (WG III)

As a basis for prediction of future climate, various GHG emission scenarios were summarised by IPCC and were described in the IPCC Special Report on Emissions Scenarios (SRES) (Nakicenovic and Swart, 2000).

2.1.3.1. SRES

Future GHG emissions are crucial for the prediction of climate change and are dependent on the development pathway of society. However, the development of society is uncertain. Therefore, SRES were developed and used in IPCC reports to quantify the future development of society under various assumptions based on different combination of economic, technical and demographic conditions. Moreover, the IPCC SRES were widely used by environmental researchers as a way to quantify future GHG emissions. In general, four scenarios of SRES were developed namely (Nakicenovic and Swart, 2000):

- A1
- A2
- B1
- B2

The most distinguishing character of the A1 scenario is that it assumed the world population will peak around the 2050s. Three sub-scenarios under A1 were developed namely A1FI, A1T, and A1B scenarios, distinguished by the type of energy utilisation (see Table 2-1). As the A1 scenarios consider that the world population will reduce after the 2050s, the rate of GHG emissions was predicted to reduce. All three A1 sub-scenarios showed this trend (see Figure 2-3).

2. LITERATURE REVIEW

Table 2-1 SRES emission scenarios and characterisation (IPCC, 2007)

			Population growth	Economic growth	Technology development
A1	A1Fl	Fossil fuel	Population peaks in mid-century	Fast	New and more effective
	A1T	Non-fossil new energy			
	A1B	Balanced energy			
A2			Fast	Slow	Slow
B1			Population peaks in mid-century	Rapid increases in service and information economy	-
B2			Intermediate	Intermediate	-

The A2 scenario considered that population growth will be fast. As a result, the rate of GHG emissions was considered to be increasing. Compared with the highest emission scenario of A1 (A1FI) (see Figure 2-3), the A2 scenario curve was generally lower than that of A1FI in this century. After 2090, the GHG emissions of the A2 scenario begin to exceed those of the highest A1 scenarios.
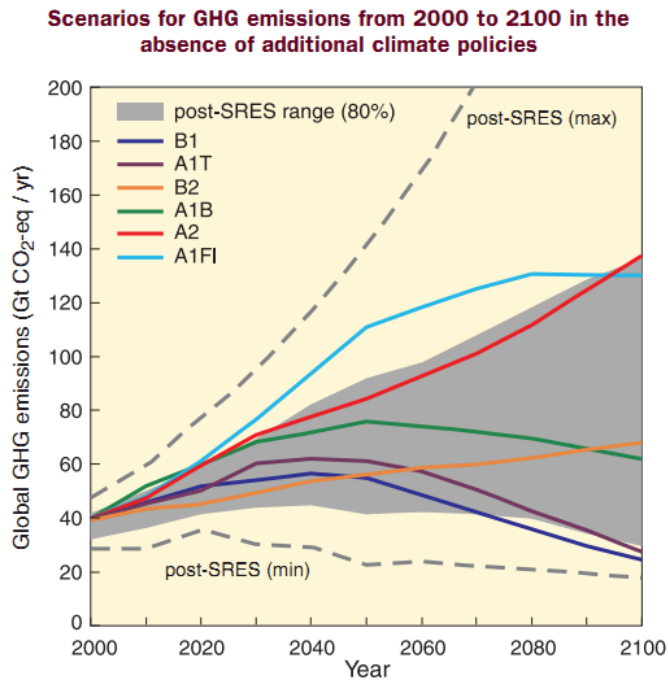
Figure 2-3 Scenarios for GHGs emissions (IPCC, 2007)

2. LITERATURE REVIEW

Population growth was considered to be lower in the B1 and B2 scenarios, compared to A1 and A2 scenarios. The B1 scenario assumes the world population will peak around the 2050s and the population growth rate of the B2 scenario was assumed to be intermediate (lower than A2). The B1 scenario is characterised by a decrease in the GHG emissions after 2040 and GHG emissions will increase steadily under the B2 scenario.

On a fundamental basis of climate projections, the emission scenarios projections reveal a general increase in the first half of the 21st century. Approximately, an upper and lower boundary was formed by the A1FI and B1 respectively, between which the GHG emissions in 2050 and 2100 will likely fall. The A1B scenario can represent an intermediate emission scenario.

AR4 Projections

Temperature

Generally, for the next two decades, an increase in the global average surface temperature of approximately 0.2 ℃ is expected. An increase of 0.1 ℃ is expected in each decade if the GHG emissions are kept at a constant level as in 2000 (IPCC, 2007). The increase will probably be larger than 0.1 ℃ due to the growing emissions of GHGs, depending on different emissions scenarios (see Figure 2-4). Furthermore, it is also very likely that hot extremes and heat waves will be more frequent.
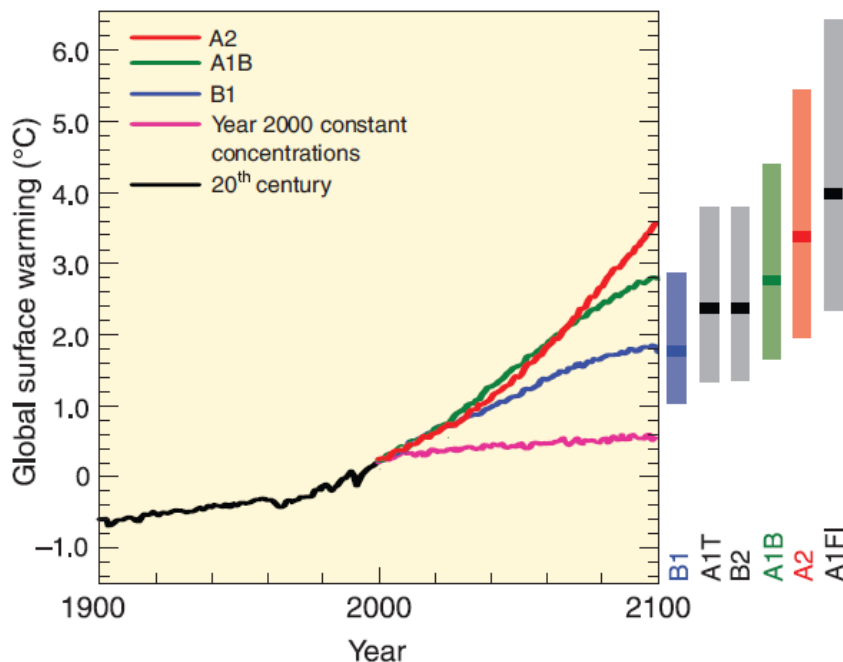
Figure 2-4 Global surface temperature change (IPCC, 2007)

Precipitation

Intensity of precipitation is likely to increase; especially it is very likely that heavy precipitation will be more frequent over most areas. Mean precipitation

is very likely to increase in high-latitude areas while decreasing in tropical areas, but the rainfall intensity will increase in both. Moreover, drought is likely to spread in a warmer future and the frequency of tropical cyclones (typhoons and hurricanes) will increase (IPCC, 2007).

Sea level

The average rate of sea level rising was 1.8 ± 0.5 mm/year between 1961 and 2003. It is very likely that this rate will be exceeded in the 21st century (IPCC, 2007).

2.1.4. Proposed regions for case studies

A recent NCHRP project had an overall assessment on the risk of climate change on highways (Meyer et al., 2013). The assessment was performed for eleven climate regions covering all states and Puerto Rico (see Figure 2-5). Taking risk as a combination of the occurrence frequency and potential consequence of highway hazard due to climate change, privilege to assess the impact of climate change on highways was given to three regions including:

1. Northwest (zone 1 on the map): This region includes Washington, most of Oregon and Idaho, and parts of Montana, Nevada, Utah, and California. It is a typical area to study because a combination of large increases in annual temperature, change in precipitation and the sea level are expected in the future.
2. Midwest (zone 3 on the map): This region covers all of Minnesota, Iowa, Wisconsin, and Indiana, most of Missouri, Illinois, and Ohio, and parts of Michigan, West Virginia, North Dakota, South Dakota, Kentucky, Kansas, and Nebraska. It is expected that the greatest increase in annual temperature will occur in these regions and thus they are worth studying.
3. Southeast (zone 5 on the map): This region includes all of Arkansas, Tennessee, South Carolina, Georgia, Alabama, Mississippi, most of North Carolina and Louisiana, and parts of Oklahoma, Texas, Florida, Virginia, Kentucky, and Missouri. It is expected that a middle range of changes will occur in this region in the future and thus it is representative as a nationally average case.
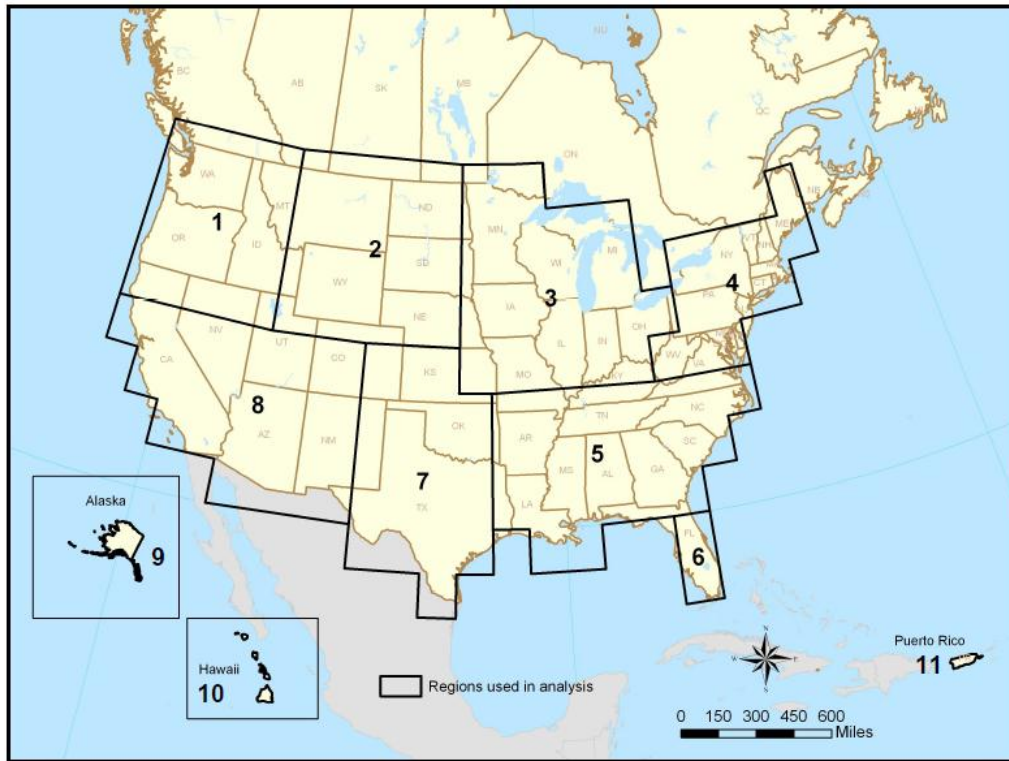
Figure 2-5 Climate regions for the assessment

2.1.5. MAGICC/SCENGEN

MAGICC/SCENGEN is an IPCC software package which is used to access global and local projections of climate change (Wigley, 2008). MAGICC/SCENGEN includes two separate tools:

- MAGICC (Model for the Assessment of Greenhouse-gas Induced Climate Change)
- SCENGEN (SCENario GENerator)

As a coupled gas-cycle/climate model, MAGICC is utilised by IPCC as a primary climatic model to predict future global average temperature increases and sea level rise. It is presumed in MAGICC that the future climate is significantly influenced by the GHGs concentration in the atmosphere. GHGs concentrations are closely related to the development of society which can be "quantified" by the SRES. Therefore, SRES are adopted as the main input of MAGICC. Stabilisation of CO_2 can be analysed in MAGICC, which can be combined with the climate feedback effect to avoid overestimation in CO_2 concentration (Wigley, 2008). Additionally, aerosol forcing can be considered in MAGICC because it can alter the energy balance of the atmosphere. Climate sensitivity, specifically defined as the increase in the temperature of the atmosphere as the concentration of CO_2 doubles, was considered to be 3 ℃ as is common practice (Wigley, 2008). The output of

18

MAGICC includes atmospheric concentration of GHGs, radiative forcing, and projections on temperature change and sea level change.

SCENGEN provides projections of local temperature, precipitation and pressure on a 5° (latitude) and 5° (longitude) grid. MAGICC/SCENGEN projections were based on an extensive database of 20 different Atmosphere/Ocean General Circulation Models (AOGCM) from many countries. The global temperature projection combines the temperature projection of chosen models that are unweighted and are normalised to an average value. It is then scaled up using an independent estimation of global-mean temperature change. The same process is also applied with precipitation.

In the United Kingdom, a similar climate change projection database called UKCP09 can be found. UKCP09 can provide climate change projections for the UK on a scale of a 25×25 km grid. The projections are based on three GHGs scenarios named high, medium and low emission scenarios corresponding to A1FI, A1B, and B1 of the IPCC SRES respectively. A subjective probability approach was applied to account for uncertainties in the projections.

2.1.5.1.MAGICC

The emission of GHG is assumed to be a main driving force of climate change in MAGICC, and thus the choice of GHG emission scenario is perhaps one of the most important MAGICC inputs. Also, a medium carbon cycle model with climate feedback effect was adopted to assist predictions. The aerosol forcing and ice melting speed was considered to be medium in the model. Furthermore, the climate sensitivity is considered to be 3 ℃ as default. The terminology "climate sensitivity" refers to the change in temperature as a consequence of change in the radiative forcing, which is commonly measured as doubled CO_2 concentration in the atmosphere.

The outputs of MAGICC include:

- Prediction of emissions (CO_2, CH_4, N_2O, and SO_2)
- Prediction of gas concentrations in the atmosphere (CO_2, CH_4, and N_2O)
- Prediction of change in average global surface air temperature and the sea level
- Radiative forcing

A general example of MAGICC output can be found in Figure 2-6 and Figure 2-7. The example shows the change in temperature and sea level from 1900 to 2100. The predictions give a policy range to account for uncertainties in the prediction and a best guess which is the median.

2. LITERATURE REVIEW
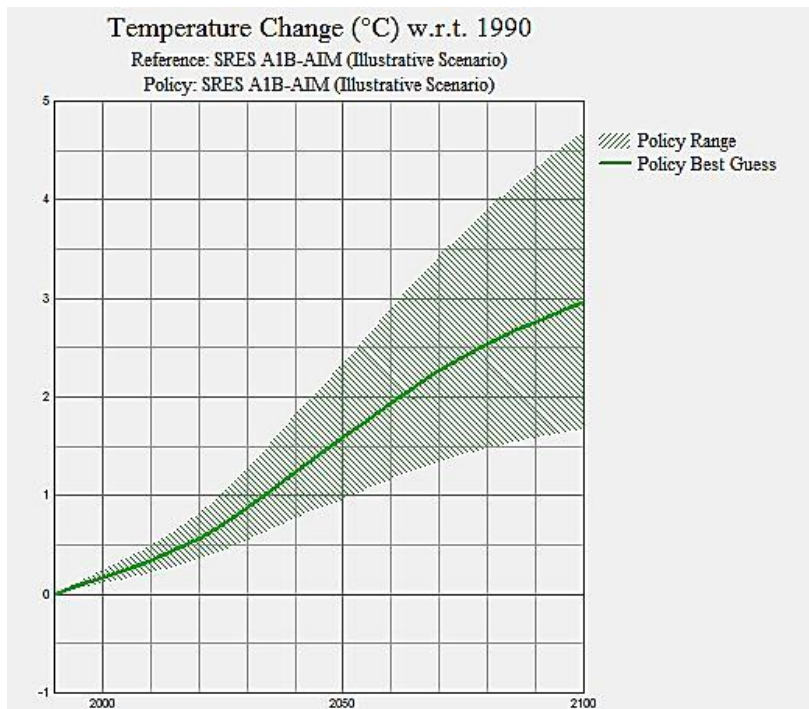
Figure 2-6 MAGICC output: global change in surface air temperature under scenario A1B
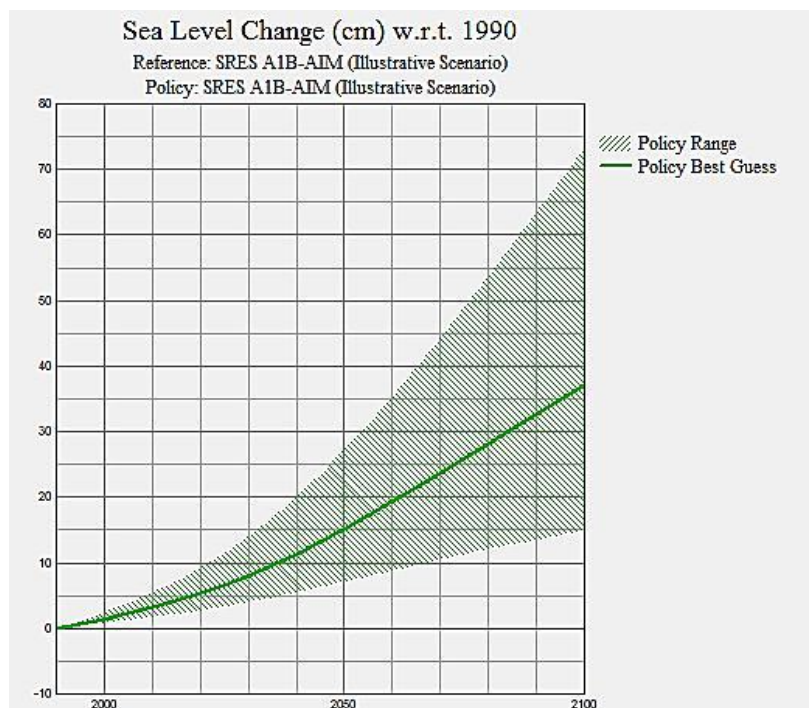
Figure 2-7 MAGICC output: global change in the sea level under scenario A1B

According to MAGICC output under scenario A1B, the global temperature will increase approximately 1.6 °C until 2050 compared to the 1990s. In 2100, the global temperature will be approximately 2.8 °C higher than a century ago. Under scenario A1FI, the global temperature in 2100 will be 4 °C higher than in 2000 and it is unlikely that the temperature will increase

20

more than 4 ℃. Compared to the 1990s, the sea level will increase approximately 15 cm until 2050 and 35 cm until 2100 under scenario A1B. Under scenario A1FI, the numbers are 15 cm and 46 cm respectively. More results on global temperature and sea level rise projections are attached in the Appendix (Figure A-8 to Figure A-13).

2.1.5.2. SCENGEN

Although an extensive choice of AOGCM were available, only some were selected to interpolate the local climate because they can better represent the investigated regions (Meyer et al., 2013). The chosen models included:

- NCARPCM1 from National Center for Atmospheric Research, USA.
- GFDLCM2.1 model from Geophysical Fluid Dynamics Laboratory, USA.
- IPSL_CM4 model from Institute Pierre Simon Laplace, France.
- MIROC (Medium) model Center for Climate System Research, Japan.
- MRI-2.3.2A model from Meteorology Research Institute, Japan.
- MPIECH-5 model from Max Planck Institute for Meteorology, Germany.
- HadCM3 and HadGEM1 models from Hadley Centre for Climate Prediction and Research, United Kingdom.

An example of the outputs of SCENGEN is shown in Figure 2-8 and Figure 2-9. With the Global Positioning System (GPS) coordinates, the location can be found on the map to find the local change in temperature and precipitation.
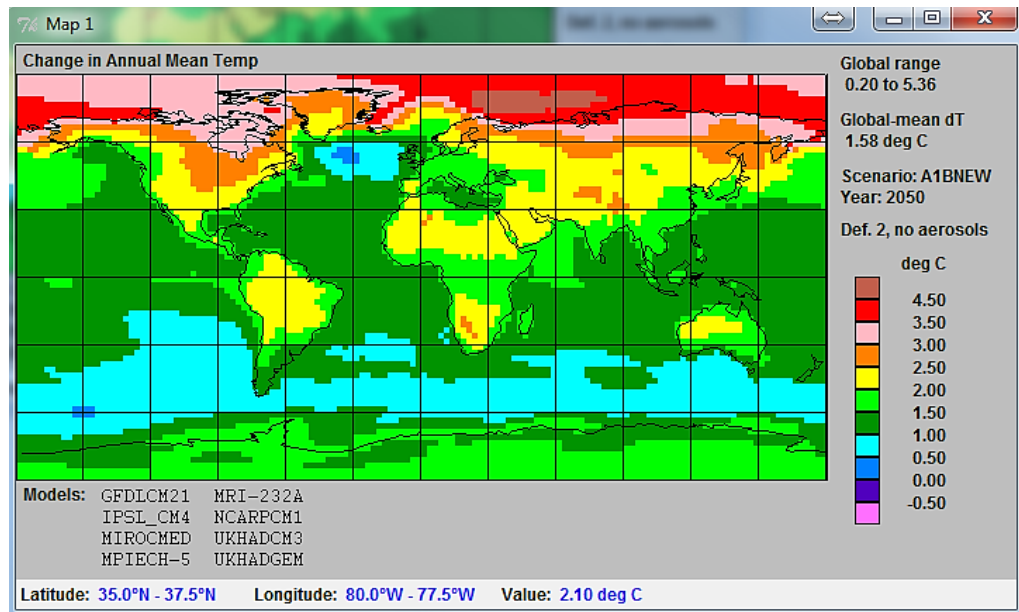
Figure 2-8 Change in annual mean temperature (℃) under A1B scenario in 2050
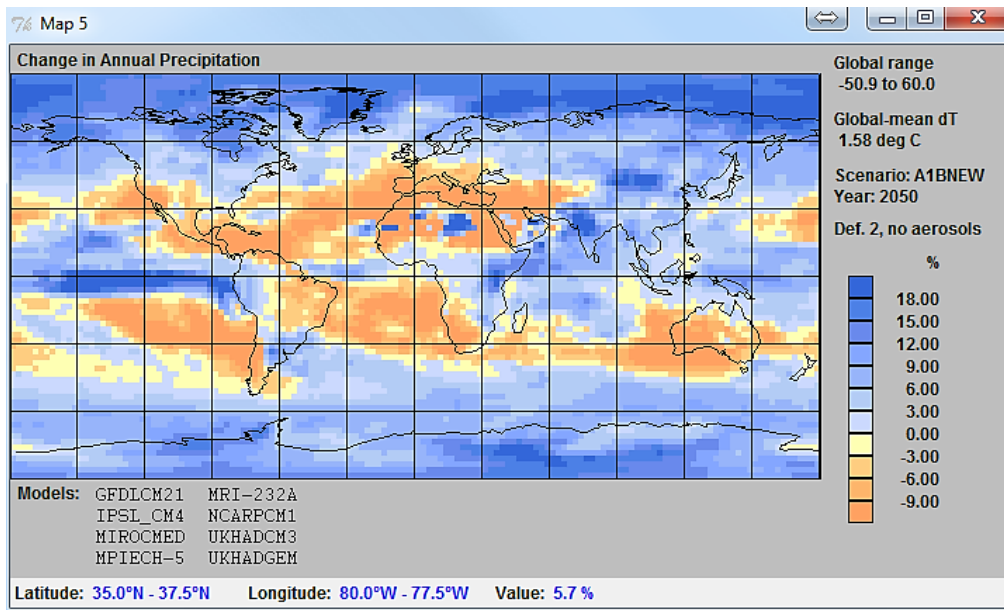
Figure 2-9 Change in annual precipitation (%) under A1B scenario in 2050

2.1.6. MAGICC/SCENGEN Climate change prediction limitations

MAGICC/SCENGEN is probably the most well-known climate change prediction package and is widely used by policy makers and researchers. However, the climate of the earth is such a complex system that it is difficult to be fully understood with current knowledge. Therefore, unpredictability and uncertainties exist in MAGICC/SCENGEN projections. Nevertheless, some of the significant uncertainties can be appreciated and managed to some degree. So far, MAGICC/SCENGEN can only give climate change projections including the change in the global average surface temperature, precipitation, sea level, as well as local change in the average surface temperature and precipitation. Climatic extremes e.g. hotter summer, colder winter, hotter days, colder nights, and more frequent hurricanes/typhoons/flooding can be observed from past records in certain regions, but to predict and locate such events on a map has been extremely difficult.

MAGICC considers that future climate is most influenced by the future emissions of GHGs. As the future GHG emissions are dependent on the development pathway of society, therefore significant error can be expected if the development pathway is biased. The uncertainty in the prediction of GHG emissions is dealt with using various SRES. SRES assumes various development pathways principally according to population, economic conditions, and energy sources. These emission scenarios provide users an opportunity to select scenarios which can suit their own interests and at their own risk. The highest and lowest emission scenarios create an upper and lower boundary between which the future emissions are very likely to range.

A fundamental question for prediction of temperature response to the concentration of carbon dioxide i.e. climate sensitivity was not fully answered. How much will temperature increase when the atmospheric concentration of carbon dioxide doubles? Researchers have attempted to bring down the uncertainty and it was reported that the climate sensitivity is likely to range between 2 to 4.5 ℃ with the best estimation of 3 ℃ (IPCC, 2007). Furthermore, it was added that the climate sensitivity is extremely unlikely to be less than 1 ℃ and very unlikely to be more than 6 ℃ (IPCC, 2013).

MAGICC/SCENGEN projection results are based on runs of selected AOGCMs. Therefore, the outputs may be influenced by the number of runs and type of selected models. AOGCMs are invented and developed in different countries and have their own advantages and disadvantages. Moreover, some models are more reliable for some regions than for others (Meyer et al., 2013). Therefore, a good choice of AOGCMs can help to reduce errors in the prediction.

Uncertainties in the IPCC projection results can be assessed by quantitative approaches and using expert judgement. Eventually, the uncertainties in the results have to be defined. A list of the expressions and their associated probability of occurrence can be found in the table below:

Table 2-2 Uncertainty expression used by IPCC

Expressions	Probability of occurrence
Virtually certain	>99%
Extremely likely	>95%
Very likely	>90%
Likely	>66%
More likely than not	>50%
About as likely as not	33% - 66%
Unlikely	<33%
Very unlikely	<10%
Extremely unlikely	<5%
Exceptionally unlikely	<1%

2.1.7.   Climate change and demographic change

Demographic change is usually considered to be significantly influenced by population growth, urbanization and migration. Recent studies discovered that climate change, as an environmental pressure, may contribute to demographic change (Reuveny, 2007, Barnett and Adger, 2007). Climate change may deteriorate the environment of an inhabited place and reduce the availability of resources. Furthermore, it can induce conflicts in a region (Nordås and Gleditsch, 2007). All of these impacts may lead to migration. For instance, coastal lines may retreat due to rise in the sea level. Under such condition, land

may face salinity and erosion problems. In an extreme, coastal cities may be fully or partly submerged, or, at least, the perceived rises may discourage inhabitants. Under those conditions, people must or may wish to migrate to other cities. Furthermore, climate change can increase the frequency and intensity of heat waves, storms, and flooding. The increase in frequency or intensity of these events can all lead to demographic change.

Demographic change is expected to have an influence on the traffic demand. Population increase in a metropolis tends to generate more traffic for urban roads and roads between cities, thus accelerates deterioration of these roads.

The prediction of migration as a consequence of climate change is currently unfeasible and there is still a long way to go until any clear methods are developed over the next 50 years (Black et al., 2008, Brown, 2008). And it is unclear how far climate change can dominate migration, compared to the significance of economic, social and political concerns. Even so, the significance of migration can never be underestimated because of the importance of the amount of traffic loading on pavement deterioration.

2.2. Pavement performance modelling and MEPDG

2.2.1. Introduction

Pavement structural design and analysis has been developing for many decades. As early as the 1880s, Boussinesq developed a theory that assumes pavements as a one-layer structure which is elastic, homogeneous, and isotropic and the stress in the pavement under a point load can be calculated. Later in 1947, Odemark developed an equivalent thickness method which considers the thickness and modulus of different pavement layers. Around 1959 -1961, a series of AASHTO (the American Association of State Highway and Transportation Officials, previously AASHO) road tests was performed in the United States and a pavement design guide called "AASHO Interim Guide for the Design of Rigid and Flexible Pavements" was issued as a result of the extensive road tests. In 1986, the AASHTO Guide for Design of Pavement Structures started to be adopted in the United States (AASHTO, 1993). The design procedure was empirical, and was based on the extensive road tests from the late 1950s (AASHTO, 2009). However, as the traffic loading, vehicle type, pavement materials, and even the environment has been changing since then, the empirical design may not be suitable for design in the 21st century. Therefore, there is a need to integrate new mechanistic knowledge into the empirical design to extend utilization of the design guide under various traffic, loading, structural, material, and environmental conditions.

2.2.2.   Stress and strain response

The stress and strain state of the pavement can impact the pavement performance in the long-term. High stress and strain states can cause more deterioration and this is not desirable in the pavement. Given a vehicle load, the stress-strain response in the pavement can be determined by the resilient modulus of each layer. The resilient modulus is based on the recoverable strain under repeated loads and can be defined as (Huang, 2004):

$$M_R = \frac{\sigma_d}{\epsilon_r}$$
<div align="right">Equation 2-1</div>

where,

M_R = resilient modulus

σ_d = deviator stress (axial stress difference in compression tests)

ϵ_r = recoverable strain

The resilient modulus of pavement materials is typically stress-dependent and dependent on various material and climatic factors.

2.2.2.1. Influential parameters

The magnitude of stress level, stress history, number of loading cycles, loading conditions, material properties and environmental conditions may affect the resilient modulus of granular materials.

Load and stress

Resilient modulus, for the same material, differs depending on the magnitude of the stress level induced by the applied load. Many researchers have discovered the significance of stress level to resilient modulus of road materials (Williams, 1963, Uzan, 1985). In particular, strong correlation has been revealed between resilient modulus and bulk stress (the sum of principal stresses) or confining stress in laboratory testing (Uzan, 1985, Sweere, 1990), while deviator stress which represents shear has much less effect on the resilient response of the material (Mogan, 1996). Furthermore, Poisson's ratio is also found to be associated with the state of applied stress (Brown and Hyde, 1975).

Stress history is found to have impact on resilient modulus (Dehlen, 1969). For instance, progressive compaction and particle rearrangement of unbound granular materials occurs under repeated traffic loading, which can result in a change of resilient modulus. The resilient modulus is reported to increase with an increase of loading cycles (Moore et al., 1970). Resilient modulus can stabilise after, for instance, several thousand loading repetitions

2. LITERATURE REVIEW

(Allen and Thompson, 1974). Loading conditions such as load duration and frequency are also believed to have impact on the resilient modulus although the impact may not be significant (Thom and Brown, 1987).

Material properties

Material properties of binder and granular materials and mix design are connected with resilient response. The resilient property of asphalt mixture is commonly associated with temperature because asphalt mixture can be considered as a visco-elastic material. Temperature may have a significant impact on the deformation property of such materials. For granular materials, the shape of aggregates can have an influence on the resilient modulus. For instance, crushed aggregates and rough particles provide better grip between particles and better loading spreading ability, thus higher resilient modulus can be expected (Allen and Thompson, 1974, Hicks, 1970). Although the shape and roughness of aggregates are usually neglected in real modelling, their effect on resilient modulus cannot be underestimated.

Environmental parameters

Temperature can have significant influence on the stiffness of asphalt concrete. Under high temperature, asphalt binder softens and loses stiffness (Buttlar and Roque, 1996, Monismith et al., 1965). The ability to spread stress can reduce and stress can be concentrated under loads. Therefore, critical stress (at the bottom of the asphalt layer or on top of subgrade) can be increased and lead to more deterioration. Under low temperature, asphalt layers gain stiffness. When a pavement is frozen, additional stiffness can be gained. Surface mixtures are in direct contact with air temperature and can be more impacted by temperature than base mixtures. The resilient modulus in unbound layers including unbound base layers, subbase, and subgrade is rarely affected by temperature, except in areas where there can be deep winter frost penetration. Furthermore, repetitions of high and cold temperature can cause the asphalt concrete to expand and shrink and thus lead to thermal stress (Lytton et al., 1983). Thermal fatigue cracking can initiate when the thermal stress is great enough and repeats for a large number of times.

Moisture can significantly impact the resilient modulus of unbound granular materials and subgrade (Monismith et al., 1975, Hicks, 1970, Thom, 1988, Thom and Brown, 1987). Due to precipitation and variation in the groundwater level, the moisture content of subgrade may change all the time. The degree of saturation was found to have significant influence on the resilient response of subgrade (Hicks, 1970). The resilient modulus may increase or decrease when the moisture content drops below optimum depending on the suction that is developed. When the moisture content exceeds the optimum, the resilient modulus reduces with an increase in the moisture

content (Hicks, 1970). At high saturation level, stiffness and strength of subgrade can reduce significantly because of the reduction in the effective stress as a consequence of excessive pore pressure. The magnitude of the modulus decrease is dependent on the soil (Drumm et al., 1997).

2.2.2.2.Dynamic modulus

Dynamic modulus is one of the fundamental material properties to describe the stress-strain response of hot-mix asphalt (HMA). It was found that dynamic modulus can provide a better characterisation than the resilient modulus tests. This is because temperature and loading frequencies are considered in this test giving it more realism (Loulizi et al., 2006). Dynamic modulus can be affected by various factors including temperature, loading rates, age, as well as mixture properties (binder stiffness, binder content, aggregate gradation, and air voids percentage (Witczak, 2004, El-Badawy et al., 2012)).

The dynamic (complex) modulus E^* is used to define the stress-strain response under a continuous sinusoidal loading, which can be formulated as (Witczak, 2004):

$$E^* = \frac{\sigma_0 sin\omega t}{\varepsilon_0 \sin(\omega t - \emptyset)}$$
<div align="right">Equation 2-2</div>

where,

σ_0 = peak stress

ε_0 = peak strain

t = time (s)

ω = angular velocity

$\emptyset$ = phase angle (degree)

In the MEPDG, the modelling method of E^* depends on different input levels. Strictly, the dynamic modulus is defined by the absolute value $|E^*| = \sigma_0/\varepsilon_0$ and is usually denoted as E^* in conventional practice. Dynamic testing data according to AASHTO protocols TP5 (AASHTO, 1998) are required for input Level 1. The Witczak E^* predictive equation is adopted for input Levels 2 and 3. No laboratory data is needed for Level 3 and only some volumetric information is required. For all input levels, the dynamic modulus of asphalt is obtained from a master curve, which is derived from either laboratory testing or E^* predictive models, depending on the input level.

MEPDG input Level 1

2. LITERATURE REVIEW

For input Level 1, a dynamic modulus testing result is required, which describes the dynamic modulus of an asphalt mixture under various temperatures (e.g. 14, 40, 70, 100, and 130 ℉; -10, 4.4, 21.1, 37.8, 54.4 ℃ respectively) and loading frequencies (e.g. 0.1, 0.5, 1, 5, 10, and 25 Hz). Then, a master curve is constructed by firstly selecting a reference temperature (70 ℉ in the MEPDG; 70 ℉ = 21.1 ℃) and then data at different temperature are shifted with respect to time (Apeagyei and Diefenderfer, 2011). Eventually, a smooth curve is obtained by numerical optimization.

Before this, the relation between viscosity and temperature of asphalt binder needs to be established using linear regression. Firstly, the stiffness of asphalt binder is correlated to viscosity, which can be described as follows (Witczak, 2004):

$$\eta = \frac{G^*}{10}\left(\frac{1}{sin\delta}\right)^{4.8628} \qquad\qquad \text{Equation 2-3}$$

Then the viscosity and temperature can be correlated by the linear formula (Witczak, 2004):

$$loglog\eta = A + VTS * logT_R \qquad\qquad \text{Equation 2-4}$$

where,

η = viscosity

G^* = complex shear modulus (Pa)

δ = asphalt phase angle (degree)

A, VTS = regression factors

T_R = temperature ($°Rankine$)

MEPDG input Level 2 and 3

The Witczak E^* predictive model is adopted for input levels 2 and 3. The model (NCHRP 1-37 A viscosity-based E^* predictive model) can be formulated as (Witczak, 2004, Andrei et al., 1999):

$$logE^* = -1.249937 + 0.02923\rho_{200} - 0.001767(\rho_{200})^2 - 0.002841\rho_4 -$$

$$0.058097V_a - 0.82208(\frac{V_{beff}}{V_{beff}+V_a}) +$$

$$\frac{3.871977 - 0.0021\rho_4 + 0.003958\rho_{38} - 0.000017(\rho_{38})^2 + 0.00547\rho_{34}}{1+e^{(-0.603313-0.313351\log(f)-0.393532\log(\eta))}} \qquad \text{Equation 2-5}$$

where,

E^* = dynamic modulus (10^5 psi)

η = asphalt viscosity (10^6 Poise)

f = loading frequency (Hz)

V_a = air void content (%)

V_{beff} = effective asphalt content (%)

ρ_{34} = cumulative percentage retained on 3/4 in (19 mm) sieve

ρ_{38} = cumulative percentage retained on 3/8 in (9.5 mm) sieve

ρ_4 = cumulative percentage retained on #4 (4.76 mm) sieve

ρ_{200} = percentage passing No. 200 (0.075 mm) sieve

For the master curve of a specific mixture, the equation can be expressed as (Witczak, 2004):

$$Log|E^*| = \delta + \frac{a}{1+e^{\beta+\gamma(logt_r)}} \qquad \text{Equation 2-6}$$

where,

$|E^*|$ = dynamic modulus (10^5 psi)

$\delta = -1.249937 + 0.02923\rho_{200} - 0.001767(\rho_{200})^2 - 0.002841\rho_4 - 0.058097V_a - 0.82208(\frac{V_{beff}}{V_{beff}+V_a})$

$a = 3.871977 - 0.0021\rho_4 + 0.003958\rho_{38} - 0.000017(\rho_{38})^2 + 0.00547\rho_{34}$

$\beta = -0.603313 - 0.313532log(\eta_{T_r})$

$\gamma = 0.313351$

t_r = reduced time of loading at reference temperature (21.1 ℃)

η_{T_r} = asphalt RTFOT (Rolling Thin Film Oven Test) viscosity at the reference temperature (10^6 Poise)

It was reported that 2750 test points and 205 different HMA mixtures were used for the calibration of the model and another 5700 test points were added after 2004 (Witczak, 2004).

The Witczak predictive model is a widely used dynamic modulus model, and is adopted by the MEPDG. Early versions of the MEPDG (0.7 to 0.9) used a Witczak model developed in 1999 (Andrei et al., 1999). This model considered properties of asphalt material including binder viscosity (at design temperature and loading frequency), aggregate gradation, and volumetric properties of mixtures. In new versions of MEPDG (1.0 and 1.1), a revised version of the Witczak model (NCHRP 1-40 G^* based E^* predictive model)

considering the dynamic shear modulus was adopted and believed to advance the prediction (Ceylan et al., 2009), which can be formulated as (Bari and Witczak, 2006):

$$logE^* = 0.02 + 0.758(|G^*|^{-0.0009} \times \left(6.8232 - 0.03274\rho_{200} + \right.$$

$$0.00431\rho_{200}{}^2 + 0.0104\rho_4 - 0.00012\rho_4{}^2 + 0.00678\rho_{38} - 0.00016\rho_{38}{}^2 -$$

$$0.0796V_a - 1.1689\left(\frac{V_{beff}}{V_a+V_{beff}}\right) \Big) +$$

$$\frac{1.437+0.03313V_a+0.6926\left(\frac{V_{beff}}{V_a+V_{beff}}\right)+0.00891\rho_{38}-0.00007\rho_{38}{}^2-0.0081\rho_{34}}{1+e^{(-4.5868-0.8176log|G^*|+3.2738log\delta)}}$$

Equation 2-7

where,

G^* = dynamic shear modulus (psi)

However, it was reported that the Witczak models may overestimate the influence of temperature by understating the effects of other mixing properties and show greater errors at extreme low/high modulus (Bari and Witczak, 2006, Dongre et al., 2005). An updated Witczak model was reported to improve the predictability of the model under extreme temperatures and take short and long term hardening effects into consideration (Witczak and Fonseca, 2007).

The Hirsch model is an alternative for the prediction of dynamic modulus (both dynamic shear modulus and dynamic extensional modulus) of asphalt concrete (Christensen Jr et al., 2003). Several versions of the Hirsch model were evaluated and it was reported that the most effective one was the simplest one which only incorporated binder modulus, air voids in aggregates, and voids filled with binder (Christensen Jr et al., 2003).

Another dynamic predictive model was reported to take the microstructure of HMA mixtures into consideration (Shu and Huang, 2008). It was found that this model can reflect the trend of dynamic modulus despite underestimation. The underestimation may be caused by the lack of consideration of aggregate interlocking and underestimation of aggregate surface area (Buttlar and Roque, 1996).

2.2.2.3. Resilient modulus

For decades, the resilient modulus of subgrade soil has been studied and many models have been developed to calculate resilient modulus of unbound granular materials. It is commonly agreed that stress and moisture are the most

2. LITERATURE REVIEW

crucial parameters (Lekarp et al., 2000a). Most of the models take consideration of stress and some of them take moisture into account as well. The MEPDG has three input levels to account for the resilient modulus of granular materials to achieve different levels of accuracy. High accuracy (level 1) can be achieved using modulus predicted from cyclic triaxial testing data ("k-θ" model as described later by Equation 2-8). Level 2 (medium accuracy) uses models to correlate the resilient modulus to parameters such as soil plasticity index and strength properties. Level 3 (low accuracy) uses default values for the resilient modulus.

One of the most well-known models is called the "k-θ" model, which can be formulated as (Hicks, 1970):

$$M_R = k_1 \theta^{k_2} \qquad \text{Equation 2-8}$$

where,

M_R = resilient modulus

θ = bulk stress $(\sigma_1 + \sigma_2 + \sigma_3)$

k_1, k_2 = factors

This model correlates resilient modulus exclusively to the bulk stress, which reflects the stress level in the material, while other parameters, especially the environmental parameters are not taken into consideration. It is known that the resilient modulus of subgrade soil generally shows seasonal variations as separated or combined effects of temperature, moisture, and frost/thaw (Hassan et al., 2003). Therefore, it can be a solution for seasonal variation that the "k - θ" model is validated under different environmental conditions throughout a year to obtain monthly values for k_1, k_2.

Many regression models have been developed to take the influence of environmental parameters into account. Most of the regression models correlate resilient modulus with stress level, moisture content, soil dry density, temperature and degree of saturation (Witczak et al., 2000; Jin et al., 1994). Thus the prediction of resilient modulus gains flexibility in exhibiting seasonal variations. An example regression model can be taken from a study by Jin et al (1994), where the resilient modulus is formulated as:

$$log M_r = a + b \times log\theta - c \times \left(\frac{w}{c}\right) - d \times (T) + e \times \gamma_d \qquad \text{Equation 2-9}$$

where,

M_r = resilient modulus (MPa)

θ = bulk stress (kPa)

2. LITERATURE REVIEW

$\left(\dfrac{w}{c}\right)$ = percent water content

T = temperature (℃)

γ_d = dry density (kg/m^3)

a, b, c, d, e = regression factors

These regression models can deal with resilient prediction within a specific location with calibrated factors, over a time span e.g. a year. But regression models have limited application for soil with different classifications and new validations should be performed for another type of soil. From a study by Carmichael & Stuart (1985) on over 250 soil types, it was found that soil parameters, such as plasticity index and aggregate size, are also influential to the resilient modulus. Further, the regression model developed in this study for fine-grained soil can be expressed as:

$$M_r = 37.431 - 0.4566PI - 0.6179w - 0.1424F + 0.1791CS -$$

$$0.3248\sigma_d + 36.422CH + 17.097MH \qquad \text{Equation 2-10}$$

where,

M_r = resilient modulus in ksi

PI = plasticity index in percent

w = water content in percent

F = percent passing sieve No. 200

CS = confining pressure in psi

σ_d = deviator stress in psi

CH, MH = material factors

The material factors (CH and MH) and plasticity index allow this model to account for fine-grained soils with different classifications. In this model, the resilient modulus is related to the stress level with both confining pressure and deviator stress taken into account.

The AASHTO method for resilient modulus (Drumm et al., 1997) correlated resilient modulus to the degree of saturation of soils as follows:

$$M_{r(wet)} = M_{r(opt)} + \frac{dM_r}{dS}\Delta S \qquad \text{Equation 2-11}$$

where,

$M_{r(wet)}$ = resilient modulus

$M_{r(opt)}$ = resilient modulus at optimum water content

$\frac{dM_r}{dS}$ = gradient of resilient modulus with respect to saturation

ΔS = change post-compaction degree of saturation

The gradient of resilient modulus with respect to saturation $(\frac{dM_r}{dS})$ is empirical. According to AASHTO (1992), the gradient is almost linear for soil samples under static confining and deviatoric pressure. With the empirical gradient values for various soils and the resilient modulus at optimum water content from direct testing, resilient modulus can be calculated at any degree of saturation.

2.2.3. Pavement performance

2.2.3.1. Introduction

Pavement distress is a common phenomenon, observed mainly on the road surface, which is caused by traffic loading and deficiencies in construction, materials and maintenance. The types of distress are various and can be described as either structural or functional. Structural distress is associated with the ability to carry the designed load while functional distress is related to the ride quality and safety aspects. It is of importance that each type of distress should be considered and a failure criterion established for the development of pavement design. It is essential to identify different types of distress as well as their severities by measurements of pavement performance. The Distress Identification Manual for the Long-term Pavement Performance Program (Miller and Bellinger, 2003), published by the Federal Highway Administration in 2003, is a comprehensive manual which provides a solid basis for identification of distress and collecting of data.

2.2.3.2. Cracking

A crack is an unplanned break or discontinuity in the integrity of the pavement surface. Cracks may appear as small openings or partial fractures on pavement surfaces or bottoms of asphalt layers. Cracks are precisely defined by AASHTO with a minimum length of 25 mm and a minimum width of 1 mm (NCHRP, 2004). The term "cracking" refers to the process of a crack developing.

Cracks can be affected by traffic loading, the environment, or the combination of both. Commonly, cracks can propagate in two ways which are top-down cracking and bottom-up cracking. Cracks are always a symbol of a pavement defect. Cracks allow for infiltration of water into the sub-layers of a

pavement and thus, will accelerate pavement deterioration to some extent. Pavement deterioration rate is found to be much greater once cracking has initiated (ISOHDM, 1995). Some common cracking phenomena are discussed as follows.

Fatigue cracking

Fatigue cracking is a series of interconnecting cracks caused by the fatigue failure of an asphalt surface or stabilised base under repeated traffic loading (Huang, 2004). The horizontal stress at the bottom of the asphalt layer is generally lower than the tensile strength of the material. However, after a number of loading repetitions, the material tends to exhibit fatigue damage and cracks start to propagate upwards. Therefore, fatigue cracking may sometimes be called bottom-up cracking. After the initial stage (interconnecting cracks), this form of fatigue cracking will deteriorate into sharp-angled pieces with many sides. The pieces are normally less than 0.3 metre side length. An alligator pattern will occur in a late stage, therefore, the term "alligator cracking" is a synonym of "fatigue cracking".

Alligator cracking often appears on roads with high volumes of heavy vehicles and occurs in the wheel-path. Moreover, fatigue cracking will not occur until numerous loadings have been induced. After initiation, fatigue cracking will increase rapidly as the pavement weakens. Pavement quality will reduce largely because of fatigue cracking. It is considered to be a major structural distress and a sign of a severely damaged road.

Fatigue cracking is measured in square metres (or feet) per unit surface area (%). It is a common practice that the severity of the fatigue cracking are ranked and specified by a certain level e.g. high, medium and low severity.

Longitudinal cracking

Longitudinal cracking consists of linear cracks which generally develop in the direction of the pavement centreline. Longitudinal cracking can appear as single cracks or a series of nearly parallel cracks. The reason for longitudinal cracking is mainly because of shrinkage of the asphalt surface under low temperature or asphalt hardening. When temperature gets colder, asphalt concrete shrinks and tensile thermal stress will be induced. With asphalt hardening, asphalt becomes brittle and is more prone to cracking. Furthermore, longitudinal cracks can also be associated with subgrade movements due to moisture (Moffatt and Hassan, 2006). Generally, longitudinal cracking is environmentally related but can be associated with traffic loading (Casey et al., 2012a), especially when the cracking locates in a wheel path.

2. LITERATURE REVIEW

Measurements are recorded both for wheel path longitudinal cracking and non-wheel path longitudinal cracking. Longitudinal cracking is measured by total length per unit road length (m/km or inch/mile).

Transverse cracking

Transverse cracking means linear cracks which predominantly develop perpendicular to the pavement centreline. Similar to longitudinal cracking, transverse cracking can occur as a single crack or a series of parallel cracks.

The reason for the transverse cracking is believed to be environmentally associated. Common causes for transverse cracking are shrinkage cracks in asphalt surfacing under low temperature or asphalt hardening, as for longitudinal cracking. The same as longitudinal cracking, transverse cracking can be load related (Casey et al., 2012b). Usually, transverse cracking occurs in bound flexible pavements. Transverse cracking is measured in total length per unit road length (m/km or in/mi).

Block cracking

Block cracking consists of a series of cracks which divides pavements into rectangular pieces. Block cracking can be mistaken to be combination of longitudinal and transverse cracking. Typically, the size of the blocks ranges from approximately 0.1 to 10 m^2 (1 to 100 ft^2, 1 ft $\approx$ 0.3 m). If the size is larger than this, the cracking is considered to be the combination of longitudinal or transverse cracking (Miller and Bellinger, 2003).

Shrinkage of hot mixed asphalt is believed to be the main reason for block cracking. The shrinkage occurs due to cycling of daily temperature which results in cyclic stress and strain. Block cracking can occur in areas without traffic loadings; thus block cracking is not load associated, although loads can increase its severity.

Block cracking is commonly measured as percentage per square metre with a severity level for each square metre. If fatigue cracking lies in a block cracking area, the area should be reduced by excluding areas under fatigue cracking.

2.2.3.3. Rutting

A rut is a longitudinal surface depression in the wheel path. Rutting is a character of the transverse profile of a road surface. Rutting is undesirable for many reasons. It can provide a potential means of water intrusion through asphalt layers into unbound pavement layers. Or in a worse case, when rutting has deformed the subgrade surface, it will act to keep water in the pavement at the pavement-subgrade interface, thereby leading to rapid pavement decay.

During cold weather, rutting may retain water at the surface which can develop into ice thus reducing skid resistance. Hydroplaning risks are increased as well.

Rutting is caused by traffic loading and the environment. Traffic loading, especially heavy loading will have substantial effect on rutting, by means of abrasion, shear deformation and compaction. Environmental considerations including water, temperature and freeze-thaw cycles can have an impact on structural materials in pavements and thus can aggravate rutting. The type of rutting is various due to different mechanisms. Dawson and Kolisoja (2006) propose four modes of rutting taking into consideration compaction, wheel shear, weak subgrade and particle damage according to different road types and traffic conditions. Although the mechanism of rutting is complex, it is commonly believed that surface rutting consists of two parts: namely asphalt rutting and UGM rutting.

Asphalt rutting can be concluded as two types: consolidation and material flow (Kandhal and Cooley, 2003). The consolidation is one-dimensional densification or vertical compression without occurrence of asphalt shoving, while lateral flow of the material occurs due to inadequate shear strength or an insufficient amount of air voids (Witczak, 2007). In a well compacted mix, the impact from densification is small compared to the shear deformation, thus the dominant material behaviour for asphalt rutting is shear deformation (Long, 2001). Creep recovery tests were developed to evaluate the rutting resistance of asphalt mixtures by investigating the creep deformation in bitumen and mastics (Elnasri et al., 2014, Elnasri et al., 2013).

Rutting in UGM is permanent (plastic) deformation of UGM, including the unbound base layer, subbase layer as well as subgrade. It has been proved by accelerated pavement tests that up to 30% to 70% of rutting is generated from the granular layers (Arnold, 2004, Korkiala-Tanttu et al., 2003) for some pavements. Therefore the rutting in UGM can be dominant in many cases. The permanent deformation in UGM is associated with repeated traffic loading, various material and structural factors and by the environment (Lekarp et al., 2000b). The material factors include the properties of the aggregates such as grain shape, surface roughness, maximum grain size, content of fines, grain size distribution, and degree of compaction. Other factors include, for example, the number of load repetitions, temperature, moisture condition, geometry of the structure and stress history (Korkiala-Tanttu, 2008).

2.2.3.4. Roughness

Roughness is the measurement of the longitudinal unevenness of the pavement. Roughness is an important indication of road serviceability and riding comfort because it has an impact on vehicle dynamics. It can also affect the dynamic loading which can accelerate the deterioration of a pavement. An increase of

roughness on a pavement is believed to cause an increase in road user's cost (Archondo and Faiz, 1994, Greenwood and Christopher, 2003) as well as accidents (Ihs and Sjögren, 2003). Therefore, for better road management, it is of importance to have precise and up-to-date measurement of roughness.

To provide a common quantitative measurement for road roughness, the International Roughness Index (IRI) was developed under the sponsorship of the World Bank at the International Road Roughness Experiment which was held in Brazil in 1982. After that, guidelines for roughness measurements were published by the World Bank (Sayers et al., 1986). Strong evidence has been shown that IRI measured from different regions are compatible with each other (Sayers and Karamihas, 1998).

IRI is a roughness scale, based on dynamic response of a profilometer at 80 km/hr (known as RARS80, i.e., IRI). The profilometer can be either a topographic survey or a mechanical profilometer, which records the vertical motion of a quarter car. The vertical movements will be translated into the elevation of the longitudinal profiles, then to a summarised IRI. IRI is expressed in m/km (or inches/mile). IRI is the property of a single wheel track and it is recorded in segments. IRI is defined by the Average Rectified Slope (ARS), as a ratio of the accumulated suspension motion to the distance travelled of a standard quarter car at the standard speed (80 km/h). ARS can be illustrated as in Figure 2-10:
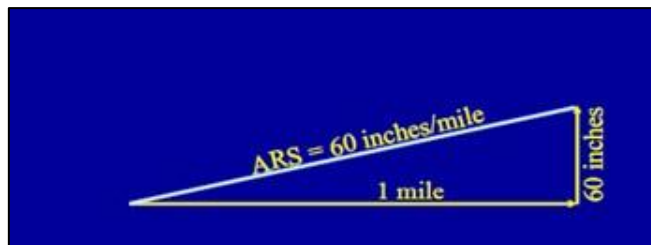
Figure 2-10 ARS illustration

Generally, each type of pavement has a certain range of initial IRI and its IRI needs to be in that range to ensure driving quality (see Figure 2-11). The lower the IRI value is, the better the quality of the pavement. Thus, a lower IRI value indicates better driving comfort and better performance of the pavement.
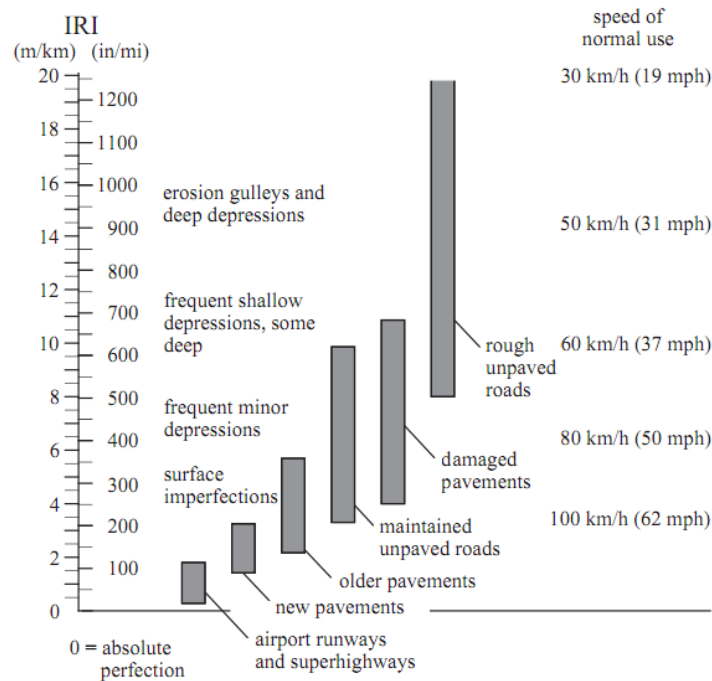
Figure 2-11 Suitable IRI range for different pavements (Sayers and Karamihas, 1998)

2.2.4. Pavement performance and environmental factors

Temperature and moisture are probably the most discussed "enemies" of a flexible pavement. To be more specific, the performance of asphalt concrete is highly associated with its temperature and moisture content, which plays an important role for the deformation properties of unbound granular materials. Heat in the pavement comes principally from the solar radiation and air temperature and is related to the properties of the materials to receive and retain the energy including albedo, heat capacity, and thermal conductivity. Additionally, wind can change the surface convection and thus impact pavement temperature. Moisture in the pavement can be related to precipitation and the groundwater level. Therefore, five environmental factors were discussed in the study, including temperature, precipitation, solar radiation, wind speed, and groundwater level. These factors were all considered by the Enhanced Integrated Climatic Model (EICM) in MEPDG.

2.2.4.1. Asphalt rutting

Asphalt rutting refers to the accumulation of permanent deformation in the asphalt layer and bituminous base layer. Asphalt concrete is a viscoelastic material and the stiffness can be significantly influenced by the temperature of the material. Moreover, resistance to permanent deformation can be reduced

when temperature increases. Therefore, it can be inferred that increasing of air temperature and solar radiation can accelerate rutting in asphalt layers. Furthermore, wind can enhance convection and thus impact pavement temperature.

The stiffness of asphalt concrete may reduce dramatically when temperature increases. Moreover, larger asphalt rutting is expected under higher asphalt temperatures, especially when the traffic volume is large and the traffic speed is slow. Therefore, the majority of asphalt rutting occurs when the temperature is higher. Temperature increasing caused by climate change may increase the frequency of high temperature and thus lead to greater asphalt rutting.

2.2.4.2. Subgrade rutting

Dramatic increases in moisture in pavements due to rainfall should be avoided in good pavement design and practise. A well-designed drainage system is indispensable in areas with plentiful precipitation. However, moisture increase due to precipitation is difficult to avoid, especially when drainage is bad. There are several pathways for the rainfall to reach the unbound layers of a pavement as mentioned before, including subsurface seepage, cracking and rise of water table. Nonetheless, pavement cracking may be less important in water infiltration compared to subsurface seepage and rise of water table (Birgisson and Ruth, 2007). The infiltration will increase the moisture content of the unbound layers but the extent to which the moisture changes depends also on the property of the soil.

In cold areas with increasing precipitation, moisture content in UGM including subgrade is expected to increase, which indicates weaker resistance to permanent deformation for the road. Generally, moisture exists in soils. A moderate amount of moisture content is desirable because it benefits the stiffness thus provides better resistance to permanent deformation. However, excessive moisture contents can result in a reduction in resilient modulus and stiffness; therefore the road is prone to greater permanent deformation (Werkmeister, 2003). The reduction of effective stress due to excessive pore pressure is believed to be the reason for the reduction in permanent deformation resistance (Lekarp et al., 2000b). Researchers have confirmed this by experiment that high water content in UGM can lead to significant permanent deformation (Thom and Brown, 1987). Furthermore, it seems that soils have an optimum water content, above which the permanent deformation propagates rapidly (Gidel, 2001).

In areas where subgrade is frozen during winter and thaws in spring, the moisture content in the subgrade can be significantly high in spring. Pavements' strength and stiffness can be significantly reduced especially if the

pavement has bad drainage. A considerable amount of rutting may occur during this period. Furthermore, other distress including cracking, potholes, and roughness can be exacerbated. Frost heave and spring thaw usually occur at high altitude. In frost regions, temperature increase due to climate change may be:

- great enough to keep the pavement frost-free. Under this condition, climate change may reduce pavement deterioration by eliminating frost heave and spring thaw. However, the frost period when pavements gain strength can be eliminated as well.
- medium to reduce the frost period. Such cold areas may have a generally warmer winter but still with a frost period. The frost period can be reduced and thus the period when pavements gain strength is also excluded. Even worse, the thawing period may be extended so that periods with greater deterioration rate may be extended. In such areas, the effect of climate change on pavement performance needs to be more carefully considered.
- little and have no effect on frost heave and spring thaw.

Furthermore, groundwater level rise due to climate change can be expected in coastal areas because of the sea level rise, which can increase the moisture content in the subgrade. For instance, a study has been performed on New Haven, a coastal city in the State of Connecticut, U.S.. With a substantial part of the city at less than 30 feet above the sea level, the groundwater level is likely to increase due to the sea level rise (Bjerklie et al., 2012). Furthermore, many underground utilities may be flooded in the future. In contrast, others found that the global sea-water rise can result in depletion of groundwater (Wada et al., 2012). The excessive extraction of groundwater may result in lower groundwater level and lead to more surface runoff which can contribute to the sea level rising. This can be common in urban areas where groundwater is excessively extracted. Altitude is a factor when considering effects of sea level rising on the groundwater level and infrastructure as a consequence. The groundwater level in coastal areas may be considerably closer to the land surface compared to that of high altitude regions.

2.2.4.3. Cracking

In a hotter climate, as a consequence of age hardening, the asphalt surface becomes brittle and vulnerable to cracking. When pavements cool from a hot condition, thermal tensile stresses can cause cracking initiation and propagation. Therefore thermal cracking will be more serious in areas with more extreme daily/seasonal/annual hot and cold weather.

In general, there are two different types of thermal cracking, which are low-temperature transverse cracking and thermal fatigue cracking. The former is caused by the shrinkage of asphalt due to cold extremes, while the latter results from asphalt ageing and residual stress due to a large number of loading cycles. Increasing average temperature can lead to a higher pavement temperature. Age hardening is either desirable or undesirable, depending on the position. Age hardening is undesirable on the road surface, because it can reduce the ability of pavement to flex under traffic. Nevertheless, age hardening may be acceptable in pavements with thick bituminous base layer because the stiffness of the material increases due to age hardening, thus better load spreading ability is expected.

2.2.5. MEPDG performance prediction models

2.2.5.1. Design procedure

Pavement design using the 2002 Design Guide is achieved by a trial-verification-modification loop, i.e., it does not give the layer thickness or a structural number as in the AASHTO Guide for Design of Pavement Structures (AASHTO, 1993). A trial design is assumed, verified, and adjusted if any specific criteria are not met. The final design needs to meet all design criteria. The design procedure of the 2002 design guide can be followed by three steps (AASHTO, 2009) (see Figure 2-12):

1) Input the trial design (traffic, structure, material, and climate)
2) MEPDG calculates the responses and damage accumulation over the design life
3) The design is verified against the performance criteria and, if not satisfying, modified.
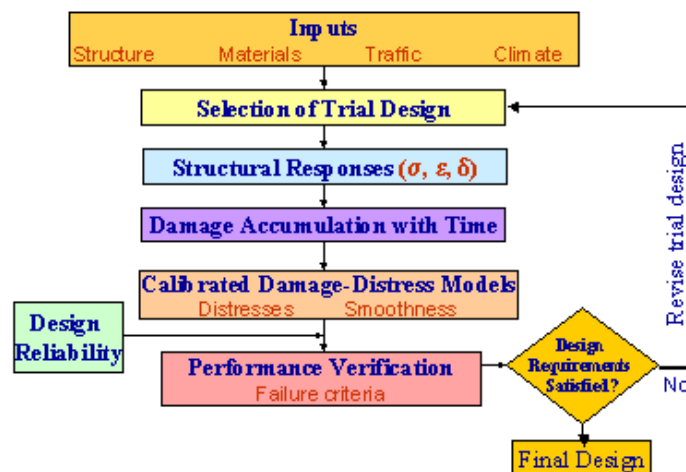
Figure 2-12 Design procedure of 2002 Design Guide (AASHTO, 2009)

2. LITERATURE REVIEW

The material input hierarchy provides different levels of accuracy for pavement response and performance modelling (AASHTO, 2009). The designer can choose different input levels for certain material properties depending on their need and the availability of necessary input data.

The stress-strain response is calculated using multi-layer elastic response models with the finite element method. Then the pavement performance is evaluated by an incremental damage approach. The approach divides the analysis period into time increments of 1 month for rigid pavements and 1 month or 0.5 month for flexible pavements. Within each increment, variations in material properties, traffic and, climate are taken into consideration and the combination of factors that affect pavement response and damage are unique to that increment. Calibrated pavement performance models including bottom-up cracking, fatigue cracking, roughness, and rutting models are available for pavement performance predictions. Field measurements of pavement condition from the Long Term Pavement Performance (LTPP) database and some other field data (AASHTO, 2009) were adopted for model calibration.

The pavement performance predictions at a selected reliability level can be compared to performance criteria. If the trial design satisfies performance criteria, a feasible design is made. Otherwise the design needs to be modified and re-assessed by the design procedure, until a feasible design is found. Furthermore, improvement of the trial can be made by modification of the trial (e.g. thinner layer) and verified by the design process until a better design is found.

2.2.5.2. Inputs

The inputs of MEPDG consist of four categories, which are traffic, structural, material, and climatic input.

Traffic category includes Annual Average Daily Traffic (AADT), truck percentage, monthly/hourly vehicle distribution, vehicle class distribution, axle type, lateral wandering, and traffic growth rate. Structure category involves pavement layer thickness and material properties.

For flexible pavements, the material (including asphalt mixture, unbound granular materials, and subgrade) properties have three input levels. Input Level 1 requires sophisticated laboratory testing or field measurements and thus represents the highest accuracy. Regression equations are used in input Level 2, i.e. parameters are correlated to other material property(s). Relatively, input Level 2 has intermediate accuracy. Input Level 3 uses typical values from estimation and thus has lowest accuracy (AASHTO, 2009). The structural input includes layer type and thickness.

2. LITERATURE REVIEW

Climate input is used to predict the environment of a pavement, i.e. pavement temperature and moisture profile is derived from the EICM. The climate conditions of any location can be represented by a nearby station or interpolated from the 6 closest stations, which are inversely weighted by the distance from the location (AASHTO, 2009).

2.2.5.3. Enhanced Integrated Climatic Models

Climate inputs are used to predict pavement temperature and moisture profile by the EICM which is a one-dimensional coupled heat and moisture flow programme. The EICM includes three major models, which are:

- The Climatic-Material-Structural Model
- The Cold Regions Research and Engineering Laboratory (CRREL) Frost Heave and Thaw Settlement Model
- The Infiltration and Drainage Model

The climatic inputs for EICM are hourly data of climatic conditions, including temperature, precipitation, wind speed, sunshine percent, and groundwater level. Other general inputs include latitude, longitude, elevation, and daily records of sunrise/sunset time. EICM can "translate" the inputs, i.e. external environment, to the internal environment including temperature, moisture, and frost depth. Together with EICM, there are several parameters that determine the temperature in, and moisture profile of, a pavement:

- Thermal conductivity (temperature)
- Heat capacity (temperature)
- Infiltration (moisture)

Thermal conductivity quantifies the ability of a material to conduct heat. It is the quantity of heat that is transmitted through a unit thickness, normally to the surface of a unit area, per unit of time for a given temperature gradient. Heat capacity is used to describe the ratio of heat added to a material to the increase in the temperature. The infiltration parameter defines the potential for net infiltration of water into a pavement.

2.2.5.4. Fatigue cracking

In general, fatigue cracking can be categorised by the direction of crack propagation, which includes bottom-up fatigue cracking and surface-down fatigue cracking (AASHTO, 2009). Bottom-up fatigue cracking initiates at the bottom of the asphalt layer and propagates upwards to the pavement surface. The cracks become inter-connected on the surface and form an alligator pattern over a long time, and thus it is termed alligator cracking (AASHTO, 2009). Alligator cracking may be used as a synonym of fatigue cracking elsewhere

(Huang, 2004). Surface-down cracking initiates from the surface of a flexible pavement and propagates downwards. This type of cracking usually appears parallel on the surface of flexible pavements and thus is termed longitudinal cracking. Generally, fatigue cracking is load associated and may be also related to environment conditions (Huang, 2004).

Bottom-up fatigue cracking (alligator cracking)

Usually, fatigue cracking is measured in square metres (or feet) of surface area with a severity level. If the severity of an area is so bad that it cannot be determined by the existing level, the entire area should be rated as highest severity. Furthermore, fatigue cracking can also be measured as a percentage of the surface area, which is adopted in MEPDG.
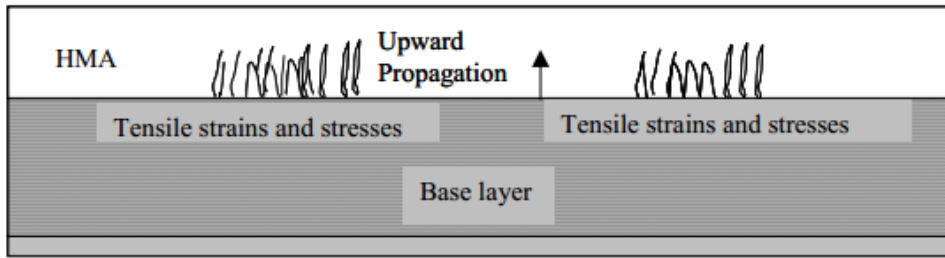
Figure 2-13 An illustration of bottom-up fatigue cracking

In the Design Guide, the bottom-up cracking is related to the bottom-up fatigue damage as follows (NCHRP, 2004):

$$FC_{down} = \left(\frac{C_3}{1 + e^{C_1 C_1' + C_2 C_2' log_{10}(100D)}} \right) \times \frac{1}{60} \qquad \text{Equation 2-12}$$

$$C_2' = -2.40874 - 39.748(1 + h_{AC})^{-2.856} \qquad \text{Equation 2-13}$$

$$C_1' = -2C_2' \qquad \text{Equation 2-14}$$

where,

FC_{down} = bottom-up fatigue cracking (%)

D = bottom-up fatigue damage

h_{AC} = asphalt layer thickness

C_1, C_2, C_3 = model factors

The damage is calculated based on Miner's law, which is formulated as (NCHRP, 2004):

$$D = \sum_{i=1}^{T} \frac{n_i}{N_i} \qquad \text{Equation 2-15}$$

where,

D = damage

n_i = number of load repetitions in period i

N_i = number of load repetitions allowed under conditions in i

The number of load repetitions to failure (cracks start to develop) can be expressed as (NCHRP, 2004):

$$N_f = Ck_1 \left(\frac{1}{\varepsilon_t}\right)^{k_2} \left(\frac{1}{E}\right)^{k_3}$$ Equation 2-16

where,

N_f = number of load repetitions to failure

ε_t = tensile strain at the critical position

E = material stiffness

C = laboratory to field adjustment factor

k_1, k_2, k_3 = regression factors

Surface-down fatigue cracking (longitudinal cracking)

Studies suggest that longitudinal cracking can also be associated with traffic loading especially when the cracking is located in the wheel path. Longitudinal cracking can be related to the wheel load and tyre pressure. Wheel load can induce tensile stresses, resulting in the initiation and propagation of longitudinal cracking. Shearing of the HMA mixtures can also cause cracks to initiate and propagate, especially from the radial truck tyres (Myers et al., 2001, AASHTO, 2009). Furthermore, aging of the HMA surface mixture can accelerate the initiation and propagation of longitudinal cracking (AASHTO, 2009). In addition, longitudinal cracking can also be caused by badly constructed paving of a lane joint (Huang, 2004).
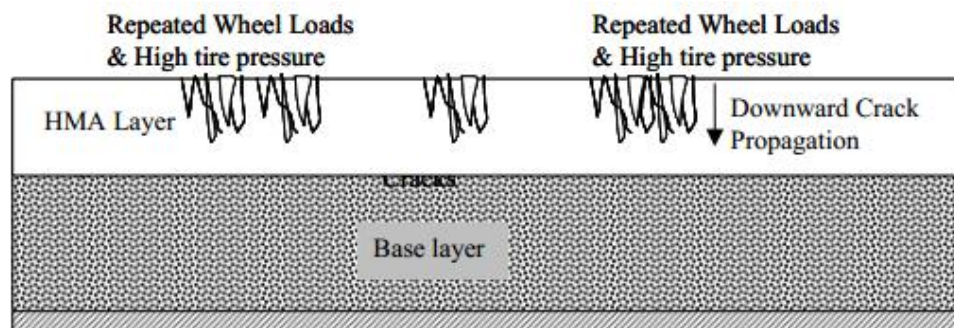
Figure 2-14 An illustration of surface-down cracking

Occasionally, longitudinal cracking with sealant in good condition may be also included in measurements, because a new crack and a sealed crack may

not be distinguished easily by the scanner in road condition surveys. This also applies to the measurements of other types of cracking with sealant treatment.

In MEPDG, the longitudinal cracking model, referred to as surface-down fatigue cracking, relates longitudinal cracking to the top-down fatigue damage and can be formulated as (NCHRP, 2004):

$$FC_{top} = \left(\frac{C_3}{1+e^{C_1-C_2 log_{10}(100D')}} \right) \times 10.56 \qquad \text{Equation 2-17}$$

where,

FC_{top} = top-down fatigue cracking (m/km)

D' = top-down fatigue damage

C_1, C_2, C_3 = model factors

2.2.5.5. Thermal cracking (transverse cracking)

Thermal cracking is caused by low temperature or temperature cycling (AASHTO, 2009). Thermal cracking caused by low temperature is termed low temperature (thermal) cracking. Low temperature thermal cracking occurs when the tensile strength of the asphalt material is exceeded by the additional tensile stress due to shrinkage of the material under low temperature (Monismith et al., 1965). Thermal cracking caused by temperature cycling is termed thermal fatigue cracking. Thermal fatigue cracking is caused by the thermal stress due to daily/seasonal temperature cycling, which is not necessarily related to low temperature (Lytton et al., 1983). Therefore, thermal fatigue cracking may occur on pavements in relatively moderate climates. Thermal cracking may occur in the form of block cracking as the asphalt ages and becomes brittle (AASHTO, 2009).

In MEPDG, the amount of thermal cracking is related to the crack depth and can be expressed as (NCHRP, 2004):

$$C_f = \beta_1 N(z) \left(\frac{logC/h_{ac}}{\sigma} \right) \qquad \text{Equation 2-18}$$

where,

C_f = amount of thermal cracking

$N(z)$ = standard normal distribution

C = cracking depth

σ = standard deviation of $logC$

h_{ac} = thickness of the asphalt layer

β_1 = regression factor

The propagation of thermal fatigue cracking as a result of thermal cooling cycles can be calculated using Paris law of cracking propagation (NCHRP, 2004):

$$\Delta C = A\Delta K^n$$
<div align="right">Equation 2-19</div>

where,

ΔC = change in crack depth due to a cooling cycle

K = change in the stress intensity factor caused by the cooling cycle

A, n = fracture parameters of the asphalt mixture

Parameter n can be determined by the regression factor derived from the creep compliance curve and A is related to stiffness and tensile strength of the asphalt mixture.

2.2.5.6. Permanent deformation

Introduction

Rutting is related to traffic loading and the environment. Traffic loadings, especially heavy loadings will have substantial effect on rutting, by means of compaction and abrasion. The damage of a heavy axle on a flexible pavement is magnified by the fourth power law, according to early AASHTO road tests (Cebon, 1989, Dawson, 2008). Environmental considerations including excessive water, high temperature and freeze-thaw cycles can have impact on structural materials in pavements and thus can aggravate rutting (AASHTO, 2009, Korkiala-Tanttu, 2008, NCHRP, 2004, Huang, 2004). The type of rutting is various due to different mechanisms. Dawson and Kolisoja (2006) included four modes of rutting for low-volume pavements, which are:

- Mode 0: Rutting is caused by compaction in non-saturated materials immediately after trafficking. The compaction can prevent further compaction and increase the stiffness of materials. Therefore, it is generally seen as a self-stabilizing process of the materials.
- Mode 1: In flexible pavement with weak granular material, local shear may occur closed to the wheel. The aggregate adjacent to the wheel may be subject to shear deformation and dilation as a consequence. Furthermore, mode 1 rutting is common in areas affected by seasonal frost (Dawson and Kolisoja, 2006).
- Mode 2: In flexible pavement with granular material of high quality, the pavement ruts as a whole. In seasonal frost areas, the subgrade may

2. LITERATURE REVIEW

experience excessive moisture during spring thaw. This may reduce the stiffness of subgrade soil and mode 2 rutting may occur.

- Mode 3: Mode 3 rutting generally refers to the wear of the pavement. In permanent frost areas where subgrade is frozen, pavements gain strength. In such areas, abrasion from studded tyres may become the dominating mode of rutting. In fact, the utilisation of studded tyres exists not only in permanent frost areas but also in general cold climate zones, where studded tyres are used to increase the friction between tyres and pavement surface.
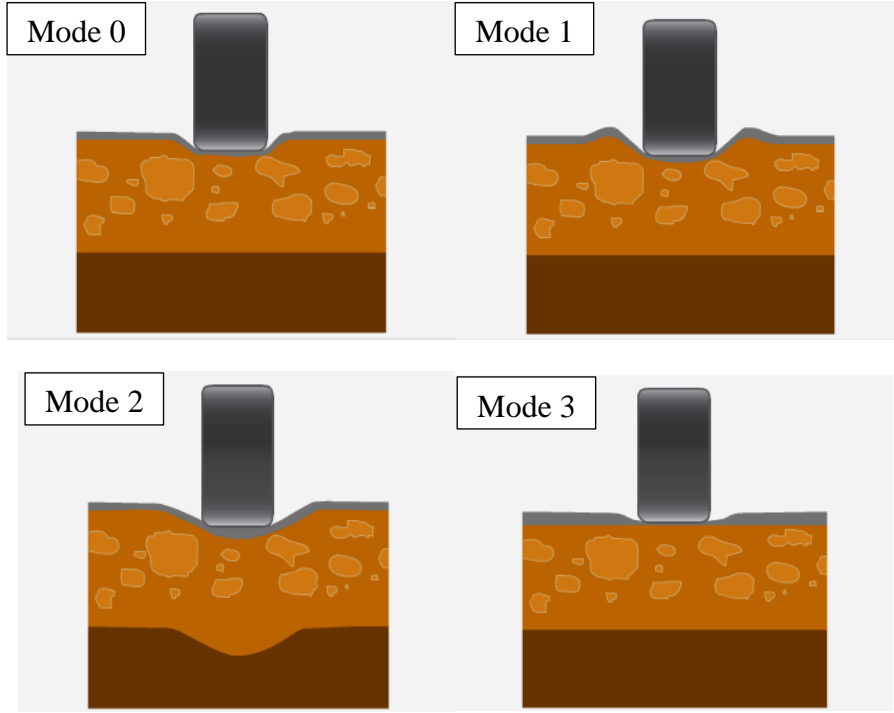
Figure 2-15 Four modes of rutting (Dawson and Kolisoja, 2006)

Although several rutting modes exist, permanent deformation of a pavement is usually calculated from the sum of permanent deformation of all pavement layers and subgrade (see Equation 2-20, 2-21) (Korkiala-Tanttu, 2008, Werkmeister, 2003, NCHRP, 2004, AASHTO, 2009). The permanent deformation prediction models are different between asphalt layers and granular layers (unbound granular layers and subgrade).

$$RD = \sum_{i=1}^{n} \Delta RD_i \qquad \text{Equation 2-20}$$

$$\Delta RD_i = \varepsilon_{pj} \times \Delta h_j \qquad \text{Equation 2-21}$$

where,

RD = rut depth

ΔRD_i = permanent deformation in structural layer i

ε_{pj} = plastic strain in finite element layer j

Δh_j = thickness of finite element layer

Permanent deformation of asphalt materials

The permanent strain in asphalt mixtures can be related to the elastic strain, temperature, and number of loading cycles as (NCHRP, 2004):

$$\frac{\varepsilon_p}{\varepsilon_r} = a_1 T^{a_2} N^{a_3}$$

Equation 2-22

where,

ε_p = permanent strain

ε_r = elastic strain

T = temperature

N = number of loading cycles

a_1, a_2, a_3 = regression factors

      Field calibration factors were adopted for the further development of the model and this model was adopted by the MEPDG, which can be formulated as (NCHRP, 2004):

$$\frac{\varepsilon_p}{\varepsilon_r} = \beta_{r1} a_1 T^{\beta_{r2} a_2} N^{\beta_{r3} a_3}$$

Equation 2-23

where,

$\beta_{r1}, \beta_{r2}, \beta_{r3}$ = field calibration factors

Permanent deformation in unbound materials

There have been many permanent deformation prediction models which relate plastic strain (or deformation) to number of loading cycles, elastic strain, stress level, and material properties such as internal friction angle. A modified Tseng and Lytton model was adopted in the Design Guide and can be formulated as (NCHRP, 2004, Tseng and Lytton, 1989):

$$\delta_a(N) = \beta_1 \left(\frac{\varepsilon_0}{\varepsilon_r}\right) e^{-\left(\frac{\rho}{N}\right)^\beta} \varepsilon_v h$$

Equation 2-24

where,

δ_a = permanent deformation

N = number of load repetitions

ε_r = resilient strain

$\varepsilon_0, \beta, \rho$ = material properties from testing

ε_v = calculated average vertical resilient strain from primary response model

β_1 = calibration factor

h = layer thickness

Model factor β was further developed to be related to water content as follows (NCHRP, 2004):

$$log\beta = -0.61119 - 0.017638W_c \qquad \text{Equation 2-25}$$

where,

W_c = water content (%)

The advantage of this model is the capability of predicting the permanent deformation under various moisture conditions in pavement unbound granular layers and subgrade, and thus take seasonal variation of the moisture content in unbound granular layers into consideration. With rutting measurement from 88 road sections of 23 States in the U.S. from the LTPP database, the model factors were nationally calibrated and can be found in the Design Guide (NCHRP, 2004). Furthermore, the accuracy of rutting prediction may rely much on the accuracy of applied rutting models for unbound granular layers as a high percentage of total rutting can occur in these layers (Qiao et al., 2014).

2.2.5.7.International Roughness Index (IRI)

Prediction of IRI can be made by correlating IRI to other pavement performance indices including rutting, bottom-up fatigue cracking, top-down fatigue cracking, and thermal cracking (NCHRP, 2004). Other distress types, e.g. potholes are associated with road roughness and serviceability but may not be adopted to derive IRI because of a lack of modelling method of these distress types. Such models are usually based on in-situ measurements of distress. In MEPDG, prediction of IRI is considered to be depending on the type of base such as unbound granular, asphalt treated, and chemically stabilised bases. The selected road sections for case studies are all with granular base and subgrade and the other two types will not be mentioned.

The IRI, unlike other distress type, starts at a particular initial value. The initial IRI may be determined by pavement structure, materials, and compaction in construction. For flexible pavements with unbound granular base and subgrade, the development of IRI can be formulated as (NCHRP, 2004):

2. LITERATURE REVIEW

$$IRI =$$

$$IRI_0 + 0.0463\left[SF\left(e^{\frac{age}{20}} - 1\right)\right] + 0.00119(TC_L)_T + 0.1834(COV_{RD}) +$$

$$0.00384(FC)_T + 0.00736(BC)_T + 0.00115(LC_{SNWP})_{MH}$$

Equation 2-26

where,

IRI = international roughness index (m/km)

IRI_0 = initial IRI (m/km)

SF = site factor

age = age in years

$(TC_L)_T$ = total length of transverse cracking (m/km)

$(FC)_T$ = fatigue cracking in wheel path (% total lane area)

$(BC)_T$ = block cracking (% total lane area)

COV_{RD} = coefficient of rut depth variation (%)

$(LC_{SNWP})_{MH}$ = length of sealed longitudinal cracking of medium and high severity outside wheel path (m/km)

The site factor is associated with a combination of climatic factors and properties of the unbound materials and can be formulated as (NCHRP, 2004):

$$SF = \left(\frac{(R_{SD})(P_{0.075}+1)(PI)}{2\times10^4}\right) + \left(\frac{In(FI+1)(P_{0.02}+1)[\ln(R_m+1)]}{10}\right)$$

Equation 2-27

where,

R_{SD} = standard deviation of the monthly rainfall (mm)

$P_{0.075}$ = percentage passing the 0.075 mm sieve

$P_{0.02}$ = percentage passing the 0.02 mm sieve

PI = plasticity index

FI = average annual frozen index (℃-days)

R_m = average annual rainfall (mm)

2.2.5.8. Reliability

The uncertainties in the MEPDG prediction results are due to various reasons, such as uncertainties in inputs, models, and LTPP data for calibration. Due to simplification, some input factors are considered to be constant throughout the design life of a pavement. However, these parameters may vary significantly. For instance, the traffic inputs may be significantly changed over the design life of a pavement, which is typically $20 - 40$ years. Considering the traffic condition of 30 years ago, e.g. the traffic growth rate, percentage of trucks, type of vehicles has significantly changed compared to present. Furthermore, the yearly/monthly/daily/hourly vehicle distribution may not necessarily be identical. Similarly, the climate may change over the design period of a pavement. Therefore, uncertainties can be introduced. Other inputs such as laboratory testing, material properties, and structure layer thickness are all subject to errors in measurements. The pavement performance models are mechanistic-empirical and usually calibrated from measurements. The measurements are subject to both systematic and random error. Therefore, it is unavoidable that the calibrated models will include uncertainties. Obviously, the uncertainty of some factors is more significant due to the larger sensitivity of the system to their values.

The reliability of pavement performance prediction is defined as (also see Figure 2-16):

$$R = P(distress\ over\ design\ period < critical\ distress\ level)$$

(Equation 2-28)

where,

R = reliability

P = probability
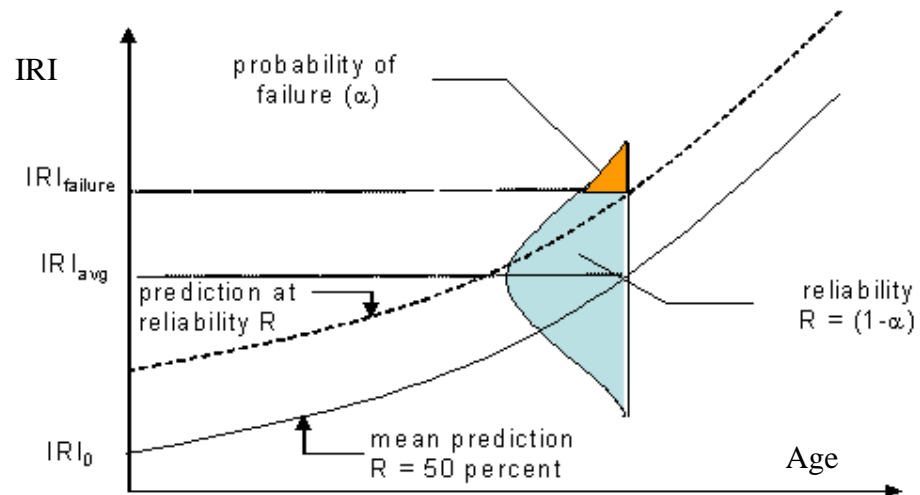
Figure 2-16 Reliability concept (IRI) (AASHTO, 2009)

For instance, due to all uncertainties considered, the roughness in IRI at a particular year follows a normal distribution. The mean roughness IRI_{avg} represents the roughness at 50% reliability, i.e., the probability for the roughness to be higher than IRI_{avg} at that year is 50%. For another example, the probability of failure (failure criteria: $IRI > IRI_{failure}$) is assumed to be 3% at the end of a pavement design life. This means the reliability of the roughness prediction is 97%.

2.2.6.　　　Pavement serviceability and service life

Pavement serviceability is a functional property of a pavement, which describes the ability of a specific section of pavement to withstand traffic in its existing condition. Pavement serviceability can be reflected by many functional characteristics of pavements, e.g. safety related indices, ride quality, and roughness. Pavement serviceability can also be related to distress and structural measures. Present Serviceability Rating (PSR) was developed as a subjective index for rating the serviceability of a pavement. The PSR is obtained from experts' judgement on driving experience after trial rides. It was found that the PSR showed good correlation with some particular pavement distress types e.g. IRI (Terzi, 2006). The numerical index Present Serviceability Index (PSI) is developed for prediction of PSR, which is made from the mathematical combination of different distress measurements based on data from the AASHTO Road test.

Pavement service life is the time from opening to traffic until the pavement provides a substandard performance level that is determined by one or more performance indices. The substandard performance level can usually be seen by the maintenance thresholds, which are determined by road authorities. The maintenance threshold that is triggered earliest defines the

pavement's service life. The service life can be expressed by the following equation:

$$SL = min(SL_1, SL_2, SL_3 \dots)$$ Equation 2-29

where,

SL = pavement service life

$SL_1, SL_2, SL_3 \dots$ = service life calculated with distress types 1, 2, 3, and...

The service life of individual distress is measured from opening to traffic until the maintenance threshold of the distress is triggered. If maintenance thresholds are not triggered over the entire pavement design life, the pavement service life is considered to be equal to the design life. Pavement service life indicates the durability of a pavement without maintenance. When the pavement service life has been reached for a pavement, interventions need to be performed, given sufficient budget.

2.3. Pavement maintenance

2.3.1. Introduction

A combination of traffic loading and environmental effects leads to the deterioration of pavements. As time goes by, the functional condition of pavements can fall to a critical level when the comfort for driving on the road is poor, or even unacceptable. The serviceability of the road is then under challenge. Poor serviceability may also result in reduced driving safety and increased costs for the road users. Therefore, maintenance should be performed at this point to provide a better service for road users.

For road authorities, the choice of maintenance methods is based on pavement age, condition and availability of funding. Technically, pavement condition measures such as rutting, roughness and cracking are the most common considerations to initiate maintenance. An unacceptable level of pavement condition can be indicated by these distress types when they exceed threshold values (see Figure 2-17), referred to as trigger values. The trigger values are the maximum acceptable distress indices, suggesting the uppermost tolerable levels of distress for pavements. As soon as the indices of distress (for instance, roughness) exceed the trigger values as a result of pavement performance deterioration, intervention strategies (for instance, rehabilitation) need to be considered to repair the road to a better condition.
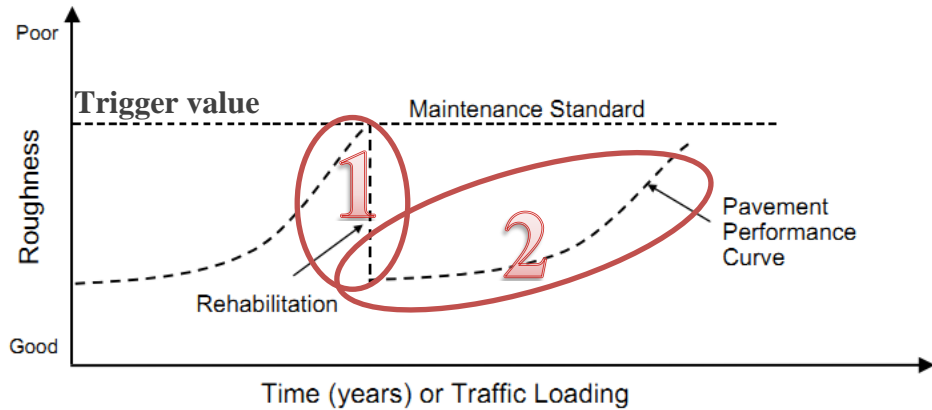
Figure 2-17 Roughness deterioration, trigger value and intervention strategy (1:the immediate effect of maintenance, 2: the long-term effect of maintenance) (Kerali et al., 2006)

2.3.2. Types of maintenance

Generally, pavement maintenance interventions can be described in several categories according to the frequency intensity, and costs for maintenances. In HDM-4, preservation road works are defined in three work classes including routine maintenance, periodic maintenance and special maintenance (Odoki and Kerali, 1999). Typically, routine maintenance is performed to improve pavement condition every year. Common routine maintenance may include crack sealing and filling, edge patching, shoulder repair, pothole repair and drainage works. Periodic maintenance includes preventive maintenance, resurfacing (restoration), rehabilitation and reconstruction. Special maintenance refers to maintenance for emergency conditions such as traffic accident and snow removal. Pavement maintenance is categorized elsewhere as preventive maintenance, corrective maintenance and emergency maintenance (Johanns and Craig, 2002). Due to the ambiguous boundaries between each category, pavement maintenance categories may vary among different road agencies. However this does not mean the individual maintenance methods are different. A summarised category for some common pavement maintenance interventions that can treat cracking, or rutting, or roughness problems is as follows:

- *Routine maintenance*
  - *Crack sealing and filling*
  - *Pothole repair*
  - *Drainage works*
- *Preventive maintenance*
  - *Seal coat*
  - *Microsurfacing*
  - *Thin overlays*
- *Corrective (reactive) maintenance*

- o *Thick asphalt overlays*
- *Rehabilitation*
  - o *Mill and fill*
  - o *Reconstruction*

2.3.2.1. Routine maintenance

Routine maintenance is performed in response to regularly occurring (e.g. every 1 or 2 years) minor distress as a "light" treatment. Typical routine maintenance includes crack sealing and filling, pothole repair, and drainage work.

Crack sealing and filling is usually applied by utilising emulsified bitumen or modified asphalt as a bond to seal the crack walls so that intrusion of water and dust into the pavement from the cracking can be prevented for a period. Crack sealing and filling can also be used to form an impermeable surface before preventive, corrective maintenance, and rehabilitation. For better effectiveness, crack sealing and filling should be applied on pavement surface that is dry and clean. Therefore, crack sealing and filling may help to retard further pavement deterioration. Furthermore, crack sealing and filling requires intensive labour work, thus it is not preferable when the cracking problem is severe because high labour costs may be incurred.

The formation and development of a pothole is complicated. Heavy traffic, asphalt fatigue and inadequate bonding between bitumen and aggregates can all contribute and aggravate a pothole. A pothole is a sign of bad road condition and patching must be applied to repair it.

The purpose of drainage work is to provide the road a successful drainage path which can reduce the excessive water content in the pavement structure.

2.3.2.2. Preventive maintenance

Preventive maintenance is the planned strategy of cost-effective treatments on existing roadway systems to improve the functional condition of the road without substantially changing its structural capacity. Successful preventive maintenance is able to improve pavements' functional condition, retard further deterioration, and thus improve road safety. The most cost-effective time to apply the preventive maintenance is typically before significant distress is exhibited (Hicks et al., 2000). Moreover, costs of preventive maintenance are usually reasonably low compared to corrective maintenance and rehabilitation. Nevertheless, for pavements with structural problems such as rutting, preventive maintenance is not applicable.

2. LITERATURE REVIEW

Seal coats

Seal coats and microsurfacing are very common preventive maintenance applications. Seal coats are the application of a thin layer of emulsified or modified asphalt topping on the pavement surface. Sometimes, a cover of fine aggregates can be added on top of the seal coat.

The exposure of a pavement to sunshine, wind, and precipitation can accelerate the aging of the asphalt surface. After decades, asphalt oxidises and its ability to bend and flex under traffic is restricted. Seal coats are generally considered to be used for restoring the functional property of the pavement surface e.g. skid resistance. Moreover, roughness can be improved after seal coats including chip seal and slurry seal (ISOHDM, 1995). Seal coats are generally considered as time efficient interventions. For instance, fog seal is applied using low viscosity diluted asphalt emulsion and can have an operation speed of 25,000 square yards per day (approximately 20,000 square metres). Seal coats can usually last for 3 – 5 years (Van Kirk, 2004). Nevertheless, seal coats are incapable of addressing rutting (Johanns and Craig, 2002).

Microsurfacing

Microsurfacing (ultra-thin overlay) refers to the application of polymer modified asphalt emulsion with aggregates, mineral filler and water on existing pavement surfaces. Microsurfacing is performed by a paver, which can have an efficiency of approximately 6.6 lane-miles/day (approximately 10.6 lane-km/day). This considerable efficiency can lead to less work zone costs and thus may reduce road user costs. Microsurfacing may last for approximately 7 to 10 years (Johanns and Craig, 2002).

Unlike seal coats, microsurfacing is capable of addressing rutting (up to 1.5 inches, approximately 38 mm) problem (Johanns and Craig, 2002). Besides, microsurfacing creates a new surfacing, which helps to prevent surface distress such as ravelling. However, microsurfacing is incapable of dealing with cracking, base failure and plastic shear deformation in HMA layers (MTAG, 2008).

Thin overlay

Overlays refer to the application of a layer of hot mixed asphalt on an existing pavement surface. Overlays may be either preventive or corrective, mainly depending on the thickness of the added layer. Overlays with thicknesses less than 1.5 inches ($\approx$ 38 mm) are usually considered to be preventive in practice and are referred to as "thin overlays" (MTAG, 2008). Furthermore, several preventive maintenance methods including chip seal and microsurfacing may be sometimes referred to as thin overlays because the layers are thin and offer

no structural improvement to the pavement. The thin overlay discussed in this thesis does not refer to these types of interventions.

Thin overlays are considered to have no effect on the structural properties i.e. bearing capacity and stress distribution, of pavements. Thin overlays applied on structurally sound pavements can extend the service life of the existing pavements (typically 4 – 6 years) and mitigate distress including ravelling, potholes, visible cracking, and alleviate rutting and roughness (MTAG, 2008, Hicks et al., 2000). Moreover, the new surface may provide better skid resistance.

2.3.2.3. Corrective maintenance

Overlays

Overlays are considered corrective maintenance when they deliver structural enhancement to the existing pavement and are typically thicker than 1.5 inches ($\approx$ 38 mm). The term "overlays", discussed later, is used to name this type of overlay. Overlays are adopted when pavements exhibit serious evidence of deterioration. The installation of the overlay will establish a new surface for the road, thus distress such as cracking and potholes will be repaired. Surface functional properties such as skid resistance can be improved. Roughness and rutting problems can also be alleviated after an overlay. When structural distress triggers thresholds, such an overlay can be applied instead of routine maintenance or preventive maintenance.

As more materials are used, overlays usually cost much more compared to routine and preventive maintenance. The installation of an overlay can also take longer thus more user delay can be expected.

2.3.2.4. Rehabilitation

Fill and mill

Rehabilitation refers to a major modification of a road structure, usually by means of milling out old damaged material and resurfacing. The thickness of resurfacing may depend on the condition of the pavement, the anticipated traffic load and budget. From experience, a pavement with a PSR = 2.5 will be considered for some rehabilitation (Huang, 2004). The rehabilitated pavement is expected to have an 8 to 12 years' service life (Tayabji et al., 2000). Furthermore, for roads with structural distress, rehabilitation has proved to be the most effective technique (HDMR, 1995).

Reconstruction

Reconstruction refers to the complete removal and replacement of pavement layers down to the subbase or subgrade. Reconstruction is not common unless the pavement structure has failed or the subgrade needs to be strengthened.

2.3.3.　　Maintenance effects modelling

The immediate effect can be indicated by a sudden change in pavement serviceability or pavement performance indices after a specific intervention. Most immediate maintenance effects models relate pavement performance indices after the intervention to that before the intervention by a linear regression model. The linear model is widely applied for the immediate maintenance effects of routine maintenance (e.g. cracking filling and sealing (Odoki and Kerali, 1999)), preventive maintenance (e.g. chip seal and slurry seal (ISOHDM, 1995, Odoki and Kerali, 1999)), and corrective maintenance (e.g. overlays (Djärf et al., 1995, NDLI, 1991, ISOHDM, 1995). The general principle of the model can be expressed as (Djärf et al., 1995, NDLI, 1991):

$$IRI_a = a_0 + b_0 * IRI_b$$

Equation 2-30

where,

a_0, b_0 = model coefficient

　　　The model coefficients are observed to be different in a study from Sweden ($a_0 = 0.55$, $b_0 = 0.29$), compared to that ($a_0 = 1.87$, $b_0 = 0.25$) from Thailand, which suggested that the reduction in roughness due to overlays may vary from practise to practise (NDLI, 1991). Some linear models considered the thickness of the new surface. (ISOHDM, 1995):

$$IRI_a = a_0 + a_1 * \max(IRI_b - a_0, 0) * \max(a_2 - HNEW, 0)$$

Equation 2-31

where,

HNEW = the thickness of overlay (mm)

a_0, a_1, a_2 = model coefficients

2.3.4.　　Summary

In general, different maintenance interventions are able to treat one or more distress types. In general, the "heavier" an intervention is, the more distress type it can treat. From "light" to "heavy", the maintenance categories are routine maintenance < preventive maintenance < corrective maintenance < rehabilitation < reconstruction. Different interventions may be combined to have better effects. For instance, previous to preventive and corrective maintenance, crack seal and fill is always preferable to seal the old surface. Moreover, the same intervention can be applied twice if necessary. For instance, a chip seal is the application of emulsified asphalt on pavement

surface which is then covered with aggregate, followed by rolling compaction. Chip seals can be applied one on top of another to perform a double bituminous surface treatment in practice.

The treatment capability of the discussed interventions is summarised in Table 2-3. All of the discussed interventions can address visible cracking. Rutting and roughness needs to be solved by corrective maintenance or rehabilitation. Although crack seal and fill has a minor effect on roughness (Odoki and Kerali, 1999), it is designed to treat cracking problems. Seal coats can only improve the functional surface of a pavement and are generally considered to have no effect on rutting or roughness, although limited improvement on roughness can be expected (ISOHDM, 1995). Microsurfacing can have minor effect on rutting but is not intended for addressing the rutting problem and its effect on roughness is insignificant. Rutting and roughness can be improved by thin overlay or overlay. A road with severe rutting and roughness problems can only be addressed by rehabilitation.

Table 2-3 Treatment capability ("+" = more capable; "-" = less or not capable)

	Intervention	Cracking	Rutting	Roughness
Routine maintenance	Crack fill and seal	+	-	-
Preventive maintenance	Seal coats	+	-	-
	Microsurfacing	+	+	+
	Thin overlays	+	+	+
Corrective maintenance	Overlays	+ +	+ +	+
Rehabilitation	Mill and fill	+ + +	+ + +	+ +
	Reconstruction	+ + +	+ + +	+ + +

2.4. Life-cycle cost analysis

2.4.1.   Introduction

LCCA is an assessment tool for evaluating the total monetary value of a product from cradle to grave. The purpose of LCCA is to evaluate the discounted long-term value of a product to support investment decisions. For highways, LCCA was used to sum the total direct and indirect costs to the agency, the road user, as well as the environment over the service life of a pavement (approximately 40 – 50 years) (Huang, 2004), in order to evaluate the total costs and, more importantly, to enhance long-term decision-making.

The LCC is calculated as the Net Present Value (NPV) of the total costs. NPV is the discounted net benefit, which is calculated by subtracting

costs from benefits. NPV for a highway can also be expressed only by costs, when benefits are the same among different alternatives such as (Huang, 2004):

$$\text{NPV} = \text{InitialCost} + \sum_{k=1}^{N} RehabCost_k \left[\frac{1}{(1+i)^{n_k}} \right] \qquad \text{Equation 2-32}$$

where,

N = number of rehabilitations

i = discount rate

n = year of expenditure

The NPV value converts the future cash flow to the present costs, using a discount rate. The Federal Highway Administration (FHWA) reviewed the national pavement design in the United States and recommended the discount rate in current practice of pavement LCCA to be around 3-5%.

Generally, the LCC of a road includes three components and can be expressed as follows:

$$\text{LCC} = \sum_{n=1}^{n} \frac{AC_n + UC_n + EC_n}{(1+i)^{n-1}} \qquad \text{Equation 2-33}$$

where,

AC = agency costs

UC = user costs

EC = environmental costs

i = discount rate

n = year

The LCC sums the discounted annual costs over the life cycle of a pavement, which includes the agency costs, road user costs, as well as environmental costs. The three components are described as follows.

2.4.2.   Agency costs

Agency costs are all costs incurred directly by the agency over the life of the project; this mainly consists of preliminary engineering, contract administration, construction costs, maintenance costs and salvage costs (Huang, 2004). Sometimes, operating costs and labour costs are also included as agency costs (Huang, 2004). Initial construction is a major component of agency costs and it may account for 70 – 90% of the agency costs. Maintenance may cost 10 – 25% of the agency costs. Salvage cost refers to the remaining value of the road at the end of the analysis and is counted as a negative cost. In the end of a pavement's service life, the salvage cost can be negligible (Timm, 2007).

2.4.3. User costs

In highway LCCA, user costs refer to the apparent and hidden costs incurred by the motoring public, including vehicle operating costs (VOC), delay costs and accident costs (Huang, 2004). In the case of construction, maintenance or rehabilitation, additional costs will occur due to the disturbance for the traffic flow, namely work zone (WZ) costs. Road user costs are the summation of three components:

$$UC = VOC + DC + AC \qquad\qquad \text{Equation 2-34}$$

where,

RUC = road user costs

VOC = vehicle operating costs

DC = delay costs

AC = accident costs

2.4.3.1. VOC

VOC usually includes costs associated with fuel, lubrication oil, tyre wear, and vehicle maintenance.

Fuel consumption is different among various vehicles. In general, heavy vehicles consume more fuel compared to passenger cars. For the same type of vehicle, fuel consumption rate is dependent on the state of operation, which can be divided into idling, acceleration, deceleration, and maintaining speed (Zaniewski et al., 1982). Speed can also have an influence on fuel consumption. Commonly, the relation between fuel consumption and vehicle speed follows a "U" shape i.e. fuels consumed more at low or high speed and the most fuel efficient vehicle speed is around 40-60 km/h (Greenwood and Christopher, 2003). Furthermore, fuel consumption can be affected by road conditions, such as slopes and roughness (Greenwood and Christopher, 2003).

The consumption of lubrication oil is associated with vehicle classes, speed, and roughness (Zaniewski et al., 1982). For a specific highway section, where the vehicle classes and speed are certain, the lubrication oil cost can be directly related to road roughness. Zaniewski (1982) related lubrication oil consumption to the road roughness measured by a quarter-car. This model was tested and validated on Indian roads and was found to have good prediction (CRRI, 1985).

Tyre wear can be a major cost of road users and it may cost as much as 23% of the average running costs of a typical truck (Watanatada et al., 1987).

2. LITERATURE REVIEW

Tyre wear is mainly caused by the abrasion between tyre and road surface (Parry et al., 2001). The abrasion will cause greater damage to the tyre when the vehicle is climbing, accelerating, or braking.

Vehicle maintenance costs include maintenance parts costs and labour costs. Maintenance parts costs are associated with maintenance and repair on vehicle parts including engine, transmission, body, chassis, brakes and electrical parts and other parts. Maintenance parts cost is found to be significantly affected by road roughness and vehicle age (Chesher and Harrison, 1987). Labour costs are incurred due to vehicle maintenance and repair.

VOC model

Early VOC models related VOC to road roughness by a simple linear model. An example of it can be described as follows (NCHRP, 1985):

$$Passenger\ car\ VOC = 120.7 + 18.65 IRI \qquad \text{Equation 2-35}$$

$$Articulated\ vehicle\ VOC = 933.2 + 135.88 IRI \qquad \text{Equation 2-36}$$

where,

VOC = vehicle operating costs (US$/1000km)

IRI = international roughness index (m/km)

This model tends to exaggerate increment of VOC with increase in IRI, thus another model is adopted by NCHRP, which is formulated as:

$$Passenger\ car\ VOC = 438.73 + 4.38 IRI + 2.51 IRI^2 \qquad \text{Equation 2-37}$$

$$Large\ truck\ VOC = 2607.73 + 181.67 IRI + 2.3 IRI^2 \qquad \text{Equation 2-38}$$

The parabolic function has been observed to have good prediction under low to high levels of roughness (IRI: 1-10 m/km) (Ockwell, 1999). As VOC is a combination of different cost components which are affected by traffic and vehicle conditions, the factors of the model will vary from place to place. In other words, model calibration may improve the accuracy of the model.

Another way to calculate VOC is to sum up components of VOC, which primarily consist of fuel consumption costs, oil consumption costs, tyre wear costs, maintenance costs as well as depreciation.

Fuel consumption model
The fuel consumption is affected by many factors. Firstly, the fuel consumption is different among various vehicle classes. Heavy vehicles tend to have more powerful engines, thus they are prone to more fuel consumption.

2. LITERATURE REVIEW

Small cars tend to have less power and are commonly designed to be fuel efficient, so the fuel consumption is expected to be comparatively lower. Moreover, it can be expected that fuel efficiency of vehicles will be improved, attributed to the development in automotive technology. Secondly, the fuel consumption is related to vehicle speed. For the same vehicle, the rate of fuel consumption varies during constant speed, acceleration, deceleration, and idling (Zaniewski et al., 1982). Finally, road conditions including curvature, elevation (uphill and downhill), roughness, and skid resistance can also have impact on fuel consumption. Road surface conditions are claimed to have significant impact on fuel economy (Zaniewski, 1989).

Zaniewski et al. (1982) developed a model to calculate fuel consumption, which considered the fuel consumption at different states of vehicle operation (idling, acceleration, deceleration and maintaining constant speed). Factors such as vehicle speed, time and distance for acceleration and deceleration were considered by the model.

An early fuel consumption model correlates fuel consumption to vehicle type, speed, road elevation and roughness. This model has been validated in developing areas including India, Kenya and Caribbean areas. The model can be expressed as follows (Greenwood and Christopher, 2003):

$$FC = a_0 + \frac{a_1}{S} + a_2 S^2 + a_3 RISE + a_4 FALL + a_5 IRI \qquad \text{Equation 2-39}$$

where,

FC = fuel consumption in L/1000 km

S = vehicle speed (km/h)

$RISE, FALL$ = rise or fall of the road (m/km)

$a_0, a_1, a_2, a_3, a_4, a_5$ = Model coefficients

In HDM-3, Fuel consumption is correlated to the tractive power and engine speed as described below (Greenwood and Christopher, 2003):

$$UFC_0 + (a_3 + a_4 RPM)P_{tr} + a_5 P_{tr}^2 \ (P_{tr} \geq 0) \qquad \text{Equation 2-40}$$

$$IFC = UFC_0 + a_6 P_{tr} + a_7 P_{tr}^2 \ (NH_0 \leq P_{tr} \leq 0) \qquad \text{Equation 2-41}$$

$$UFC_0 + a_6 NH_0 + a_7 NH_0^2 \ (P_{tr} < NH_0) \qquad \text{Equation 2-42}$$

$$UFC_0 = a_0 + a_1 RPM + a_2 RPM^2 \qquad \text{Equation 2-43}$$

where,

IFC = the instantaneous fuel consumption (mL/s)

P_{tr}= the tractive power

RPM = the engine speed in revolutions per minute

UFC_0 = the amount of fuel required to maintain engine operation

$a_0, a_1, a_2, a_3, a_4, a_5, a_6, a_7, NH_0$ = model parameters

In this model, two different regimes for engine power are assumed, under which different rates of fuel consumption are expected. The positive power regime $(P_{tr} \geq 0)$ is aimed at modelling fuel consumption when the engine provides traction force, while the negative power regime $(NH_0 \leq P_{tr} \leq 0)$ is used in circumstances when the rolling and aerodynamic resistance exceeds the gravitational acceleration. The fuel consumption is found to be asymptotic to a minimum when the tractive power is smaller than a certain value $(P_{tr} < NH_0)$.

Some development has been made with this HDM-3 fuel consumption model and is adopted by HDM-4:

$$IFC = f(P_{tr}, P_{accs} + P_{eng}) = Max(\alpha, \xi * P_{tot} * (1 + dFuel))$$

<div align="right">Equation 2-44</div>

where,

P_{tr} = required power to overcome traction force (kW)

P_{accs} = required power for engine accessories (kW)

P_{eng} = required power for engine friction (kW)

α = Idling fuel consumption (mL/s)

ξ = engine efficiency (mL/kW/s)

$dFuel$ = excess fuel consumption by congestion

The HDM-4 fuel consumption model becomes highly sophisticated because of a great amount of factors involved. On one side, the complexity of the model reveals comprehensive links between relative factors. And it thus provides better accuracy for prediction of fuel consumption for a specific vehicle. On the other hand, nevertheless, the complexity of the model requires substantial work of model validation to achieve the accuracy, which restricts the wide application of the model.

Lubrication oil consumption
Early studies on lubrication oil consumption on good condition pavement discovered that the lubrication oil consumption is associated with vehicle

classes and speed (Zaniewski et al., 1982). Some other studies associated lubricants consumption with road roughness, which can be expressed as:

$$AOIL = a + b * QI \qquad\qquad \text{Equation 2-45}$$

where,

$AOIL$ = the lubricants consumption

a, b = model coefficient

QI = roughness

QI is a conventional roughness index measured by a quarter-car index scale, which is found to be approximately proportional to IRI. This relation was given by Watanatada (1987):

$$QI = 13 * IRI \qquad\qquad \text{Equation 2-46}$$

Validation of this model has been performed on Indian roads and typical model coefficients found for some classes of vehicles (Institute, 1982).

Tyre wear costs

Tyre wear cost is believed to be a major road user cost and it may comprise 23% of the average running cost of a typical truck (Watanatada et al., 1987). Carcass wear and tread wear are the major modes of tyre wear. The carcass wear is quantified by how many retreads are needed before the tyre is finally scrapped. Tread wear is defined by the fraction of tyre wear per 1000 tyre-km. Thus the tyre wear can be denoted as (Watanatada et al., 1987):

$$CTW = \frac{CN + CRT * NR}{DISTOT} \qquad\qquad \text{Equation 2-47}$$

$$DISTOT = \frac{1}{TWN} + \frac{NR}{TWR} \qquad\qquad \text{Equation 2-48}$$

where,

CTW = tyre wear cost (1000 tyre-km)

CN = the cost of a new tyre

CRT = the cost of a retread

NR = the average number of retreads

$DISTOT$ = the total distance of travel

TWN = wear rate of a new tyre

TWR = wear rate of a retread

2. LITERATURE REVIEW

Another method to calculate the tyre wear is the "cost equivalent" method, which relates the tyre wear cost to the cost of equivalent new tyre. The principle of this method can be expressed as follows (Archondo and Faiz, 1994):

$$Cost\ per\ 1000\ vehicle - km = EQNT\ new\ tyre\ cost \qquad \text{Equation 2-49}$$

Validation of this model has been made using tyre wear and other data from Brazil (Archondo and Faiz, 1994). For passenger cars, this model is expressed with consideration of roughness:

$$EQNT = NT(0.0114 + 0.001781 * IRI) \qquad for\ 0 < IRI \le 15$$

Equation 2-50

$$EQNT = 0.0388 * NT \qquad for\ IRI > 15$$

Equation 2-51

where,

NT = the number of tyres per vehicle

For trucks and buses, the tyre wear is formulated as:

$$EQNT = NT\left(\frac{\frac{(1+0.01NR)TWT}{1+NR}}{VOL} + 0.0027\right) \qquad \text{Equation 2-52}$$

where,

NT = the number of tyres per vehicle

NR = the number of retreads

TWT = the predicted volume of rubber loss $(dm^3/1000\ tyre - km)$

VOL = the average volume of rubber per tyre

Maintenance parts costs

Maintenance parts costs are associated with maintenance and repair of vehicle parts including engine, transmission, body, chassis, brakes and electrical parts. Another part of maintenance parts cost is the labour cost associated with vehicle maintenance and repair and will be mentioned later. Maintenance parts cost is found to be affected by road roughness and vehicle age (Chesher and Harrison, 1987). Maintenance parts costs can be formulated as (Archondo and Faiz, 1994):

$$PC = 100CKM^{KP} * CP_0 * \exp(CP_q * IRI * 13) \qquad for\ IRI \le QIP_0$$

Equation 2-53

$$PC = 100CKM^{KP} * (a_0 + a_1 * IRI * 13) \qquad for\ IRI > QIP_0$$

<div align="right">Equation 2-54</div>

$$a_0 = CP_0 * \exp(CP_q * QIP_0)(1 - CP_q * QIP_0)$$

<div align="right">Equation 2-55</div>

$$a_1 = CP_0 * CP_q * \exp(CP_q * QIP_0)$$

<div align="right">Equation 2-56</div>

where,

CKM = the average age of vehicles measured by distance (km)

KP, CP_0, CP_q = model coefficient

QIP_0 = transitional roughness in IRI (m/km)

For passenger cars and other light vehicles, the relation between maintenance parts costs and road roughness is exponential when the road roughness is considerable small ($IRI \leq QIP_0$), while on a rougher road, the relation becomes linear. The transitional roughness (QIP_0) is adopted to account for the two relations in the calculation. However, for heavy trucks, the relation tends to be linear, regardless of roughness, thus the QIP_0 value is set to 0 for heavy vehicles. Moreover, this model has been validated by study in Brazil (Archondo and Faiz, 1994).

Maintenance labour costs

The labour costs are incurred due to vehicle maintenance and repair. Thus the maintenance parts costs are used to estimate labour costs. Moreover, road roughness has also been considered and the labour costs can be expressed as (Archondo and Faiz, 1994):

$$LH = CL_0 \left(\frac{PC}{100}\right)^{CL_p} * \exp(CL_q * IRI * 13)$$

<div align="right">Equation 2-57</div>

where,

LH = maintenance labour costs

CL_0, CL_p, CL_q = model coefficients

2.4.3.2. Delay costs

Delay costs mainly refer to the increase in travelling time due to detours and rerouting; reduced road capacities thus limited speed; and new facilities which prevent users from gaining travel time benefits (Daniels et al., 1999). Delay costs may be a dominant component of user costs (Zhang et al., 2008). Delay costs are determined by the monetary value of crews' delays as a comparison to a free flow situation. The costs can be controversial because the monetary value delays are believed to be associated with drivers' purposes such as work

2. LITERATURE REVIEW

or leisure. Furthermore, the value of time is typically difficult to define and may vary from place to place. Despite the controversies, multiplication of the delay time and the monetary value of time is widely applied to calculate traffic delay costs.

Delay can occur under many circumstances including over capacity, work zone operation, and accidents. As defined by the Highway Capacity Manual (TRB, 2000), highway capacity refers to the maximum traffic flow rate of a lane of a highway section under specific conditions. The highway capacity can be affected by the geometric, traffic, environmental and control conditions.

A properly designed highway usually takes traffic and traffic growth rate into consideration so that the capacity criteria can be fulfilled throughout the life span of the highway. The highway capacity can be associated with the environment. For instance, in cold areas where the pavement is covered with snow for long periods, vehicle speed may be considerably lower compared to a non-frozen road and thus the highway capacity may be influenced. Therefore, climate change may change the highway capacity, especially with more frequent extreme weather. However, extreme weather events can have greater return period; i.e. such event can be rare. Furthermore, the duration of extreme weather is usually not significant compared to the life span of a highway. Therefore, the impact of climate change on capacity of a highway is generally considered to be insignificant over the road's life cycle and thus delays due to over capacity are neglected from the study. However, over capacity due to WZ operation was considered, because the WZ operation may be affected by climate change.

WZ delay is the additional time for road users to pass a WZ or detour around it. Due to safety reasons, traffic speed needs to be reduced when passing a WZ. Delays occur during the reduction of the speed until vehicles accelerate back to the normal departure speed. Therefore the delays may consist of delays when vehicles decelerate, maintain a lower speed throughout the WZ (moving delay), accelerate to normal departure speed, and queue if there is any (Memmott and Dudek, 1982, Mallela and Sadasivam, 2011). Climate change may result in significant change in maintenance decision-making and thus affect WZ delay. Due to this, the WZ delay will be considered in the study. Furthermore, this study focuses on a road rather than a network of roads, so considerations will not be given to detour, although detour may account for a part of the total delay. Thus this may become a limitation to investigate WZ time delay for urban roads which are commonly inter-connected, where drivers tend to detour to find other alternative routes in case of traffic jams. Nevertheless, detour delay may be a minor issue on interstate highways, where detour options are limited.

2. LITERATURE REVIEW

Delay can occur due to accidents. Climate change, if it can impact accident rate, will have an influence on consequent delays. For instance, when temperature increases in a permafrost area, a frozen pavement surface may thaw and gain friction. Accident rate can be reduced due to this and delays due to accidents can be reduced. In contrast, climate change can also increase accident rate and increase delays. For example, in areas where extreme weather e.g. storms become more frequent, accident rates may increase and thus lead to more delays. Therefore, it is difficult to find a general conclusion regarding the relation between climate change and delays due to accidents. Furthermore, safety measures are taken to reduce accident rate and accidents, although perhaps not eliminated, will be significantly reduced. Therefore, fatal and non-fatal accidents may not be as many as today and the consequent delays can be considerably less. Therefore, delays due to accidents will not be discussed in this study.

Work zone delay

WZ delay, as discussed, may consist of three components, including:

- Deceleration/acceleration delay
- Moving delay
- Queueing delay

Deceleration/acceleration delay refers to the time loss when vehicles reduce normal speed to WZ speed or increase the WZ speed to normal speed, compared to the situation when it maintains normal speed. The deceleration/acceleration can be completed in seconds and is insignificant compared to moving delay and queueing delay. Due to this, the deceleration/acceleration is neglected in this study and moving delay and queueing delay was chosen to represent the WZ delay.

Moving delay

During maintenance activities, vehicles approach the WZ and reduce speed. The moving delay is referred to as the delay when vehicles maintain a lower speed throughout the WZ. The moving delay can be expressed by the following equation (Chien et al., 2002):

$$\text{If } \left(Q(i) + q(i) \right) \leq C_w t_p(i); \quad t_M(i) = \left(\frac{L}{V_w} - \frac{L}{V_a} \right)(Q(i) - q(i))$$

Equation 2-58

$$\text{If } \left(Q(i) + q(i) \right) \geq C_w t_p(i); \quad t_M(i) = \left(\frac{L}{V_w} - \frac{L}{V_a} \right) C_w t_p(i)$$

Equation 2-59

where,

$Q(i)$ = Flow rate during period i

$q(i)$ = Accumulated queue length from period i $-$ 1 (veh) ($q(i) =$ $\sum_{j=k}^{i-1}(Q(i) - C_w t_p(j))$ for i $> k$)

C_w = Roadway WZ capacity

$t_p(i)$ = Duration of period i

$t_M(i)$ = Moving delay in period i

V_w = WZ speed

V_a = Average approaching speed

L = WZ Length

Queuing delay

During maintenance, one or several lanes sometimes need(s) to be closed and thus induce a bottleneck for the highway. The bottleneck can limit the capacity of the road and lead to or aggravate a queue during maintenance operation. Queuing delay is believed to make a significant contribution to the passengers' total delay. For instance, queuing delay can account for more than 90% of a motorist's total travel time under extreme circumstance (Mannering et al., 2009).

In general, two methods exist to calculate the queue delay. The first one is deterministic queuing theory, which has been used for decades in practice. The second one is the shock wave method, which assumes the traffic flow behaves analogous to fluid flow. The shock wave model is based on the traffic density and velocity of individual vehicles (Richards, 1956). Nevertheless, the traffic density is sometimes difficult to measure, which limits the utilisation of it (Chien et al., 2002). Based on the deterministic character of the traffic modelling approach, deterministic queueing theory can be applied to calculate queueing delay. To be more specific, a D/D/1 discipline was used, denoting a deterministic arrival pattern, a deterministic departure pattern with only one departing channel. The D/D/1 queue delay normally can be solved by a graphical solution. The queuing delay can be expressed by the following equation (Chien et al., 2002):

$$Delay = \frac{t_1^2(C - C_w)(Q - C_w)}{2(C - Q)} \qquad \text{Equation 2-60}$$

where,

Q = Traffic flow rate

C = Roadway capacity under normal operation

2. LITERATURE REVIEW

C_w = Roadway capacity under WZ

t_1^2 = Maintenance duration
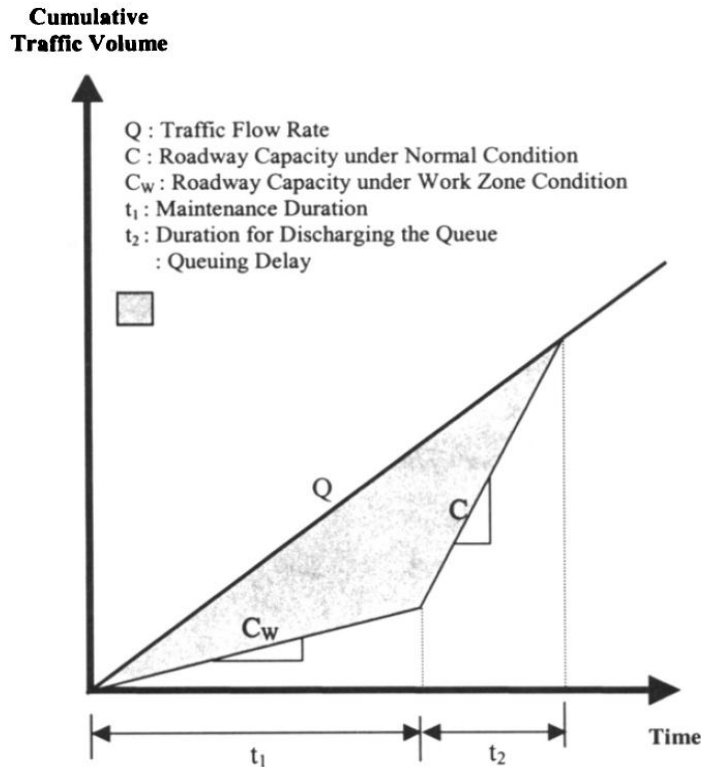
Figure 2-18 Deterministic graphic solution for queuing delay (Chien et al., 2002)

The total vehicle delay (veh*h) can be indicated by the shadow area in Figure 2-18. The queue started to accumulate at time 0, when the traffic demand exceeded the capacity of the WZ. The maximum queue length (veh) occurred at time t_1, when the maintenance work finished and the closed lane(s) opened to traffic again. After t_2, the queue dissipated and the traffic operated normally again.

Work zone capacity

During the operation of a work zone, when one or several lanes need(s) to be closed, the capacity will be reduced as a consequence. The WZ capacity is generally considered as the traffic flow over at which interruption to existing flow (i.e. congestion) occurs in a WZ.

WZ capacity can be obtained by in-situ measurements, typically in two ways (Borchardt et al., 2009). The first one is applied by measuring the largest traffic volume through the work zone, practically accepted as the peak 15-minute traffic flow rate. Nevertheless, this method is believed to be unsustainable from a long-term perspective. The other method is based on measurement of traffic volume in a work zone during congestion. In practise,

the identification methods of WZ capacity differ between different States in the U.S. Although influenced by many factors, the WZ capacity can be affected primarily by WZ configuration, work activity, roadway conditions and environmental conditions (Borchardt et al., 2009). WZ configuration may refer to WZ characterisations such as the number of closure lanes, the length of the WZ and the WZ layout. The number of closure lanes is believed to have significant impact on WZ capacity; thus it is considered in many WZ capacity prediction models (Kim et al., 2000). WZ intensity, which is another significant factor, can have an influence on vehicle speed and thus affects WZ capacity (Chitturi et al., 2008). Other WZ activity characterisation such as work time and intensity can also have impact on the WZ capacity (Borchardt et al., 2009). Roadway conditions may include roadway elevation, pavement conditions and lane width. It seems likely that the WZ speed will be higher on a flatter, better conditioned and wider pavement, and thus a higher capacity can be expected. Furthermore, environmental hazards such as heavy rainfall can restrict the WZ capacity. Many models have been developed to predict the WZ capacity and can be found in literature (Abrams and Wang, 1981, Memmott and Dudek, 1982, Karammes and Lopez, 1992, TRB, 2000, Kim et al., 2000). Most of these models are regression models that can be calibrated to local situations. The Memmott and Dudek (1982) model is utilised in this study, due to the low requirements for model coefficients. The WZ capacity can be expressed by the following formula:

$$C = a - b(CERF)$$
<div align="right">Equation 2-61</div>

where,

C = estimated WZ capacity

$CERF$ = risk factor

a, b = coefficients (see Table A-34 in Appendix)

As a disadvantage, many relevant factors are not considered in this model except for the open/closed lanes. However, this model was proved to have decent prediction for some freeways in North Carolina and Indiana (Kim et al., 2000), which indicated one of the most influential parameters i.e. number of closure lanes can properly reflect the WZ capacity to some degree.

2.4.3.3. *Accident costs*

Accident costs are costs incurred by traffic accidents, including damage to vehicles, damage to public or private properties as well as accident injuries. The accident rate is related to the pavement conditions such as crossings, traffic sight distance, skidding and aquaplaning (Ihs and Sjögren, 2003, Parry and Viner, 2005). Existing studies on accident costs are scarce and only a few

accident costs models are available. Accident costs are calculated as the cost sum of three components: fatal accident, non-fatal injury accidents and property damage (Daniels et al., 1999). Fatal costs may include medical treatment costs before death, lost labour, and costs from the suffering of relatives and friends of the casualties. Non-fatal injuries can be defined by medical treatment costs, for instance treatment costs and hospital stay costs. Property damage, compared to the fatal or non-fatal costs, is more objective and can be defined by the costs due to the damage of vehicles and drivers' and passengers' belongings.

Fatal and non-fatal accident costs can be subjective and are based or partially based on a "willingness to pay" basis. The "willingness to pay" approach is subjective and thus the costs can vary significantly from person to person. Therefore, the accident costs are not considered, although climate change can affect accident costs in both a direct and indirect way. Directly, climate change, especially extreme weather, e.g. extreme precipitation, may reduce the visibility, reduce skid resistance, and even lead to aquaplaning, and thus lead to a higher accident rate. However, such impact may not always be negative. For instance, drivers tend to reduce speed in heavy rainfall. Therefore, fatal accident rates may be reduced. Indirectly, accident rate can be affected by additional pavement deterioration and consequent work zone operations. However, little research has been performed to relate accident costs to climate change up to date.

2.4.4.　Environmental costs

Environmental costs refer to the cost caused by environmental hazards such as emissions of GHGs, toxic gases and noise, through the life-cycle of a pavement. Environmental costs exist in the stage of raw material acquisition, construction, maintenance, traffic congestion, and end-of-life recycling. Environmental hazard e.g. noise has been considered more seriously as road users today put more emphasis on driving comfort and thus noise is undesirable. Noise reduction technology has been applied on some roads to reduce the noise and can benefit both drivers and surrounding residents (Parry and Roe, 2000). However, some environmental costs such as noise are difficult to be quantified in monetary value.

Measures have been taken to assess the environmental costs of road projects. A popular method named Life-Cycle Assessment (LCA) has been widely applied to compare environmental footprints of alternative road projects, construction materials, and maintenance interventions (Huang and Parry, 2014, Giustozzi et al., 2012). The LCA methodology, distinguished from LCCA, assesses the emissions of a product rather than the monetary costs. Using LCA, emissions of GHGs and toxic gasses or a normalised Global Warming Potential (GWP) value can be evaluated during material acquisition, transport,

and the manufacturing process of the product. Due to the extent of this study, the environmental costs were not discussed. Furthermore, the environmental costs only can account for a very small percentage in the whole life-cycle of a road (Zhang et al., 2008); thus it is considered to be insignificant.

2. LITERATURE REVIEW

3. METHODOLOGY

3.1. Introduction

The methodology of this study focused on developing a detailed framework upgraded from the overall framework as described in Figure 1-1. The detailed framework included four tasks as the overall framework including investigation of climate change, pavement performance modelling, pavement maintenance effects, and maintenance optimisation involved LCCA. Taking climate change as a variant, the developed framework can provide differences in pavement performance, maintenance decision-making as well as LCC as outputs. The developed framework identifies the key elements of each task and discovers the connection between tasks. Furthermore, case studies on six highway sections were used to derive the detailed framework and demonstrate its applications.

3.2. Detailed framework

The detailed framework is presented in Figure 3-1. The framework starts with projections of climate change by IPCC's MAGICC/SCENGEN programme (see later in Section 3.4.2), which is considered to be the most widely used and authoritative tool for the projection of climate change. This study focused on the direct impact of climate change on pavements with considerations over a long-term, i.e. it is suspected that changes in climate may result in significant changes on pavement deterioration, maintenance decision-making, or LCC. SRES were utilised by IPCC to account for major uncertainties in the prediction of climate change which corresponded to the future development pathway of society. Furthermore, high, medium, and low emission scenarios were used in the climate change projections.

3. METHODOLOGY
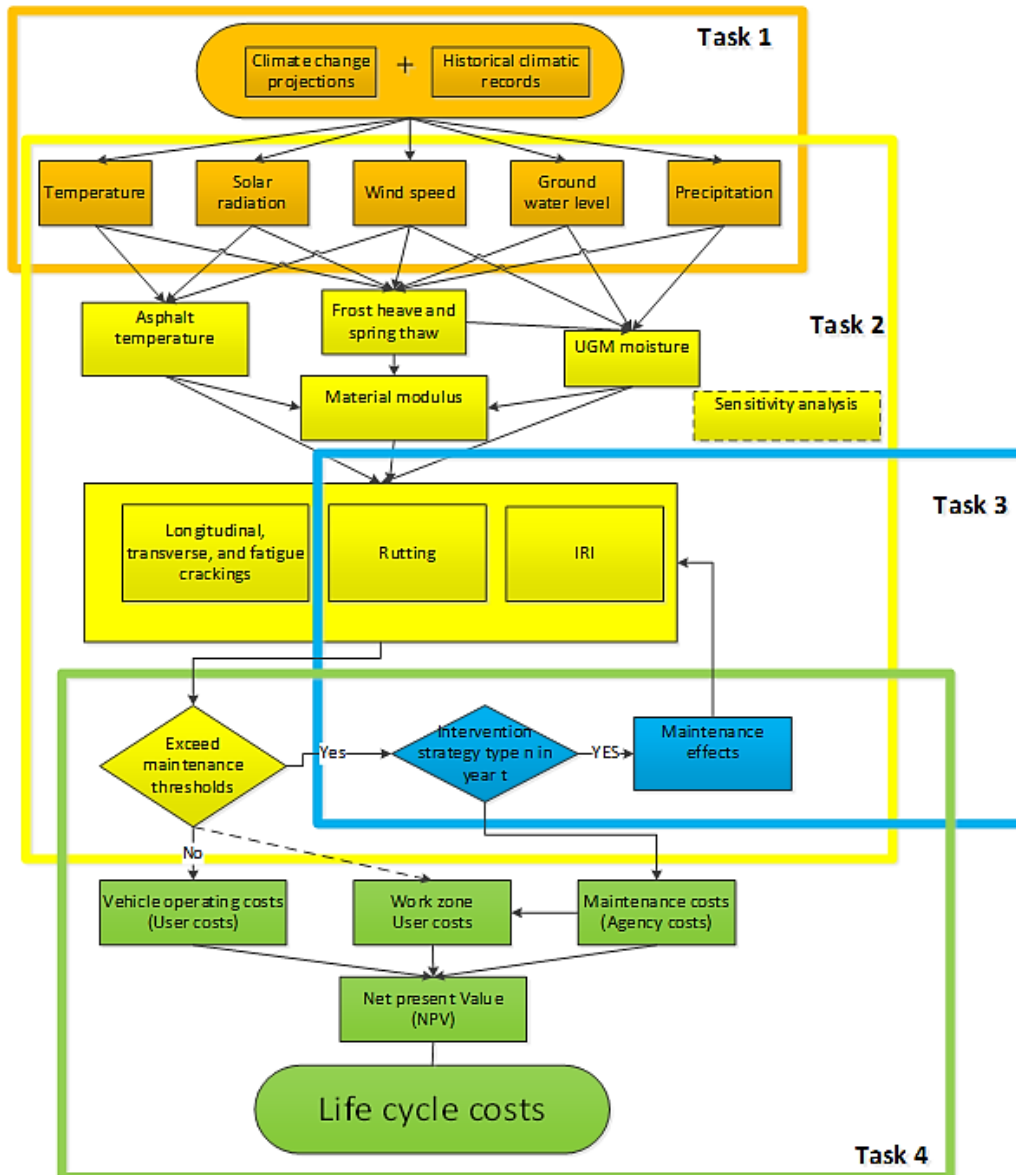
Figure 3-1 Detailed framework

The performance of flexible pavements is affected by environmental factors, especially temperature and moisture. Increases in future temperature, precipitation, and sea water level can be predicted by MAGICC/SCENGEN, and thus the environmental factors of pavements in the future can be estimated. The prediction is based on climate predictions on the average increase/decrease in temperature, precipitation, and sea level. However, other environmental parameters that may influence pavement deterioration including wind speed, solar radiation, and seasonal temperature variations should not be neglected (Crispino and Nicolosi, 2001). To achieve this, a sensitivity analysis (see later in Section 3.5.1) of pavement performance due to climatic factors needs to be performed. The aim of the sensitivity analysis is to identify the importance of various climatic factors and manage uncertainties. The sensitivity was performed for the six studied cases (see later in Section 3.3). Based on the sensitivity analysis, prediction of pavement performance using MEPDG can be

managed with reduced uncertainties. The MEPDG can take combinations of climate change predictions and historical climate (see later in Section 3.4) into consideration using EICM (see Section 2.2.5.3). This advantage reinforces the adequacy of the MEPDG programme. As an environmental sensitive structure, a flexible pavement can be most crucially impacted by temperature and moisture. High temperature can reduce the stiffness and rutting resistance of asphalt layers and excess/lack of moisture can reduce the stiffness and rutting resistance of unbound granular materials. Combination effects of temperature and moisture can be seen during the frost-thaw period and can contribute to significant amounts of distress.

The additional pavement deterioration induced by climate change may trigger maintenance significantly earlier, therefore future maintenance and the consequent LCC can be affected by climate change. Changes in pavement service lives were calculated (see Section 2.2.6 and 3.5.2). To investigate the impact of climate change on maintenance in the future, a section-based maintenance optimisation algorithm was created to represent the decision-making process in the future (see later in Section 3.7.3). The algorithm aimed to arrange maintenance interventions with minimised total LCC including agency and user costs while keep their balance in order to achieve fair road economy (see later in Figure 3-17). LCC components that are related to climate change were selected and described in Section 3.7.2. Three real road sections in Virginia were used to evaluate the impact of climate change on pavement maintenance and its consequent LCC. Firstly, the maintenance effects of the most common interventions in Virginia including thin overlay, thick overlay, and mill & fill on IRI and rutting are considered. Typical linear models to predict immediate maintenance effects on IRI and rutting were validated using Virginia PMS data (described in Section 3.6). Secondly, three maintenance decision-making alternatives were used to represent different maintenance concepts including do nothing, strict trigger, and opimised maintenance. The impact of climate change on the maintenance and LCC were compared under each alternative. Eventually, differences in LCC caused by climate change can be derived.

Maintenance decision-making is dependent on pavement performance level and costs. More frequent or "heavier" interventions can incur more agency costs but can keep pavement performance at a better level. User costs may be reduced significantly, as user costs such as VOC can be directly related to pavement performance level i.e. IRI. Task 3 and 4 are combined to find the optimised intervention strategies.

3.3. Introduction to Case studies

Case studies were performed for flexible pavements from different climatic regions in the U.S. to demonstrate the methodology of this study. The case

studies were performed for American highways because of the availability of a suitable performance prediction tool (i.e. MEPDG) and maintenance data. In total, six sections were selected for the case study, including:

- 3 created sections (Test section 01 (SecT01), Test Section 02 (SecT02), and Test section 03 (SecT03)), assumed to be from Seattle, WA, Minneapolis, MN, and Richmond, VA respectively. The sections are from regions of high risk to assess the impact of climate change proposed by Meyer et al. (2013) (described in 2.1.4).
- 3 real sections (Section 01 (Sec01), Section 02 (Sec02), and Section 03 (Sec03)) from Virginia.

The three created sections will be used in the earlier phase of the methodology to test the sensitivity of pavement performance to climatic factors. Typical pavement structures with typical traffic volumes were used in the evaluation and thus study on these sections can reflect the general situation. Furthermore, the regions where these sections are selected from are the nationally "at risk" regions for the study of the impact of climate change on pavements, thus case studies on these three sections can reflect the national worst case (SecT01 and SecT02) or average (SecT03) situations on how climate change will influence performance and service life of flexible pavements.

The three real sections will be used to test the whole framework. All of them were selected from climate zone 5 (Figure 2-5), where a medium change in climate will occur in the future. Therefore, the study on these cases represents a nationally average situation on how climate change can affect performance, maintenance planning, and subsequent costs of flexible pavements. Moreover, it is vital to this study that data and information on distress measurements, pavement material costs and treatment costs are available in this region.

3.3.1. SecT01, SecT02, and SecT03

These sections were created based on investigation on the typical pavements in the LTPP database from the three regions. The traffic level on the three created sections was assumed to be 3800 AADTT each, which is a typical heavy traffic volume on interstate highways according to the LTPP. The same amount of traffic was considered for all the three sections to make comparison easier. The structure and material of the roads is shown in Table 3-1:

3. METHODOLOGY

Table 3-1 Structure and material of sections SecT01. SecT02, and SecT03
(Qiao et al., 2013b)

SecT01				
Layer	Type	Thickness (in)	Specifications	MEPDG input level
1	Asphalt concrete	4	PG grade: 52-10	3
2	Asphalt concrete	5	PG grade: 52-10	3
3	Granular base	8	A-3, Resilient modulus (psi): 24500	3
4	Subgrade	-	A-7-6, Resilient modulus (psi): 8000	3
SecT02				3
Layer	Type	Thickness (in)	Specifications	3
1	Asphalt concrete	6	PG grade: 52-34	3
2	Asphalt concrete	6	PG grade: 52-34	3
3	Granular base	12	A-1-a, Resilient modulus (psi): 42000	3
4	Subgrade	-	A-7-6, Resilient modulus (psi): 11500	3
SecT03				3
Layer	Type	Thickness (in)	Specifications	3
1	Asphalt concrete	4.5	PG grade: 70-22	3
2	Asphalt concrete	3	PG grade: 70-22	3
3	Granular base	5	A-1-a, Resilient modulus (psi): 42000	3
4	Subbase	6	A-7-6, Resilient modulus (psi): 12000	3
5	Subgrade	-	A-7-6, Resilient modulus (psi): 8000	3

(1 inch = 25.4 mm; 1 psi = 6.89 kPa)

The subgrade of the three sections was categorised as medium quality soil. A strong subgrade may give good support for upper layers, which has less deterioration and vice versa. Therefore, a medium quality subgrade can better

represent the average cases. The choice of PG grade was made according to the most frequently used design PG grade from the states.

The structure of the three sections was similar, which included two asphalt layers, and a granular base layer. SecT03 had an additional subbase layer. The subgrade was chosen as a clay material with low resilient modulus for the three sections because pavements with weaker subgrade have worse ability to spread the traffic load and are thus prone to more deterioration. It is more interesting to see the impact of climate change on a road with more deterioration rather than a perfect pavement, in order to compare the pavement performance with or without the climate change. The thickness of the pavements ranged from 43 cm to 60 cm, including asphalt layer, granular base, and subbase. The binder PG grade was chosen as typical PG grade from the state. Furthermore, aggregate grading was set to be default.

3.3.2. Sec01, Sec02, and Sec03

The three road sections in Virginia (see Figure 3-2 and Figure 3-3) were used to test the whole framework of the methodology because of the abundant pavement management data to find specific information about the pavements and validate maintenance effects, especially in three districts that are considered to have the most frequent maintenance activities including:

- Bristol
- Salem
- Richmond
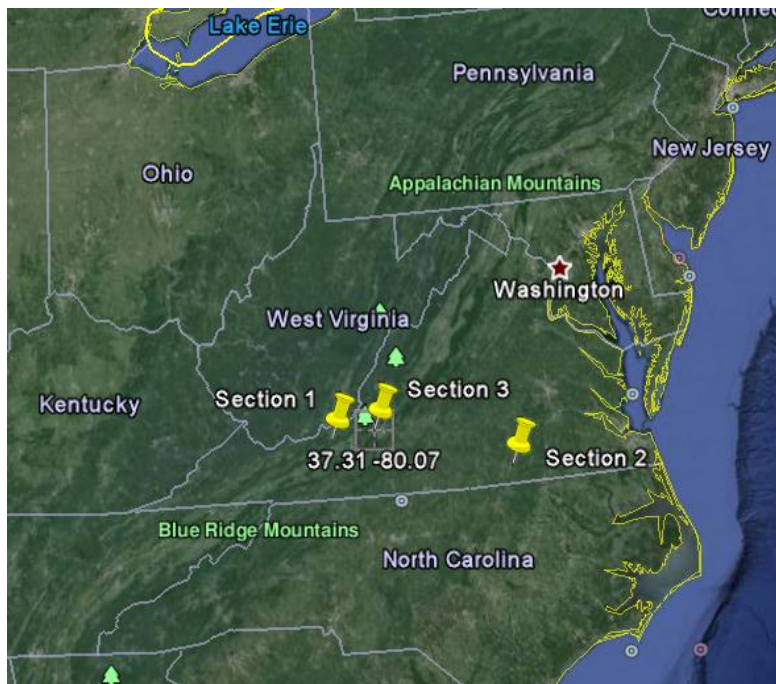
Figure 3-2 Three sections in Virginia for case studies

3. METHODOLOGY

Figure 3-3 Google street view of Sec01, Sec02 and Sec03

The google street views of the sections or nearby (exact location for Sec03 not available) can be seen on Figure 3-3. The three sections are just below the top edge of the climate zone 5 on Figure 2-5. Due to the particular location, the climate for the sections may also be under the influence of climate zone 4.

Study for Virginia can be representative for the national average situation in terms of climate change. The three sections were selected from the PMS database of the Virginia Department of Transportation (VDOT), including a primary road section (Sec01), and two interstate road sections (Sec02 and Sec03). The selection was based on a low (Sec01), medium (Sec02), and high traffic (Sec03) level in Virginia, judging from the investigated sections' AADTT in 2010 (See Figure 3-5). The structure and material for the three sections are as follows:

Table 3-2 Structure and material of sections Sec01, Sec02, and Sec03 (1 in = 25.4 mm)

Sec01				
Layer	Type	Thickness (in)	Specifications	MEPDG input level
1	Asphalt layer	1.5	SM-2A (PG grade: 64-22)	3
2	Base layer	4	B-3 (PG grade: 64-22)	3
3	Subbase	10	No. 21A (A-1-a), Resilient modulus: 29000 psi	3
4	Subgrade	-	A-3	1
Sec02				
Number	Layer and material	Thickness (in)	Specifications	MEPDG input level
1	Asphalt layer	1.5	SM-12.5D	1
2	Asphalt base	2	BM-25.0	1
3	Subbase	12	A-3, Resilient modulus:24500 psi	3

Number	Layer and material	Thickness (in)	Specifications	MEPDG input level
4	Subgrade	-	A-3, Resilient modulus:24500 psi	3
Sec03				
Number	Layer and material	Thickness (in)	Specifications	MEPDG input level
1	Asphalt layer	1.5	SMA-12.5E	1
2	Asphalt layer	1.4	SM-12.5D	1
3	Asphalt layer	1.2	CB-1 or H-2 (PG grade: 70-22)	3
4	Base layer	7.5	H-3 (3) (PG grade: 70-22)	3
5	Subbase	6	No. 21, Resilient modulus: 19215 psi	3
6	Subgrade	-	Select Unstabilised material, Resilient modulus: 39000 psi	3

(material codes see VDOT Road and Bridge Specifications (2002), 1 psi = 6.89 kPa)

The Virginia PMS recorded pavements' history over a long period. The material specification and code used earlier may be different compared to the current ones. The properties of the old classified materials were "translated" to current materials by experience. The decision on the MEPDG input level depended on the availability of testing results on similar materials, which can be found in VDOT and VTRC (Virginia Transportation Research Council) reports. These included testing for dynamic modulus and creep compliance for asphalt mixtures (Prowell, 1999, Apeagyei and Diefenderfer, 2011) and resilient modulus testing for unbound granular materials (Hossain, 2010).

3.3.3. Traffic condition

Three parts of Virginia PMS data was focused on, which are construction history, yearly distress rating, and traffic volume. The structure and materials of the three real road sections were picked up from the construction history. The yearly distress rating is used for validation of maintenance effect models. Traffic volume information is used for choice of sections for analysis and pavement performance modelling.
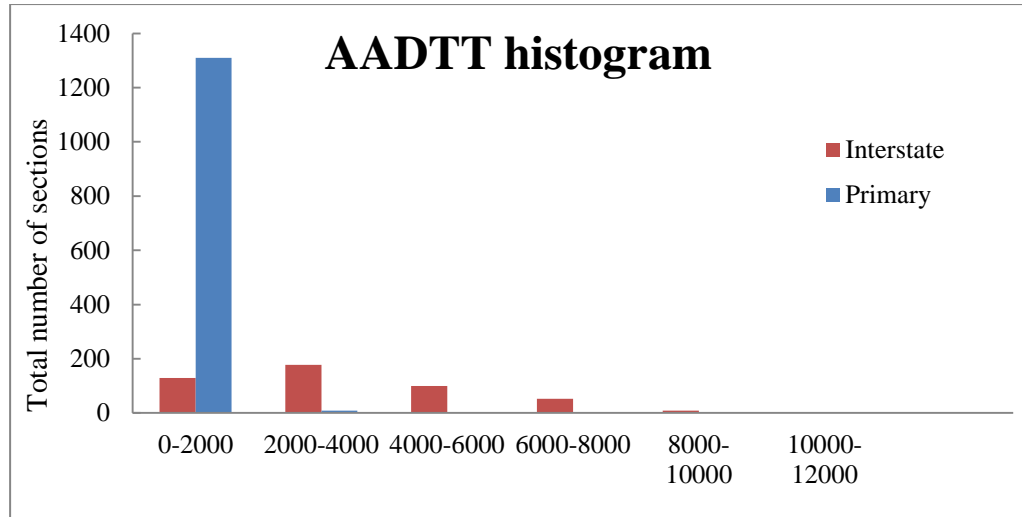
Figure 3-4 A histogram of sections' AADTT for interstate and primary roads in Bristol, Salem, and Richmond

Traffic information (AADTT) in 2010 of 1337 sections of primary sections and 569 interstate sections from the three districts was investigated. It can be observed from Figure 3-4 that the heavy truck volume has a wider spectrum from a low level (< 2000 AADTT) to a high level (>10000 AADTT). The heavy truck volume for primary roads is generally less than 2000 AADTT.
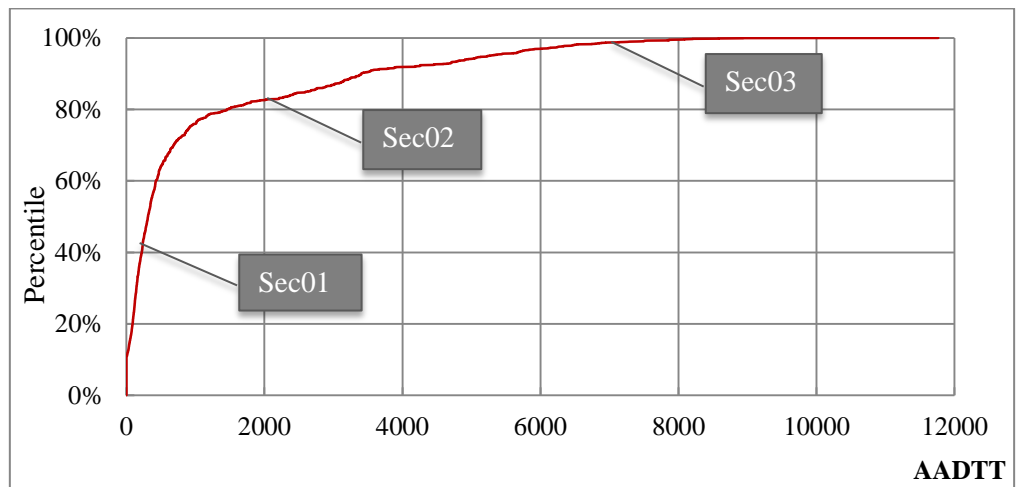
Figure 3-5 Sections' AADTT accumulative percentage in Districts of Bristol, Salem, and Richmond in 2010

Figure 3-5 shows the heavy traffic volume on the primary and interstate roads from the three districts in 2010 in terms of AADTT by the accumulative percentage from the three districts. According to statistics (see Figure 3-5), approximately 43% road sections from the three districts have lower truck traffic volume compared to Sec01, and thus Sec01 can represent the median traffic volume for the three districts. Approximately 83% of road sections have less than 2017 AADTT, which means Sec02 can be an example of a high traffic volume road. Only approximately 1% of sections have more traffic than

7119 AADTT and Sec03 can be representative for an extreme busy road. The sections' basic information can be found in Table 3-3.

The choice of the three districts, as described before, was made due to the fact that frequent maintenance activities were known to be performed in the districts. It is known that frequent maintenance is typically operated on pavements with worse conditions, e.g. roads with higher heavy traffic volume or thinner structure thickness, therefore, the low/medium/high volume judged by the three districts is likely to be greater than Virginia average low/medium/high volume. Meanwhile, the design of pavements including structure and materials is related to the volume of heavy traffic and thus the pavements designed for the three locations may be thicker or use better materials than Virginia's average.

Table 3-3 General information of Sec01, Sec02, and Sec03

	Sec01	Sec02	Sec03
Route ID	SR00100NB*	IS00085NB	IS00081NB
Classification	Primary	Interstate	Interstate
District	Salem	Richmond	Salem
Begin Mile	41.04	15.68	92.37
End Mile	41.49	19.52	94.04
Length (km)	0.16	1.23	1.23 (assumed; GPS coordinates not available)
Lane width (m)	3	3.5	3.4
Approximate elevation (feet)	1860 (567 m)	370 (113 m)	1150 (351 m)
Total lane number each way	2	2	2
AADTT	241	2017	7119
Truck percentage	5%	10%	16.5%

*NB = North bound

3.4. Investigation of climate change

3.4.1. Historical climatic data

Sec02 (Latitude: 36.76, longitude: -78.09) locates in the District of Richmond in southern Virginia with a general humid subtropical climate. The elevation of the section is approximately 378 feet above sea level. The section's climatic information was generated using EICM. The EICM interpolated the weather data from the vicinity of the given location which was calculated inversely weighted by distance (AASHTO, 2009). The climate was generated with from six nearby climate stations as in Figure 3-6.

3. METHODOLOGY

☑ 45.9 miles ROANOKE RAPIDS, NC - HALIFAX COUNTY AIRPORT Lat. 36.26 Lon. -77.43 Ele. 251 Months: 88 (M1)

☑ 58.1 miles RICHMOND, VA - RICHMOND INTL AIRPORT Lat. 37.31 Lon. -77.19 Ele. 167 Months: 116 (C)

☑ 62.5 miles WAKEFIELD, VA - WAKEFIELD MUNICIPAL ARPT Lat. 36.59 Lon. -77.01 Ele. 111 Months: 100 (C)

☑ 63.0 miles LYNCHBURG, VA - LNBRG RGNL/P. GLENN FLD AP Lat. 37.2 Lon. -79.13 Ele. 1000 Months: 115 (M1)

☑ 63.2 miles RICHMOND/ASHLAND, VA - HANOVER CO MUNICIPAL ARPT Lat. 37.43 Lon. -77.26 Ele. 207 Months: 116 (C)

☑ 72.0 miles DANVILLE, VA - DANVILLE REGIONAL AIRPORT Lat. 36.34 Lon. -79.2 Ele. 584 Months: 67 (C)

Figure 3-6 Climatic stations used to interpolate historical climatic of Sec02 (distance, location, airport, latitude, longitude, elevation in feet and record duration)

Due to the inversely weighted distance factor, the interpolated weather condition was more influenced by closer weather stations. Arguably, the climate of a location may be highly influenced by the altitude, which was probably underestimated during the interpolation. It is a common rule of thumb that temperature drops approximately 1 ℃ as the altitude increases 100 meters on the surface of the earth. Therefore, change in the elevation of the interpolated locations may play a significant role in determination of the climate. Certainly, the reversed distance factor tends to interpolate weather more similar to the closest station(s), which, in a way, means that the interpolation is more influenced by the altitude of the nearest station(s). This can be true for flatlands but the accuracy needs to be discussed for hilly areas. The vicinity of Sec02 is flat and thus it can be generally considered that the interpolation was not biased because of the elevation.

Furthermore, the climate of a location can also be affected by the landscape and vegetation cover. For instance, the surface temperature of a pavement constructed in the shadow may be significantly lower compared to the same pavement under sunshine. Moreover, vegetation may create shadow and increase moisture in the air due to transpiration. Therefore, the general assumption for a pavement under interpolated weather conditions is a pavement under direct exposure to sunlight.
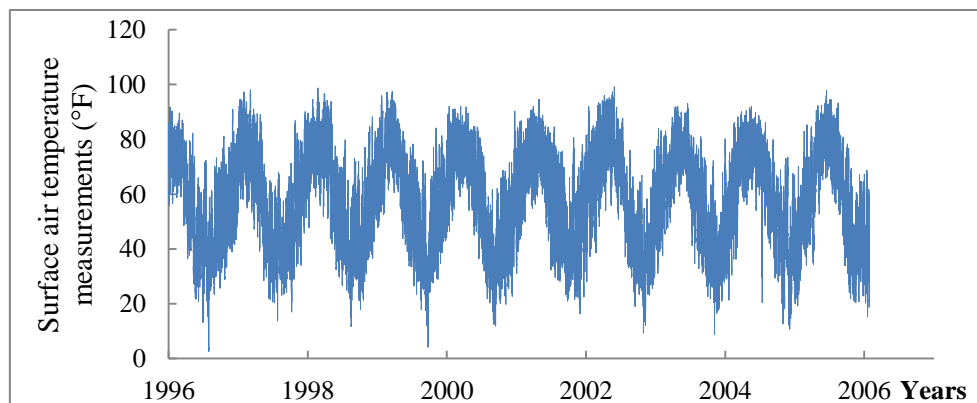
Figure 3-7 Hourly surface air temperatures in Fahrenheit between 0:00 1st Jul 1996 and 23:00 28th Feb 2006 (NCHRP, 2004)

87

3. METHODOLOGY

The approximate 10-year period for the measured temperature is a bit short to observe the increase in temperature that occurred during this period for all sections. The measurement approximates to a sine function with peaks in summers and valleys in winters.
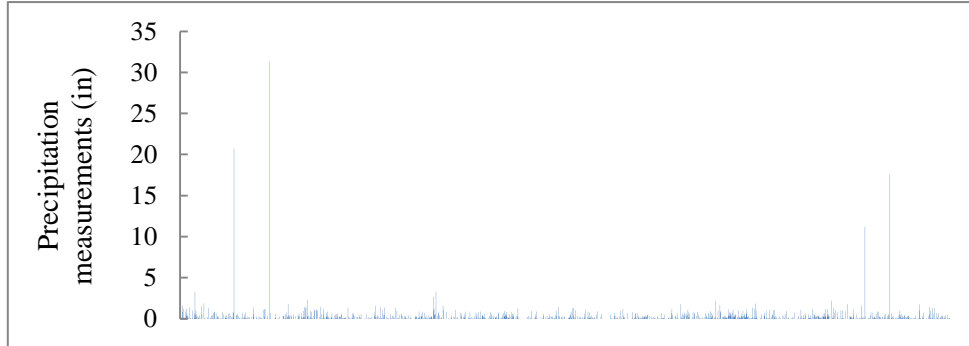
Figure 3-8 Hourly precipitation between 0:00 1st Jul 1996 and 23:00 28th Feb 2006 (1 in = 24.5 mm)

In Figure 3-8, some of the peak hourly precipitation values seem to be too high and unrealistic. This is because daily precipitation was improperly used in nearby stations instead of hourly precipitation. However, this is unlikely to have an effect on the result because the pavement performance prediction in MEPDG uses an incremental method, which means the climate condition is monthly based instead of hourly based. Under the same mechanism, errors in the measurement of climatic factors can be smoothed by adopting the average values. The incremental method tends to neglect extreme weather events e.g. hot extremes and maximum precipitation, and thus underestimates distress, which is sensitive to extreme environmental conditions.

The interpolated weather including hourly surface air temperature and precipitation during a period of approximately 10 years was presented in Figure 3-7 and Figure 3-8. The average/total values of the interpolated hourly climatic factors are presented in Table 3-4.

Table 3-4 Interpolated present climate condition of Sec02

Average annual surface air temperature ($°F$)	Average annual precipitation (in)	Average annual wind speed (mph)	Average annual sunshine percentage (%)	Average annual groundwater level (feet below ground surface)
57.81	52.57	4.48	62.31	21.5

(57.81 $°F$ = 14.3 $°C$, 52.57 in = 1.3 m, 4.48 mph = 7.2 km/h, and 21.5 feet = 6.6 m)

The average annual groundwater level is obtained from the average of historical measurements of groundwater depth of the closest borehole. The groundwater information was obtained from the United States Geological Survey (USGS) online groundwater database (USGS, 2014).

3.4.2. Climate change predictions

With assumptions on different levels of GHG emissions, the future climate change can be projected in terms of change in the surface air temperature, precipitation, and sea level rise. MAGICC was used to give climate change prediction results including change in average surface air temperature and the sea level on a global base and SCENGEN was used to provide this information on a local base. The emission scenario discussed included (also see Table 2-1):

- 2100 high emission scenario (A1FI)
- 2100 medium emission scenario (A1B)
- 2100 low emission scenario (B1)
- 2050 high emission scenario (A1FI)
- 2050 medium emission scenario (A1B)
- 2050 low emission scenario (B1)

The 2100 high emission scenario was used to represent the maximum extent of the climate change according to the current predictability within a hundred years. This scenario can represent an upper boundary of the change in pavement performance and road economy in 2100. The 2050 scenarios represent the situation in the near future and explore, if flexible pavements of traditional design are constructed and operated under the climate of 2050, what will be the change in pavement performance, maintenance planning, and road economy as a consequence. The high and low emission scenarios of 2050 form an upper and lower boundary of the 2050 climate change and the medium emission scenario is believed to be the most likely case.

Local climate change prediction for SecT01, SecT02, and SecT03 was made under the medium emission scenario of 2050 for Seattle (WA), Minneapolis (MN), and Richmond (VA). Local climate change prediction for Sec01, Sec02, and Sec03 was made under scenario A1FI, A1B, and B1 in 2050 and 2100. Sec01 and Sec03 are within the same climate change pixel (see Figure A-14 to Figure A-25) and thus the prediction results in terms of temperature, precipitation, and sea level are the same. A summary of the prediction results for all studied cases can be found in Table 3-5 (also see Figure A-14 to Figure A-25):

Table 3-5 Global and local climate prediction for the three sections

Scenario	SecT01		SecT02		SecT03		Global
2050 A1B	T (℃)	P (%)	T (℃)	P (%)	T (℃)	P (%)	Sea level (cm)
	1.79	-1.2	2.58	5.3	1.74	4.5	15

Scenario		Sec01		Sec02		Sec03		Global	
		T (℃)	P (%)	T (℃)	P (%)	T (℃)	P (%)	T (℃)	Sea level (cm)
2050	A1FI	2.52	7.0	2.47	6.7	2.52	7.0	1.8	15
	A1B	2.14	5.9	2.10	5.7	2.14	5.9	1.6	13
	B1	1.89	5.2	1.61	5.0	1.89	5.2	1.4	5
2100	A1FI	5.96	16.5	5.85	15.8	5.96	16.5	4.4	46
	A1B	4.00	11.1	3.92	10.6	4.00	11.1	3.0	35
	B1	3.04	8.4	2.98	8.0	3.04	8.4	2.2	30

T = increase in temperature; P = increase/decrease in precipitation

The purpose of including SecT01, SecT02, and SecT03 is to have a general idea of the sensitivity of pavement performance to climatic factors in the three high risk regions. Therefore, only the medium emission scenario in 2050 was used to represent the climate change prediction that is likely to occur. For Sec01, Sec02, and Sec03, scenario A1FI, A1B, and B1 in 2050 and 2100 were selected to have a detailed control on the climatic factors so that the impact on pavement performance due to the variations in the climatic factors can be revealed with more details.

A general observation from the climate change prediction is that the temperature increase in all sections is greater than the global average. The precipitation will increase in all sections except for SecT01 (State of Washington), where less precipitation is expected in 2050.

3.4.3. Combination: historical climatic data and climate change projections

3.4.3.1. Temperature

The increase in temperature in each decade was not significant enough for the change to be revealed by the historical hourly measurement graphs (see Figure 3-7). From the climate change prediction, the maximum increase in temperature in a decade was found to be less than 0.5 ℃ even under the high emission scenario (See Figure 3-9). Such difference in temperature is usually not considered to be significant for the performance of a flexible pavement,

especially when hot extremes were not considered. Therefore, the climate models in MEPDG assume constant climate, which uses the 10-year climatic measurements to represent the climate conditions for each decade of the design life of the pavement. To some extent, the MEPDG result is about the pavement performance under repeated 10-year climate conditions as measured between 1990s and 2000s.
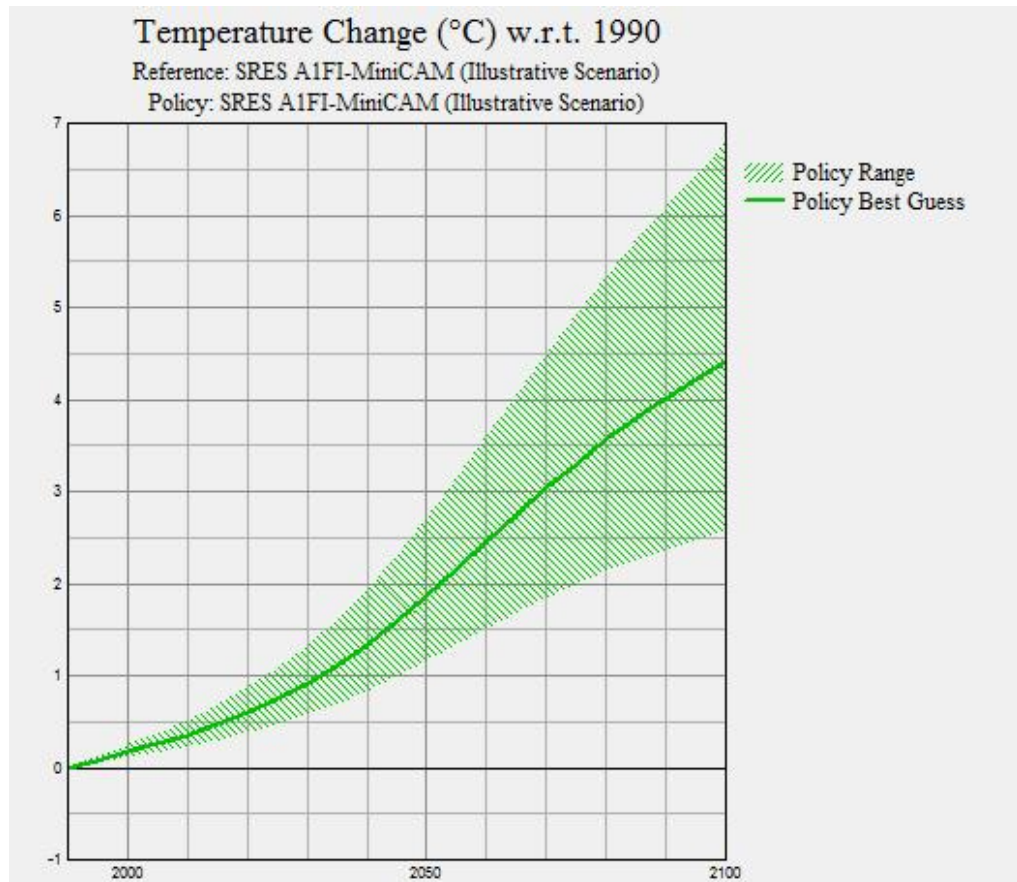
Figure 3-9 MAGICC output: Change in global surface temperature in this century under high emission scenario

The temperature record was combined with climate change predictions to create a "likely" climate profile for the future. The modification included two functions (see also Figure 3-10):

- A sine function
- A linear function

3. METHODOLOGY
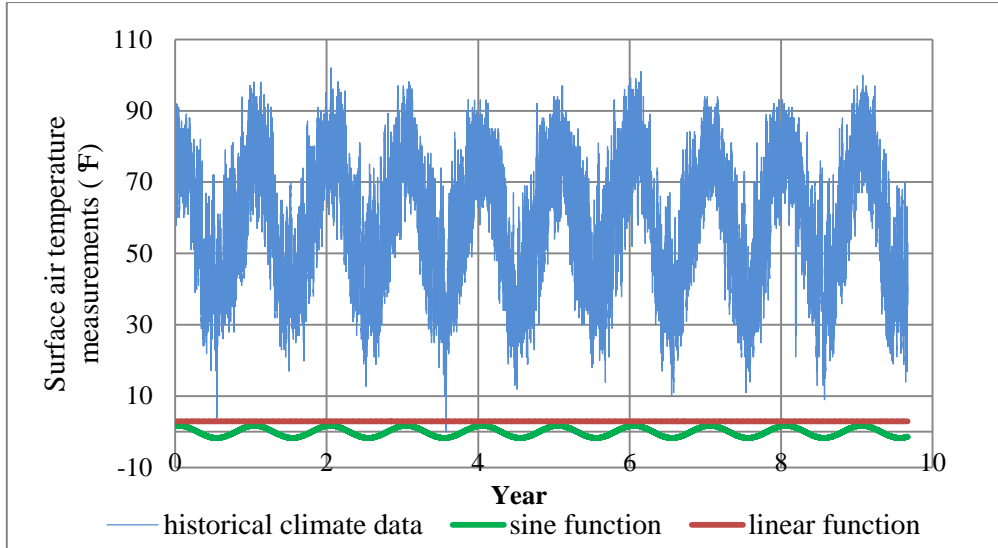
Figure 3-10 An example of temperature modification (Richmond, VA) (Qiao et al., 2013b)

The sine function was used to represent the seasonal temperature variation (hotter summer and colder winter). This function is used for SecT01, SecT02, and SecT03 to give a general idea on the influence of temperature variation on pavement performance. However, as the extent of the variation cannot be quantified, this function was not adopted to evaluate the real sections. The sine function can be expressed as:

$$T_s = a \times \sin(b \times Y + C) \qquad \text{Equation 3-1}$$

where,

T_s = sine function to be added to climatic records

Y = time of temperature measurement (year)

a, b, c = calibration factors

The sine function is able to add variation to the temperature and keep the total unchanged within a period. The factors a, b, c were calibrated from the historical climatic records respectively for SecT01, SecT02, and SecT03. The maximum/minimum value of the sine function was determined by the factor a, which was calculated from the extreme hot and cold temperature with a certain confidence level (95%). Factor b is determined by the period of the sine function, which equals one year ($b = 2\pi/1$). Factor c is determined by the time of the year of the first measurement.

The linear function (T_l) (see Figure 3-10) was used to represent the increase in the average temperature. The linear function equals a constant, which can be expressed as:

$$T_l = constant \qquad \text{Equation 3-2}$$

where,

T_l = linear function to be added to climatic records

For the sensitivity analysis of pavement performance (SecT01, SecT02, and SecT03) to climatic factors, the constant was calculated by multiplying the sensitivity (5%) with the mean annual temperature. To evaluate the real sections, the prediction of climate change under different scenarios was taken to be the constant. By adding the predicted increase in temperature to the hourly measurement (Equation 3-3), this also gave the same increase in the average annual temperature. Meanwhile, this increased the frequency of extreme hot hours (see Figure 3-11). For instance, the extreme hot hours between 100-110 ℉ occurred 35 times after the modification compared to 0 times for the baseline. The hours between 90-100 ℉ occurred 2418 times, which was three times as many as the baseline. Therefore, extreme hot hours were added as a consequence. However, the technique required to predict the extreme weather is not available and thus there is no evidence to claim the accuracy of the increase in hot extremes. As the up-to-date climate models can only predict the average value of increase in the temperature, the increase in the frequency of extreme hot hours was only considered to be the result of increase in the average temperature.
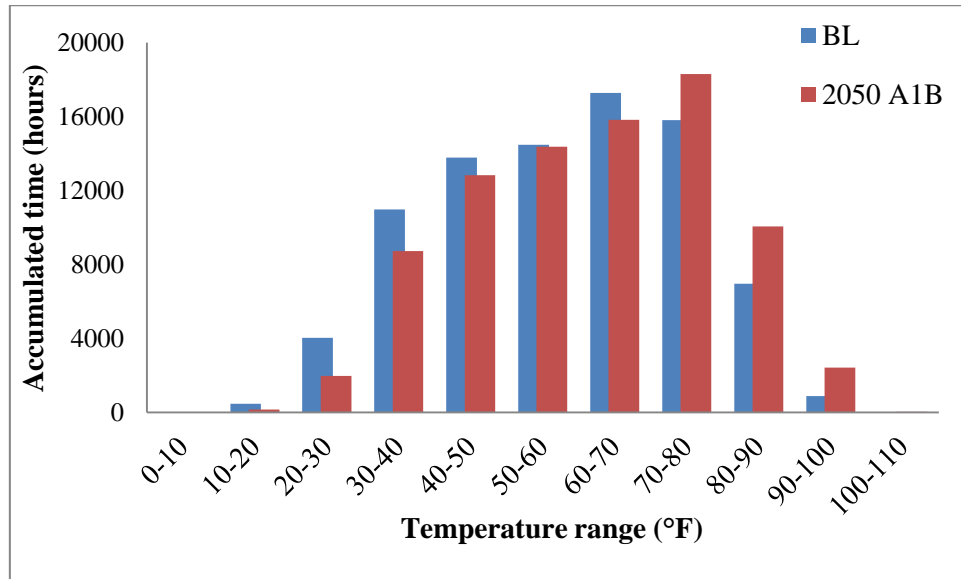
Figure 3-11 Histogram comparison of hourly temperature frequency after modification for Sec02

Eventually, temperature modification can be made using the equation below:

$$T_m = T_{original} + M \qquad \text{Equation 3-3}$$

where,

T_m = modified temperature

$T_{original}$ = original temperature from measurement

M = modification using either T_s or T_l

The available measurement period was usually approximately 10 years. Although the climate is stable in a region, the weather conditions are highly random. Without consideration of climate change, the temperature histogram may be significantly different compared to that in the next decade. However, the difference between the average temperatures is usually not significant.

The linear function increases the average temperature by adding an increase in the hourly temperature. This function represents the part of climate change prediction which is with the highest level of confidence, i.e. increase in the average temperature. It can be observed from Figure 3-11 that the frequency of hot hours increased and cold hours reduced. Without changing the average temperature, the sine function can increase the frequency of hot and cold hours, which is one of the major differences between the effect of the linear and sine functions.

3.4.3.2. Precipitation

The prediction of increase/decrease in precipitation is as a percentage. The modification of precipitation can be expressed by the following equation:

$$P_m = P_{original} \times (1 + p/100) \hspace{3cm} \text{Equation 3-4}$$

where,

P_m = modified precipitation

$P_{original}$ = original precipitation from measurement

p = predicted increase/decrease (+/-) in precipitation in percentage

With the modification, the hourly precipitation is increased/decreased proportionally and the total precipitation is increased/decreased to the same proportion. This modification can also change the frequency of extreme precipitation events. As the rainfall is random, it is almost impossible to predict a pattern of precipitation and thus there is not a sound technique to modify the precipitation pattern e.g. seasonal variation.

3.4.3.3. Groundwater and sea level

With a maximum consideration for the effect of sea level rise, it was assumed that the increase of sea level leads to the same increase in groundwater level. As flexible pavements are sensitive to environment and subgrade moisture plays an important role for the spreading of traffic loading and road

deterioration, therefore, this assumption avoids the effect of groundwater rise being underestimated. The modification of groundwater level can be expressed by the following equation:

$$GW_m = GW_{original} - D_s \qquad\qquad \text{Equation 3-5}$$

where,

GW_m = modified groundwater level (to ground or road surface)

$GW_{original}$ = original groundwater level

D_s = rise in the sea level

The groundwater level information of Sec01, Sec02, and Sec03 was collected from the USGS database which includes information of groundwater table measurements in a number of boreholes in the U.S.. The nearest boreholes were chosen to investigate the groundwater level for the three sections (see an example in Figure 3-12).
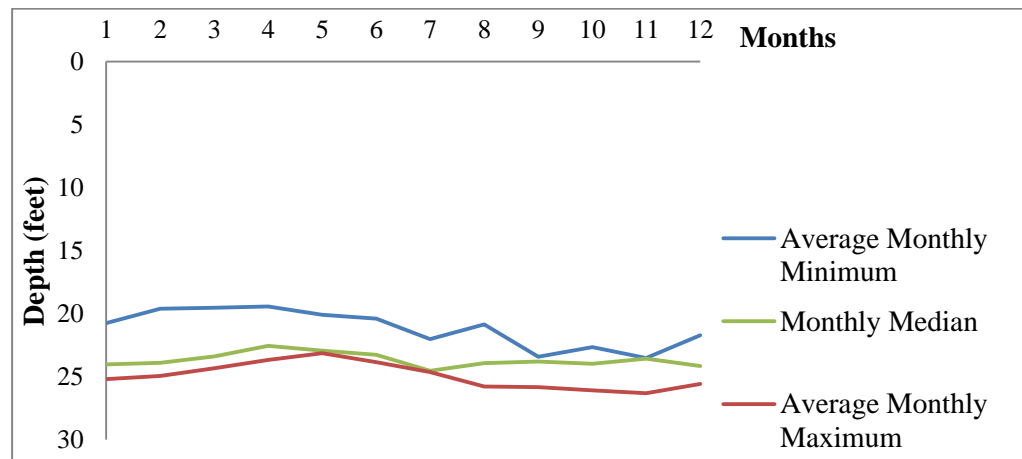
Figure 3-12 Groundwater depth measurements near Sec02 (1 foot ≈ 0.3m)

The groundwater level was calculated by the distance between the ground surface and the average annual/seasonal groundwater level. For Sec01, seasonal groundwater level was used because the groundwater level was comparatively high (3.7 feet (≈ 1.1 m) from the ground surface) and the variation was great (standard deviation: 0.799 feet (≈ 0.24 m)). The groundwater level in Sec02 and Sec03 was considerably lower and the deviation was less. The groundwater level of SecT01, SecT02, and SecT03 was assumed to be 5 feet below the pavement surface. The groundwater level of Sec01, Sec02, and Sec03 can be found in the Appendix (Table A-23).

3.4.4.   Summary

Climate change is likely to occur in the future and it is predictable to some extent. The climate change that occurred in the past decades was closely associated with human emission of GHG. The IPCC created several emission

scenarios according to different development pathways of our society to quantify the amount of GHG emissions. Under various emission scenarios, climate models can be used to project global and local climate. The MAGICC/SCENGEN programme was run under this principle with a choice of various climatic models or their combinations to evaluate global and local climate change including changes in average temperature, precipitation, and sea level rise.

The climate database included hourly measurement of temperature, precipitation, wind speed, solar radiation, and groundwater level in many weather stations in the U.S. over a period of approximately 10 years. Weighted inversely by distance, the weather conditions in a specific location can be interpolated from its nearby stations. Furthermore, groundwater measurements from the USGS database can provide another alternative to estimate the groundwater level for a specific location.

Modification was made to combine the climate change projections and historical climatic records to represent a "likely" future climate. The modification included an increase/decrease in hourly temperature and precipitation, additionally hot/cold extremes in summer/winter, and an increase in the groundwater level. Although methods to predict the (daily/seasonal) extreme weather events, wind speed, and solar radiation are unavailable based on current knowledge, attempts will be made to discuss their uncertainties linked to the prediction of pavement performance by a sensitivity analysis (see Section 3.5.1).

3.5. Pavement performance modelling

3.5.1. Sensitivity analysis

Currently IPCC climate change projections contain uncertainties and are incapable in predicting climatic conditions including wind speed and solar radiation. The method discussed previously to combine climate records and climate predictions to generate future climate profiles can also induce uncertainties to the system. To enable these uncertainties to be studied and possibly quantified, a sensitivity analysis was performed to identify the most influential climatic factors on pavement performance.

The sensitivity analysis was performed by increasing/decreasing the climatic factors one at a time by a percentage, which will result in a change in pavement performance as a consequence. The sensitivity was calculated using the equation as follows:

$$Sensitivity = \frac{\Delta PP(t) / PP(t)}{\Delta CF / CF} \qquad \text{Equation 3-6}$$

3. METHODOLOGY

where,

$PP(t)$ = pavement performance

ΔPP = change in pavement performance

CF = climatic factor

ΔCF = change in the climatic factor

The calculated sensitivity is a relative sensitivity, which can be compared with other sensitivities and show the importance of each climatic factor to the system. The involved climate inputs included hourly records of:

- temperature (T)
- precipitation (P)
- wind speed (WS)
- sunshine percent (SP)
- groundwater level below road surface (GW)

In the study, a sensitivity analysis was performed for all six sections with a 5% or 10% (or both) increase in climatic inputs to the MEPDG as follows:

- 5% increase for SecT01, SecT02, and SecT03
- 5% and 10% increase for Sec01, Sec02, and Sec03

In the sensitivity analysis, the climatic factors were increased/decreased 5% and 10% because 5% can approximately reflect the climate condition of 2050 and 10% can approximately represent that of 2100, in terms of the average annual temperature (in °F), average total annual precipitation (in inch), and groundwater level below road surface (in foot). The increases were applied to T, P, WS, and SP. Decreases with the same percentages were applied to GW, which means the groundwater level rises as a result of climate change. Figure 3-13 is an example from Sec02 which revealed the match between the climatic inputs modified with percentage increases and climate predictions.
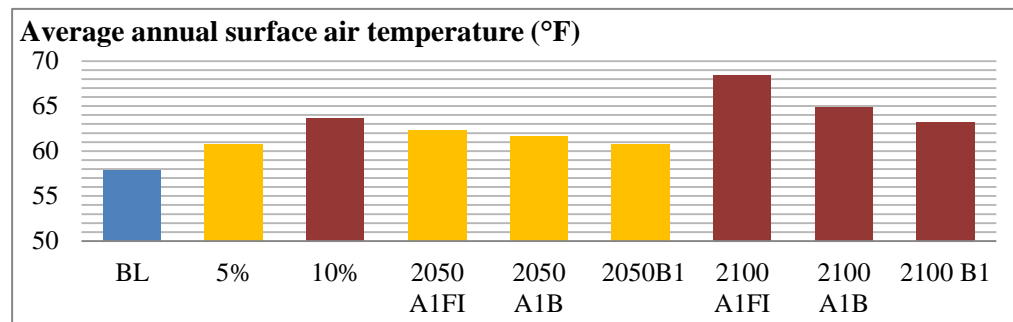
3. METHODOLOGY
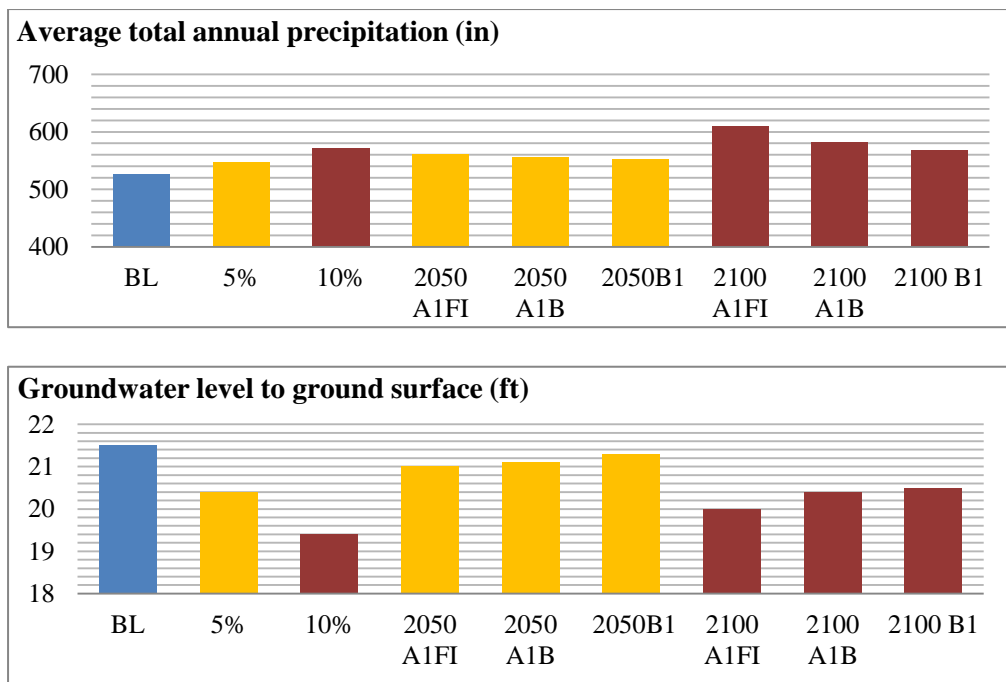
Figure 3-13 Modified climatic factors comparison under BL, 5% increase. 10% increase, and some emission scenarios for Sec02 (BL = baseline, 1 in = 25.4 mm, and 1 foot ≈ 0.3 m)

For the other climatic factors, wind speed and solar radiation, the same percentage was applied for the sensitivity analysis. Although no prediction was available for these factors, it was reasonable to increase the hourly values of such factors by the same percent and test their sensitivities. Furthermore, the maximum sunshine percentage was 100%. Any modified hourly sunshine percentage higher than this value was considered to be 100%.
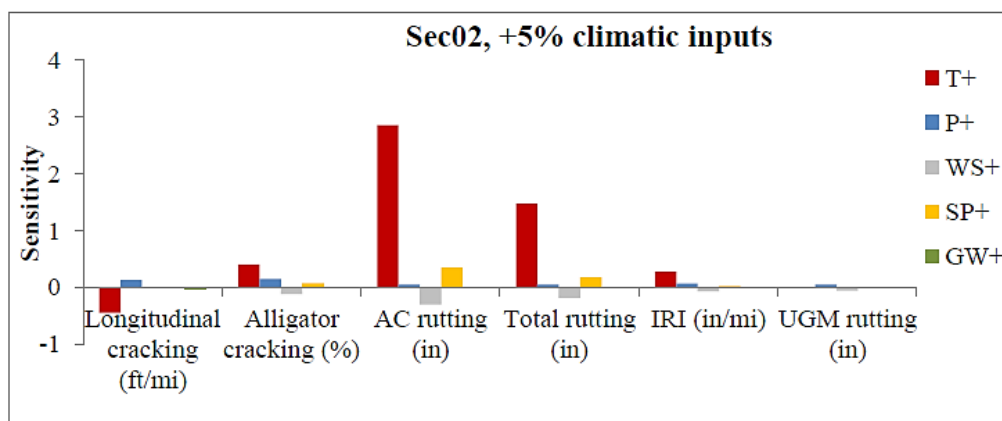
Figure 3-14 Sensitivity analyses of pavement performance to climatic factors (Sec02, 5% increase in variables)

Figure 3-14 is an example of the sensitivity analysis performed for Sec02 with a 5% increase in variables. It can be observed that the pavement performance index that is most influenced by environmental factors is the AC rutting. For AC rutting, the most influential environmental factor is

temperature. Rutting accumulated in unbound granular layers is the least affected performance index.

3.5.2.   Pavement service life

Climate change can have impact on pavement deterioration and thus reduce the service life of the pavement. After prediction of pavement performance with or without climate change, the service life of pavements can be analysed. The pavement service life is calculated using the Equation 2-29 and distress including IRI and rutting with defined thresholds (see later in Table 4-5).

Pavement service life can be sensitive to certain performance indices. For instance, the rutting development of a flexible pavement can be fast in the beginning because of the compaction from vehicles. Typically after a few years, the accumulation of permanent deformation tends to slow down. If the service life is determined by rutting when the accumulation is slow, even a small increase in rutting can result in significant reduction in the service life. Similarly, the choice of threshold may have significant impact on the pavement service life. An example of service life can be observed in Figure 3-15. The example is from Sec01. Assuming the pavement service life is only determined by rutting, the service life is 30 years with a rutting threshold of 0.75 in (≈ 19 mm). Under climate change conditions, service life is reduced by 18 years, comparing the 2100 A1FI and BL scenario. If the threshold is increased to 1 in, the service life is 40 years for both baseline and climate change scenarios. If the threshold is reduced to 0.6 in (≈ 15 mm) for instance, the service life of the pavement under the baseline is 10 years and climate change under the 2100 A1FI scenario can reduce the service life by approximately 6 years.
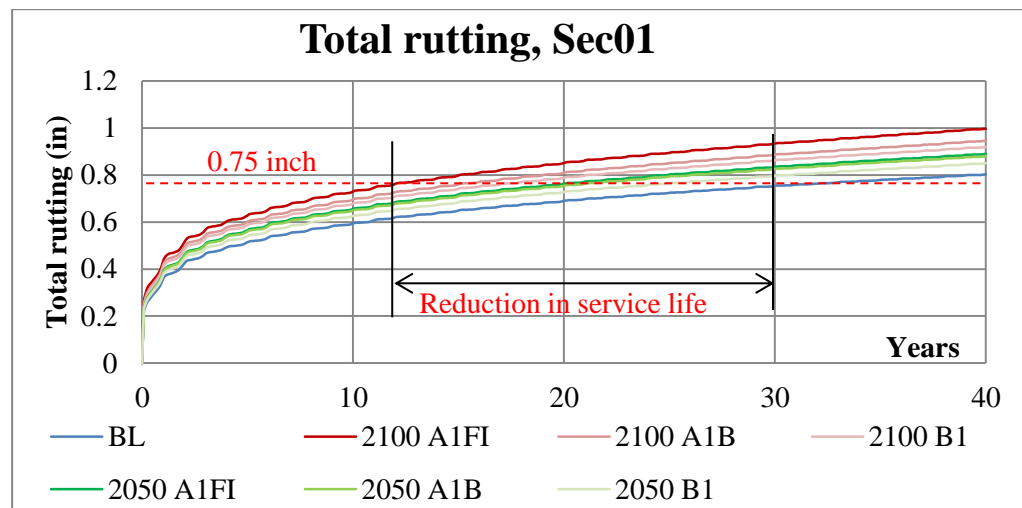
Figure 3-15 Pavement service life analysis for rutting (1 in = 25.4 mm)

3.6. Maintenance effects

3.6.1. Introduction

Pavement service life and maintenance decision-making are linked to pavement performance. Climate change may impact on pavement service life and thus it is doubted that maintenance decision-making in the future may be affected by climate change. Therefore, it is interesting to investigate how maintenance decision-making is affected by climate change, in terms of frequency and costs of interventions.

For conventional responsive interventions, maintenance is triggered when performance thresholds are reached. Based on this principle, maintenance decision matrices have been developed by various road authorities with consideration of several distress modes. Furthermore, pavement performance indices (especially IRI) can be used in maintenance optimisation to achieve minimised total costs (Qiao et al., in press-a, Qiao et al., in press-b). Pavement maintenance decision-making is usually made on the basis of performance levels.

Furthermore, the choice of interventions can impact performance. Different interventions have different capability to address distress and ability to improve pavement performance indices. Therefore, the maintenance effects of various interventions need to be investigated for successful maintenance decision-making.

In this section, maintenance effects of various interventions will be discussed. A linear model was used to model maintenance effects of three types of interventions including thin overlay, thick overlay, and mill & fill. The validated maintenance effects models were used in case studies for Sec01, Sec02, and Sec03. Furthermore, a data selection process was defined to extract useful data from the database and will be discussed later.

3.6.2. Maintenance effect overview

Maintenance decision-making refers to the process to select one or several types of interventions and apply them at a certain time of the pavements' life time. The selection needs to be constrained by maintenance thresholds, serviceability level, available maintenance equipment, and budget. Different maintenance interventions are designed to address different distress types. In general, the maintenance effects of interventions can include two parts:

- An immediate effect: the immediate improvement in pavement performance indices indicated by the differences between performance measurement before and after the intervention.
- A long-term effect: the ability to retard future deterioration.

In this study, only the immediate effect is considered. The long-term effect is neglected because the long-term effect is difficult to measure. The long-term effect is only meaningful when compared to the original development of deterioration. The long-term effect of a certain intervention can only be seen by comparing the development of deterioration of a section with the intervention and an identical section without the intervention. Due to the variability of traffic and environment, this is difficult.

3.6.3. Pavement management data

A PMS is a set of tools assisting pavement management in order to achieve better decision-making. Traffic conditions, pavement structure and materials, condition surveys are essential parts of a PMS. In the U.S., the LTPP is a popular PMS on a national level, including pavement data from many states. Each state may have its own PMS. For instance, the PMS used in this study is from VDOT, which is one of the most complete PMSs of all the states. The VDOT's PMS provided useful information on traffic, structure, material, and performance measurements for the three real sections of the case studies.

The maintenance data from the three most frequently maintained districts in Virginia including Bristol, Salem, and Richmond were selected for validation of maintenance effect models. Two sets of data were involved namely construction history and performance measurements. The oldest construction history in the investigated regions dated back to the 1960s. In the construction history, the thickness and the material of each layer was recorded with a material code according to a Virginia standard. Maintenance interventions were also documented and information on the material and thickness can be obtained. Performance measurements included in-situ measurements of distress including cracking, roughness, rutting, patching, bleeding, and potholes since 2007. Pavement performance including IRI and rutting was included. Both construction history and performance measurements were recorded in sections at a minimum scale. The length of the sections is approximately 1 mile (1.61 km). However, the sections' begin/end mile posts for construction history and performance measurements did not always coincide.

To combine section data and correlate construction history and pavement performance, a matching algorithm was created to combine the two sets of data. The matching is based on criteria including route hierarchy, route ID, directions, mile posts, and time of the intervention and measurements.

3.6.4. Immediate maintenance effects model formulation

For the investigated interventions, the different thicknesses for each investigated intervention were too few to be used in the regression analysis.

Therefore, the thickness of overlay was not used as a parameter in the model but was rather reflected by a model coefficients. Therefore, the linear model used in this study only considered pavement performance indices before interventions as a variable. Furthermore, to emphasise the improvement in performance indices due to the intervention, the linear model (Equation 2-30) was transformed into the following equation:

$$\Delta IRI_n = a * IRI_{n0} + b \qquad\qquad \text{Equation 3-7}$$

where,

ΔIRI_n = improvement in IRI due to an intervention (in/mi)

IRI_{n0} = roughness before the intervention (in/mi)

a, b = regression factors

The same linear relation can be used to model the immediate maintenance effects of interventions on rutting (Hall et al., 2002) and can be expressed as follows:

$$\Delta Rut_n = c * Rut_{n0} + d \qquad\qquad \text{Equation 3-8}$$

where,

ΔRut_n = improvement in rutting due to an intervention (in)

Rut_{n0} = rutting before the intervention (in)

c, d = regression factors

In principle, Equation 3-7 is the same linear model as Equation 2-30 but Equation 3-7 and 3-8 have an emphasis on the reduction in IRI and rutting due to an intervention.

3.6.5. Model validation

The immediate maintenance effects models are crucial to predict pavement performance after maintenance and thus are of importance to the performance prediction over the life cycle of a pavement. Furthermore, the accuracy and precision of the used model is dependent on the model coefficient i.e. model validation is essential for more accurate and precise predictions. Therefore, Virginia PMS data were adopted to validate the models to the local conditions. The validated maintenance effects models were used in case studies on Sec01, Sec02, and Sec03.

The combined construction history and pavement performance data can provide information on the latest intervention and performance indices in and after the year of the intervention, which is considered to represent pavement

3. METHODOLOGY

performance before and after the intervention. According to this, the improvement in IRI and rutting due to maintenance can be expressed as:

$$\Delta IRI_n = IRI_{n0} - IRI_{n1} \qquad\qquad \text{Equation 3-9}$$

$$\Delta Rut_n = Rut_{n0} - Rut_{n1} \qquad\qquad \text{Equation 3-10}$$

where,

IRI_{n1} = roughness measured in the year after the intervention (in/mi)

Rut_{n1} = rutting measured in the year after the intervention (in)

n = the number of data points (0, 1, …, n)

In theory, IRI_{n0} and IRI_{n1} represents IRI immediate before and after an intervention so that ΔIRI_n can indicate the maintenance effect. However, both the construction history and performance measurements are recorded by the year of operation. Thus, if the intervention and performance measurements are recorded to be performed in the same year, it is impossible to know which one was made first. Moreover, human factors can introduce uncertainties to the measurements. Therefore, some additional measures and assumptions were made to improve the calculation on the immediate effects and assist maintenance effects modelling:

1. If ΔIRI_n and ΔRut_n are calculated to be negative, the data points (IRI_{n0}, IRI_{n1}) and (Rut_{n0}, Rut_{n1}) will be removed from the analysis. This is because the negative ΔIRI_n and ΔRut_n (i.e. $IRI_{n0} < IRI_{n1}$ and $Rut_{n0} < Rut_{n1}$) indicate that the intervention is not performed between the two measurements. This is because if the intervention is performed between the two measurements, a sudden improvement in IRI and rutting can be observed i.e. $IRI_{n0} > IRI_{n1}$ and $Rut_{n0} > Rut_{n1}$. Certainly, this is based on the fact that the discussed intervention is capable of addressing IRI and rutting.
2. In fact, the differences in IRI and rutting calculated using Equation 3-9 and 3-10 included two effects: the improvement in performance indices and additional deterioration between the two measurements. However, the deterioration in a year is insignificant compared to the immediate maintenance effects according to experience. Furthermore, this study mainly focuses on corrective maintenance which is typically applied in the later phase of the pavements' life when pavements have stabilised i.e. yearly deterioration is relatively slight. Therefore, the additional deterioration is neglected.
3. Errors exist in the database. A pavement section with an IRI of 1750 in/mi was found in the database. The IRI value was too high according to experience (30 – 1200 in/mi (0.47 – 19 m/km)) (Sayers and

Karamihas, 1998). This may be because of an unexpected item on the section that biased the results and the result cannot reflect the real roughness of the pavement. Some such errors are obvious and noticeable as discussed but some of them are not easy to discover due to the size of the database. In the regression analysis (validation) of the maintenance effects models, the obvious errors in the measurements are commonly problematic because they have greater influences on the regression. To avoid this, regression diagnosis with a Cook's Distance (CD) method was applied to remove those outliers, which may have an influence on the derived regression equation.

Furthermore, it can be observed from VDOT PMS that the standard speed for IRI measurements (80 km/h) is usually difficult to keep to in measurements and the real speed can typically range between 50 and 100 km/h. Although lower or higher speed can introduce errors in IRI measurements, it is considered that validation of maintenance effect models are not affected, because a large number of IRI measurements were used in the regression analyses.

3.6.6. Cook's distance

In statistics, CD is a measurement of the influence of a data point on least square regression analysis. CD is applied in this study to identify points that need to be checked for validity and excluded if necessary. The analysis was performed by the SPSS statistics software package for screened data points (ΔIRI_n versus IRI_{n0} and ΔRut_n versus Rut_{n0}, satisfying $\Delta IRI_n > 0$ and $\Delta Rut_n > 0$) with the following equation:

$$D_i = \frac{\sum_{j=1}^{n}(\widehat{y_j}-\widehat{y_j}(i))^2}{pMSE}, i = 1, 2, \dots, n \qquad \text{Equation 3-11}$$

where,

$\widehat{y_j}$ = the estimate of the conditional mean

$\widehat{y_j}(i)$ = the estimate of the conditional mean without point i

p = the number of coefficient in the regression model

MSE = mean squared error

For CD, there is no strict threshold over which the points can be considered influential in the regression analysis because the CD is comparative. However, points with a CD that meets $D_i > 0.7$ are usually considered influential, the validity of which needs to be checked (McDonald, 2002). Therefore, the CD threshold was set to be 0.7 in this study to identify influential points. Any section with a CD that was greater than 0.7 was removed, either for IRI or rutting.

3.6.7. Summary

From the investigated data from the three most frequently maintained districts, three interventions were considered because the construction history and performance measurements of the interventions were sufficient in the validation of maintenance effects models. The three interventions were (1 in = 25.4 mm):

- Op1: Overlay (1.5 or 2 in)
- Op2: Overlay (topping overlay and an intermediate layer; 3.5 or 4.5 in total)
- Op3: Mill & fill (2 or 4 in)

Op1 was an overlay of surface mixture with a nominal maximum aggregate size of 12.5 mm. Op1 can be either preventive or corrective maintenance because 1.5 in ($\approx$ 38 mm) is typically the limit between a preventive thin overlay and corrective overlay. Therefore, it was difficult to judge the maintenance category of the 1.5 in ($\approx$ 38 mm) overlay. The 2 in overlay was generally considered corrective. Op2 was considered to be corrective. Op2 was made of an intermediate layer of base mixture with a nominal maximum aggregate size of 25.0 mm and was topped with the same surface layer as Op1. Op3 used the same surfacing for the fill stage. The mill and fill were both 2 in so the elevation of the pavement surface remained unchanged. The estimated costs of the three interventions can be found in Table 3-6. The costs included the costs of the material, machinery costs and labour costs. Op2 was thicker and consisted of more materials and thus was more expensive than Op1. Op 3 included the mill phase which required more labour work and machinery costs and thus was the most expensive. The operation duration of Op3 was longest because of the additional milling work. The vehicle operation speed on the three sections was assumed to be 65 mph ($\approx$ 105 km/h), which is common on interstate highways. The WZ speed was assumed to be 35 mph ($\approx$ 56 km/h).

Table 3-6 Costs and others information of the three interventions

	Op1	Op2	Op3
Costs (USD/square yard)	5.0	6.0	8.0
Operation duration (days)	5	6	10

(1 square yard $\approx$ 0.8 square metres)

It needs to be appreciated that the material costs, labour costs and machinery costs may vary significantly from place to place. The figures above are assumed based on literature (Peshkin et al., 2011) and are only used for demonstration purposes.

3.7. Life-cycle cost analysis and maintenance optimisation

3.7.1. Maintenance decision making and LCC

Maintenance decision-making is mainly based on pavement performance, budget, and availability of equipment. In practice, different road authorities have their own way to maintain pavements according to the required serviceability level. A decision-making tree/matrix is a common method to schedule cost-effective interventions based on available resources (Hicks et al., 2000, Johanns and Craig, 2002). In the past decades, computer aided maintenance optimisation algorithms were created to solve maintenance planning with multi variables including pavement performance and costs to achieve more economic decision-making (Ferreira et al., 2002, Lamptey et al., 2008, Rashid and Tsunokawa, 2012, Santos and Ferreira, 2012).

As climate change can impact pavement deterioration and reduce a pavement's service life, pavement maintenance and the consequent LCC are suspected to be affected. In this study, three maintenance decision-making alternatives were included:

- Alternative 0 (do nothing)
- Alternative 1 (strict trigger)
- Alternative 2 (optimisation)

It is assumed no maintenance will be performed during the pavement's entire life under Alternative 0. As no maintenance is assumed, the agency costs and WZ costs are not involved. Thus changes in user costs due to climate change can be derived.

Alternative 1 represents a conventional decision-making process, which is dependent on strict maintenance thresholds. This alternative aims to minimise the agency costs while keeping performance level below thresholds. As an extra output, the pavements' service life can be calculated under Alternative 1.

Alternative 2 represents a future decision-making process using a computational algorithm. The optimisation considers pavement performance, agency and user costs, and maintenance thresholds, however, with unlimited budgets. This results in costly maintenance interventions because user costs dominate. However, current practice suggested such investment was unrealistic because of the limited agency budget. To address this, the agency costs can be magnified by a factor to be weighted more in the analysis as will be discussed later.

3.7.2.   Cost components

Life-Cycle Cost Analysis (LCCA) is used to assess the long-term economic efficiency of alternative investment options. In general, LCCA is used to calculate the cash flow from cradle to grave of a project. In this study, the LCCA was applied as a tool to compare the differences in LCC as a result of climate change. Thus the absolute value of the LCC was not of importance but the difference was. Therefore, LCC components that are not related to climate change and its consequent effects are neglected. After the literature review (Section 2.4), selected LCC components were:

- Maintenance costs (Agency costs)
- VOC, WZ delay costs, and WZ VOC (User costs)

Based on the analysis that climate change will affect the deterioration of flexible pavements, maintenance decision-making needs to adapt to the changes. Maintenance costs were thus selected to demonstrate the adaptions (see Table 3-6). Construction costs as another major component can also be changed due to climate change. For instance, to adapt to a hotter future climate, stiffer binder can be used to satisfy stiffness and permanent deformation requirements (see Qiao et al. (2013a)). The cost-benefit of such adaptions can be evaluated using the framework with added agency costs components.

Several components of user costs were selected because these costs were related to the discussed consequence of climate change which included pavement performance and maintenance operations. VOC can be associated with pavement performance indices, especially IRI (Chatti and Zabaar, 2012, Zaniewski et al., 1982, Watanatada et al., 1987).

As VOC is a combination of different cost components which are affected by traffic and vehicle conditions, the factors of the model may vary from place to place, i.e. model calibration may improve the accuracy of the model. However, the aim of including these models is not to calculate the absolute value of the VOC but rather to use it as a reference for comparisons. Linear models were considered to be good enough to achieve this and thus Equation 2-35 and 2-36 were used to compute VOC under normal vehicle operation. For calculation of VOC under WZ conditions, speed was an important factor to consider and thus the general models for computing VOC (Equation 2-35 and 2-36) were not considered to be appropriate. VOC component models discussed in the literature review (Equation 2-39, 2-45, and 2-49 to 2-52) were used for modelling the major components of WZ VOC including fuel consumption, lubrication oil costs, and tyre wear costs.

WZ delay costs started with calculation of peak capacity and WZ capacity. The peak capacity was calculated using standard procedures for estimating highway capacity by Federal Highway Administration (HPMS,

2000). The WZ capacity was calculated using the Memmott and Dudek (1982) model (Equation 2-61). The hourly traffic distribution was considered to be constant and was set as the default traffic distribution as in MEPDG (AASHTO, 2009) (see in Figure 3-16). The maintenance interventions were assumed to be performed between midnight and 8:00 to avoid interruption on high traffic flows. WZ delays were calculated by summing the major components including moving delay (Equation 2-58 and 2-59) and queueing delay models (Equation 2-60) as described in the literature review.
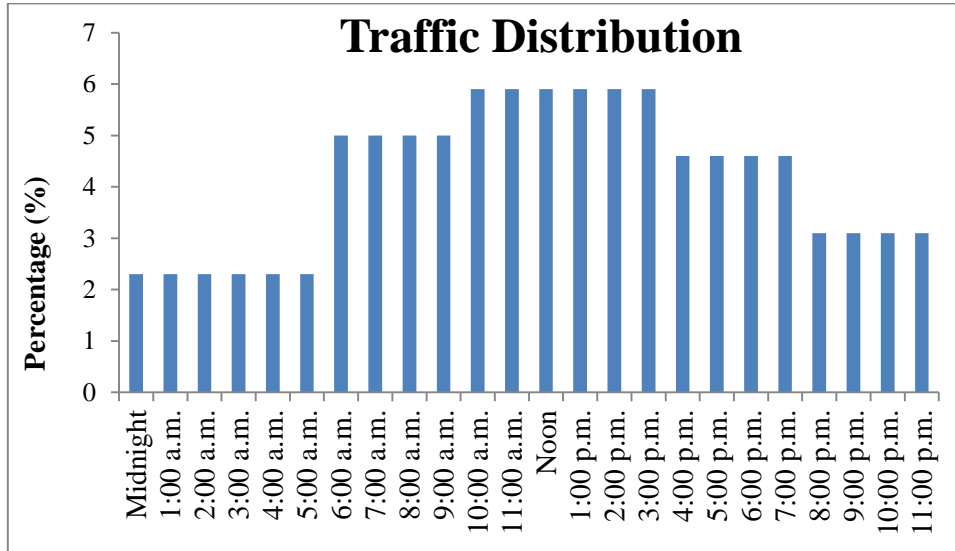
Figure 3-16 MEPDG default hourly traffic distribution

During maintenance operations, one lane of the two lane highway (one direction) of the case studies was considered to be closed, resulting in an increase in the traffic demand for the other lane. In case the traffic demand exceeded the capacity of the lane, a queue was considered to form. The queueing delays were calculated with Chien's model (Equation 2-60) (Chien et al., 2002) under the D/D/1 discipline. The time delays were multiplied by the value of time for drivers to calculate the delay costs.

The value of time refers to the opportunity costs of time of vehicle drivers. The value of time is dependent on the purpose of travelling and is different from person to person. In general, the value of time for a trucker or cargo driver is higher than a passenger car's driver because trucks or cargo vehicles are for business and passenger cars are for travelling and leisure purpose. In this study, the value of time was assumed to be 8 USD/hour for car drivers and 15 USD/hour for truck drivers.

3.7.3.   Maintenance optimisation

Since the 1980s, the importance of establishing a PMS was recognised and various PMSs were developed by road agencies around the world. In general, a PMS has two functions: prediction of pavement performance using a set of prediction tools validated using in-situ measurements; and tools to assist

maintenance decision-making to achieve cost-benefit. The optimisation of maintenance is an important aim of PMS.

Although based on the particular situations of agencies, the principle of the maintenance optimisation is similar, that is to find the most economical solution within budget. The relation between performance level and costs can be expressed in Figure 3-17. To have a better performance level, more agency costs need to be invested in pavement maintenance with careful planning. The costs can be spent on increasing the application frequency of interventions or change to more expensive interventions that can have greater effects. User costs can be related to road conditions. For instance, user costs including VOC can be related to the IRI of pavements. Therefore, the extra investment in maintenance can help to reduce VOC for road users. More investment in maintenance can also increase road user costs. For instance, more frequent interventions may cause more delays for road users. Therefore, the user costs may not trend as continuous as shown in Figure 3-17. However, user costs will be higher on a worse pavement in general. Therefore, the total LCC appears as a "U" shaped curve against the average performance level of pavements and can be minimised at a certain performance level with a certain maintenance investment. When the maintenance intervention strategy can keep the total LCC at the minimal value, the maintenance is said to be optimised.
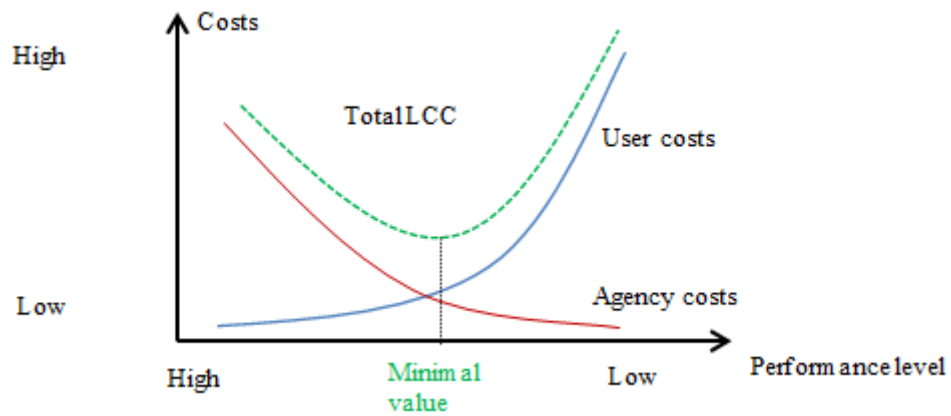
Figure 3-17 Agency costs, user costs, and total LCC

When the maintenance is optimised, the cost benefit is largest from the perspective of society. However, the minimised LCC may be at the cost of unrealistic agency costs which the agency may not be able to afford. Therefore, the minimisation of LCC may be based on limitations on the agency costs i.e. budgetary constraint (Ferreira et al., 2002, Lamptey et al., 2008, Santos and Ferreira, 2012). As this study is theoretical, the budgetary constraint does not exist. A similar approach was used to set budgetary constraint by multiplying the agency costs with a factor as applied in this study. A sensitivity study of the optimisation to the multiplication weighting factor was made with these factors (see Section 4.6.3.1.).

3. METHODOLOGY

As a basis, the prediction of pavement performance is of importance to maintenance optimisation. In early maintenance optimisation methods, simple performance prediction models were used such as the probabilistic models validated using the Markov Decision Process (Golabi et al., 1982, Cheng et al., 2015). Due to the inaccuracy of the purely empirical performance models, the optimised maintenance interventions may not be the most economical solution. Pavement performance models are much more developed now and can predict performance more accurately with various inputs. The deterministic models are quantitative and can give performance predictions of various distress types using a mechanistic-empirical approach (Ferreira et al., 2002, Santos and Ferreira, 2012, Sanchez-Silva et al., 2005). Present Serviceability Index (PSI) is a common performance index used for maintenance optimisation (Ferreira et al., 2002, Santos and Ferreira, 2012). The PSI is the prediction of Present Serviceability Rating (PSR), which is an evaluation of driving comfort judged by an assessment panel. However, the PSR is subjective and less comparable than the technical indices. IRI and rutting are probably the most studied performance indices and the theory on the development of these indices are the most developed. Therefore, the development of IRI and rutting was modelled by MEPDG to enhance maintenance optimisation.

Climate change may significantly reduce a pavements' service life and thus impact pavement maintenance and the consequent LCC. Furthermore, it may affect the minimised total LCC i.e. climate change can incur more costs for flexible pavements in the future. This information will be meaningful for both road authorities and road users. If agency cost increases due to climate change, road authorities need to consider an increase in the budget in maintaining pavements to the same performance level as before. Besides, considerations will be needed to modify the current pavement design method to adapt to the climate change. If user costs increase because of climate change, users can be aware of these additional costs.

The maintenance optimisation in this study was focused on a section of a highway instead of a road network. This can represent the case where a section of a highway is carefully maintained. This is likely to occur in the future because the construction phase of highways has almost been completed in developed countries and maintenance of existing highways has become the primary task. Therefore, a higher budget for pavement maintenance may be expected in the future and flexible pavements may be maintained with greater effort than before.

In this study, a binary non-linear programming algorithm was created to optimise the type and application time of interventions from three studied interventions for the three real sections. The algorithm can be expressed as follows:

3. METHODOLOGY

Minimise:

$$LCC = \sum_{t=1}^{t} \sum_{n=1}^{n} \left[X_{t,n} \times \left[AC_{t,n} \times f + WZVOC_{t,n} + WZdelay_{t,n} \right] + VOC_t \right]$$

Equation 3-12

Subject to:

$$IRI_{t,n} < IRI_{max}$$ Equation 3-13

$$Rut_{t,n} < Rut_{max}$$ Equation 3-14

where,

t = analysis year

n = intervention type

LCC = life-cycle costs

f = weight factors between agency costs and user costs

IRI_{max}, Rut_{max} = maintenance thresholds

$X_{t,n}$ = decision of application of intervention type n in year t; $B_{t,op} = 0$ (intervention) or 1 (no intervention)

$IRI_{t,n}, Rut_{t,n}$ = prediction of IRI and rutting depth in year t, also affected by maintenance history

$AC_{t,n}$ = agency costs for intervention type n in year t

VOC_t = vehicle operating costs

$WZVOC_{t,n}$ = work zone vehicle operating costs in year t

$WZdelay_{t,n}$ = work zone delay costs for intervention type n in year t

The predictions of IRI and rutting ($IRI_{t,n}, Rut_{t,n}$) were determined by the MEPDG performance predictions and the maintenance effects of interventions if there are any. IRI and rutting values will drop proportionally to the indices before maintenance. VOC_t and $WZVOC_{t,n}$ was related to IRI and thus was associated with deterioration rate and maintenance history. In the optimisation, other constraints were made as follows:

$$IRI_{t,n} > IRI_{min}$$ Equation 3-15

$$Rut_{t,n} > Rut_{min}$$ Equation 3-16

where,

IRI_{min}, Rut_{min} = lower boundary of IRI and rutting depth

3. METHODOLOGY

These two constraints were introduced for two reasons. Firstly, the constraints can set different average pavement performance levels (as will be discussed later). Secondly, this can ensure that IRI and rutting after maintenance will not be lower than the initial IRI and rutting, which suggests that the pavement performance level will not be better than that when the pavement was built.

For the three real sections in the case studies, the analysis year t was assumed to be after 40 years. Compared to the normal flexible pavements' service life (approximately 20 years), it was assumed that the pavements will be abandoned after 40 years (reasons as discussed in section 2.4.2). However, the effect of climate change is long-term and may not be easily seen over a short period. Therefore, a longer pavement design life was considered. Under the careful maintenance scheme the optimisation provided, 40 years of design life can be achieved. Furthermore, the salvage value was not considered at the end of the design life. Although, the assumption allowed maintenance optimisation to keep pavement performance at a high level near the end of the pavements' design life.

In theory, to schedule the three investigated interventions over 40 years without constraints, this yields 2 (0 or 1) to the power of 120 (3×40) possibilities. Each possibility corresponds to a LCC value. The optimisation attempted to find the least LCC value among these 1.32×10^{36} possibilities with various constraints. To achieve this, a genetic algorithm with a gradient based optimisation routine was used. The optimisation was performed in Microsoft Excel using a plugin called Frontline Solver. Genetic algorithms, as search heuristics that imitate the natural selection process, have been widely applied for optimisation and search problems. Genetic algorithms have been applied for pavements' maintenance optimisation for many years (Chan et al., 1994, Flintsch and Chen, 2004). The algorithm was only used as a mathematical approach to find optimised intervention strategies and the algorithm itself will not be discussed here. A genetic algorithm can simplify problems and reduce calculation time to find the wanted combination of interventions. However, the genetic algorithm may lead to several optimal solutions or even a local solution and an initial solution is needed in the selection process. Therefore, an initial solution was created and the optimisation results under all climate change scenarios were based on this solution. Because of this, the results are comparable.

As different lower boundaries of IRI or rutting were set, a minimised LCC value can be obtained at different performance levels. By interpolating this information (average IRI, LCC), a total LCC curve can be plotted as in Figure 3-17. The average IRI over a pavement's design life was defined by:

3. METHODOLOGY

$$IRI_{avg} = \left.\int_0^T IRI_{t,n}\right/T \qquad\qquad \text{Equation 3-17}$$

where,

IRI_{avg} = average IRI

T = design life of a pavement

By comparing the total LCC curve under current climate and future climate, the difference in LCC due to climate change can be discovered.

IRI_{avg} = average IRI

3. METHODOLOGY

4. RESULTS AND DISCUSSIONS

4.1. Introduction

A framework was created to evaluate the impact of climate change on the deterioration, maintenance, and LCC of flexible pavements. The framework was developed as the methodology of this study and the application was demonstrated using case studies on six road sections. The framework started with investigation of climate change and used the combination of historical climate and climate change projections to predict pavement performance. With locally validated maintenance effects models, changes in pavement maintenance to adapt to climate change can be estimated, based on the prediction of pavement performance indices under present or future climate.

The three outputs of the study can respectively answer the three questions proposed in the aims and objectives section. Output 1 included evaluations the sensitivity of pavement performance to climatic factors and predictions of performance indices under climate change and BL scenarios. Output 2 gives changes in maintenance decision-making due to climate change, under three maintenance regimes, namely do nothing; strict trigger with lowest agency costs; and optimised interventions with the lowest total LCC. Eventually, Output 3 can reveal the impact of climate change on the LCC of flexible pavements.

4.2. Climate change predictions

As an input for the framework, climate change projections formed a basis of the methodology. This study focuses on pavements' response to climate change rather than climate change itself. Therefore, details about the projections of climate change are not discussed and default inputs (see Appendix Figure A-1 to Figure A-7) of MAGICC/SCENGEN were used which may result in relatively conservative projections. As one of the most important climate change prediction parameters, several emission scenarios were involved to help to understand uncertainties in the projections. The high emission scenario A1FI was used as the upper limit of climate change and the low emission scenario B1 was adopted for the lower limit. The medium emission scenario was used to predict climate change that is very likely to occur in the future.

Two output years were used for the climate change projections, which were 2050 and 2100. The 2050 projections can represent the near future. With the life span (40 years) of pavements discussed in this project, flexible pavements constructed today (2014) will eventually be operating under the climatic conditions in 2050. Climate projections in 2100 can represent the greatest changes in this century and thus can be used as the worst case.

115

4. RESULTS AND DISCUSSIONS

The temperature and precipitation predictions for the studied sections are presented in Table 4-1. The global sea level rise predictions are also included. It can be observed that temperature will increase in all the six locations. Furthermore, increasing in precipitation was observed in the prediction for all the investigated locations except for SecT01. The temperature increase in Minneapolis is the greatest under 2050 scenarios (see Table 4-1). This made Minneapolis (from the Midwest) highly susceptible to the consequence of climate change related to high temperature on flexible pavements as suggested by Meyer et al (2013).

Table 4-1 Climate change projections (T = temperature, P = precipitation)

Scenario		SecT01 Seattle, WA		SecT02 Minneapolis, MN		SecT03 Richmond, VA		Global
		T (℃)	P (%)	T (℃)	P (%)	T (℃)	P (%)	Sea level (cm)
2050 A1B		+1.78	-1.2	+2.55	+5.3	+2.14	+5.9	+15
+5%		+1.44	+5.0	+1.33	+5.0	+1.61	+5.0	+7.6
Scenario		Sec01 Bristol, VA		Sec02 Salem, VA		Sec03 Richmond, VA		Global
		T (℃)	P (%)	T (℃)	P (%)	T (℃)	P (%)	Sea level (cm)
2050	A1FI	+2.52	+7.0	+2.47	+6.7	+2.52	+7.0	+15
	A1B	+2.14	+5.9	+2.10	+5.7	+2.14	+5.9	+13
	B1	+1.89	+5.2	+1.61	+5.0	+1.89	+5.2	+5
2100	A1FI	+5.96	+16.5	+5.85	+15.8	+5.96	+16.5	+46
	A1B	+4.00	+11.1	+3.92	+10.6	+4.00	+11.1	+35
	B1	+3.04	+8.4	+2.98	+8.0	+3.04	+8.4	+30

4.3. Sensitivity analysis

Sensitivity analysis was performed on SecT01, SecT02, and SecT03 to test the impact of climatic factors on the performance of typical flexible pavements from the three most sensitive climate regions in the United States. The sensitivity of pavement performance to climatic factors indices was calculated using Equation 3-6. The climatic factors for SecT01, SecT02, and SecT03 included hourly measurements of air temperature (℉), precipitation (in), wind speed (mph), sunshine percent (%), and the assumed groundwater level (5ft (= 1.524 m) from the pavements' surface). A 5% increase in these factors was added to hourly measurements of temperature, precipitation, wind speed and sunshine percentage one at a time to perform the sensitivity analysis. If hourly sunshine percentage exceeded 100% in the analysis, it was limited to 100% in that case. This means an original hourly sunshine percentage (CF) that is greater than 95.2% (=1/(1+0.05)) will round to 100% (CF + ΔCF). The hourly sunshine percentage would increase by less than 5% rather than 5%. However,

4. RESULTS AND DISCUSSIONS

an hourly sunshine percentage that is greater than 95.2% is rare in the investigated climatic records, thus it was generally considered that the underestimation is negligible. Moreover, a 5% increase in groundwater level meant that the distance between the groundwater level and the pavement surface was reduced by 5%. The pavement performance indices of the three sections (SecT01, SecT02, and SecT03) were predicted by MEPDG under a baseline scenario and modified climate with 5% increments. The sensitivity analysis was performed five times, applying a 5% increment on each climatic factor at a time. The pavement performance ($PP(t)$) indices included longitudinal cracking, transverse cracking, fatigue cracking, IRI, asphalt rutting and total rutting. Furthermore, the 5% increment was also applied to the seasonal variation of temperature (Equation 3-1).

An increase of 5% in climatic factors was chosen for the sensitivity analysis because 5% can approximately represent the medium emission scenario of 2050, which is likely to occur in the near future. For detailed study for Sec01, Sec02, and Sec03, both a 5% and 10% increment in climatic factors were considered in the sensitivity analysis. The 10% increment was used to represent the medium emission scenario in 2100, which was likely to occur in the more distant future.

The performance predictions excluded transverse cracking from the sensitivity analysis because no transverse cracking was predicted in any of the six sections over 40 years. This might indicate that the locations of the studied cases did not provide great daily temperature differences that are enough for the transverse cracking to develop, as transverse cracking is mainly associated with thermal stress. Moreover, an increase in the temperature was likely to reduce the amount of transverse cracking because the temperature increase might lead to less shrinkage of the asphalt concrete and consequently less transverse cracking. However, the increase in yearly/seasonal/daily temperature variations can potentially increase the chance of low temperature and thus increase the amount of transverse cracking. Nevertheless, no transverse cracking was observed in the prediction even when a 5% increment in seasonal temperature variation was added.

It was found that the most critical environmental factors included temperature, precipitation, and groundwater level. These factors were found to dominate certain distress types. Wind speed and sunshine percentage was not observed to have dominated any distress in the case studies. In most of the case studies, the magnitude of sensitivity to wind speed and sunshine percentage was much less than temperature, precipitation or groundwater level. Moreover, the sensitivity of performance indices to wind speed and to sunshine percentage was opposite, e.g. a 5% increase in wind speed can reduce all distress types and a 5% increase in sunshine percent can increase all distress types in the case studies. Therefore, their effects on pavement performance

were considered minor and to cancel each other out. Although future prediction of wind speed and sunshine percentage was unavailable, the sensitivity analysis suggested that their effects were negligible.

Most of the cases showed that temperature was the dominating climatic factor on performance indices compared to the rest (SecT01, SecT02, SecT03, Sec02, and Sec03). However, it was found that precipitation and groundwater level may also have significant influence under some circumstances (Sec01). As Sec01 was thinnest, this might indicate that thin pavements were more prone to distress brought in by climate change.

4.3.1. Temperature

A general conclusion could be drawn from the sensitivity analysis that temperature was the most influential parameter for pavement performance. Commonly, the impact of temperature dominated other environmental factors on pavement performance (see Appendix Figure A-26, Figure A-27, Figure A-28, Figure A-31, Figure A-32, Figure A-33, and Figure A-34). Moreover, both an increase in the average air temperature and seasonal temperature variation can be influential. In general, the impact of an increase in average temperature on pavement performance can be of the same magnitude of that due to temperature variation (see Appendix Figure A-26 to Figure A-28). From the investigated sections, it can be observed that some distress types may be more sensitive to temperature including longitudinal cracking, alligator cracking, and rutting. IRI and rutting from UGM was found to be less sensitive to temperature.

The sensitivity to temperature was found to be more significant for longitudinal cracking than for other distress types in some cases (see Appendix Figure A-28, Figure A-33, and Figure A-34), sometimes which was also observed by other researchers (Hoff and Lalague, 2010, Kim et al., 2005). However, the sensitivity of longitudinal cracking to temperature was also observed to be negligible or even negative sometimes (see Appendix Figure A-31 to Figure A-32) i.e. temperature increases may help to reduce longitudinal cracking. The MEPDG longitudinal cracking prediction was based on the tensile strain near the surface of the asphalt layer. On one side, the increasing temperature could reduce the resilient modulus of asphalt layers and thus reduce its ability to spread load. Consequently, tensile strain might become greater near the surface of asphalt layers and thus more longitudinal cracking could be expected (positive sensitivity). On the other side, increasing temperature could make the asphalt layers become less brittle. Therefore, initiation and developing of longitudinal cracking might be retarded, although the tensile strain increased (negative sensitivity). This suggests that an increase in temperature can either accelerate or retard the development of longitudinal cracking. The longitudinal cracking discussed in this study referred to the top-

down fatigue cracking i.e. longitudinal cracking as a result of low temperature was excluded.

A 5% increase in the temperature was found to have increased the amount of alligator cracking. Prediction of alligator cracking (bottom-up fatigue cracking) was based on the excessive tensile strain at the bottom of the asphalt layer. The increase in temperature might have reduced the resilient modulus of the asphalt layer and lead to worse distribution of traffic loading, resulting in higher tensile stress/strain at the bottom of the asphalt layer. Therefore, more alligator cracking may be expected.

Rutting was observed to be sensitive to temperature changes. As rutting from UGM was insensitive to temperature, the increase in rutting due to the increase in temperature was mainly from the asphalt layers. As temperature increased, the resilient modulus of the asphalt layers reduced. As the plastic strain is related to elastic strain by the asphalt rutting model (see Equation 2-23) in the MEPDG, the permanent deformation tends to increase. Furthermore, the increase in temperature could reduce the resilient modulus of asphalt layers and thus reduce its ability to spread loading. Therefore, stress and strain in asphalt layers may become greater and thus asphalt rutting becomes more.

Relatively, IRI was found to be less affected by temperature and other investigated environmental factors. Although IRI is related to cracking and rutting in practice (NCHRP, 2004), it seems the variations were not great enough to make a difference in the IRI.

4.3.2. Precipitation

Precipitation was found to have much less impact on distress compared to temperature for SecT01, SecT02, SecT03, Sec02, and Sec03. The 5% increase in precipitation had slight influence on IRI and rutting. Its influence was only noticeable in Sec01 where the amount of longitudinal and alligator cracking increased with an increase in the precipitation. This may due to the fact that precipitation increased the content of moisture in the subgrade together with the contribution of the high groundwater level thereby reducing the support, which changed the tensile stress distribution in the asphalt layers.

4.3.3. Groundwater level

The influence of the groundwater level rise was only noticeable for Sec01. The amount of alligator cracking, rutting, and IRI increased due to the rise in groundwater level and the amount of longitudinal cracking decreased. Sec01 was the thinnest among the sections with high groundwater level, thus the result may indicate that groundwater level rise can significantly impact the performance of thin flexible pavements. The assumption that the groundwater rise equalled the sea level rise probably reflects a worse situation of groundwater rise. In fact, the investigated sections were not close to the sea

and at high altitude, hence the assumption might exaggerate the impact of the rise in the sea level. However, as the impact of groundwater level may have significant impact on pavement performance, flexible pavements in low-altitude coastal areas, and in other areas where water may collect are susceptible to a sea level rise. Furthermore, groundwater level can be influenced by rainfall. It can be inferred that deterioration will be accelerated on pavements with high groundwater level from regions where precipitation will increase.

4.4. Performance predictions

Pavement performance of Sec01, Sec02, and Sec03 under various emission scenarios was analysed with MEPDG. The investigated pavement performance indices included longitudinal cracking, alligator cracking, total rutting, and IRI. Climate change projections made by MAGIC/SCENGEN were applied as the input of the framework (Figure 3-1). The projections included change in temperature, precipitation, and the sea level predicted under high/medium/low emission scenarios for 2050 and 2100.

Previous sensitivity analysis excluded transverse cracking from the analysis because no transverse cracking was predicted to appear for the investigated sections. Therefore, transverse cracking was excluded from the performance prediction. The effects of wind speed and sunshine percentage were excluded from the climatic factors because their influences on performance of the studied pavements were found to be insignificant and likely to cancel each other out (see Appendix Figure A-26 to Figure A-34). Climate change projections for 2050 and 2100 were chosen because 2050 symbolised the change in the near future and 2100 represented the greatest change in this century. A combination of local historical climatic records and climate change projections for 2050 or 2100 was performed to create possible future climate. As the duration of the local historical climatic records were typically approximately 10 years, they were modified and repeated four times to suit the assumed life span (4×10 years) of studied pavements to represent baseline climate. Therefore, rather than focusing on the creation of approximate future climate over 40 years and predict the future pavement performance based on that, the prediction focused on what will be the deterioration of a flexible pavement if it operates under a certain possible future climate. The latter method avoided the difficulty of the creation of a completely new possible future climate profile. The pavement performance prediction results can be found in the Appendix (Figure A-35 to Figure A-46).

In general, longitudinal cracking, alligator cracking and rutting can be more influenced by climate change compared to IRI, which was in accordance with the results from the sensitivity analysis. The longitudinal cracking prediction for Sec01 seemed to be little influenced by climate change (see

4. RESULTS AND DISCUSSIONS

Appendix Figure A-35). This is likely to be caused by the combined impact of temperature, precipitation, and groundwater. The influence of individual climatic factors on longitudinal cracking was found to be significant from the sensitivity study (see Appendix Figure A-29 and Figure A-30) but the combined effects did not have an impact. Furthermore, the assumption that the groundwater level rise equalled the sea level rise may overestimate the influence of sea water level rise on longitudinal cracking, which is particularly true due to the high altitude location of Sec01 (see Table 3-3). Therefore, the impact of sea level might be less and thus the impact of temperature and precipitation could dominate the change in longitudinal cracking i.e. climate change might cause significant increase in longitudinal cracking for Sec01. As it was difficult to relate the groundwater rise to the climate change, it was preferable for the effect of sea level to be considered rather than neglected. The change percentages of predicted performance indices under various climate change scenarios compared to the baseline scenario are presented in Table 4-2.

Although it is the increase in the groundwater level that is of concern, the actual groundwater level was also important for pavement performance. When the groundwater level was high, even a small increase in the groundwater level could cause significant additional deterioration.

Alligator cracking was found to increase with an increase in climate change indicators (2100 A1FI > 2100 A1B > 2100 B1> 2050 A1FI > 2050 A1B >2050 B1) (see Table 4-2). The impacts of temperature, precipitation, and groundwater level all had positive sensitivity to alligator cracking. Rutting in Sec01 was found to increase between approximately 6 − 24 % under various scenarios. The increase in rutting was mainly caused by the increase in temperature and groundwater level (see Appendix Figure A-29 and Figure A-30). The sensitivity of rutting to temperature and groundwater level was almost equally significant, especially for a higher increase in the inputs (10% compared to 5%, see Appendix Figure A-29 and Figure A-30). The increase in IRI of Sec01 was found to be less than 1.5% even under the highest emission scenario. Moreover, the increase in IRI was less than 1% under 2050 scenarios.

4. RESULTS AND DISCUSSIONS

Table 4-2 Change percentage of performance indices in year 40 as a result of climate change

Scenarios	2100 A1FI	2100 A1B	2100 B1	2050 A1FI	2050 A1B	2050 B1
Longitudinal cracking						
Sec01	-1.93%	-3.31%	-5.52%	-4.42%	-4.97%	1.66%
Sec02	-5.71%	-2.17%	-0.68%	0.14%	2.17%	2.72%
Sec03	197.41%	110.34%	76.72%	61.21%	50.86%	43.97%
Alligator cracking						
Sec01	52.02%	40.73%	34.68%	25.40%	22.98%	13.31%
Sec02	11.67%	10.12%	9.34%	8.56%	8.75%	8.17%
Sec03	55.83%	35.28%	26.11%	21.39%	17.78%	15.56%
Rutting						
Sec01	24.16%	17.68%	14.45%	10.83%	9.59%	5.85%
Sec02	32.82%	25.00%	21.37%	19.41%	18.16%	16.34%
Sec03	39.00%	25.00%	18.67%	15.17%	12.83%	11.17%
IRI						
Sec01	1.18%	1.30%	1.30%	0.83%	0.83%	0.18%
Sec02	4.74%	4.49%	4.25%	4.15%	4.20%	4.05%
Sec03	1.14%	0.82%	0.63%	0.51%	0.44%	0.38%

Unlike SecT1, SecT2, SecT3, Sec01, and Sec03, the longitudinal cracking of Sec02 decreased with an increase in climate change indicators (2100 A1FI > 2100 A1B > 2100 B1> 2050 A1FI > 2050 A1B >2050 B1> BL) (see Table 4-2). This might be caused by the dominating influence of temperature on longitudinal cracking with negative sensitivity. Alligator cracking and rutting in Sec02 were found to increase with an increase in climate change indicators. A significant increase in rutting of 16.34 – 32.82 % was observed in the result. The increase in roughness was greatest in Sec02 compared to Sec01 and Sec03 (see Table 4-2). Compared to Sec01, Sec02 was hardly influenced by the groundwater level, likely because the groundwater level of Sec02 was much lower (see Appendix Table A-23). Furthermore, the assumed groundwater level rise was not able to influence pavement performance.

The increase in longitudinal cracking due to climate change was greatest for Sec03 compared to the rest. All predicted distress types for Sec03 increased as a result of increases in climate change (2100 A1FI > 2100 A1B > 2100 B1> 2050 A1FI > 2050 A1B >2050 B1) (see Table 4-2). Again, this was

due to the fact that the influence of temperature dominated distress (see Appendix Figure A-33 and Figure A-34).

It can be concluded that the influence of temperature dominated pavement performance for all the three sections and the significance of temperature was far more than the impact of other environmental factors for Sec02 and Sec03 (see Appendix Figure A-31 to Figure A-34). Sensitivity analysis on SecT01, SecT02, and SecT03 (see Appendix Figure A-26 to Figure A-28) confirmed this conclusion. Furthermore, temperature variations may also significantly impact pavement performance. Unfortunately, daily/seasonal/annual temperature variations were not included in the performance predictions because there was no evidence to determine how much the variations can be. Furthermore, the temperature variations simply added extreme hot and cold hours to the climatic records in principle, i.e. increased the frequency of high and low temperature. In fact, the frequency of high temperature can also be increased with an increase in the average temperature (see Figure 3-11). Therefore, the increase in the average temperature can account for the extreme hot hours to some extent, although the extent was not strictly controlled.

4.5. Immediate maintenance effects modelling

4.5.1. Maintenance effects

The immediate maintenance effects models (Equation 3-7, 3-8) of three previously described interventions, namely thin overlay, thick overlay, and mill & fill, were validated using PMS data from VDOT. The data was selected to obtain IRI and rutting before and after the three interventions. A data mining process (described in 3.6.5) was applied to exclude data that was considered to be invalid (reasons described also in 3.6.5). After mining, 284 sections (each with data points of (IRI_{n0}, IRI_{n1}), (Rut_{n0}, Rut_{n1})) satisfied the selection criteria and could be used for the validation of maintenance effects models. The data sections mainly came from Interstate Route 81 and 77. Among these data points, three points were identified using Cook's D (> 0.7) (described in 3.6.6), which were considered too influential for the regression analysis. The selected data points, improvement of IRI and rutting, and calculated Cook's D can be found in the Appendix (see Table A-25, Table A-26, and Table A-27).

Statistics on the selected data revealed the mean and standard deviation of IRI and rutting immediately before (IRI_{n0} , Rut_{n0}), and after the maintenance (IRI_{n1}, Rut_{n1}), as well as their improvement (see Table 4-3). It can be observed that the immediate improvement of IRI was almost equivalent for Op2 (ΔIRI_n = 30.9 in/mi (≈0.488 m/km)) and Op3 (ΔIRI_n = 30.2 in/mi (≈0.477 m/km)), both of which were greater than that of Op1 (27.1 in/mi (≈0.428 m/km)). From Table 4-3, it can be seen that Op3 was performed on

4. RESULTS AND DISCUSSIONS

sections with greater roughness (IRI_{n0} = 86.3 in/mi ($\approx$1.36 m/km)). Op2 was found to have more capability for treating rutting because the improvement in rutting was greatest (ΔRut_n = 0.15 in (=3.81 mm); see Table 4-3).

Table 4-3 Statistics on performance indices before and after interventions and improvement (1 in/mi $\approx$ 0.0158 m/km)

Intervention	Op1 (thin overlay)		Op2 (overlay)		Op3 (mill & fill)	
Number of valid data points	114		45		122	
Performance indices	Mean (μ)	Standard deviation (σ)	Mean (μ)	Standard deviation (σ)	Mean (μ)	Standard deviation (σ)
IRI_{n0} (in/mi)	78.6	16.6	74.7	11.5	86.3	24.3
IRI_{n1} (in/mi)	51.5	10.7	43.6	8.7	56.1	9.8
ΔIRI_n (in/mi)	27.1	13.7	30.9	9.0	30.2	21.5
Rut_{n0} (in)	0.23	0.05	0.27	0.08	0.20	0.06
Rut_{n1} (in)	0.13	0.04	0.12	0.06	0.13	0.05
ΔRut_n (in)	0.10	0.05	0.15	0.07	0.07	0.05

Plots of ΔIRI_n versus IRI_{n0} and ΔRut_n versus Rut_{n0} are presented in the Appendix (Figure A-47 to Figure A-56). Linear regression lines were added and it was found that fair (0.37 – 0.84) R^2 values were obtained for the plots. Estimated regression factors are presented in Table 4-4. The regression factors were found to be comparable to a Swedish (a= 0.75, b = -24.8) (Djärf et al., 1995) and an American LTPP experience (a = 0.49, b = -82) (Hall et al., 2002). Hall et al. examined the maintenance effects of a thick overlay (5 in (=12.7 cm)) on flexible pavements. Factor b was considerably smaller in this study and this is likely to be because the thickness of the overlay in this study was much less.

Futhermore, it was observed that the thickness of the fill did not significantly affect the immediate maintenance effect on IRI and rutting for Op3 (see Appendix Figure A-55 and Figure A-56). However, it can be observed that data points of thicker overlay or fill are typically located in the upper part of the data cloud, implying that an influence of thickness existed (see Figure A-54). With an increase in the thickness of the overlay, the maintenance effects may be affected significantly, given pavement structure cannot have an influence on immediate maintenance effects (Morian et al., 1998). As argued before, although the linear regresssion model did not take overlay (or fill) thickness into consideration, it was still considered by the

4. RESULTS AND DISCUSSIONS

regression equations from the validation using in-situ data. The regression factors for Equation 3-7 and 3-8 are presented in Table 4-4.

Table 4-4 Results: regression factors for the immediate maintenance effects models (1 in/mi ≈ 0.0158 m/km and 1 in = 25.4 mm)

	IRI (in/mi)		Rutting depth (in)	
	a	b	c	d
Op1	0.6307	-22.491	0.5956	-0.0401
Op2	0.5234	-8.0962	0.5874	-0.0117
Op3	0.811	-39.74	0.4752	-0.0234

The immediate maintenance effects of the three interventions are plotted in Figure 4-1. The distribution of IRI and rutting before maintenance (the horizontal axis) was considered as normally distributed and their range was estimated with $\mu \pm 2\sigma$ (μ = mean; σ = standard deviation), which accounted for approximately 95% of values.

In general, it can be observed that Op2 had greater effects on IRI and rutting than Op1. When IRI before maintenance was less than 100 in/mi ($\approx$ 1.58 m/km), the effects of Op3 on IRI and rutting was least among the three interventions. However, Op3 could be used to address high IRI. Moreover, Op2 could be applied to address serious rutting problems.
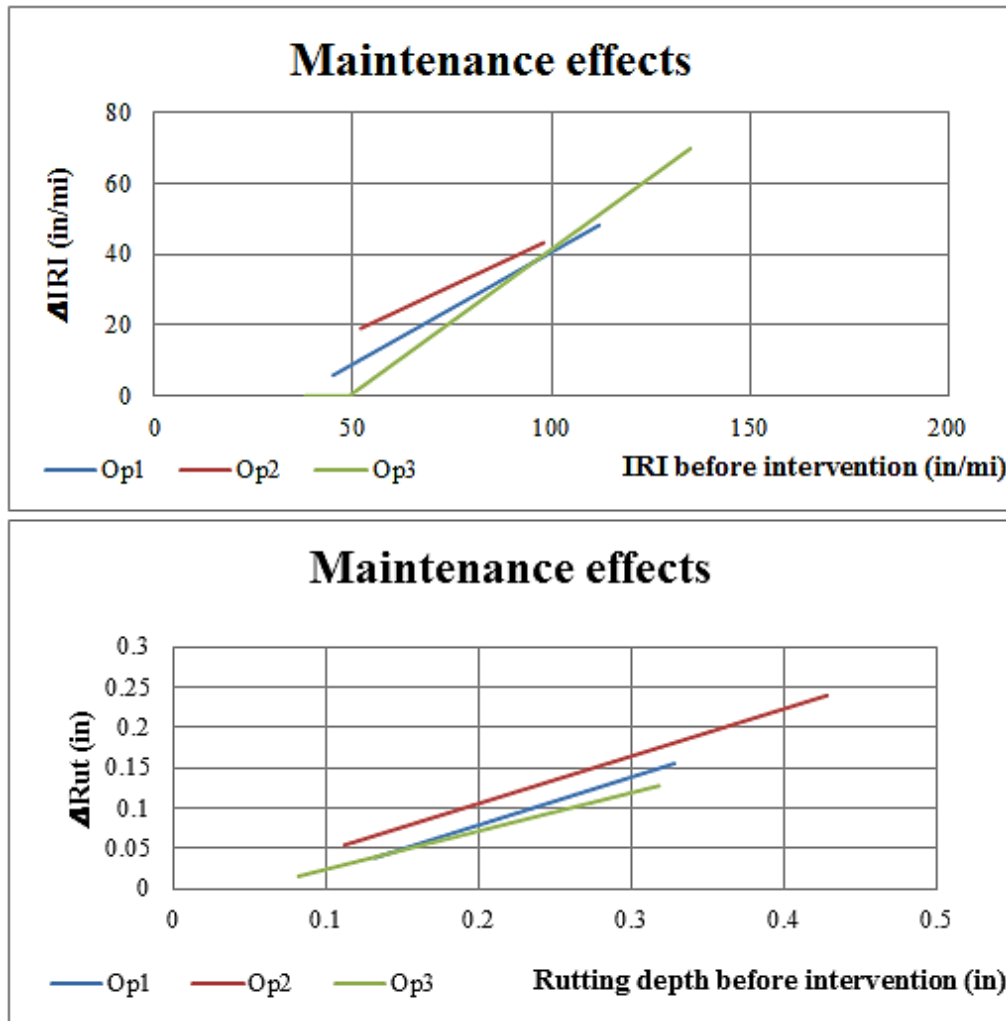
Figure 4-1 Immediate maintenance effects of Op1, Op2, and Op3

4.6. Maintenance optimisation and LCCA

Pavement performance predictions (under various climate change scenarios), maintenance effects, the maintenance optimisation algorithm (Equation 3-12 to 3-16) and selected components of LCC (as previously discussed in Section 3.7.2) were combined to obtain the results discussed in this part. IRI and rutting were used to characterise pavement performance and trigger maintenance when appropriate.

As previously described, the optimisation was assumed to be able to be performed in two ways. In the first way (Alternative 1), the maintenance interventions were optimised to achieve minimum agency costs. In principle, this reflected maintenance planning according to strict triggers, i.e. interventions were only applied when they had to be performed to prevent specification limits being breached. The most cost-effective intervention was then chosen to achieve minimum costs. In the second way (Alternative 2), the intervention optimisation was based on the minimisation of the total costs (agency and user costs). In Alternative 2, intervention was performed when it

126

was most useful. Maintenance might be performed in advance if it could reduce the total LCC. Furthermore, a "do nothing" Alternative (0) was added to represent a situation where no maintenance was performed. Climate change scenarios including 2100 A1FI, 2050 A1FI, 2050 A1B, and 2050 B1 were considered. Scenarios of 2050 represented situations in the near future and thus were considered in more depth. Furthermore, A1B and B1 scenarios in 2100 were neglected and only the 2100 A1FI was considered to represent the maximum climate change in this century.

4.6.1. Alternative 0

Without maintenance, the total LCC was found to increase with an increase in the climate change indicators for all three sections (see Figure 4-2, and Appendix Figure A-57 and Figure A-58). In fact, the increase in LCC was only because of the increase of IRI due to climate change. It was a partly coincidence that IRI increased with the increase in climate change indicators and not all scenarios followed this trend (see Table 4-2 IRI of Sec01 under 2100 A1FI scenario and Sec02 under 2050 A1B). These exceptions occurred because some pavement responses had negative sensitivity to certain environmental factors which might dominate in the distress predictions e.g. the effect of groundwater level on longitudinal cracking for Sec01 (see Appendix sensitivity analysis Sec01 5% and 10%).
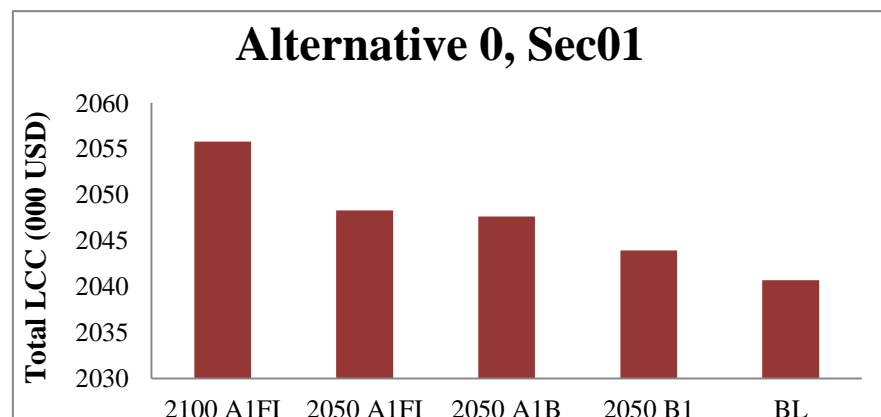
Figure 4-2 Sec01: Alternative 0, total LCC

Alternative 0 assumed no maintenance will be performed and thus LCC equalled user costs (agency costs = 0). In general, user costs of Alternative 0 increased as a result of climate change despite several exceptions. The increase in user costs was found to be relatively insignificant. For example, the maximum increase in user costs occurred under 2100 A1FI scenario and was less than 1.5% for all sections (0.74% for Sec01; 1.44% for Sec02, and 0.71% for Sec03).

The results indicated that only a minor increase in user costs may be induced by climate change. Exceptions may exist because IRI may not always increase as a result of climate change. Some environmental factors including

temperature and groundwater level were observed to have a negative relationship with longitudinal cracking (top-down fatigue cracking), which can have an influence on IRI. The increase was not observed to be significant in the case studies. This was because IRI was the only pavement performance index directly associated with user costs in this study and IRI was not found to be sensitive to environmental factors.

Longitudinal cracking (top-down fatigue cracking) was observed to have negative sensitivity to some environmental factors including temperature and groundwater level, and it can have an influence on IRI. The influence of groundwater level was found to be significant on longitudinal cracking in Sec01, which had a comparatively high groundwater level. Temperature was the only dominating environmental factor for distress in pavements without a water problem (low groundwater table). Therefore, it can be inferred that climate change will lead to an increase in LCC for flexible pavements in areas with low precipitation and low groundwater level.

4.6.2. Alternative 1

In principle, Alternative 1 considered a maintenance regime with strict specification limits (thresholds). Pavement maintenance was considered to be undertaken only when essential. The time between opening of the road and the first intervention was defined as the pavement's service life (Equation 2-29). IRI and rutting thresholds were set to trigger intervention levels. The maintenance triggers were set as in Table 4-5. Furthermore, details of each intervention in terms of costs, operation duration, and driver costs can be found in Table 4-5.

Table 4-5 Maintenance threshold values (NCHRP, 2004)

Performance indices	Threshold values
IRI	175 in/mi ($\approx$ 2.76 m/km)
Rutting	0.75 in ($\approx$ 19 mm)
Passenger costs	8 USD/hour
Truck driver costs	15 USD/hour
Free flow speed	65 mph ($\approx$ 105 km/hour)
WZ speed	35 mph ($\approx$ 56 km/hour)

An example of the results can be observed in Figure 4-3 and Figure 4-4. By comparison of the two figures, it can be seen that all the interventions are triggered when rutting reaches its threshold though, of course, remediation to address rutting also improves IRI. It can be seen that Op1 was chosen by optimisations as it was the most economical solution for minimising agency costs in this case.

4. RESULTS AND DISCUSSIONS
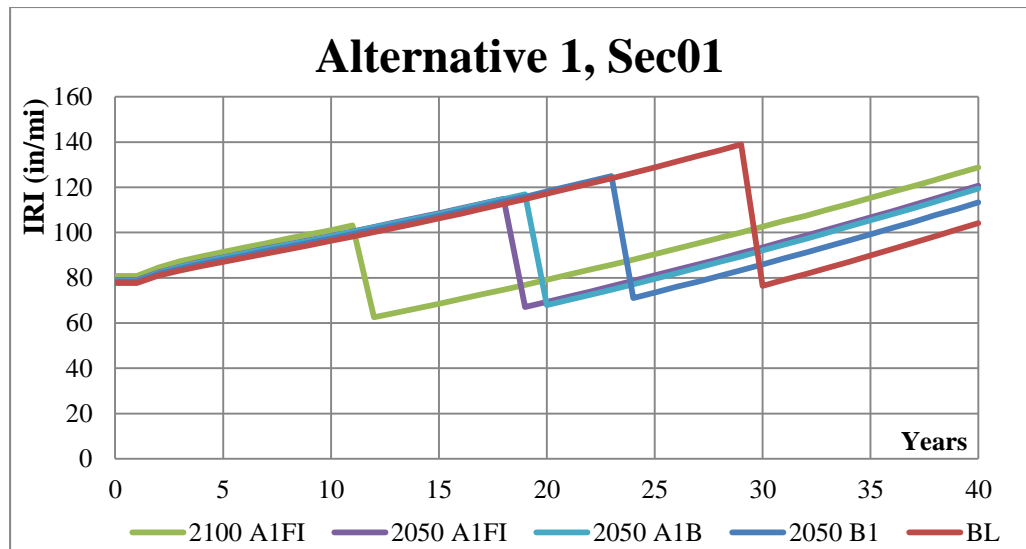
Figure 4-3 IRI curve with Alternative 1, Sec01 (1 in/mi ≈ 0.0158 m/km)
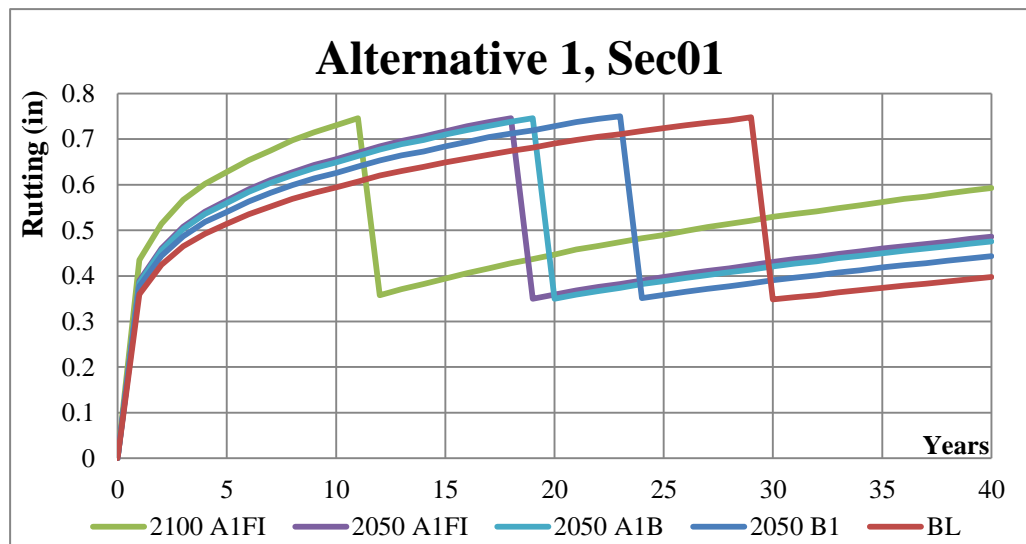
Figure 4-4 Rutting curve with Alternative 1, Sec01 (1 in = 25.4 mm)

Analyses were performed under several scenarios as shown in Figure 4-3 and Figure 4-4. Op1 was selected and performed only one time under all emission scenarios as the most economical solution to maintain Sec01 within serviceability. The service life of Sec01 under all emission scenarios was compared. It can be observed that service life was significantly influenced by climate change. Compared to the baseline, service life under 2100 A1FI scenario was reduced by 18 years. Even under 2050 A1B scenario, the service life was reduced by 10 years i.e. maintenance needed to be performed 10 years earlier than under the current climate conditions.

This situation occurred because the maintenance was triggered by rutting. IRI was found to be less sensitive to environmental factors compared to rutting. Therefore, reduction in service life triggered by IRI will not be as significant as rutting. Furthermore, it was related to the way rutting develops.

129

4. RESULTS AND DISCUSSIONS

It is typical that a flexible pavement ruts faster in the first few years after opening to traffic. The development rate decreases as time passes because of stabilisation of the material and post-compaction from traffic loadings. The shallow slope can lead to the service life of pavements determined by the rutting threshold being significantly influenced by rutting (Qiao et al., 2013b).

A similar result was observed for Sec02. The service life for the baseline it was 34 years and was reduced 16 years due to climate change under the 2100 A1FI scenario. For Sec03, IRI and rutting did not exceed maintenance thresholds under the baseline scenario and the service life was considered to be 40 years. Performance prediction under 2050 scenarios also did not trigger maintenance and thus the service life remained 40 years. Under this circumstance, climate change cannot reduce pavements' service life. Maintenance was triggered by rutting under the 2100 A1FI scenario and Op1 was triggered in year 30. To conclude, significant reduction in service life occurred under conditions in which rutting triggers maintenance.

As IRI was found to be much less influenced by climate change, maintenance triggered by IRI will not need to be performed in advance. Furthermore, the significant reduction in service life needs to be linked with the rutting problem i.e. a pavement's service life equals its design life and is not affected by climate change, if rutting cannot trigger maintenance over the pavement's life cycle. Therefore, flexible pavements that are prone to rutting problems may experience reduction in service life due to climate change, whereas those prone to roughness deterioration failure may be more resilient to climate change. For instance, flexible pavements with a high volume of heavy vehicles, thin structure, and weak subgrade are more likely to suffer from a reduced service life and earlier triggered maintenance.

Furthermore, climate sensitive distress types such as longitudinal cracking, if considered as maintenance criteria, may also cause reduction in pavements' service lives. It was found from the sensitivity analysis that longitudinal and alligator cracking may also be significantly influenced by climatic factors. Similar to rutting, reduction in pavement service life due to climate change can be expected if longitudinal or alligator cracking triggers maintenance. Although intervention threshold criteria are available for these distress types, they were not included in the optimisation because the optimisation problem would be large and a significant amount of additional computing time would be needed.

The reduction in pavements' service lives as a result of climate change may have influences on agency and user costs as a consequence. Agency costs were found to be increased as a result of climate change. The increase was because the earlier triggered intervention increased the NPV (Equation 2-33). Under the 2100 A1FI scenario, the agency cost increased approximately 6%

4. RESULTS AND DISCUSSIONS

and 5% compared to the baseline scenario for Sec01 (see Figure 4-5) and Sec02 (see Appendix Figure A-66) respectively.
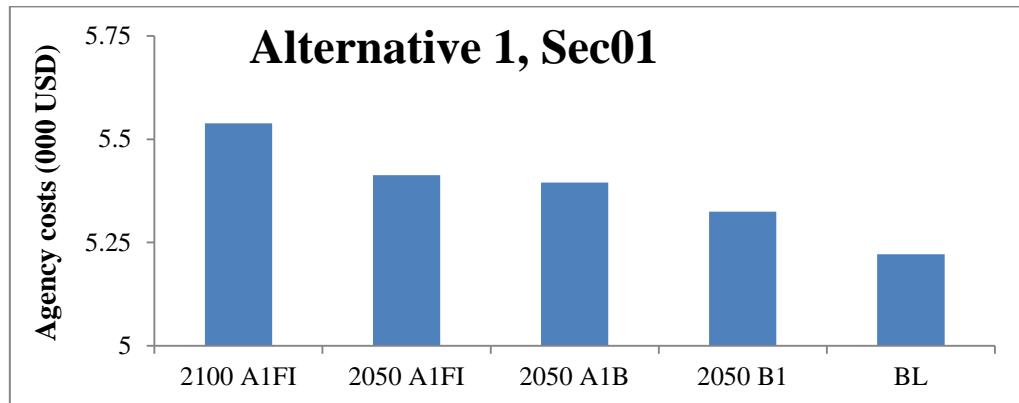
Figure 4-5 Agency costs for Alternative 1, Sec01 increased due to climate change

In contrast, user costs were observed to be reduced as a result of climate change (see an example in Figure 4-6). The reason was that earlier interventions kept the average IRI (see Figure 4-3) lower compared to the baseline, leading to lower user costs. User costs (VOC) were the highest of the cost components and dominated the total LCC (see Figure 4-7). Therefore, LCC could be reduced as a result of climate change. Similar results were also observed on Sec02.
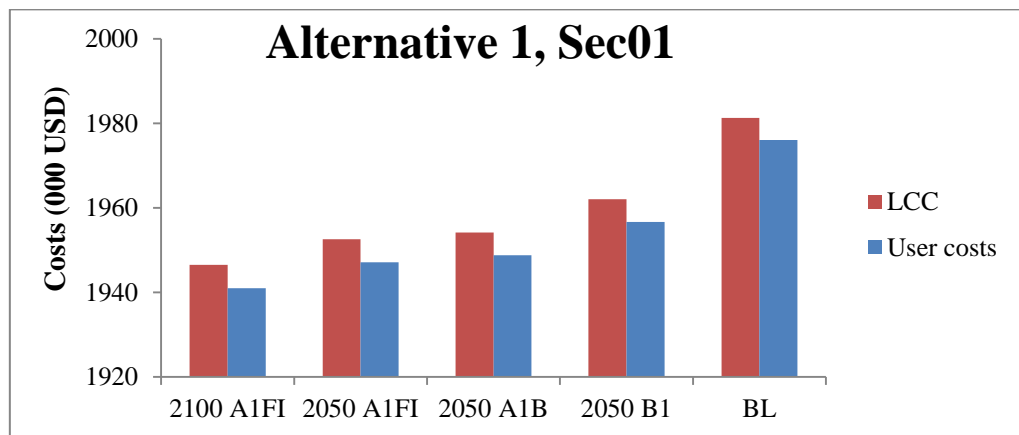
Figure 4-6 User costs and LCC for Alternative 1 Sec01 decreased due to climate

change

4. RESULTS AND DISCUSSIONS
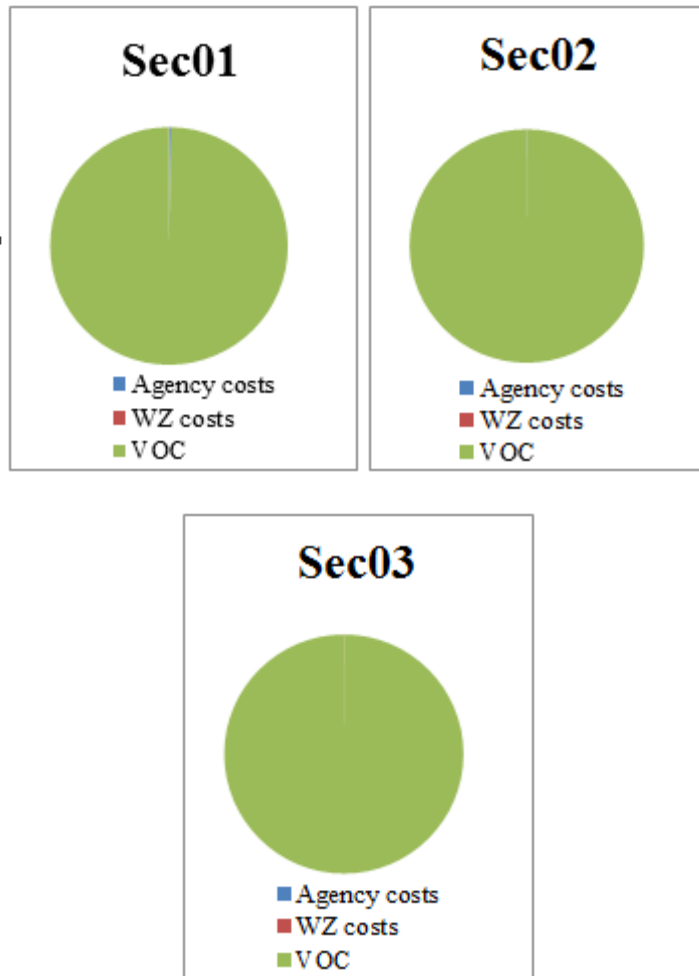
Figure 4-7 Costs components, Alternative 1, 2100 A1FI scenario

The proportion of WZ costs was negligible. The WZ costs were mainly from moving delays (from the slower movement of traffic through the WZ) for all the three sections and from queueing delay for Sec03. Of the three sections, only the traffic demand of Sec03 exceeded WZ capacity during maintenance operations (see Figure A-59, Figure A-60, and Figure A-61).

For Sec03, maintenance was only performed under the 2100 A1FI scenario. The earlier triggered maintenance reduced the IRI level and the subsequent user costs. For the remaining climate change scenarios, user costs equalled total LCC as no maintenance was performed. The increase in user costs was due to the increase in IRI as a result of climate change.

Figure 4-8 User costs and LCC for Alternative 1 Sec03 decreased due to climate change

The total LCC of Sec03 under 2050 A1FI, 2050 A1B, 2050 B1, and BL scenarios was found to increase with an increase in the climate change indicators (see Figure 4-8). This is because no maintenance was needed under these scenarios and the increase in total LCC was related to the increase in average IRI as a result of climate change. Maintenance was triggered for Sec03 under the 2100 A1FI scenario and decreased the average IRI level. Therefore, the total LCC reduced (see Figure 4-8).

4.6.3. Alternative 2

4.6.3.1. *Weighting factor*

One of the implications of the findings of Alternative 1 is that minimising LCC could be achieved by frequent maintenance intervention. Although likely to increase agency costs significantly, the reduction in user costs would be expected to be greater, given their greater magnitude (comparing values in Figure 4-6 with those in Figure 4-5). However, it is unrealistic in most jurisdictions to think that agencies would ever receive funds to achieve such frequent intervention. For this reason, an alternative approach for planning maintenance is also considered. This approach increases the importance of minimising agency costs by using a multiplication factor applied to the agency costs so that more realistic maintenance design can be made.

In this study, weighting factors of 1, 2, and 5 were used and the sensitivity of LCC to the weighting factors was analysed. Furthermore, a weight factor of 0.1 was added. The weighting factors can emphasis the importance of agency costs and may also account for overestimation or underestimation on costs. For instance, if user costs were overestimated, weighting factors greater than 1 can emphasise the agency costs and

4. RESULTS AND DISCUSSIONS

consequently reduce the importance of user costs so that the overestimation of the user costs can be corrected to some extent. Furthermore, the sensitivity of LCC to the weighting factor can be seen from comparison of LCC calculated with different weighting factors. The sensitivity study did not use the equation defined earlier (see Equation 3-6) but tested the variations in LCC due to the weighting factors.

A range was set for the lower boundary of IRI (IRI_{min} of Equation 3-15) to account for different serviceability levels after maintenance (defined by IRI). IRI_{min} can represent the minimum IRI i.e. best serviceability of a pavement section in its life cycle. According to the investigation on the three districts in Virginia, IRI after maintenance showed a wide range of distribution (see Figure 4-9). The distribution was also found to be associated with the type of intervention. However, the distribution ranged between 20 and 80 (in/mi) ($\approx$ 0.32 and 1.26 m/km) in general. Therefore, IRI_{min} of 30, 40, 50, 60, and 70 in/mi ($\approx$ 0.47, 0.63, 0.79, 0.95, 1.1 m/km respectively) was chosen to represent different levels of serviceability after maintenance, according to the 95 percentile investigated IRI levels after maintenance.
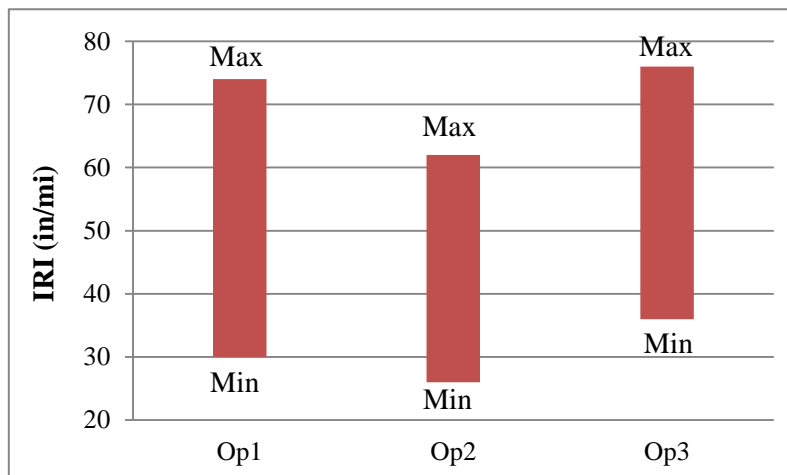
Figure 4-9 95 percentile IRI after maintenance for Op1, Op2, and Op3 from the three districts in Virginia (1 in/mi ≈ 0.0158 m/km)

The influence of the weighting factors on the LCC can be seen in Figure 4-10. There are 20 points on the figure and each point was obtained from an optimisation. For instance, an example of the optimised intervention strategy is shown in Figure 4-11 (see red arrow in Figure 4-10, the average IRI = 74.7 in/mi ($\approx$ 1.18 m/km)). The average IRI was calculated using Equation 3-17. To achieve the minimised LCC, Op2 needed to be performed in year 9 and Op1 in year 21. The corresponding IRI and rutting curves are also presented in Figure 4-11.

4. RESULTS AND DISCUSSIONS
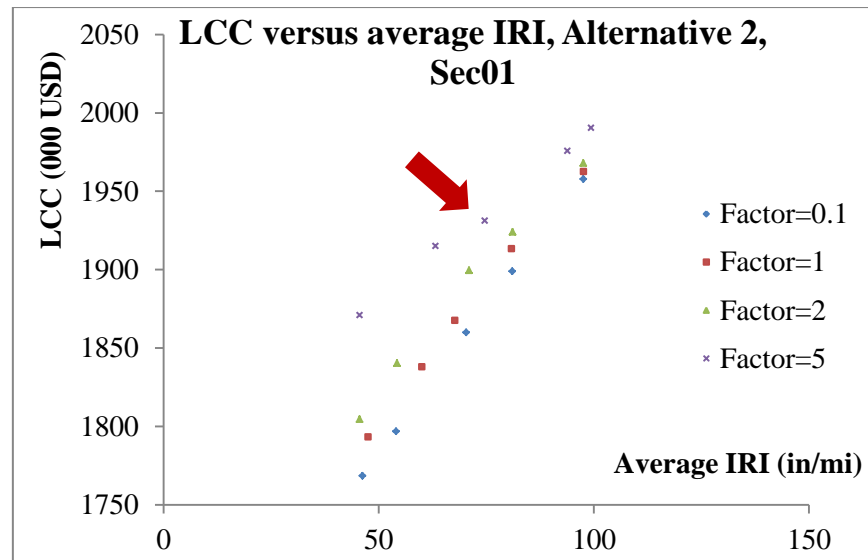
Figure 4-10 Influence of agency costs weighting factors on the LCC, Alternative 2, Sec01 (1 in/mi ≈ 0.0158 m/km)
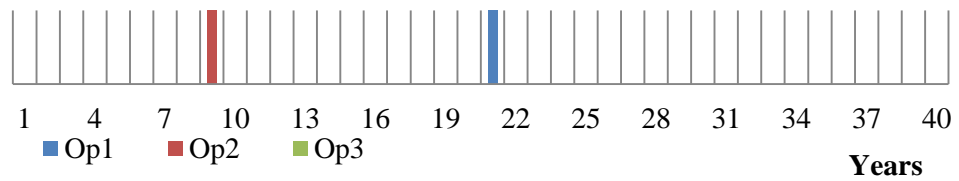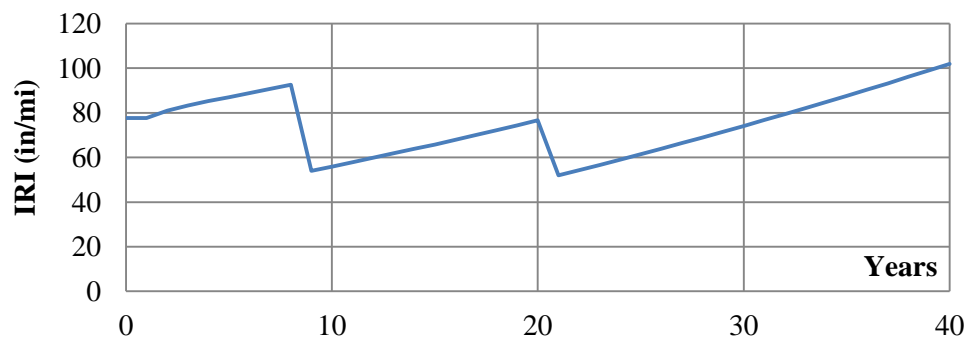
4. RESULTS AND DISCUSSIONS
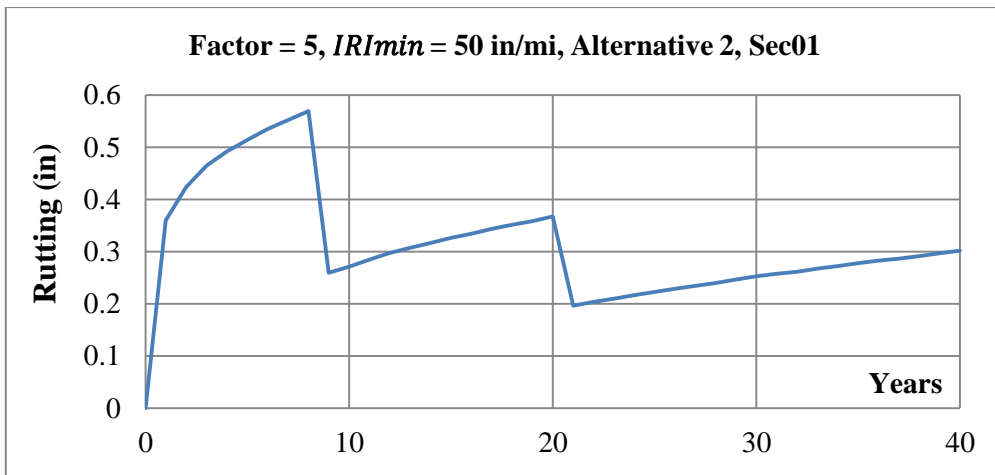
Figure 4-11 An example of optimised maintenance strategy (1 in/mi ≈ 0.0158 m/km, and 1 in = 25.4 mm)

It can be observed in Figure 4-10 that an approximately linear relation was obtained for the minimised LCC versus the average IRI. This indicated the importance of IRI to pavements' LCC. In principle, the LCC versus pavement performance curve was considered as a parabolic curve as described in Figure 3-17. However, the magnitude of agency costs was too low compared to user costs so that the balance between agency and user costs was dominated by user costs. Therefore, the curve looked approximately linear.

Clearly, the choice of weighting factor can have an influence on the optimised LCC. The weighting factors were only used in the optimisation and were not summed into the LCC. With a greater weighing factor, fewer interventions were applied and thus the average IRI was higher, leading to a higher user costs and LCC (see Figure 4-10). However, such increase was not considered to be significant in influencing the total LCC, considering the magnitude of the total LCC. For instance, the LCC of Sec01 was the most sensitive among the three sections to changes in the weighting factors. The LCC increased up to approximately 5% as the weighting factor changed from 1 to 5 (+400%). For Sec02 and Sec03, this impact was found to be even less (see Appendix Figure A-70 and Figure A-71). For Sec03, the impact was so little that the difference in LCC cannot be noticed easily. Therefore, the weighing factor was chosen to be 1 in further optimisations.

4.6.3.2. Results

Predictions of IRI and rutting under various climate change scenarios were evaluated by the intervention optimisation algorithm and the LCC was calculated. The weighting factor of agency costs was considered to be 1 as discussed earlier. For each section, the optimisation was performed 25 times, which meant 5 optimisations for each scenario including 2100 A1FI, 2050

136

4. RESULTS AND DISCUSSIONS

A1FI, 2050 A1B, 2050 B1, and BL. The 5 optimisations were distinguished by the IRI_{min} (the same values as used in weighting factor analyses). The results were originally in the form of a series of binary digits (see an example in Table A-38, Appendix). In order to have better visualisation on the results, they are shown in figures. Commonly, interventions were applied more frequently to maintain pavements at a better serviceability (as determined by the average IRI). The parameter IRI_{min} was used to control the average IRI and intervention strategies can be significantly affected by IRI_{min}. As user costs commonly dominate the LCC, it is logical to perform as many interventions as possible to reduce user costs but this is not applicable in practice because of the maximum treatability of interventions and maintenance budget constraints for agencies. Therefore, it can be observed in the results that interventions might be applied too often and too early when working to low levels of IRI_{min} (e.g. 30 or 40 in/mi ($\approx$ 0.47 or 0.63 m/km)), which is not possible to achieve in reality.

In general, it can be seen from the LCC comparison among the three maintenance assumptions that the LCC of pavements can be reduced, and their performance level increased by proper maintenance. The reduction in LCC among the three sections studied under Alternative 1 can be reduced by approximately 4.5% and 10% under Alternative 2. The average IRI can be reduced by approximately 20% and 30% by Alternative 1 and 2 respectively (see Figure 4-12). For each alternative, the scattered points indicated LCC-average IRI plots decided by different climate change scenarios including 2100 A1FI, 2050 A1FI, 2050 A1B, 2050 B1, and BL scenarios. It can be observed in all sections that plots of Alternative 0 and 1 were more divergent and these of Alternative 2 were more clustered (see Figure 4-12). This indicated that flexible pavements might be less impacted by climate change if maintained according to Alternative 2, in an optimised manner.
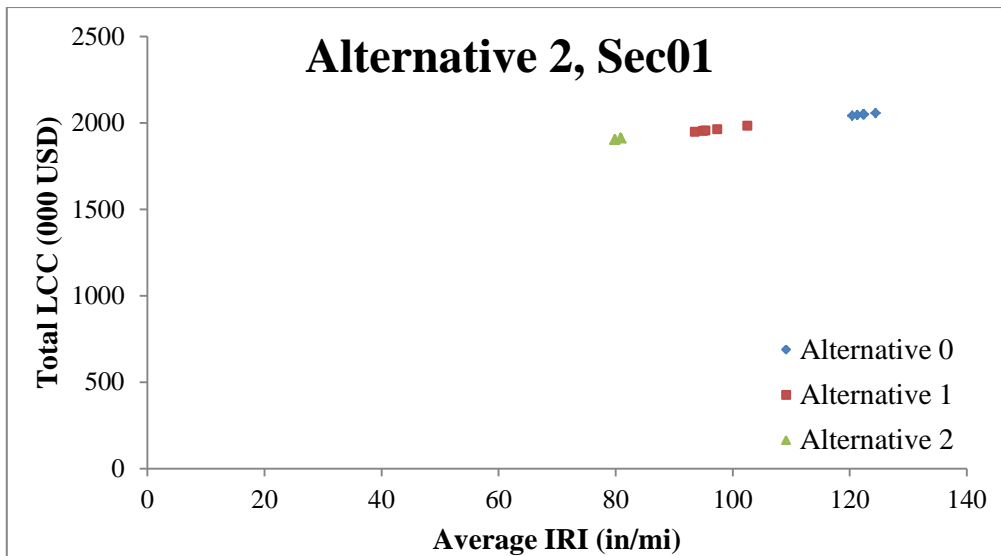
Figure 4-12 Total LCC versus average IRI for Sec01 (Alternative 2 under $IRI_{min} = 60$ in/mi (1 in/mi ≈ 0.0158 m/km))

User costs were the greatest element and dominated the LCC. This was observed for all sections, under all climate change scenarios and levels of IRI_{min}. The user costs might take up to 99% of the total costs (see Figure 4-13). Although it was assumed that the interventions were performed between $0 - 8$ a.m. (when the traffic volume was low), it was unlikely that the WZ or agency costs could have had a major impact on the LCC. Traffic volume exceeded demand only in Sec03 where queuing delay was involved. A queue was considered to form and the vehicle queuing delay was calculated (see Figure 4-14).
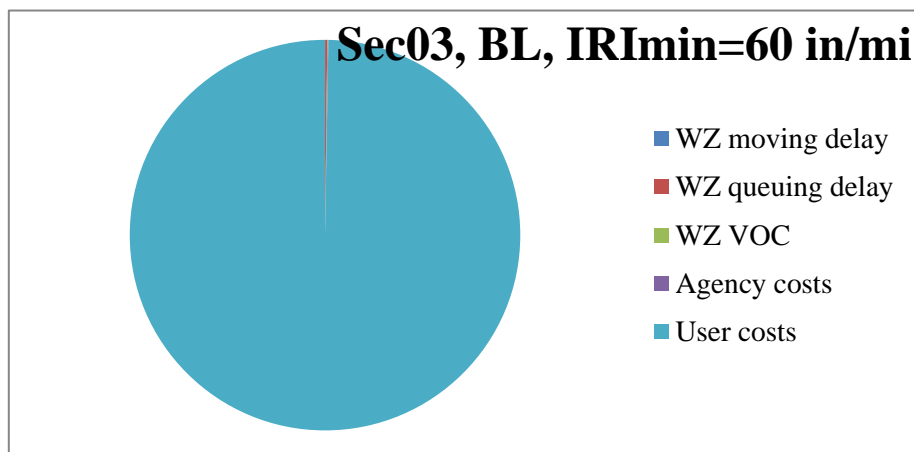
Figure 4-13 LCC components

4. RESULTS AND DISCUSSIONS
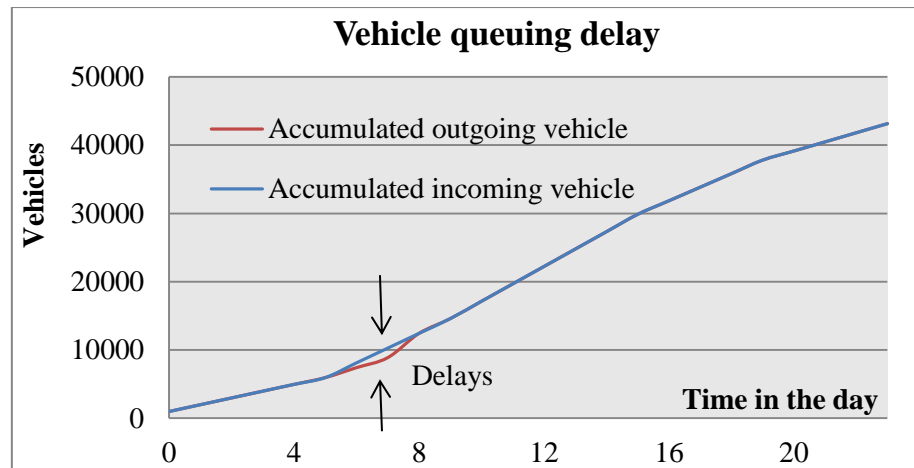
Figure 4-14 An example of vehicle queuing delay calculation

In the optimisation, the dominating part of the LCC, i.e. user costs, needed to be reduced. In this case, frequent interventions were expected, leading to significant reduction in the IRI. The upper boundary of IRI (IRI_{max}) was not important any more since the IRI curve was kept away from that maintenance threshold. The lower boundary of IRI (IRI_{min}) thus played an important role in determining the shape of the IRI curve.

Finally, the LCC versus average IRI was plotted for the three sections with the selected climate change scenarios (Figure 4-15). Approximately, the plots under each scenario followed a linear trend. The total costs versus pavement performance (in IRI) did not show a parabolic curve as in theory (see Figure 3-17). This was because the user costs were so large that they dominated the costs.

Moreover, it can be found that the linear trend under various climate change scenarios coincided. This indicated that climate change did not have significant impact on the total costs. This conclusion can only be drawn for pavements under Alternative 2 where pavement maintenance optimisation was supposed to be performed. For the others, the climate change might increase the LCC (Alternative 0) or decrease the LCC (Alternative 1). This implied that an optimised maintenance strategy can enhance the resilience of flexible pavements to climate change. Although more deterioration can be expected in the future, the LCC may not be increased if all maintenance interventions are planned and optimised.

4. RESULTS AND DISCUSSIONS

LCC-average IRI, Alternative 2, Sec01

Legend: ■ BL ▲ 2100 A1FI ✕ 2050 A1FI ✳ 2050 A1B ◆ 2050 B1

LCC-average IRI, Alternative 2, Sec02

Legend: ■ BL ▲ 2100 A1FI ✕ 2050 A1FI ✳ 2050 A1B ◆ 2050 B1

LCC-average IRI, Alternative 2, Sec03

Legend: ■ BL ▲ 2100 A1FI ✕ 2050 A1FI ✳ 2050 A1B ◆ 2050 B1
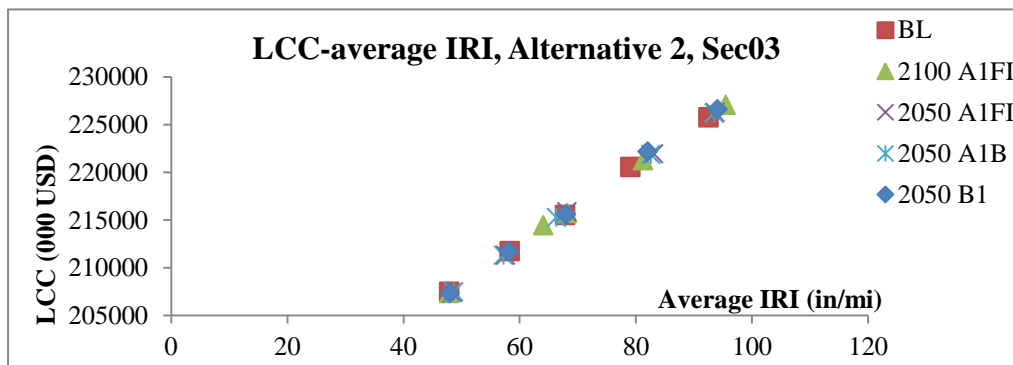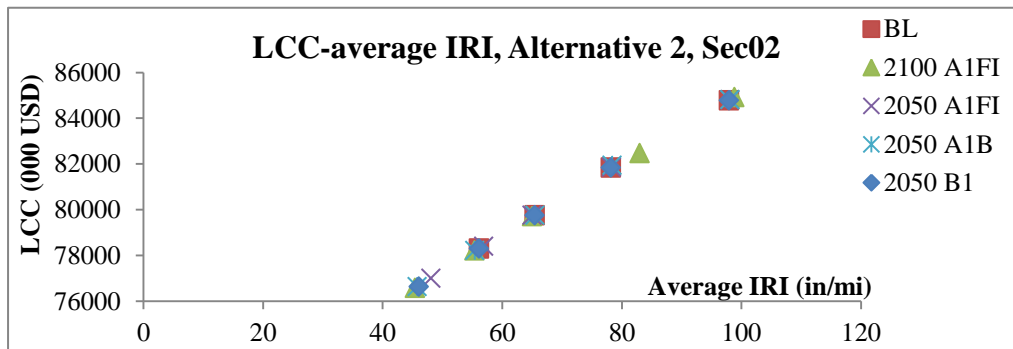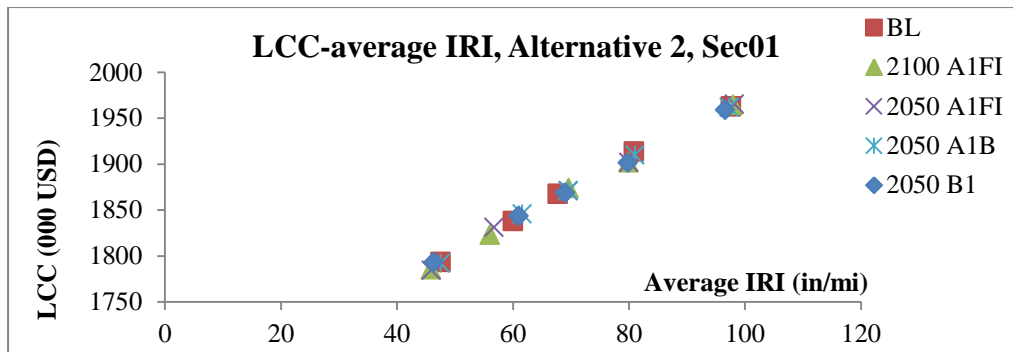
Figure 4-15 LCC-average IRI for Sec01, Sec02, and Sec03 (1 in/mi ≈ 0.0158 m/km)

Agency costs-average IRI, Alternative 2, Sec01

Legend: ■ BL ▲ 2100 A1FI ✕ 2050 A1FI ✳ 2050 A1B ◆ 2050 B1

140
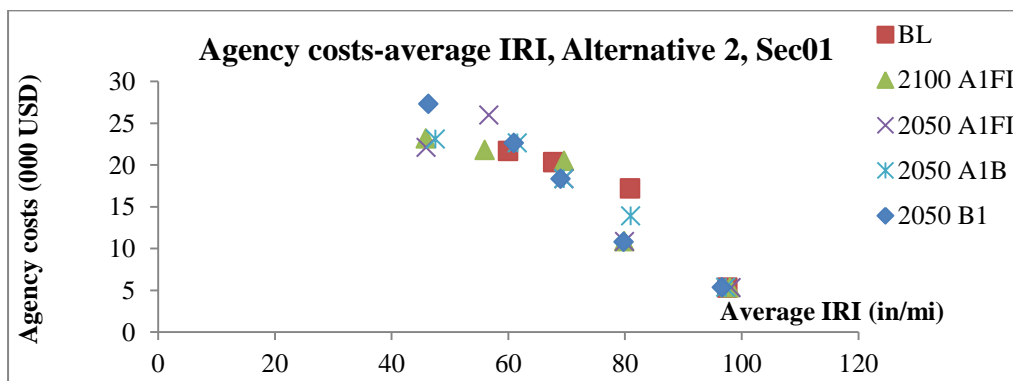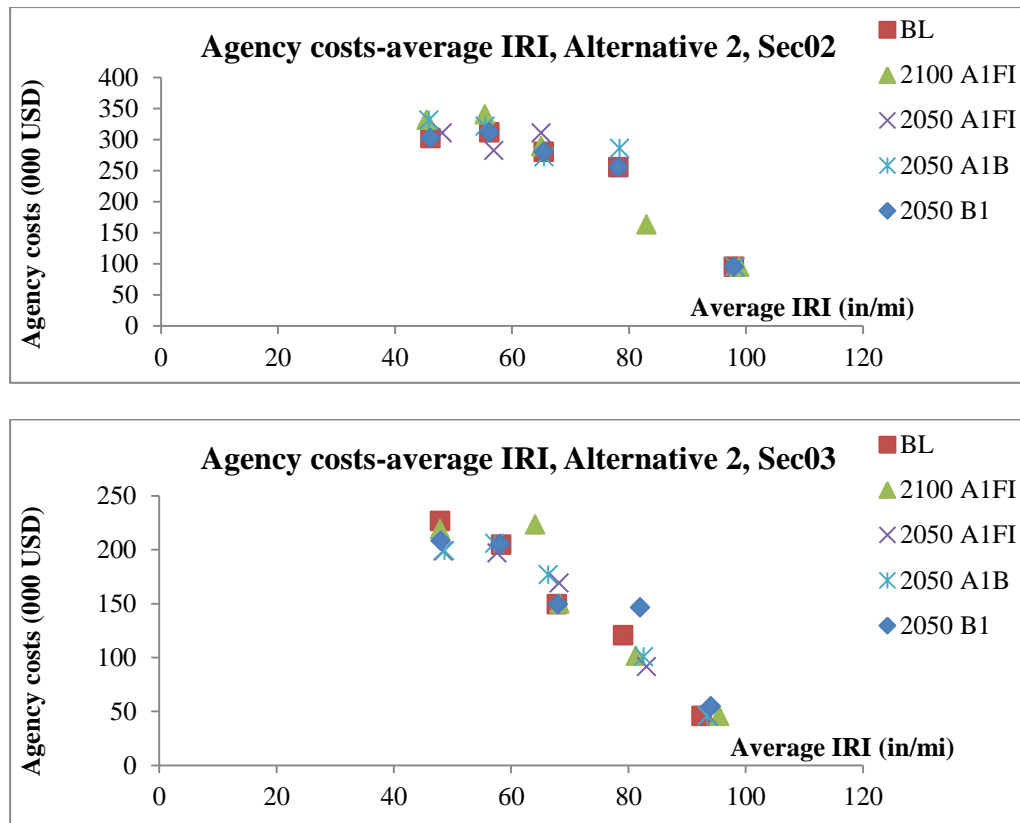
Figure 4-16 Agency costs-average IRI for Sec01, Sec02, and Sec03 (1 in/mi ≈ 0.0158 m/km)

Agency costs decreased when the average IRI was allowed to increase. The agency costs for Sec01 were least because the section was shortest so that the material costs for maintenance were lowest. Sec02 had greater agency costs than Sec03 because the road condition was worse (see Appendix Figure A-42 and Figure A-46) and thus interventions were performed more frequently.

It was not evidenced that agency costs could be associated with climate change under Alternative 2. Some pavement interventions might be performed in advance or delayed to adapt for the climate change and this resulted in minor decrease or increase in the agency costs.

4.6.4. Summary

Without maintenance (Alternative 0), it is likely that the total LCC of a flexible pavement section can increase due to climate change. In practice, some sections of a road network may not receive any maintenance treatments over the design life due to budget constraints. It can be inferred that climate change can result in an increase in the VOC for road users to drive on such sections. Although the increases were not found to be significant for the investigated sections, accumulations of such costs can make a difference for users especially when they drive over a long distance.

4. RESULTS AND DISCUSSIONS

Although the service lives of flexible pavements can be reduced, the total LCC for pavements with responsive maintenance according to strict intervention thresholds (Alternative 1) can be reduced as a result of climate change. This is because climate change may trigger corrective maintenance or rehabilitation earlier compared to the BL so that the average IRI will reduce, leading to reduction in user costs and LCC. However, the NPV of agency costs will increase. This finding also implied that responsive maintenance decision-making may not take full advantage of selected interventions. For instance, interventions triggered at the end of the pavement's design life, if is performed in advance, may reduce the average IRI and its subsequent LCC.

Alternative 2 can take full advantage of interventions so that the impact of climate change on the LCC is not significant. Furthermore, if optimisation can be applied in maintenance decision-making, the balance between agency and user costs can be almost unaffected by climate change.

5. CONCLUSIONS

A framework has been proposed to evaluate the impact of climate change on the performance, maintenance, and LCC of flexible pavements. The methodology of the framework was developed and its application was demonstrated by case studies. The framework included four parts:

- Investigation of climate change
- Pavement performance modelling
- Maintenance effects modelling
- LCCA and maintenance optimisation

The four parts were inter-connected and major links between different parts can be found from the detailed framework (Figure 3-1). Using this framework, the impact of climate change at a specific location on a defined pavement section (by structure, material, traffic, and length) with a particular maintenance regime (Alternative 0, 1, or 2) can be assessed in terms of deterioration, intervention strategy, and the subsequent LCC. From the case studies, the following conclusions can be drawn:

- Temperature, precipitation, and groundwater level were found to be influential on the performance of flexible pavements. Wind speed and sunshine percentage were found to be insignificant for pavement performance in all six investigated sections. Although current climate change predictions are not able to provide projections on wind speed or sunshine percentage for a specific location, their contributions to pavement deterioration are likely to be negligible.
- Longitudinal cracking, alligator cracking and rutting can be sensitive to climate change but the impact of climate change on IRI appears to be insignificant. However, the extent of the impact of climate change on pavement performance may be different from case to case because the distress can be impacted by the combination effects of temperature and moisture due to climate change.
- With a strict maintenance trigger, the increase in rutting due to climate change may result in a significant reduction in the service life of flexible pavements. The reduction in service life will occur under circumstances when environmentally sensitive distress (e.g. rutting) triggers maintenance under climate change scenarios. If maintenance is not triggered over a pavement's life cycle even under climate change scenarios, the service life will not be affected and will remain equal to the design life.
- Although climate change can reduce pavements' service life with strict maintenance triggers for environmentally sensitive distress, the LCC can be reduced. This is because earlier intervention can improve the overall IRI level of pavements and thus user costs can be dramatically

5. CONCLUSIONS

reduced. Usually, user costs dominate LCC. However, additional NPV for agency can be expected due to the earlier intervention.

- Considering maintenance optimisation as the future maintenance philosophy, climate change will not change road economy. Although pavement deterioration will be changed as a result of climate change, interventions can be performed in advance or delayed or changed to another type to adapt to climate change so that the most cost-effective maintenance strategies can be found. The applied maintenance optimisation can then cancel out the effects of climate change on the LCC and the balance between agency and user costs will not be disturbed.

The application of the framework can be flexible. Users can apply individual models of their own choice to substitute the models used in the case studies including models for climate change projection, pavement performance prediction, maintenance effects, LCC components, and maintenance optimisation. Other than these models, to assess the impact of climate change on flexible pavements for any location, the following information may be necessary:

- Local climate information at least including information on temperature, precipitation, and groundwater level to represent historical climate. Sensitivity analysis of pavement performance to wind speed and sunshine percentage is desirable to manage uncertainties due to the inability to predict these parameters. The climatic information may come from measurements or interpolation if local climatic measurements are unavailable.
- Information for pavement performance modeling, including traffic loadings (AADT and truck percentage), pavement layer thickness, and material properties. As maintenance optimisation can be significantly impacted by pavement performance, the accuracy of the prediction needs to be improved in order to achieve better maintenance decision-making. The accuracy of the performance prediction models can be improved by local calibrated model factors or advanced input level (e.g. dynamic modulus test instead of assumed resilient modulus).
- Local measurements of pavement performance indices before and after interventions. These data will be used in the validation of the immediate maintenance effects models. The more measurements, the more accurate the regression models can be. Obviously, the availability of such measurements may not be assured for every location. As the maintenance effects can be comparable between localities, existing maintenance effects models may be acceptable if local measurements are not available.

5. CONCLUSIONS

- Locally calibrated LCC components. With validated LCC models, the LCCA can better reflect local situations. However, the calibration process may be time- and resource-consuming while general models such as HDM-4 can achieve acceptable accuracy.

Based on this study, the following suggestions are provided to the road agencies to adapt to climate change:

- Based on the three investigated climatic regions in the U.S., the deterioration of flexible pavements is likely to be affected by climate change. Rutting will accumulate faster mainly due to the increase in temperature. Longitudinal and alligator cracking may increase or decrease as a result of a combination of increasing temperature and moisture. IRI was expected to increase in most cases (although not significantly).

- Without maintenance, the LCC of a flexible pavement is likely to have an insignificant increase as a result of climate change. The extra deterioration may lead to a greater rate of accidents which can be added to the LCC. Unfortunately, the accident costs were out of the scope of this study due to the difficulty in quantifying the costs of fatal and non-fatal accidents.

- If a flexible pavement is maintained with strict maintenance thresholds, maintenance may need to be performed much earlier but the LCC may be reduced as a result of climate change. Furthermore, this implies that strict triggers may not lead to the most cost-effective intervention strategy, because earlier performed maintenance may reduce the overall serviceability of the pavement and lead to less LCC.

- With strict maintenance thresholds, maintenance needs to be performed significantly earlier to adapt to climate change, which will increase the NPV. To avoid this, relaxation of maintenance thresholds for environmentally sensitive distress may allow agencies to avoid the extra costs but this will be by users incurring greater costs than otherwise, even if those user costs are less than at present.

- Flexible pavements with optimised intervention strategies overcame the effects of climate change on the LCC. It was observed that the time and type of intervention can be significantly influenced by pavement performance (due to climate change). This implies that maintenance optimisation relies on an accurate pavement performance model.

- As the optimisation tends to increase the frequency of interventions, budget constraints and weighting factors between agency and user costs need to be added into the optimisation to plan maintenance in a more realistic way.

5. CONCLUSIONS

6. FUTURE WORK

Although it may not significantly increase the LCC, climate change can impact maintenance decision-making. Therefore, future maintenance needs to take climate change into consideration. As a demonstrative study, the developed framework focused on the impact of climate change on flexible pavements at the section scale. The framework can have a wider application to evaluate the impact of climate change on a network of pavements so that resources can be utilised in a better way. For instance, pavement sections with weaker structure may be more prone to the impact of climate change, leading to greater costs for agency and users. Hence, priority needs to be given to interventions to be performed on these sections. Furthermore, network level assessment can provide proof for agencies to claim greater (or smaller) budgets. Therefore, climate (change) should be an essential part to be integrated into pavement decision-making. Unfortunately, few agencies have considered and applied this in practice.

Using the framework, the costs of climate change adaptation operations can be assessed with additional agency cost components. The operations may include an upgrade in asphalt binders, improvement in drainage, as well as increasing layer thickness. For instance, an upgrade in asphalt binders can reduce rutting and is desirable under a warmer climate. The costs of current binder and the upgraded binder can be added to the agency costs. Using the framework, pavement performance with current binder and upgraded binder can be analysed and compared under climate change scenarios. Furthermore, the LCC with current binder and upgraded binder can be compared. If appropriate, improvement in flexible pavement design can be made to adapt to climate change.

Improvement of the framework can improve the accuracy of the assessment and help to manage uncertainties. Generally, improvement can be considered in regard to the following aspects:

- As an indirect impact of climate change on pavements, the demographic change due to climate change needs to be considered to improve the framework, especially when the assessment is at the network level. For example, the deterioration of a flexible pavement near the sea may be accelerated by climate change if the traffic demand is kept constant. However, the traffic demand may be reduced because some residents may migrate inland due to an increase in the sea level. Hence the deterioration may not be accelerated considering the combining effects of direct and indirect impacts of climate change.
- Maintenance planning requires accurate prediction of pavement performance; thus the predictions under various climate scenarios need to be improved if possible. Firstly, updates on the climate

projections can provide environmental inputs of better quality for the performance predictions. The updates may include enhanced tools for generating the future climate and considerations of extreme weather conditions. Pavement deterioration due to climate change can be calculated more accurately, which is of importance in maintenance decision-making and LCC calculation. Secondly, locally calibrated performance prediction models can enhance the assessment.

- The long-term effects of maintenance can be added to improve maintenance effects modelling when they are available. The long-term effects can be studied with a longer period of pavement performance measurements by comparing the effects of a particular intervention of a controlled section and other sections. Alternatively, laboratory or full-scale testing e.g. accelerated pavement testing, can be used to simulate the long-term maintenance effects in a much shorter period (several decades in several months).

- As discussed, user costs dominate LCC and can impact LCC. Improvement in user costs modelling can benefit the framework. The improvement may include local calibration of user costs models and enhanced selection of user cost components. For instance, accident costs may make a difference in user costs and the accident rate is likely to be associated with climate change. Moreover, the weighting factor between agency and user costs needs to be considered and chosen carefully.

- Uncertainties were considered in this study in a qualitative way. The utilisation of various climate change scenarios represented the consideration of uncertainties in the climatic inputs. Moreover, the sensitivity analysis of pavement performance to weighting factors (in LCCA) helped to identify uncertainties and allow the assessment in a more realistic manner. Certainly, the uncertainties can be dealt with in a probabilistic way to some extent. For example, the same framework can be used but with probabilistic inputs such as a distribution of model factors. This needs to be based on profound knowledge of the probability of inputs. This is hard to achieve at present. Furthermore, uncertainties in data make this even more difficult.

- Although environmental costs are usually not considered in pavement construction and maintenance decision-making, it is being given more and more consideration. The environmental costs of roads occur with a long duration (pavement's life cycle) and on a large scale (worldwide). Furthermore, the emissions may contribute to environment deterioration including climate change. Recent research has used LCA as an environmental metric to quantify the impact of highways. In the future, integration of LCA into the framework can be

6. FUTURE WORK

a solution to incorporate environmental costs. In this way, sustainability in pavement design can be better achieved.

Certainly, other than climate, many things will be changed in the future even before the impact of climate change will show its full significance. Population and economic conditions may change from place to place, which is likely to affect the traffic demand, the inflation rate, and the perception of the value of time. In the pursuit of sustainability, public transport will be more developed and more people will adopt public transport services. Improvement in the fuel efficiency and reduction in emissions of vehicles will continue. Intelligent signalling systems have been used to control traffic flows and save time. New construction materials and maintenance treatments have been developing to improve serviceability and reduce costs and emissions. All of these and many other factors can be expected to impact agency and user costs. This means that the practical evaluation performed here may be no longer valid, but the overall framework should, with the new cost data, be valid and useful. In the future pavement design and management methods will need to be modified or changed if necessary to satisfy the requirements from the perspective of society, economy and the environment.

REFERENCES

AASHTO 1993. AASHTO GUIDE FOR DESIGN OF PAVEMENT STRUCTURES. American Association of State Highway and Transportation Officials (AASHTO).

AASHTO 1998. Method for determining the shear modulus and phase angle of asphalt binders. *In:* OFFICIALS, A. A. O. S. H. A. T. (ed.).

AASHTO 2009. Mechanistic-Empirical Pavement Design Guide (MEPDG). 1.100 ed.

ABRAMS, C., M. & WANG, J. J. 1981. Planning and Scheduling Work Zone Traffic Control. Federal Highway Administration.

AIERY, G. D. & YOUNG-KYU, C. 2002. State of the art report on moisture sensitivity test methods for bituminous pavement materials. *Road Materials and Pavement Design,* 3.4**,** 355-372.

ALLEN, J. J. & THOMPSON, M. R. 1974. Resilient Response of Granular Materials Subjected to Time-dependent Lateral Stresses. *Transportation Research Record: Journal of the Transportation Research Board***,** 1-13.

ANDREI, D., WITCZAK, M. W. & MIRZA, M. W. 1999. Development of a revised predictive model for the dynamic complex modulus of asphalt mixtures. *In:* MARYLAND, U. O. (ed.) *NCHRP 1-37.*

APEAGYEI, A. K. & DIEFENDERFER, S. D. 2011. Asphalt Material Design Inputs for User with the Mechanistic-Empirical Pavement Design Guide in Virginia. Virginia Center for Transportation Innovation and Research.

ARCHONDO, R. S. & FAIZ, A. 1994. Estimating Vehicle Operating Costs. Washington, D. C.: the World Bank.

ARNOLD, G. 2004. *Rutting of Granular Pavements.* PhD, University of Nottingham.

BARI, J. & WITCZAK, M. W. 2006. Development of a New Revised Version of the Witczak E* Predictive Model for Hot Mix Asphalt Mixtures (With Discussion). *Journal of the Association of Asphalt Paving Technologists,* 75**,** 381-423.

BARNETT, J. & ADGER, W. N. 2007. Climate change, human security and violent conflict. *Political Geography,* 26**,** 639-655.

BIRGISSON, B. & RUTH, B. E. 2007. Improving Performance Through Consideration of Terrain Conditions: Soils, Drainage, and Climate. *Transportation Research Record: Journal of the Transportation Research Board,* Volume 1819**,** 369-377.

BJERKLIE, D. M., MULLANEY, J. R., STONE, J. R., SKINNER, B. J. & RAMLOW, M. A. 2012. Preliminary Investigation of the Effects of Sea-Level Rise on Groundwater Levels in New Haven, Connecticut. *In:* 2012–1025, C. U. S. G. S. O.-F. R. (ed.).

BLACK, R., KNIVETON, D., SKELDON, R., COPPARD, D., MURATA, A. & SCHMIDT-VERKERT, K. 2008. Demographics and climate change: future trends and their policy implications for migration. University of Sussex, UK.

BORCHARDT, D. W., PESTI, G., SUN, D. & DING, L. 2009. Capacity and Road User Cost Analysis of Selected Freeway Work Zones in Texas. Texas Transportation Institute.

BROWN, O. 2008. Migration and Climate Change. International Organization for Migration.

BROWN, S. F. & HYDE, A. F. L. 1975. Significance of Cyclic Confining Stress in Repeated-load Triaxial Testing of Granular Materials. *Transport Research Record***,** 49 – 58.

BUTTLAR, W. G. & ROQUE, R. 1996. Evaluation of empirical and theoretical models to determine asphalt mixtures stiffness at low temperatures. *Asphalt Pavement Technology,* 65**,** 99-141.

CASEY, D. B., COLLOP, A. C., AIREY, G. D. & GRENFELL, J. R. Year. The effects non-uniform contact pressure distribution has on surface distress of

flexible pavements using a finite element method. *In:* 7th RILEM International Conference on Cracking in Pavements, 2012a. Springer, 347-357.

CASEY, D. B., COLLOP, A. C., GRENFELL, J. R. & AIREY, G. D. 2012b. Stress Intensity Factors at the Tip of a Surface Initiated Crack Caused by Different Contact Pressure Distributions. *Procedia-Social and Behavioral Sciences,* 48**,** 733-742.

CEBON, D. 1989. Vehicle-Generated Road Damage: A Review. *Vehicle system dynamics,* 18.1-3**,** 107-150.

CEYLAN, H., SCHWARTZ, C. W., KIM, S. & GOPALAKRISHNAN, K. 2009. Accuracy of Predictive Models for Dynamic Modulus of Hot-Mix Asphalt. *JOURNAL OF MATERIALS IN CIVIL ENGINEERING,* 21**,** 286-293.

CHAN, W., FWA, T. & TAN, C. 1994. Road‐Maintenance Planning Using Genetic Algorithms. I: Formulation. *J. Transp. Eng.,* 120**,** 693‐709.

CHARLSON, R. J., SCHWARTZ, S. E., HALES, J. M., CESS, R. D., COAKLEY, J. J., HANSEN, J. E. & HOFMANN, D. J. 1992. Climate forcing by anthropogenic aerosols. *Science,* 255(5043)**,** 423-430.

CHATTI, K. & ZABAAR, I. 2012. Estimating the Effects of Pavement Condition on Vehicle Operating Costs. NCHRP

CHENG, Z., QIAO, Y. & GUO, B. 2015. Imperfect Maintenance Model of Pavement Based On Markov Decision Process. *The Ninth International Conference on Mathematical Methods in ReliabilityThe Ninth International Conference on Mathematical Methods in Reliability.* 1-4 Jun 2015, Tokyo, .

CHESHER, A. & HARRISON, R. 1987. Vehicle Operating Costs: Evidence from Developing countries. *In:* BANK, W. (ed.) *The Highway Design and Maintenance Standard Series.*

CHIEN, S. I.-J., GOULIAS, D. G., YAHALOM, S. & CHOWDHURY, S. M. 2002. Simulation-Based Estimates of Delays at Freeway Work Zones. *Journal of Advanced Transportation,* 36**,** 131 – 156.

CHINOWSKY, P., SCHWEIKERT, A., STRZEPEK, N., MANAHAN, K., STRZEPEK, K. & SCHLOSSER, A. 2011. Adaptation advantage to climate change impacts on road infrastructure in Africa through 2011. *In:* RESEARCH, W. I. F. D. E. (ed.) *Working paper.*

CHITTURI, M. V., BENEKOHAL, R. F. & KAJA-MOHIDEEN, A. 2008. Methodology for Computing Delay and User Costs in Work Zones. *Transportation Research Record: Journal of the Transportation Research Board,* 2055**,** 31-38.

CHRISTENSEN JR, D. W., PELLINEN, T. & BONAQUIST, R. F. 2003. HIRSCH MODEL FOR ESTIMATING THE MODULUS OF ASPHALT CONCRETE. *Journal of the Association of Asphalt Paving Technologists,* 72**,** 97-121.

CRISPINO, M. & NICOLOSI, V. 2001. Temperature Analysis in Prediction of the Rutting of Asphalt Concrete Bridge Pavements. *Road Materials and Pavement Design,* 2**,** 403-419.

CROLL, J. 1864. Climate and time. *Philos. Mag.,* 28.

CRRI 1985. Road user cost study in India. New Delhi.

DANIELS, G., DAVID, R. E. & STOCKTON, W. R. 1999. Techniques for manually estimating road user costs associated with construction projects. Texas Transportation Institute, Texas A & M University.

DAWSON, A. 2014. *Anticipating and Responding to Pavement Performance as Climate Changes*, Springer.

DAWSON, A. & KOLISOJA, P. 2006. Managing Rutting in Low Volume Roads. *In:* 3, R. (ed.) *Roadex III Project*

DAWSON, A. R. 2008. Rut accumulation and power law models for low-volume pavements under mixed traffic. *Transportation Research Record: Journal of the Transportation Research Board,* 2068.1**,** 78-86.

DAWSON, A. R. & CARRERA, A. 2010. Report 11 – Overall Advice & Summary *Pavement Performance & Remediation Requirements following Climate Change.* Nottingham: University of Nottingham.

DEHLEN, G. L. 1969. *The Effect of Non-linear Material Response on the Behaviour of Pavement Subjected to Traffic Loads.* University of California.

DJ RF, L., MAGNUSSON, R., LANG, J. & ANDERSSON, O. 1995. Road Deterioration and Maintenance Effects Models in Cold Climates. Stockholm: Swedish Road and Transport Research Institute.

DONGRE, R., MYERS, L., D'ANGELO, J., PAUGH, C. & GUDIMETTLA, J. 2005. Field Evaluation of Witczak and Hirsch Models for Predicting Dynamic Modulus of Hot-Mix Asphalt. *Journal of the Association of Asphalt Paving Technologists,* 74**,** 381-442.

DRUMM, E. C., REEVES, J. S., MADGETT, M. R. & TROLINGER, W. D. 1997. Subgrade Resilient Modulus Correction for Saturation Effects. *J. Geotech. Geoenviron. Eng,* 123(7)**,** 663–670.

EL-BADAWY, S., BAYOMY, F. & AWED, A. 2012. Performance of MEPDG Dynamic Modulus Predictive Models for Asphalt Concrete Mixtures: Local Calibration for Idaho. *JOURNAL OF MATERIALS IN CIVIL ENGINEERING,* 24**,** 1412–1421.

ELNASRI, M., AIREY, G. & THOM, N. 2013. Experimental Investigation of Bitumen and Mastics under Shear Creep and Creep-Recovery Testing. *Airfield and Highway Pavement 2013@ sSustainable and Efficient Pavements***,** 921-932.

ELNASRI, M., THOM, N. & AIREY, G. 2014. Experimental study of binder-filler interaction using the modified multiple stress-strain creep recovery test. *Transport Research Arena, Paris.*

FERREIRA, A., PICADO-SANTOS, L. & ANTUNES, A. 2002. A Segment-linked Optimization Model for Deterministic Pavement Management Systems. *The International Journal of Pavement Engineering,* 3**,** 95-105.

FLINTSCH, G. W. & CHEN, C. 2004. Soft computing applications in infrastructure management. *Journal of Infrastructure Systems,* 10**,** 157-166.

GIDEL, G. 2001. A new approach for investigating the permanent deformation behavior of unbound granular material using the repeated load triaxial apparatus. *In:* CHAUSSÉES, B. D. L. D. P. E. (ed.) *RÉF. 4359.*

GIUSTOZZI, F., CRISPINO, M. & FLINTSCH, G. 2012. Multi-attribute life cycle assessment of preventive maintenance treatments on road pavements for achieving environmental sustainability. *The International Journal of Life Cycle Assessment,* 17**,** 409-419.

GOLABI, K., KULKARNI, R. & WAY, G. 1982. A statewide pavement management system. *Interfaces,* 12**,** 5-21.

GREENWOOD, I. D. & CHRISTOPHER, R. B. 2003. HDM-4 Fuel Consumption Modelling

HALL, K. T., CORREA, C. E. & SIMPSON, A. L. 2002. LTPP Data Analysis: Effectiveness of Maintenance and Rehabilitation Options. *NCHRP Web Document 47 (Project 20-50[3/4]): Contractor's final report.*

HDMR 1995. Modelling Road Deterioration and Maintenance Effects in HDM-4. *In:* MANAGEMENT, H. D. A. (ed.).

HICKS, R. G. 1970. *Factors Influencing the Resilient Properties of Granular Materials.* University of California.

HICKS, R. G., SEEDS, B. S. & PESHKIN, D. G. 2000. Select a Preventive Maintenance Treatment for Flexible Pavements. Prepared for Foundation for Pavement Preservation ed. Washington, D.C.: FHWA.

HOFF, I. & LALAGUE, A. 2010. Pavement Performance of Remediation Requirements following Climate Change (online). *Report No.7, P2R2C2 projec.*

HOSSAIN, M. S. 2010. Characterization of Unbound Pavement Materials From Virginia Sources for Use in the New Mechanistic-Empirical Pavement Design Procedure

HOUGHTON, N. & STYLES, E. 2002. Future thinking: exploring future scenarios for climate change and effects on the National Highway System. *25th Australasian Transport Research Forum (ATRF).* Canberra.

HPMS 2000. Procedures for Estimating Highway Capacity. *In:* ADMINISTRATION, F. H. (ed.) *HPMS field manual.*

HUANG, Y. & PARRY, T. 2014. *Pavement Life Cycle Assessment.*

HUANG, Y. H. (ed.) 2004. *Pavement Analysis and Design*: Pearson Education Inc.

IHS, A. & SJ GREN, L. 2003. An Overview of HDM-4 and the Swedish Management System (PMS). *In:* (VTI), S. N. R. A. T. R. I. (ed.).

IMBRIE, J. & IMBRIE, J. Z. 1980. Modeling the Climatic Response to Orbital Variations. *Science,* 207.

INSTITUTE, C. R. R. 1982. Road User Cost Study in India. New Delhi, India.

IPCC. 2007. Climate Change 2007: Synthesis Report. Contribution of Working Groups I, II and III to the Fourth Assessment Report of the Intergovernmental Panel on Climate Change.

IPCC 2013. Climate Change 2013: The Physical Science Basis. Contribution of Working Group I to the Fifth Assessment Report of the Intergovernmental Panel on Climate Change. Cambridge, United Kingdom and New York, NY, USA: Cambridge University Press.

ISOHDM 1995. Modelling Road Deterioration and Maintenance Effects in HDM-4. *International Study of Highway Development and Management Tools, RETA 5549-REG Highway Development and Management Research, Final Reports.*

JOHANNS, M. & CRAIG, J. 2002. Pavement Maintenance Manual. Nebraska Department of Roads.

KANDHAL, P. S. & COOLEY, J. R. 2003. Accelerated Laboratory Rutting Tests: Evaluation of the Asphalt Pavement Analyzer. *In:* NCHRP (ed.).

KARAMMES, R. A. & LOPEZ, G. O. 1992. Updated Short-Term Freeway Work Zone Lane Closure Capacity Values. Federal Highway Administration.

KERALI, H. G. R., ODOKI, J. B. & STANARD, E. E. 2006. Overview of HDM-4. *In:* MANAGEMENT, I. S. O. H. D. A. (ed.) *Highway Development and Management Series.*

KIM, S., CEYLAN, H. & HEITZMAN, M. Year. Sensitivity Study of Design Input Parameters for Two Flexible Pavement Systems Using the Mechanistic-Empirical Pavement Design Guide. *In:* Mid-Continent Transportation Research Symposium, 2005 Iowa, USA.

KIM, T., LOVELL, D. J. & PARACHA, J. 2000. A New Methodology to Estimate Capacity for Freeway Work Zones. *2001 Transportation Research Board Annual Meeting.* Washington D. C.

KORKIALA-TANTTU, L. 2008. *Calculation method for permanent deformation of unbound pavement materials.* Doctor of Science in Technology (Doctor of Philosophy), Helsinki University of Technology.

KORKIALA-TANTTU, L., LAAKSONEN, R. & T RNQVIST, J. 2003. Effect of the spring and overload to the rutting of a low-volume road. *HVS Nordic research.* Helsinki, Finland.

LAMPTEY, G., LABI, S. & LI, Z. 2008. Decision support for optimal scheduling of highway pavement preventive maintenance within resurfacing cycle. *Decision Support Systems,* 46**,** 376-387.

LEKARP, F., ISACSSON, U. & DAWSON, A. 2000a. State of the art. I: Resilient Response of Unbound Aggregates. *Journal of Transportation Engineering,* 126**,** 66-75.

LEKARP, F., ISACSSON, U. & DAWSON, A. R. 2000b. State of art. 2: Permanent strain response of unbound aggregates. *ASCE J. Transportation Eng'g,* 126 (1)**,** 76-84.

LI, Q., LESLIE, M. & SUE, M. 2011. The Implications of Climate Change on Pavement Performance and Design. Delware University Transportation Center.

LONG, F. M. 2001. *Permanent Deformation of Asphalt Concrete Pavements: a Nonlinear Viscoelastic Approach to Mix Analyses and Design.* PhD, University of California, Berkeley.

LOULIZI, A., FLINTSCH, G. W., AL-QADI, I. L. & MOKAREM, D. 2006. Comparing resilient modulus and dynamic modulus of hot-mix asphalt as material properties for flexible pavement design. *Transportation Research Record: Journal of the Transportation Research Board,* 1970**,** 161-170.

LYTTON, R. L., SHANMUGHAM, U. & GARRETT, B. D. 1983. DESIGN OF ASPHALT PAVEMENTS FOR THERMAL FATIGUE CRACKING.

MALLELA, J. & SADASIVAM, S. 2011. Work Zone Road User Costs: Concepts and Applications

MANNERING, F. L., WASHBURN, S. S. & KILARESKI, W. P. 2009. *Principles of Highway Engineering and Traffic Analysis*, John Wiley & Sons, Inc.

MCDONALD, B. 2002. A Teaching Note on Cook's Distance – a Guideline. *Research Letters in the Information and Mathematical Sciences,* 3, 127 - 128.

MEMMOTT, J. L. & DUDEK, C. L. 1982. A Model to Calculate the Road User Costs at Work Zones. Texas Texas Transportation Institute.

MEYER, M., FLOOD, M., DORNEY, C., LEONARD, K., HYMAN, R. & SMITH, J. 2013. Synthesis of Information on Projections of Climate Change in Regional Climates and Recommendation of Analysis Regions. National Cooperative Highway Research Project.

MILLER, J. S. & BELLINGER, W. Y. 2003. Distress Identification Manual for the Long-Term Pavement Performance Program. Federal Highway Administration.

MILLS, B. N., TIGHE, S. L., ANDREY, J., SMITH, J. T. & HUEN, K. 2007. Implications of Climate Change for Pavement Infrastructure in Southern Canada. *Final technical report*.

MILLS, B. N., TIGHE, S. L., ANDREY, J., SMITH, J. T. & HUEN, K. 2009. Climate change implications for flexible pavement design and performance in Southern Canada. *J. Transp. Eng.,* 135**,** 773 – 782.

MOFFATT, M. & HASSAN, R. 2006. Guide to Asset Management Part 5E: Cracking. *In:* AUSTROADS (ed.).

MOGAN, J. R. 1996. The Response of Granular Materials to Repeated Loading. *In:* BOARD, A. R. R. (ed.).

MONISMITH, C. L., OGAWA, N. & FREEME, C. R. 1975. PERMANENT DEFORMATION CHARACTERISTICS OF SUBGRADE SOILS DUE TO REPEATED LOADING. *In:* RECORD, T. R. (ed.).

MONISMITH, C. L., SECOR, G. A. & SECOR, K. E. 1965. TEMPERATURE INDUCED STRESSES AND DEFORMATIONS IN ASPHALT CONCRETE. *Association of Asphalt Paving Technologists Proceedings.*

MOORE, W. M., BRITTON, S. C. & SCHRIVNER, F. H. 1970. A Laboratory Study of the Relation of Stress to Strain for a Crushed Limestone Base Material. *Research No. 2-8-65-99.* Texas Transportation Institute.

MORIAN, D. A., GIBSON, S. D. & EPPS, J. A. 1998. Maintaining Flexible Pavements - the Long Term Pavement Performance Experiment. *In:* ADMINISTRATION, F. H. (ed.).

MTAG 2008. Maintenance Technical Advisory Guide. California Department of Transportation.

MYERS, L. A., ROQUE, R. & BIRGISSON, B. 2001. Propagation Mechanisms for Surface-Initiated Longitudinal Wheelpath Cracks. *Transportation Research Record: Journal of the Transportation Research Board,* 1778**,** 113-122.

MYHRE, G., HIGHWOOD, E. J., SHINE, K. P. & STORDAL, F. 1998. New estimates of radiative forcing due to well mixed greenhouse gases. *Geophysical research letters 25.14***,** 2715-2718.

NAKICENOVIC, N. & SWART, R. 2000. Special report on emissions scenarios. *Special Report on Emissions Scenarios, Edited by Nebojsa Nakicenovic and Robert Swart, pp. 612. ISBN 0521804930. Cambridge, UK: Cambridge University Press, July 2000.,* 1.

NCHRP 1985. Life-Cycle Costs Analysis of Pavements. Washington D. C.

NCHRP 2004. Guide for Mechanistic-Empirical Design of New and Rehabilitated Pavement Structures. *Part 3. Design Analysis.* National Cooperative Highway Research Program.

NDLI 1991. Thailand Road Maintenance Project. *Final report. Report to the Department of Highways, Bangkok.* Vancouver.

NORD S, R. & GLEDITSCH, N. P. 2007. Climate change and conflict. *Political Geography,* 26**,** 656-673.

OCKWELL, A. 1999. Pavement management: Development of a Life Cycle Costing Technique. *In:* ECONOMICS, B. O. T. A. C. (ed.).

ODOKI, J. B. & KERALI, H. G. R. 1999. Volume Four: HDM-4 Technical Reference Manual. HDM-4 Manual (Version V1.0E). Highway Development & Management.

PAILLARD, D. 2001. GLACIAL CYCLES: TOWARD A NEW PARADIGM. *Reviews of Geophysics,* 39**,** 325-346.

PARRY, A. R., BLACKMAN, D. & MERRILL, D. 2001. Measurements of truck tyre contact stresses and pavement wear In. *International Rubber Conference.*

PARRY, A. R. & ROE, P. 2000. The next generation of low noise asphalt road surfaces. *The 29th International Congress and Exhibition on Noise Control Engineering.* Nice, France.

PARRY, A. R. & VINER, H. E. 2005. Accidents and the skidding resistance standard for stratgic roads in England. *TRL622.* TRL, United Kingdom.

PESHKIN, D., SMITH, K. L., WOLTERS, A., KRSTULOVICH, J., MOULTHROP, J. & ALVARADO, C. 2011. Guidelines for the Preservation of High-Traffic-Volume Roadways. Strategic Highway Research Program.

PETIT, J. R., JOUZEL, J., RAYNAUD, D., BARKOV, N. I., BARNOLA, J.-M., BASILE, I., BENDER, M., CHAPPELLAZ, J., DAVIS, M., DELAYGUE, G., DELMOTTE, M., KOTLYAKOV, V. M., LEGRAND, M., LIPENKOV, V. Y., LORIUS, C., PÉPIN, L., RITZ, C., SALTZMAN, E. & STIEVENARD, M. 1999. Climate and atmospheric history of the past 420,000 years from the Vostok ice core, Antarctica. *Nature,* 399**,** 7.

PROWELL, B. D. 1999. SELECTION AND EVALUATION OF PERFORMANCE-GRADED ASPHALT BINDERS FOR VIRGINIA *In:* COUNCIL, V. T. R. (ed.).

QIAO, Y., DAWSON, A., HUVSTIG, A. & KORKIALA-TANTTU, L. 2014. Calculating rutting of some thin flexible pavements from repeated load triaxial test data. *International Journal of Pavement Engineering***,** 1-10.

QIAO, Y., DAWSON, A., PARRY, A. R. & FLINTSCH, G. in press-a. Evaluating the effects of climate change on road maintenance intervention strategies and Life-cycle Costs. *Transportation Research Part D: Transport and Environment*

QIAO, Y., DAWSON, A., PARRY, T. & FLINTSCH, G. 2013a. Quantifying the effect of climate change on the deterioration of a flexible pavement. *In:* the

9th International Conference on the Bearing Capacity of Roads, Railways and Airfields, Trondheim, Norway. Tapir fagtrykk, NTNU, 555-563.

QIAO, Y., DAWSON, A., PARRY, T. & FLINTSCH, G. in press-b. Immediate Effects of Some Corrective Maintenance Interventions on Flexible Pavements. *International Journal of Pavement Engineering*.

QIAO, Y., FLINTSCH, G. W., DAWSON, A. R. & PARRY, T. 2013b. Examining Effects of Climatic Factors on Flexible Pavement Performance and Service Life. *Transportation Research Record: Journal of the Transportation Research Board,* 2349**,** 100-107.

RAHMSTORF, S. 2007. A Semi-Empirical Approach to Projecting Future Sea-Level Rise. *Science,* 315**,** 368-370.

RASHID, M. M. & TSUNOKAWA, K. 2012. Trend Curve Optimal Control Model for Optimizing Pavement Maintenance Strategies Consisting of Various Treatments. *Computer-Aided Civil and Infrastructure Engineering,* 27**,** 155-169.

REUVENY, R. 2007. Climate change-induced migration and violent conflict. *Political Geography,* 26**,** 656-673.

RICHARDS, P. I. 1956. Shock Waves on the Highways. *Operations Research,* 4**,** 42-51.

SANCHEZ-SILVA, M., ARROYO, O., JUNCA, M., CARO, S. & CAICEDO, B. 2005. Reliability based design optimization of asphalt pavements. *International journal of Pavement Engineering,* 6**,** 281-294.

SANTOS, J. & FERREIRA, A. 2012. Pavement Design Optimization Considering Costs and Preventive Interventions. *JOURNAL OF TRANSPORTATION ENGINEERING,* 138**,** 911-923.

SAYERS, M. W., GILLESPIE, T. D. & PATERSON, W. D. O. 1986. Guidelines for Conducting and Calibrating Road Roughness Measurements. *In:* BANK, T. W. (ed.) *WORLD BANK TECHNICAL PAPER NUMBER 46.* Washington, D.C., U.S.A.

SAYERS, M. W. & KARAMIHAS, S. M. 1998. *the Little Book of Profiling*, University of Michigan.

SHU, X. & HUANG, B. 2008. Dynamic Modulus Prediction of HMA Mixtures Based on the Viscoelastic Micromechanical Model. *Journal of Materials in Civil Engineering,* 20.

SWEERE, G. T. H. 1990. *Unbound Granular Basis for Road.* PhD, University of Delft.

TAYABJI, S. D., BROWN, J. L., MACK, J. W., HEARNE, T. M., ANDERSON, J., MURRELL, S. & NOURELDIN, A. S. 2000. *Pavement Rehabilitation*.

TERZI, S. 2006. Modeling the Pavement Present Serviceability Index of Flexible Highway Pavements Using Data Mining. *Journal of Applied Science,* 6 (1)**,** 193-197.

THOM, N. H. 1988. *Design of road foundations.* PhD, University of Nottingham.

THOM, N. H. & BROWN, S. F. 1987. Effect of Moisture on the Structural Performance of a Crushed-limestone Road Base. *Transportation Research Record*.

TIGHE, S. L., SMITH, J., MILLS, B. & ANDREY, J. Year. Using the MEPDG to Assess Climate Change Impacts on Southern Canadian Roads. *In:* 7th International Conference on Managing Pavement Assets, 2008.

TIMM, D. H. 2007. Life Cycle Cost Analysis and Perpetual Pavements. *In:* WORKSHOP, P. P. D. (ed.).

TRB 2000. Highway Capacity Manual *National Research Council, Washington, DC,* 113.

TSENG, K. H. & LYTTON, R. L. 1989. Prediction of permanent deformation in flexible pavement materials. *Implication of Aggregates in the Design,*

Construction, and Performance of Flexible Pavements, ASTM STP 1016**,** 154-172.

USGS. 2014. *U.S. Geological Survey* [Online]. Available: http://www.usgs.gov/ [Accessed].

UZAN, J. 1985. Characterization of Granular Material. *Transportation Research Record: Journal of the Transportation Research Board***,** 52 – 59.

VAN KIRK, J. 2004. Long Lasting Maintenance Product, International Slurry Seal Association. *In:* WORKSHOP, S. S. (ed.). Las Vegas, Nevada.

VDOT 2002. Life Cycle Costs Analysis Pavement Options. Material division, Virginia Transportation Research Council.

VERMEER, M. & RAHMSTORF, S. 2009. Global sea level linked to global temperature. *Proceedings of the National Academy of Sciences,* 106**,** 21527-21532.

WADA, Y., VANBEEK, L. P. H., WEILAND, F. C. S., CHAO, B. F., WU, Y.-H. & BIERKENS, M. F. P. 2012. Past and future contribution of global groundwater depletion to sea-level rise. *Geophys. Res. Lett., 39,* L09402.

WATANATADA, T., DHARESHWAR, A. M. & LIMA, P. R. S. R. 1987. *Vehicle Speed and Operating Costs: Models for Road Planning and Management,* Baltimore, John Hopkins University Press.

WERKMEISTER, S. 2003. *Permanent Deformation Behaviour of Unbound Granular Materials in Pavement Constructions.* PhD, Dresden University of Technology.

WIGLEY, T. M. 2008. MAGICC/SCENGEN 5.3: User manual (version 2). *NCAR, Boulder, CO***,** 80.

WILLIAMS, G. T. 1963. Stress/Strain Relationships of Granular Soils. *Thornton Report R 1297.* Shell Research Limited.

WITCZAK, M. W. 2004. DEVELOPMENT OF A MASTER CURVE (E*) DATABASE FOR LIME MODIFIED ASPHALTIC MIXTURES. *Research Project.* Department of Civil and Environmental Engineering, Arizona State University.

WITCZAK, M. W. 2007. Specification Criteria for Simple Performance Tests for Rutting. *In:* NCHRP (ed.).

WITCZAK, M. W. & FONSECA, O. A. 2007. Revised Predictive Model for Dynamic (Complex) Modulus of Asphalt Mixtures. *Transportation Research Record: Journal of the Transportation Research Board,* 1540.

WORLD-BANK 2009. The Costs to Developing Countries of Adapting to Climate Change New Methods and Estimates.

ZANIEWSKI, J. P. 1989. Effect of Pavement Surface Type on Fuel Consumption. FHWA.

ZANIEWSKI, J. P., BUTLER, B. C., CUNNINGHAM, G., ELKINS, G. E., PAGGI, M. S. & MACHEMEHL 1982. Vehicle Operating Costs, Fuel Consumption, and Pavement Type and Condition Factors.

ZHANG, H., KEOLEIAN, G. A. & LEPECH, M. D. 2008. *An Integrated Life Cycle Assessment and Life Cycle Analysis Model for Pavement Overlay System*, Taylor & Francis Group.

APPENDIX A

Material properties of Sec01, Sec02, and Sec03

Sec01

Layer 1 and 2

Table A-1 Asphalt mixture information of Layer 1 and 2, Sec01

Asphalt property						
	PG grade	Effective binder content (%)	Air voids (%)	Total unit weight (pcf)	Thermal conductivity (BTU/hr-ft-°F)	Heat capacity (BTU/lb-°F)
Layer 1	64-22	11.6	7	150	0.67	0.23
Layer 2	64-22	11.6	7	150	0.67	0.23
Mixture Aggregate gradation						
	cumulative % retained on the ¾ in sieve		cumulative % retained on the 3/8 in sieve	cumulative % retained on the #4 sieve	% Passing #200 sieve	
Layer 1	0		12	45	6	
Layer2	0		27	62	3	

(pcf = pound per cubic feet, 1 pcf = 16.018463 kg/m^3; 1 BTU = approximate 1055 Joules)

Layer 3

No. 21A is classified by the Virginia classification. It can be categorised as A-1-a according to the AASHTO soil classification, which is a high quality granular material. The default grading material was used in the MEPDG.

Table A-2 Sieve information of Layer 3, Sec01

Sieve	Percent passing
#200	8.7
#80	12.9
#40	20
#10	33.8
#4	44.7
3/8"	57.2
1"	78.8
2"	91.6
3 1/2"	97.6

Layer 4

Level 1 MEPDG input was used for this layer because the resilient modulus testing on the same material can be found in the literature. The stresss dependent finte element method used has not been calibrated with distersses, therefore Level 1 was highly therotical. However, only the difference betweetn pavement performance under vairous climate scenarios were considered. Therefore, focus was not about the absolute value of a particular distress.

Table A-3 k values of k-θ model for the resilient modulus (Hossain, 2010)

K	Value
K_1	587.6
K_1	0.58
K_3	-0.55

Table A-4 Sieve information of Layer 4, Sec01

Sieve	Percent passing
#200	8.7
#80	12.9
#40	20
#10	33.8
#4	44.7
3/8"	57.2
1"	78.8
2"	91.6
3 1/2"	97.6

Sec02

Layer 1

Table A-5 Dynamic modulus testing results, asphalt mixture, layer 1, Sec02
(Apeagyei and Diefenderfer, 2011)

Frequency	0.1	0.5	1	5	10	25
Temperature (℉)	Mixture E* (psi)					
14	1990691	2290807	2420244	2696686	2816149	2959543
40	1245825	1580766	1730928	2054169	2195049	2372188
70	431294	612252	725043	983066	1112439	1290642
100	136621	198557	244872	377968	454838	599169
130	50280	65804	83044	139198	166842	217847

Table A-6 Binder property, Layer 1, Sec02 (Apeagyei and Diefenderfer, 2011)

Angular frequency = 10 rad/sec		
Temperature (°F)	G* (Pa)	Delta (°)
147.2	6883	80.8
158	2324	84.3
168.8	1127	86

Table A-7 Asphalt general property, Layer1, Sec02 (Apeagyei and Diefenderfer, 2011)

Effective binder content (%)	11.7
Air voids (%)	7
Total unit weight (pcf)	146.13
Thermal conductivity (BTU/hr-ft-°F)	0.67
Heat capacity (BTU/lb-°F)	0.23

Table A-8 Creep testing result, Layer 1, Sec02 (Apeagyei and Diefenderfer, 2011)

Loading time sec	Creep compliance (1/psi)		
	Temperature		
	-4 °F	14 °F	32 °F
1	1.6550E-07	2.7580E-07	6.2740E-07
2	3.3090E-07	4.1370E-07	4.6880E-07
5	3.9990E-07	4.1370E-07	7.8600E-07
10	3.9990E-07	6.2050E-07	9.4460E-07
20	3.9990E-07	6.2050E-07	1.4130E-06
50	4.6880E-07	7.6530E-07	1.5720E-06
100	5.6540E-07	9.7220E-07	2.0480E-06

Layer 2

Table A-9 Dynamic modulus testing results, asphalt mixture, layer 2, Sec02 (Apeagyei and Diefenderfer, 2011)

Frequency	0.1	0.5	1	5	10	25
Temperature (°F)	Mixture E* (psi)					
10	2937731	3259872	3401607	3701600	3818710	3990199
40	1320568	1700180	1885297	2314802	2496679	2777734
70	435113	659341	819076	1201154	1364805	1703806
100	98676	158722	256136	481380	564631	596467
130	44217	54767	75917	143933	175827	188986

Table A-10 Binder property, Layer2, Sec02 (Apeagyei and Diefenderfer, 2011)

Angular frequency = 10 rad/sec		
Temperature (°F)	Temperature (°F)	Temperature (°F)
147	5425	82
158	2533	84
168	1218	86

Table A-11 Asphalt general property, Layer2, Sec02 (Apeagyei and Diefenderfer, 2011)

Effective binder content (%)	10.3
Air voids (%)	7.6
Total unit weight (pcf)	151.32
Thermal conductivity (BTU/hr-ft-°F)	0.67
Heat capacity (BTU/lb-°F)	0.23

Layer 3 and 4

Layer 3 and 4 were assumed to be A-3 granular material with default setting as no material properties were available. The resilient modulus was chosen to be 24,500 psi and the Poisson's ratio was 0.35.

Table A-12 Sieve information of Layer 3 and 4, Sec02

Sieve	Percent passing
#200	5.2
#80	33
#40	76.8
#10	93.4
#4	95.3
3/8"	96.6
1"	98.6
2"	99.7

Sec03

Layer 1

Table A-13 Dynamic modulus input for Layer 1, Sec03 (Apeagyei and Diefenderfer, 2011)

Frequency	0.1	0.5	1	5	10	25
Temperature	Mixture E* (psi)					

(°F)						
10	1786429	2082113	2213904	2516162	2646116	2808027
40	856544	1101513	1232869	1540590	1682776	1859528
70	250964	360854	438497	637102	742738	887872
100	73360	105597	142403	239602	296699	368057
130	37657	45552	75081	125869	150834	173862

Table A-14 Binder property of Layer 1, Sec03 (Apeagyei and Diefenderfer, 2011)

Angular frequency = 10 rad/sec		
Temperature (°F)	Temperature (°F)	Temperature (°F)
158	3542	68.3
168.8	2028	70.8
179.6	1193	72.9

Table A-15 Mixture property of Layer 1, Sec03 (Apeagyei and Diefenderfer, 2011)

Effective binder content (%)	15.3
Air voids (%)	7
Total unit weight (pcf)	154.31
Thermal conductivity (BTU/hr-ft-°F)	0.67
Heat capacity (BTU/lb-°F)	0.23

Table A-16 Creep compliance input of Layer 1, Sec03 (Apeagyei and Diefenderfer, 2011)

Loading time sec	Creep compliance (1/psi)		
	Temperature		
	-4 °F	14 °F	32 °F
1	2.2750E-07	2.3440E-07	4.8260E-07
2	3.8610E-07	3.9300E-07	8.6870E-07
5	3.8610E-07	4.6880E-07	1.0690E-06
10	3.8610E-07	6.2740E-07	1.2600E-06
20	3.8610E-07	6.2740E-07	1.6480E-06
50	4.6190E-07	7.8600E-07	2.3370E-06
100	6.1360E-07	1.0960E-06	2.9300E-06

Layer 2

Table A-17 Dynamic modulus input for Layer 2, Sec03 (Apeagyei and Diefenderfer, 2011)

Frequency	0.1	0.5	1	5	10	25

Temperature (°F)	Mixture E* (psi)					
10	1990691	2290807	2420244	2696686	2816149	2959543
40	1245825	1580766	1730928	2054169	2195049	2372188
70	431294	612252	725043	983066	1112439	1290642
100	136621	198557	244872	377968	454838	599169
130	50280	65804	83044	139198	166842	217847

Table A-18 Binder property of Layer 2, Sec03 (Apeagyei and Diefenderfer, 2011)

Angular frequency = 10 rad/sec		
Temperature (°F)	Temperature (°F)	Temperature (°F)
147.2	6883	80.8
158	2324	84.3
168.8	1127	86

Table A-19 Mixture property of Layer 2, Sec03 (Apeagyei and Diefenderfer, 2011)

Effective binder content (%)	11.7
Air voids (%)	7
Total unit weight (pcf)	146.13
Thermal conductivity (BTU/hr-ft- °F)	0.67
Heat capacity (BTU/lb- °F)	0.23

Table A-20 Creep compliance input of Layer 2, Sec03 (Apeagyei and Diefenderfer, 2011)

Loading time sec	Creep compliance (1/psi)		
	Temperature		
	-4 °F	14 °F	32 °F
1	1.6550E-07	2.7580E-07	6.2740E-07
2	3.3090E-07	4.1370E-07	4.6880E-07
5	3.9990E-07	4.1370E-07	7.8600E-07
10	3.9990E-07	6.2050E-07	9.4460E-07
20	3.9990E-07	6.2050E-07	1.4130E-06
50	4.6880E-07	7.6530E-07	1.5720E-06
100	5.6540E-07	9.7220E-07	2.0480E-06

Layer 3 and 4

Table A-21 Material properties, Layer 3 and 4, Sec03

Asphalt property						
	PG grade	Effective binder content (%)	Air voids (%)	Total unit weight (pcf)	Thermal conductivity (BTU/hr-ft-$^\circ$F)	Heat capacity (BTU/lb-$^\circ$F)
Layer 1	70-22	11.6	7	150	0.67	0.23
Layer 2	70-22	11.6	7	150	0.67	0.23
Mixture Aggregate gradation						
	cumulative % retained on the ¾ in sieve		cumulative % retained on the 3/8 in sieve		cumulative % retained on the #4 sieve	% Passing #200 sieve
Layer 1	2		30		50	0
Layer2	37		46		72	3

Layer 5

Subbase material is crushed gravel, which was classified by the VDOT system as No. 21 A. The resilient modulus is 19125 and the poisson's ratio is 0.35.

Table A-22 Sieve information of subbase material, Sec03

Sieve	Percent passing
#200	9
#40	19
#10	37
3/8"	68
1"	97
2"	100

Layer 6

Subgrade was assumed to be A-3 unbound material according to the AASHTO specifications, with a range of resilient modulus between 10,000 to 60,000 psi. The resilient modulus for the subgrade of Sec03 was considered to be 39,000 psi and the Poisson's ratio is 0.35. The sieve information was identical as Layer 3 and 4 of Sec02.

Groundwater level

Table A-23 Groundwater level in the investigated sections

	SecT01	SecT02	SecT03	Sec01	Sec02	Sec03
Groundwater level to pavement surface (feet)	5	5	5	5	21.5	19.7

Climate change predictions

MAGICC/SCENGEN inputs
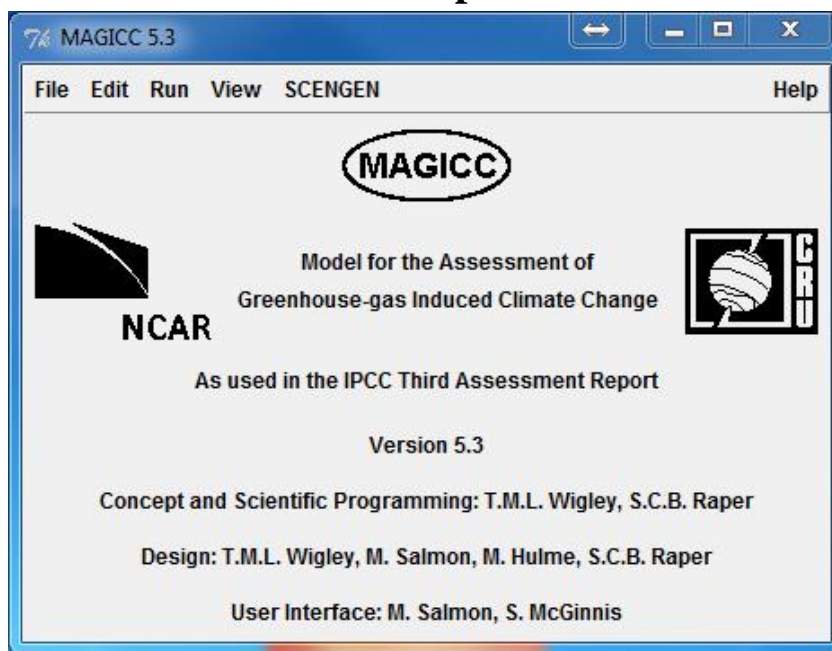
Figure A-1 MAGICC interface
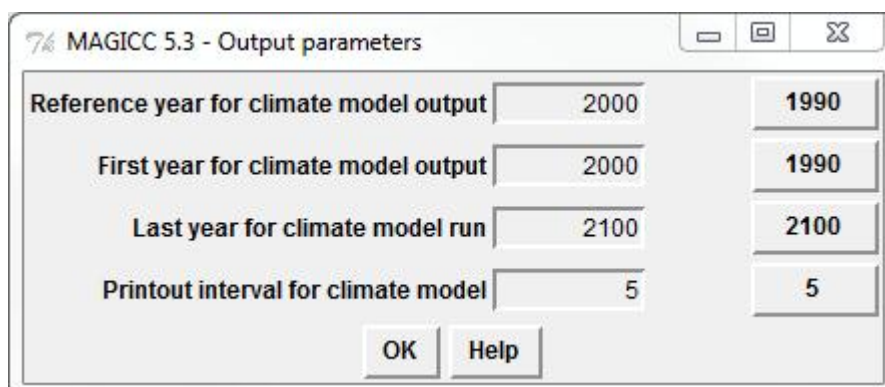
Figure A-2 MAGICC output parameters
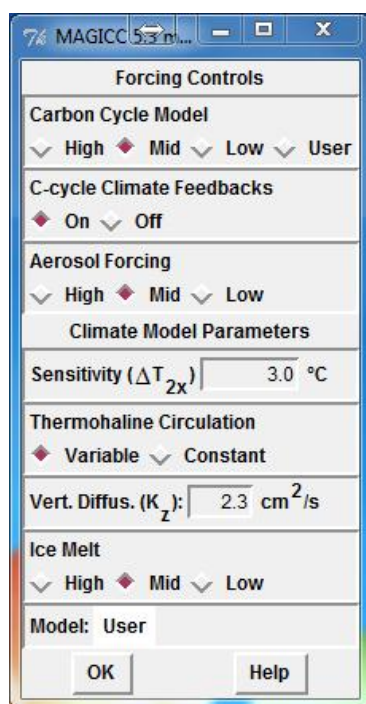
Figure A-3 MAGICC input parameters
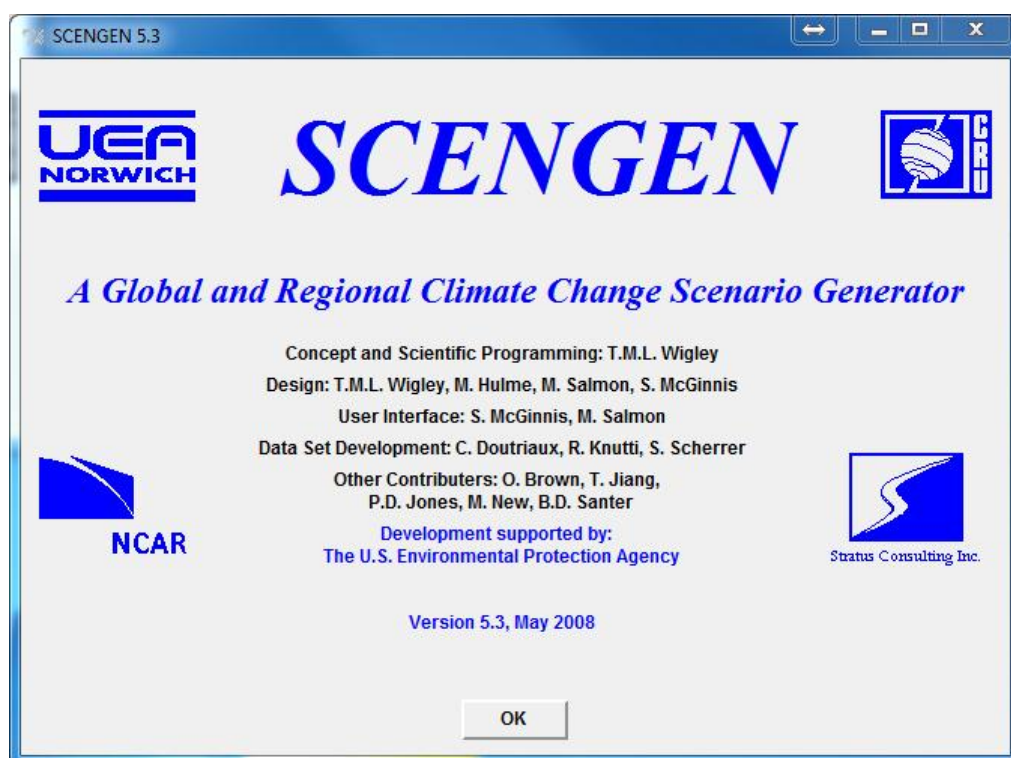
Figure A-4 SCENGEN interface
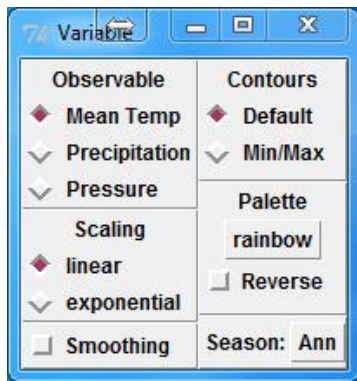
Figure A-5 SCENGEN variables
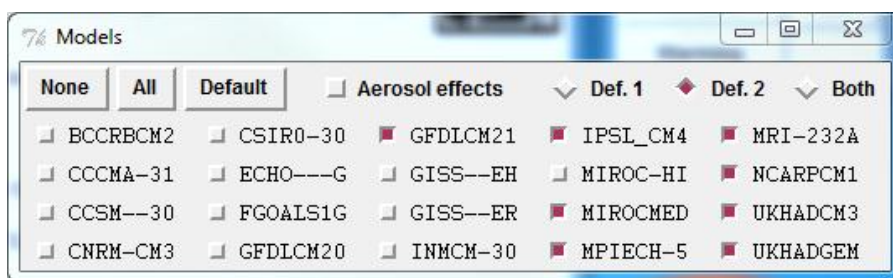
Figure A-6 SCENGEN: AOGCMs selection
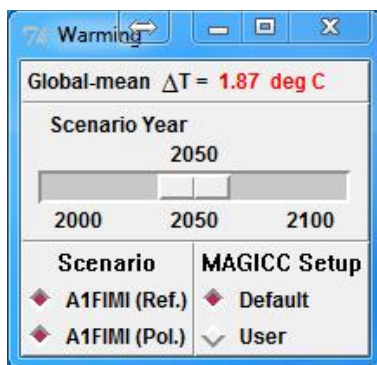
Figure A-7 SCENGEN: warming adjustment

Global average temperature
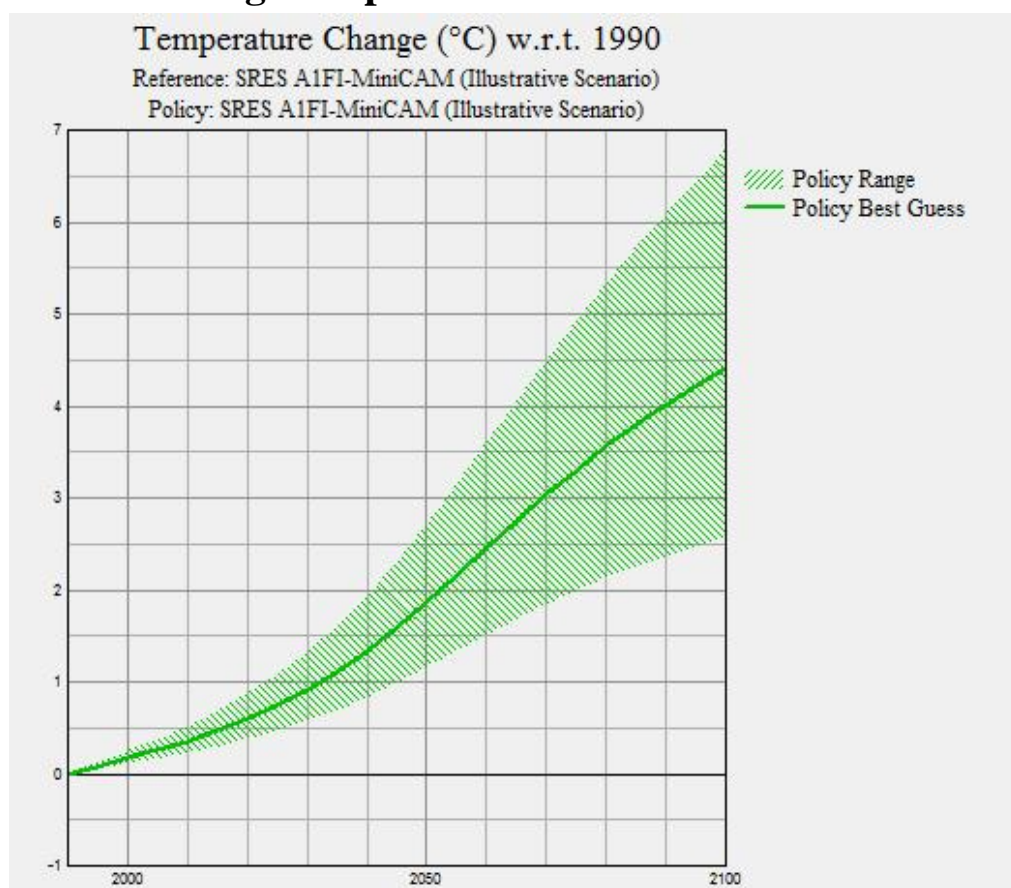
Figure A-8 MAGICC: global temperature change projection under A1FI scenario
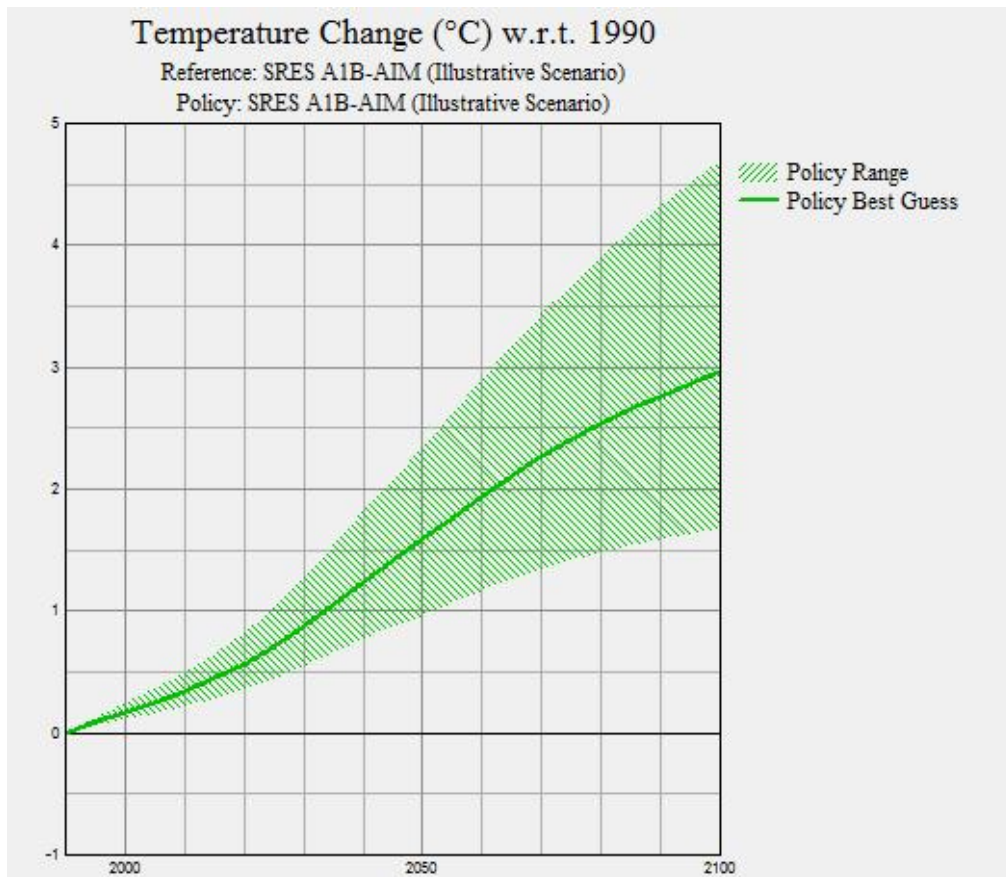
Figure A-9 MAGICC: global temperature change projection under A1B scenario
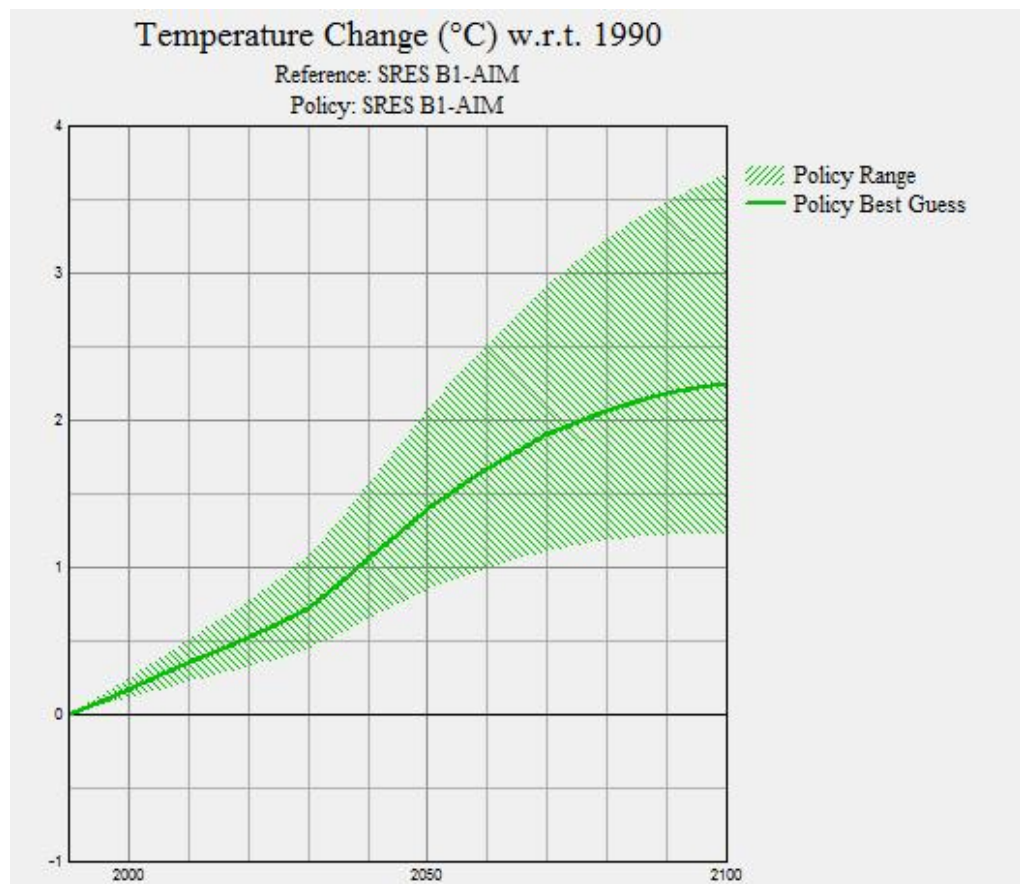
Figure A-10 MAGICC: global temperature change projection under B1 scenario

Sea water rise
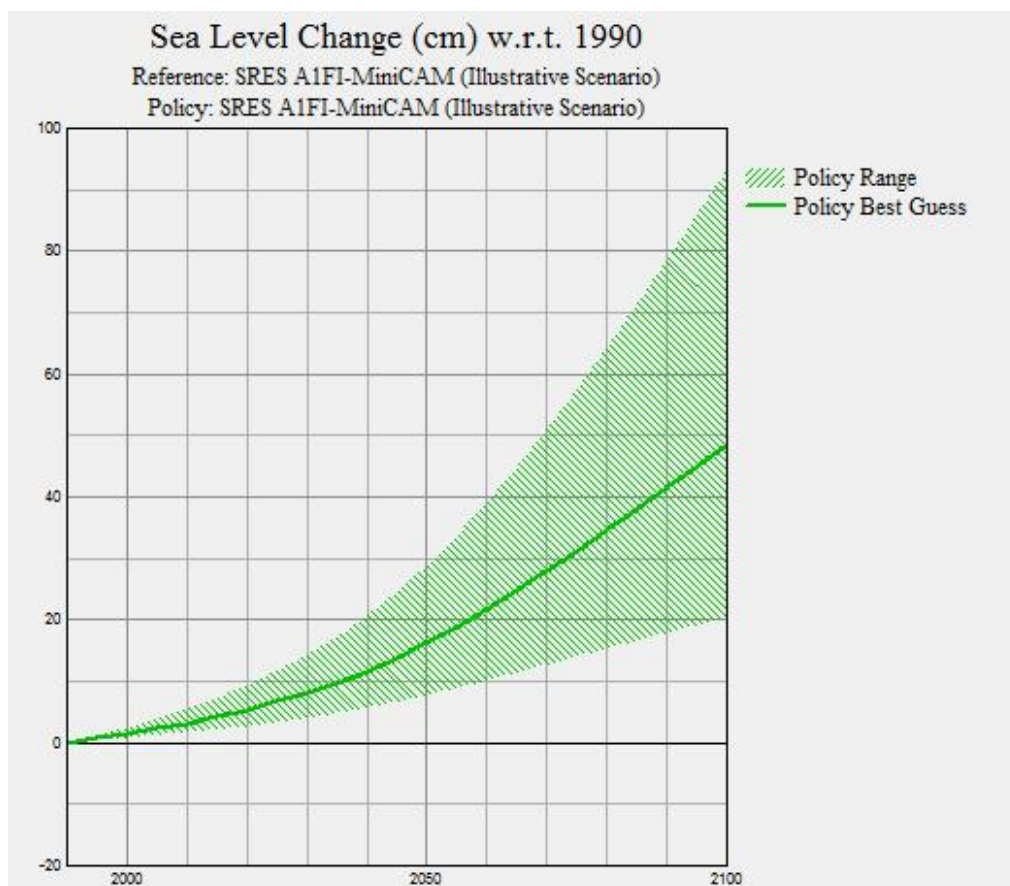
Figure A-11 MAGICC: Sea level rise projection under A1FI scenario
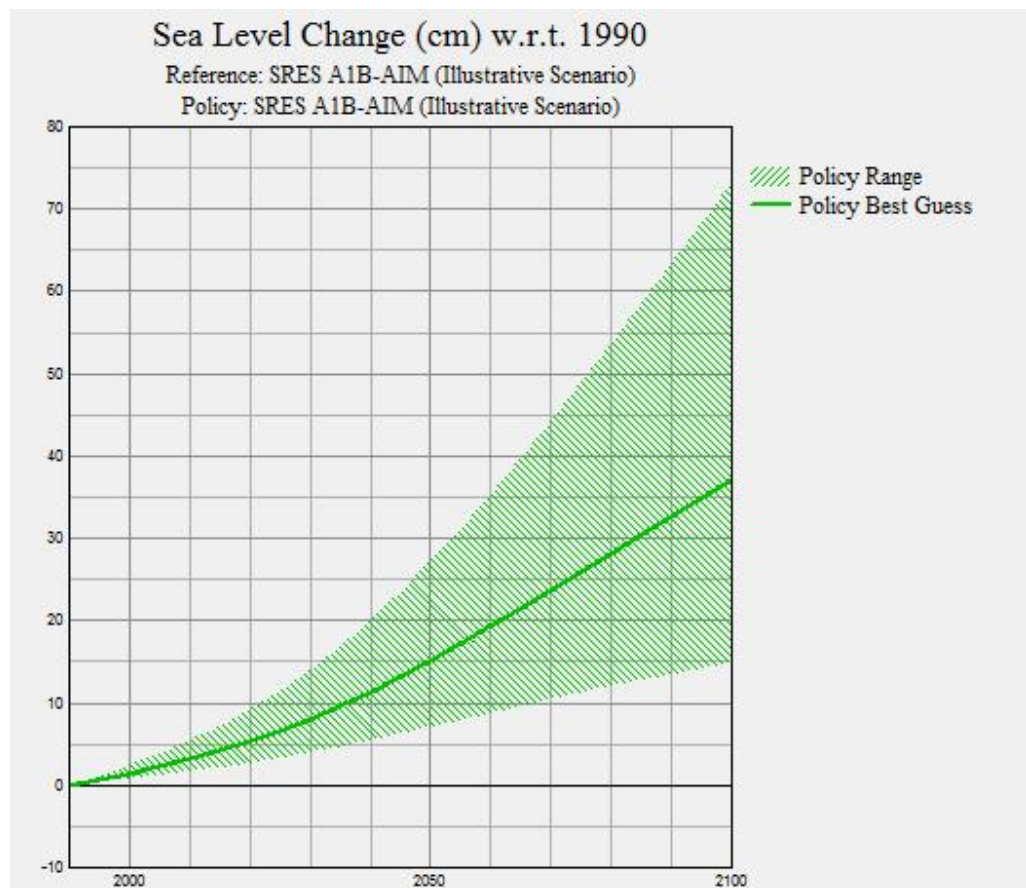
Figure A-12 MAGICC: Sea level rise projection under A1B scenario
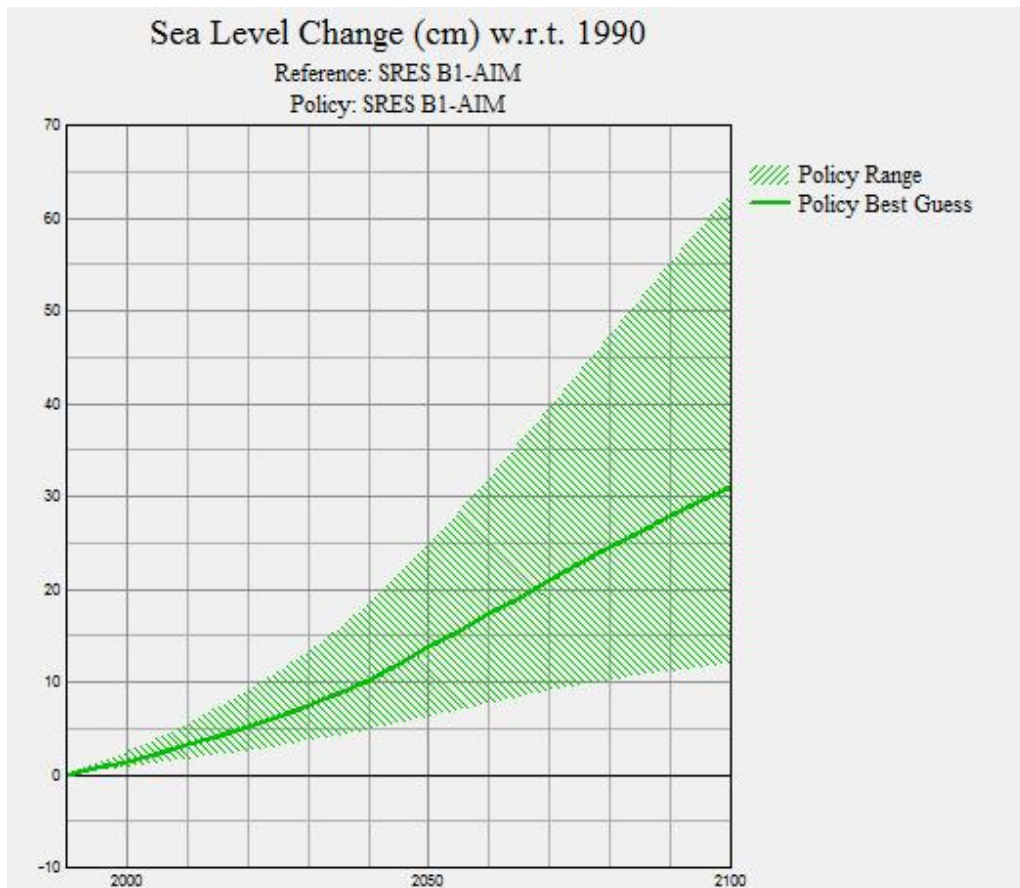
Figure A-13 MAGICC: Sea level rise projection under B1 scenario

Local temperature and precipitation predictions

Local temperature
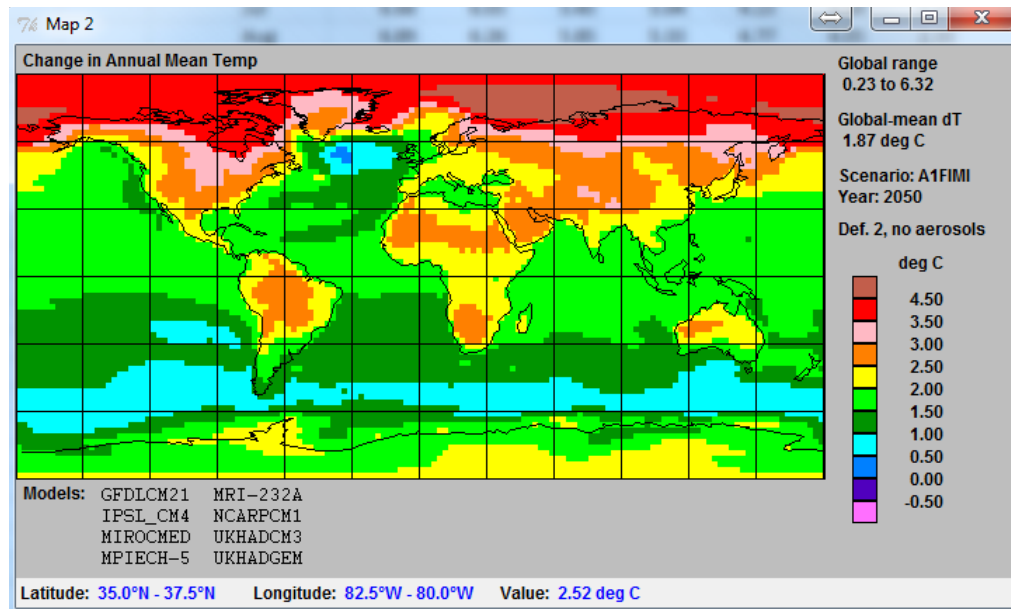
Figure A-14 SCENGEN: local temperature change projection under A1FI scenario for 2050
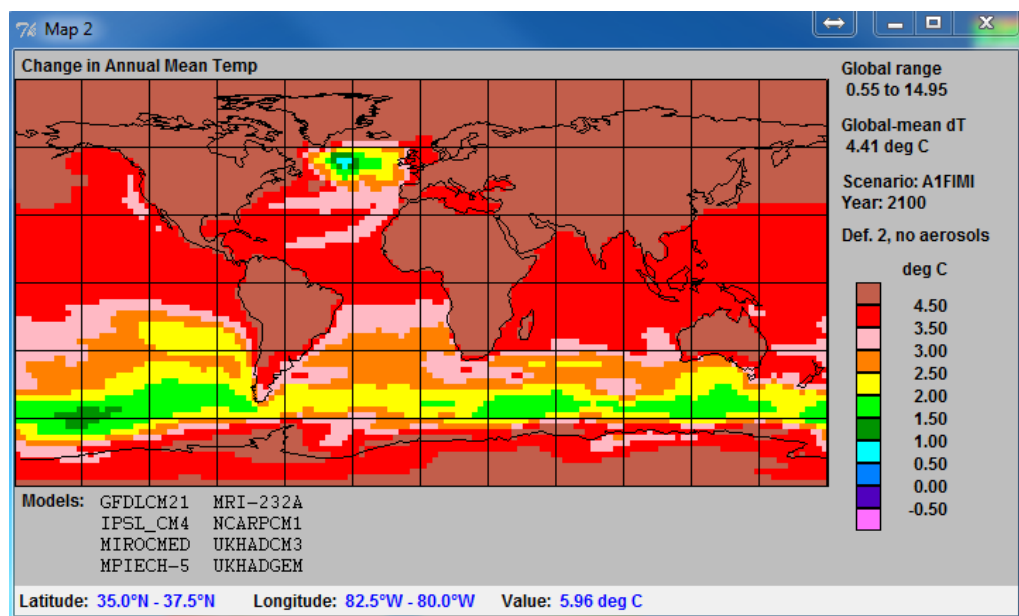
Figure A-15 SCENGEN: local temperature change projection under A1FI scenario for 2100
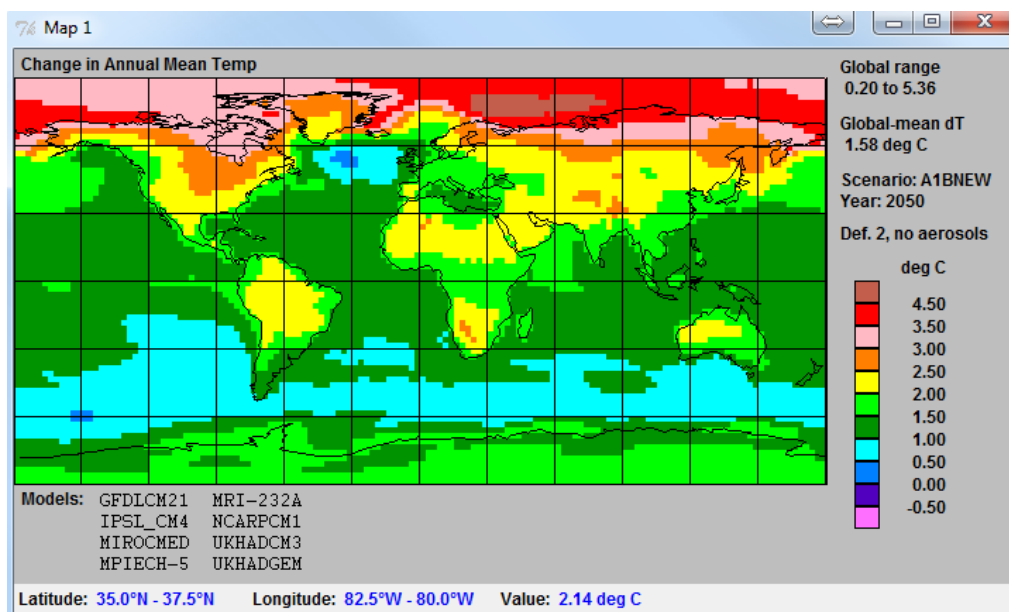
Figure A-16 SCENGEN: local temperature change projection under A1B scenario for 2050
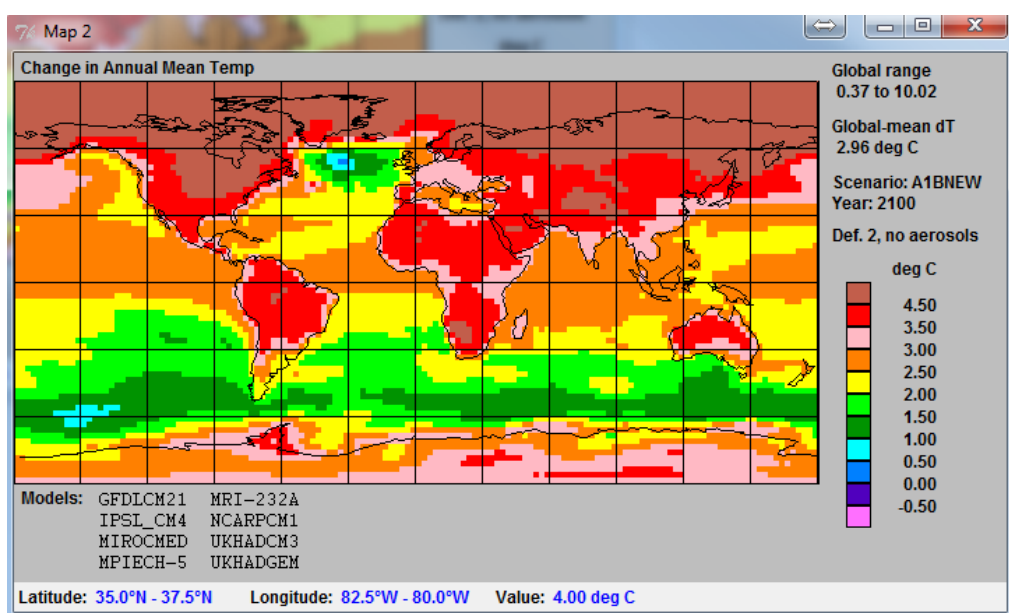
Figure A-17 SCENGEN: local temperature change projection under A1B scenario for 2100
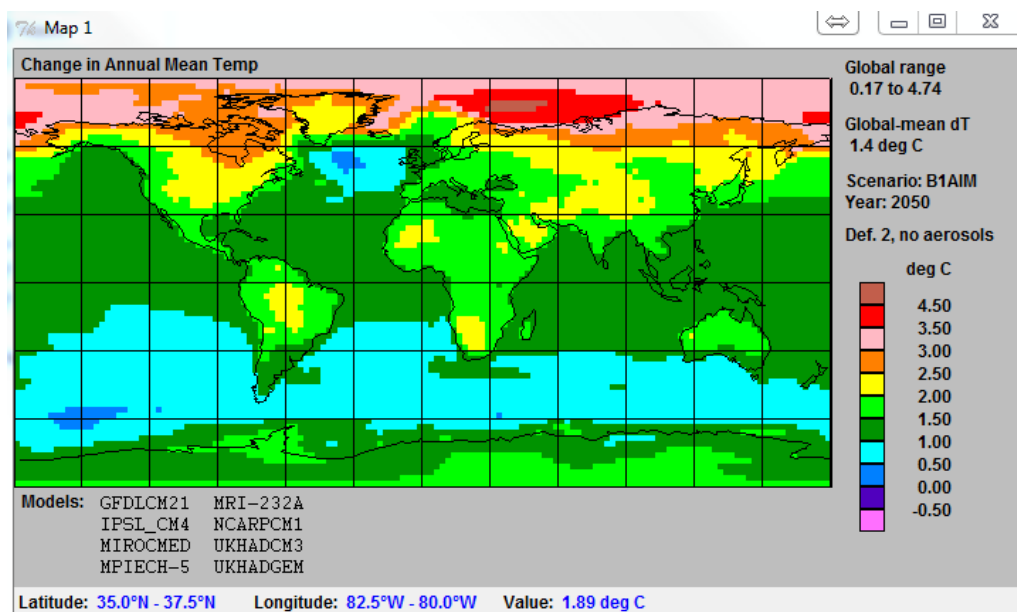
Figure A-18 SCENGEN: local temperature change projection under B1 scenario for 2050
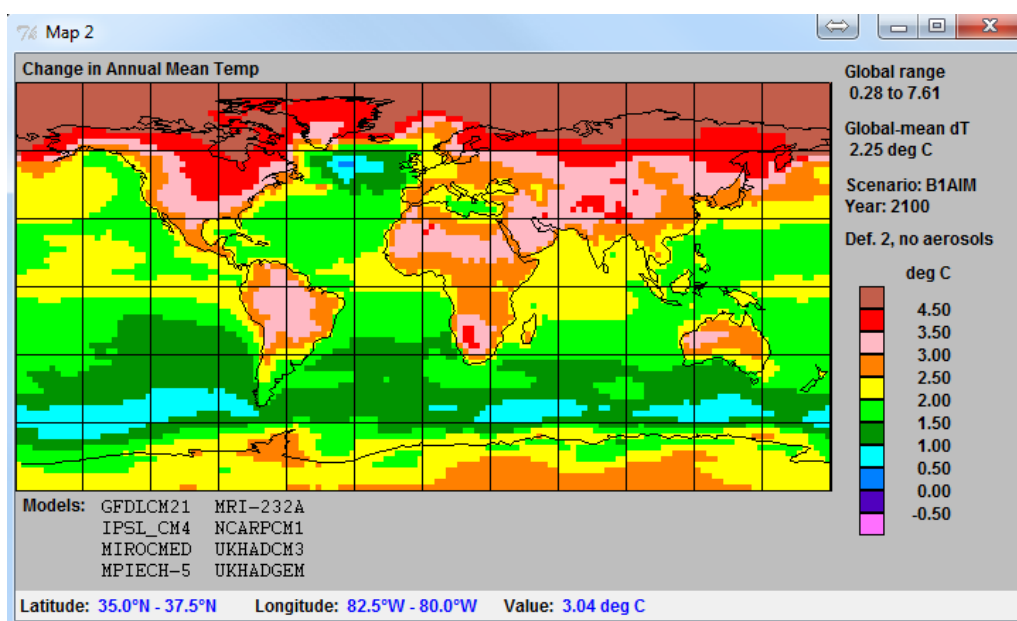
Figure A-19 SCENGEN: local temperature change projection under B1 scenario for 2100

Local precipitation
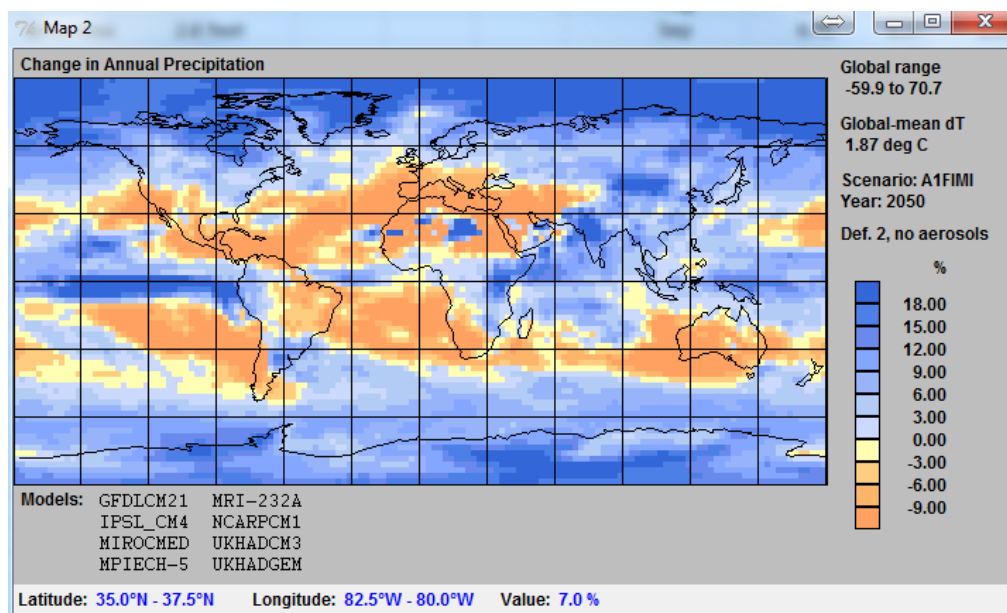
Figure A-20 SCENGEN: local precipitation change projection under A1FI scenario for 2050
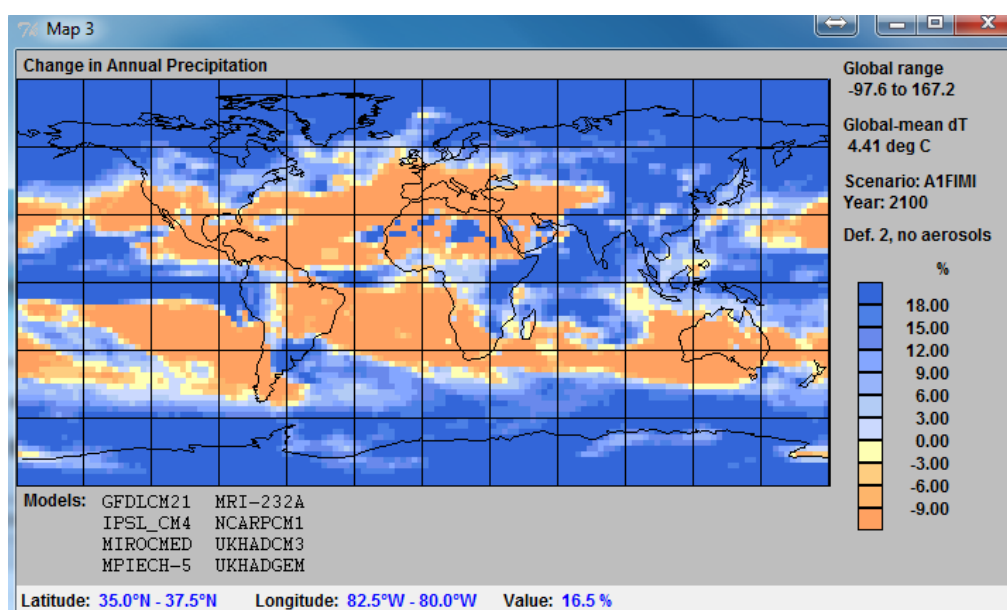
Figure A-21 SCENGEN: local precipitation change projection under A1FI scenario for 2100
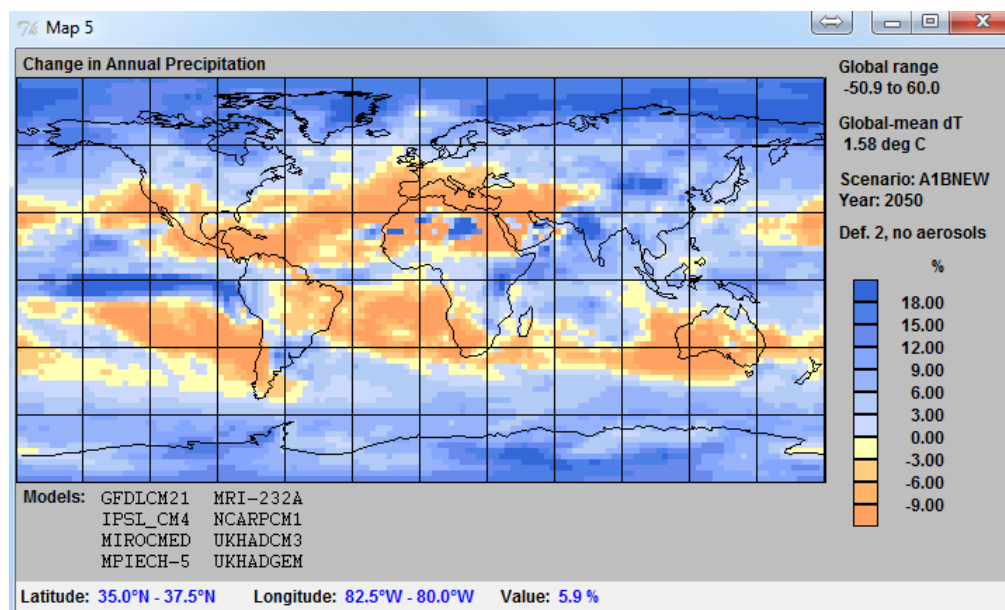
Figure A-22 SCENGEN: local precipitation change projection under A1B scenario for 2050
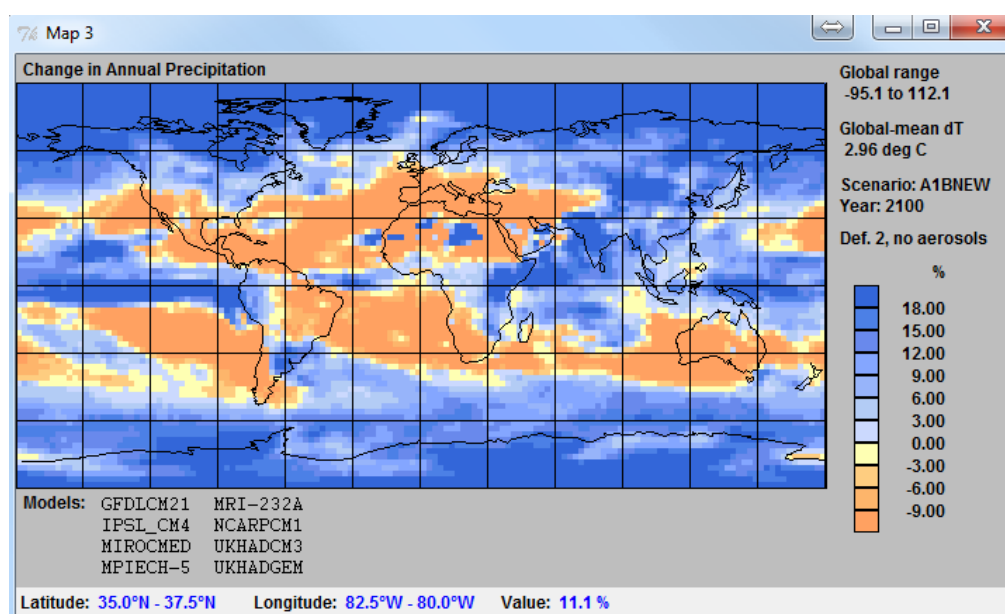
Figure A-23 SCENGEN: local precipitation change projection under A1B scenario for 2100
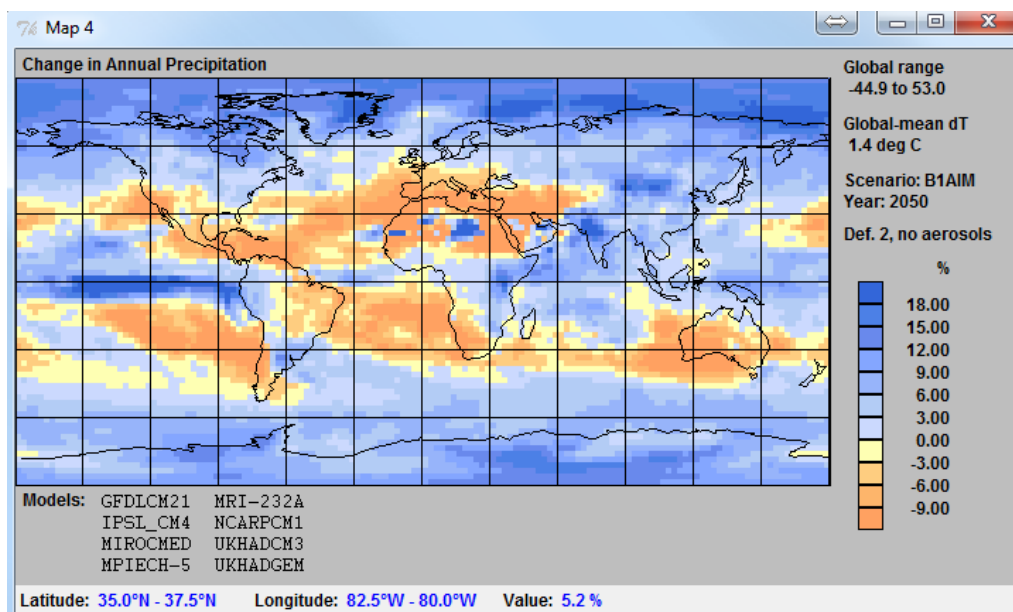
Figure A-24 SCENGEN: local precipitation change projection under B1 scenario for 2050
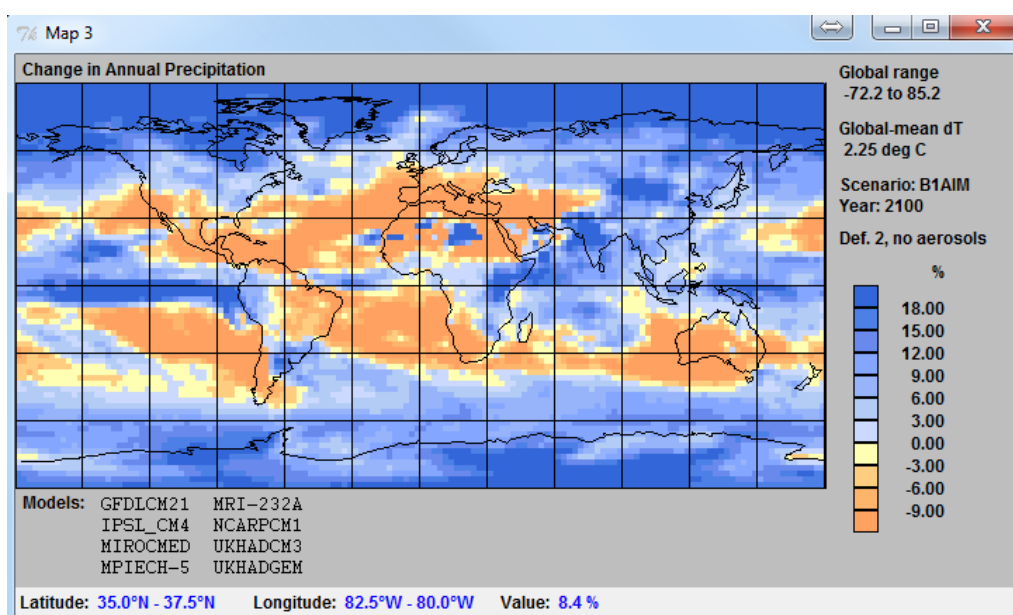
Figure A-25 SCENGEN: local precipitation change projection under B1 scenario for 2100

Sensitivity analysis

Climatic inputs

Table A-24 An example of hourly climatic record (Seattle, WA)

19961001-20060228 (monitoring period started from 1 October 1996 to 28 February 2006)					
-122.19,47.28,450,5.00,-1,-1,-1,-1,51.8344,10.155,38.1946,84.1,77.6,79.8,74.6,74.5,72.6,69.5,71.4,75.2,82.6,84.3,83.7					
(Longitude, Latitude, elevation, Annual Water Table Depth(-1 if using seasonal), spring water table depth, summer water table, fall water table, winter water table, mean annual temperature, freezing degree days, annual rainfall, monthly average humidity (12 total-start January))					
10 (month)	1 (day)	1996 (year)	6.20965 (Sunrise time (decimal-24 hour))	17.7903 (Sunset time (decimal-24 hour))	2106.92 (daily solar radiation maximum)
0 (hour)	52 (temperature)	0 (precipitation)	6 (wind speed)	0 (sunshine percent)	5 (groundwater level)
1	50	0	7	25	5
2	48.9	0	8	50	5
3	48	0	7	75	5
4	48	0	6	100	5
5	46.9	0	10	50	5
6	46.9	0	9	25	5
7	50	0	7	75	5
8	52	0	8	75	5
9	55	0	7	75	5
10	57.9	0	8	50	5
11	61.2	0	7	25	5
12	61	0	8	25	5
13	63	0	6	25	5
14	64	0	5	25	5
15	62.1	0	6	0	5
16	60.1	0	5	0	5
17	55.9	0	5	25	5
18	54	0	5	25	5
19	51.1	0	4	25	5
20	52	0	0	0	5
21	52	0	0	25	5
22	51.1	0	3	25	5
23	50	0	0	75	5
…	…	…	…	…	…

Results

Figure A-26 Sensitivity of pavement performance to climatic factors (inputs +5%, SecT01)
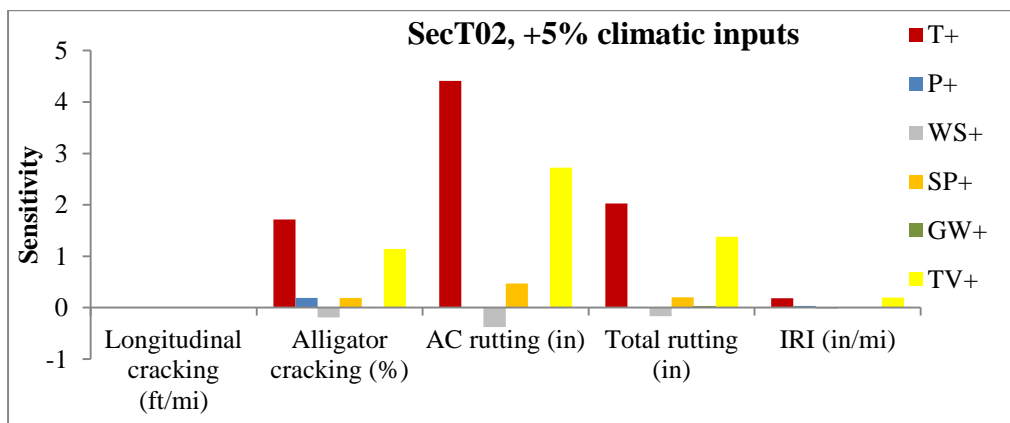
Figure A-27 Sensitivity of pavement performance to climatic factors (inputs +5%, SecT02)
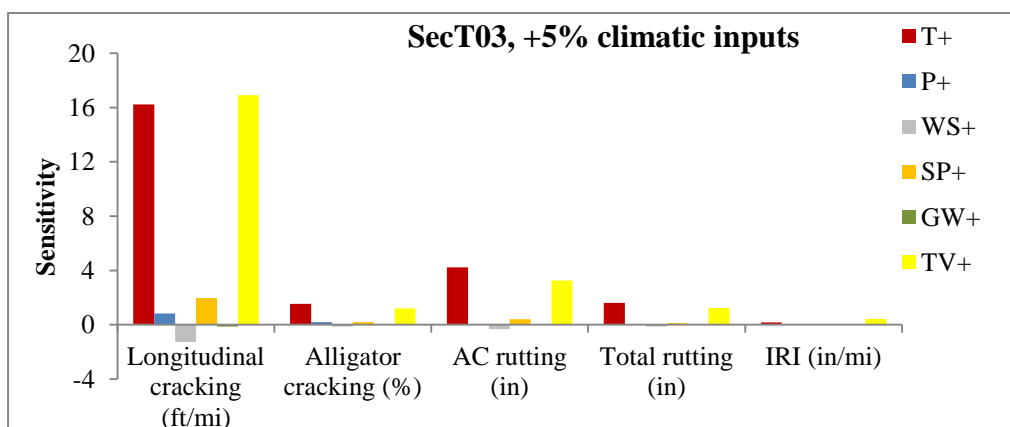
Figure A-28 Sensitivity of pavement performance to climatic factors (inputs +5%, SecT03)
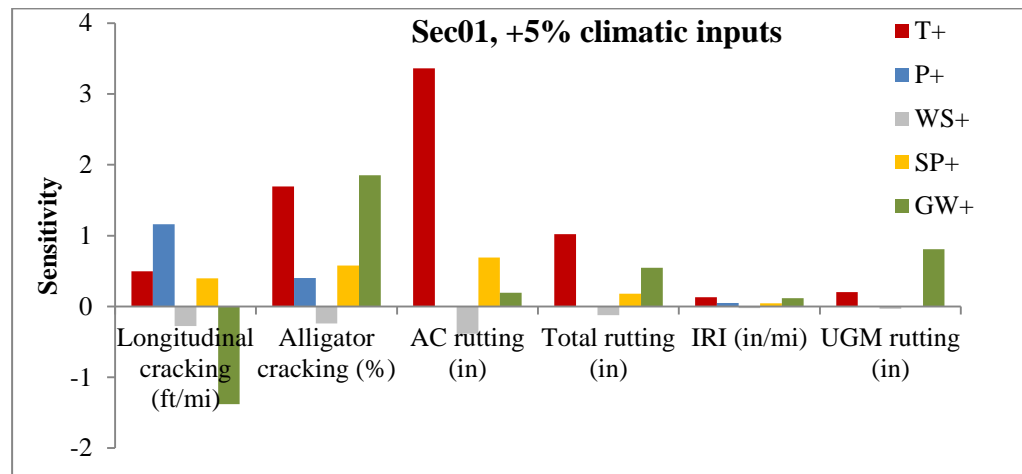
Figure A-29 Sensitivity of pavement performance to climatic factors (inputs +5%, Sec01)
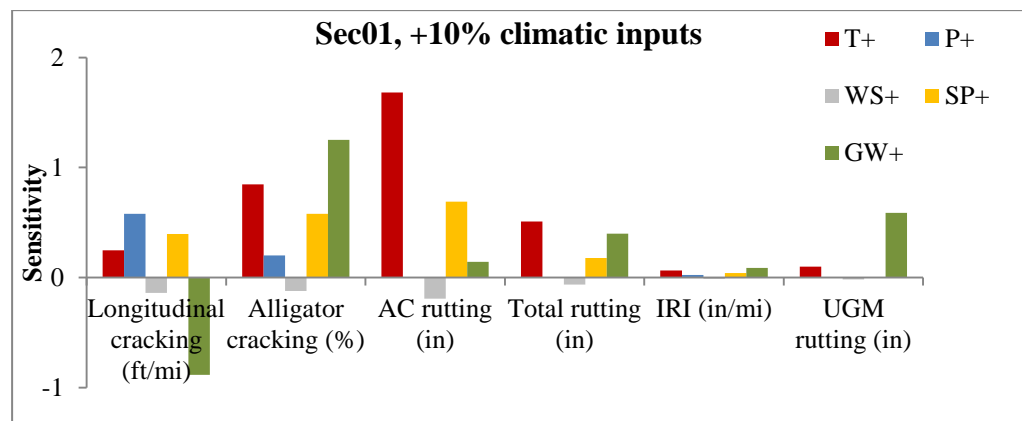
Figure A-30 Sensitivity of pavement performance to climatic factors (inputs +10%, Sec01)
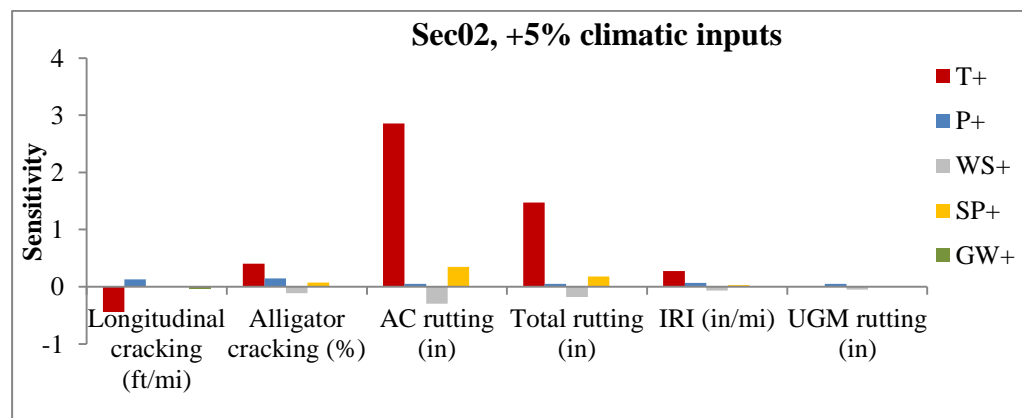
Figure A-31 Sensitivity of pavement performance to climatic factors (inputs +5%, Sec02)
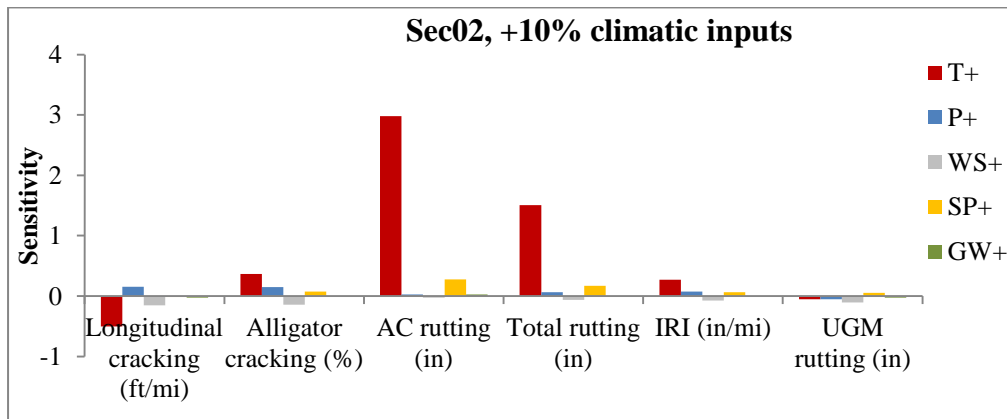
Figure A-32 Sensitivity of pavement performance to climatic factors (inputs +10%, Sec02)
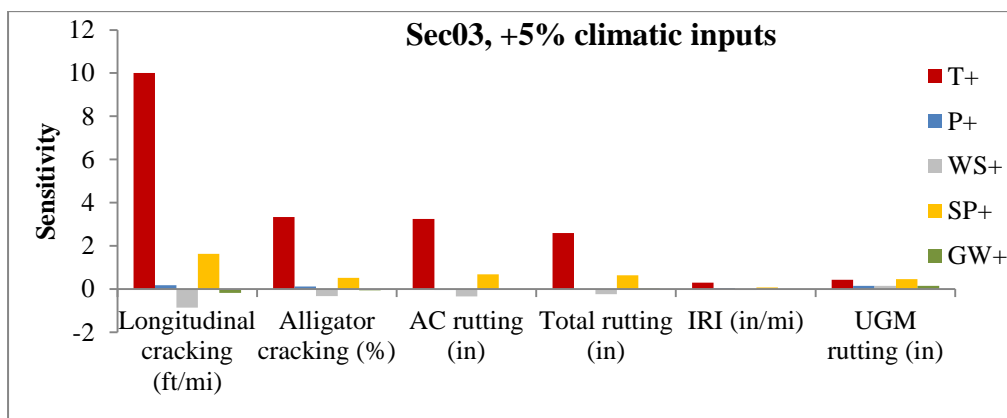
Figure A-33 Sensitivity of pavement performance to climatic factors (inputs +5%, Sec03)
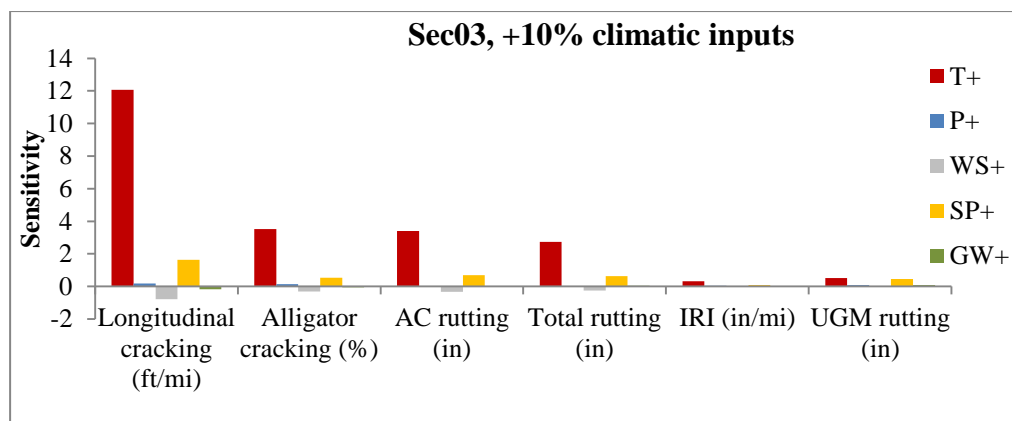
Figure A-34 Sensitivity of pavement performance to climatic factors (inputs +10%, Sec03)

Performance predictions

Sec01
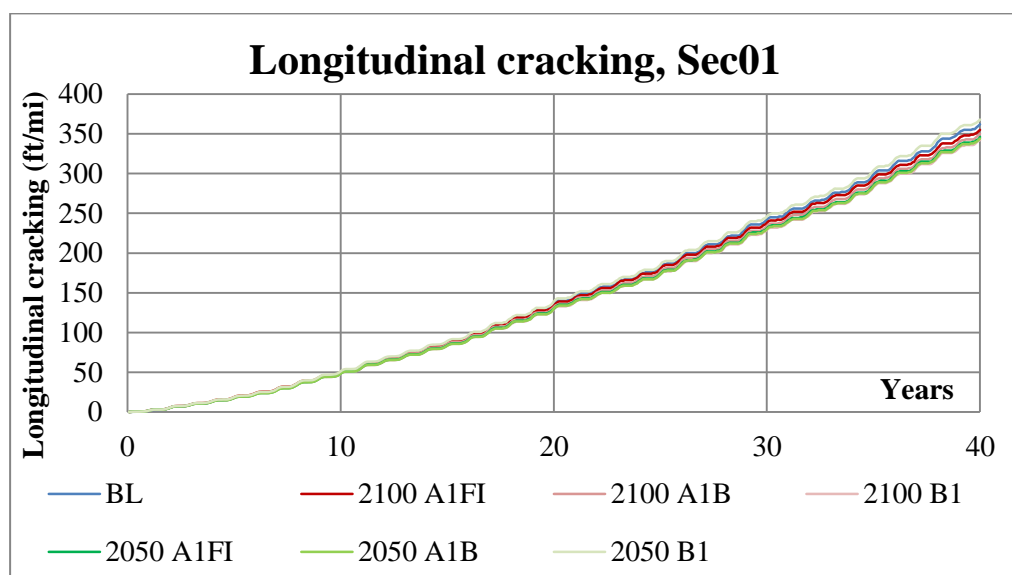
Figure A-35 Longitudinal cracking prediction under various emission scenarios for Sec01
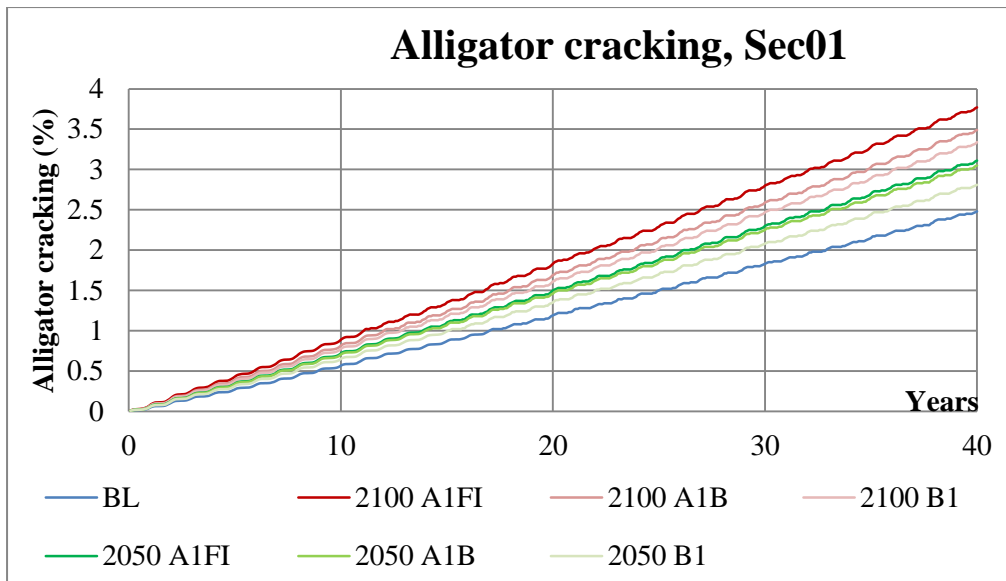
Figure A-36 Alligator cracking prediction under various emission scenarios for Sec01
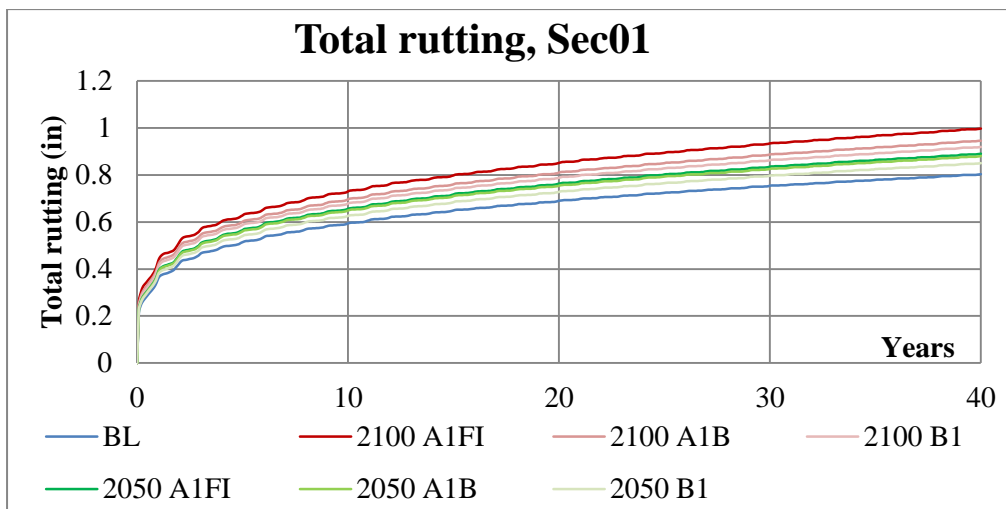
Figure A-37 Total rutting prediction under various emission scenarios for Sec01
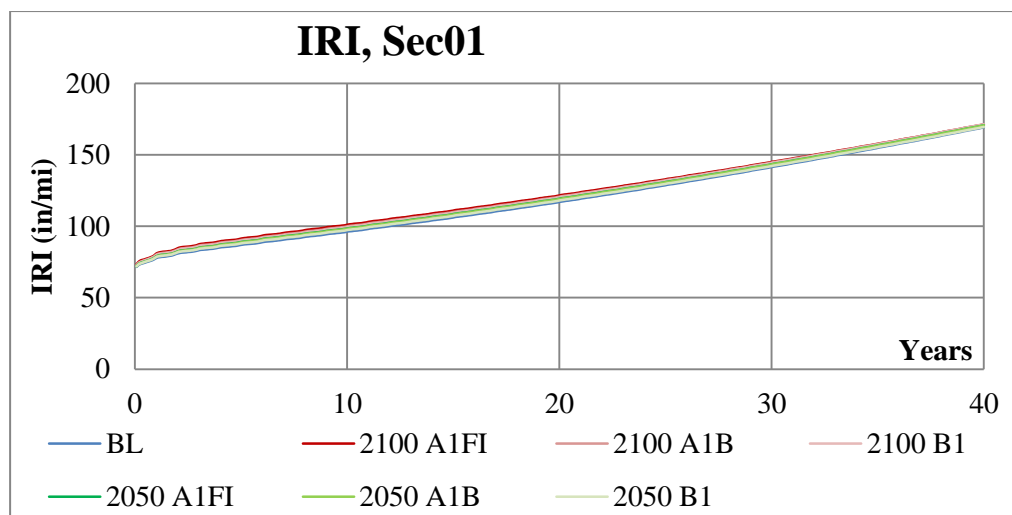
Figure A-38 IRI prediction under various emission scenarios for Sec01

Sec02
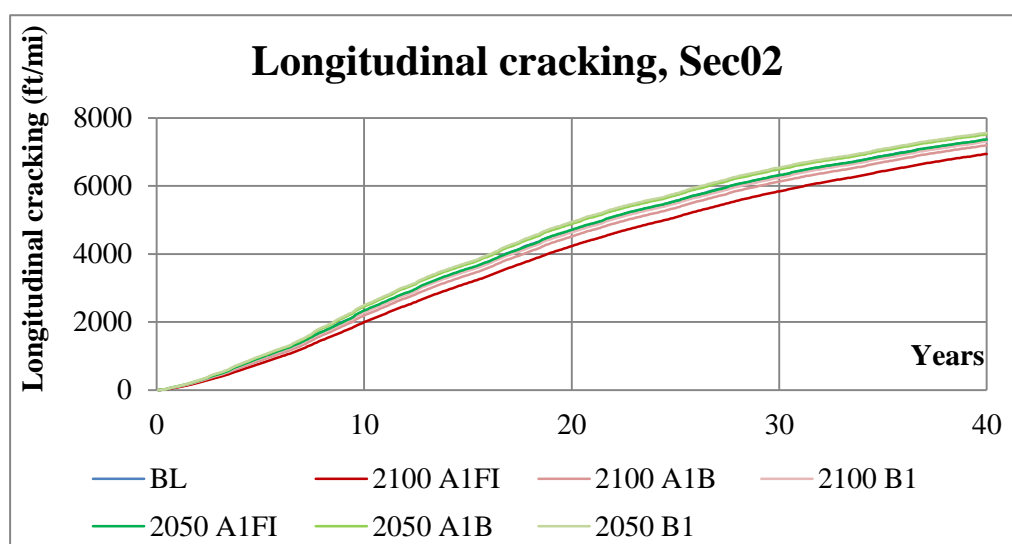
Figure A-39 Longitudinal cracking prediction under various emission scenarios for Sec02
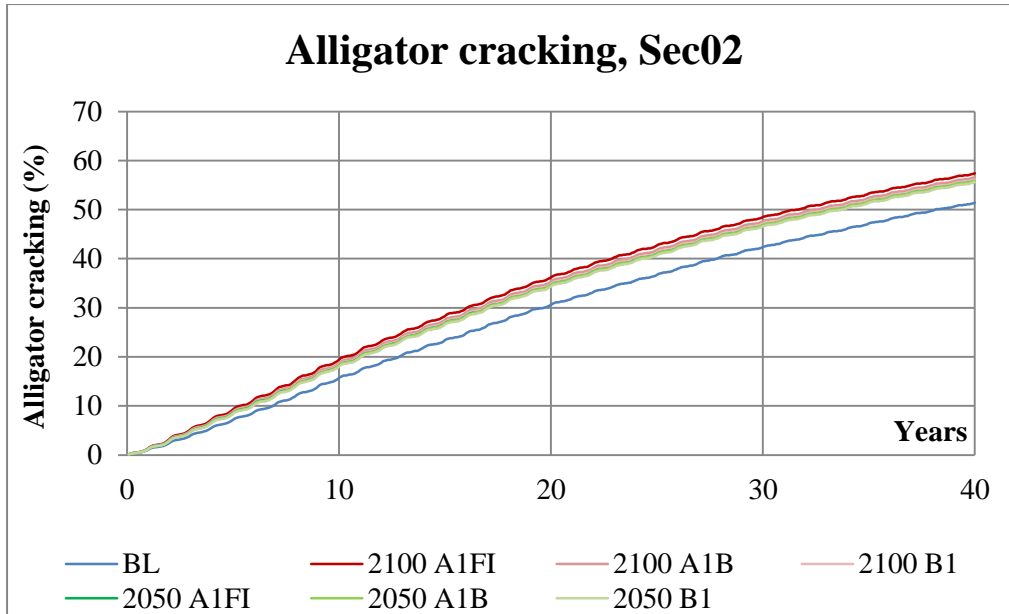
Figure A-40 Alligator cracking prediction under various emission scenarios for Sec02
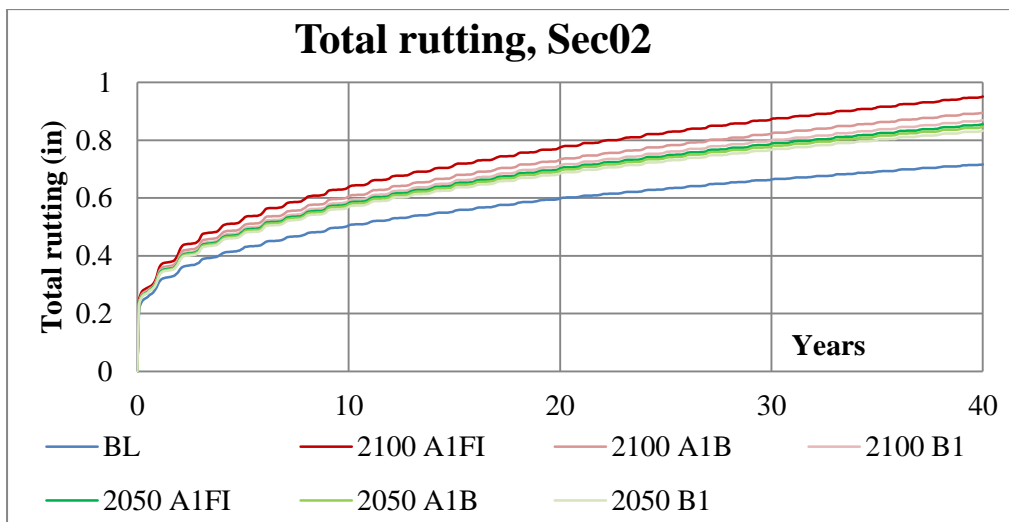
Figure A-41 Total rutting prediction under various emission scenarios for Sec02
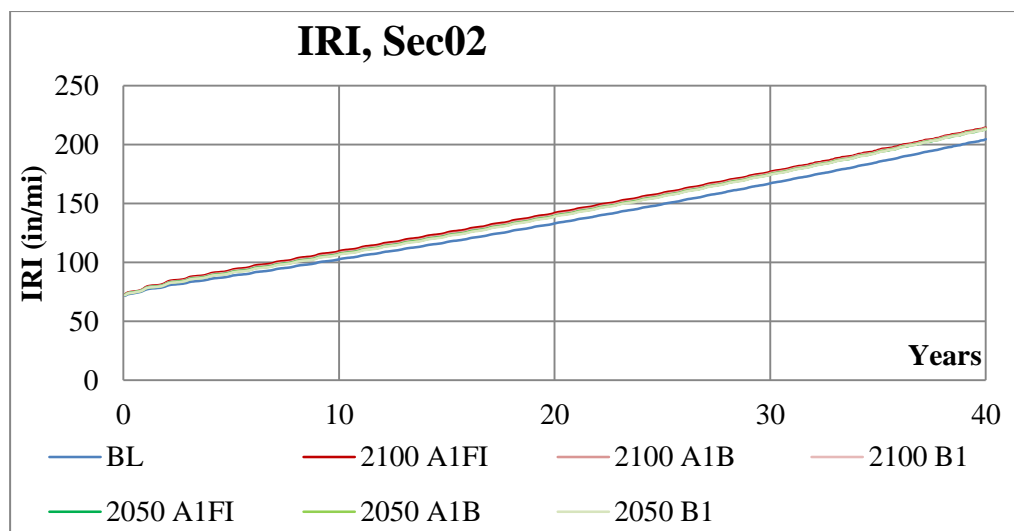
Figure A-42 IRI prediction under various emission scenarios for Sec02

Sec03
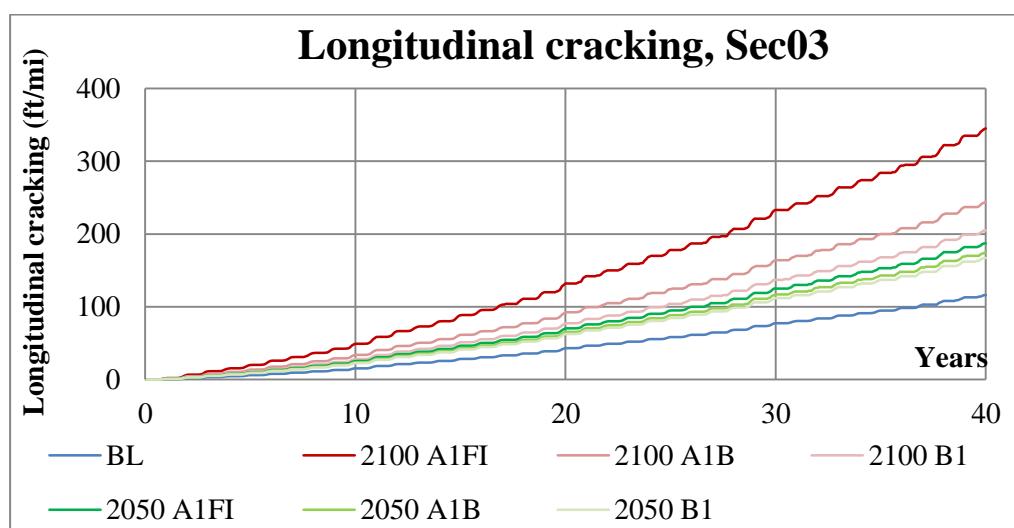
Figure A-43 Longitudinal cracking prediction under various emission scenarios for Sec03
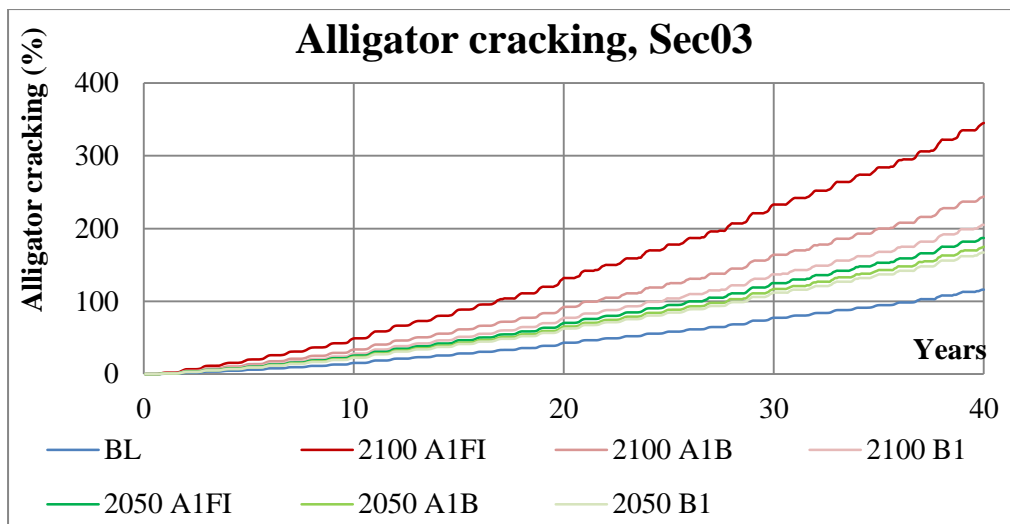
Figure A-44 Alligator cracking prediction under various emission scenarios for Sec03
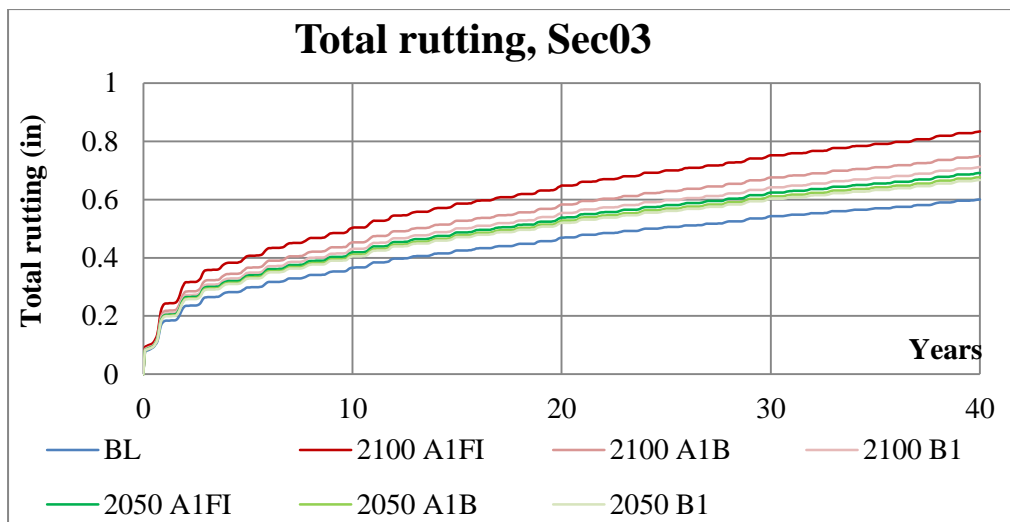
Figure A-45 Total rutting prediction under various emission scenarios for Sec03
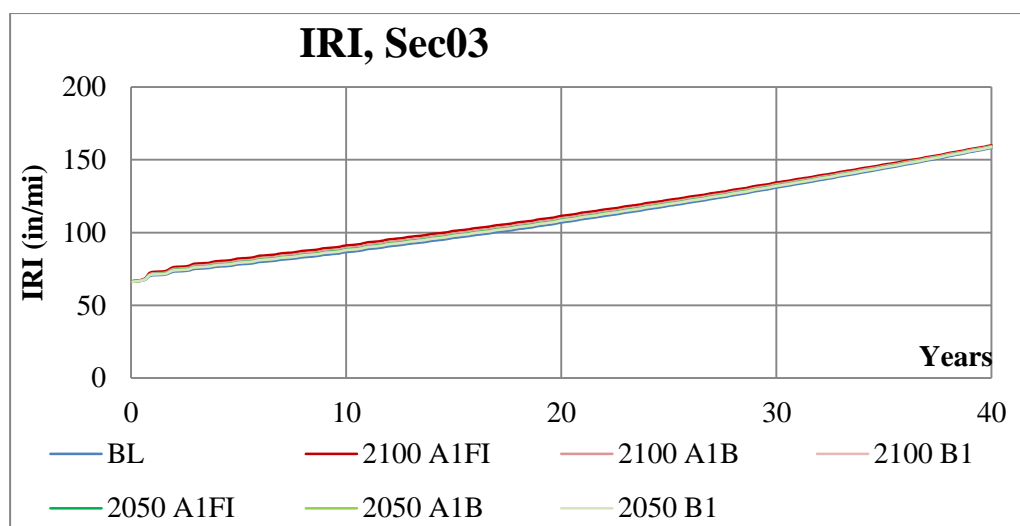
Figure A-46 IRI prediction under various emission scenarios for Sec03

Maintenance effects modelling

Data

Table A-25 Selected data for regression analysis of immediate maintenance effects models (Op1)

IRI before intervention (in/mi)	IRI after intervention (in/mi)	Rut before intervention (in)	Rut after intervention (in)	Improvement in:		Cook's D	
				IRI (in/mi)	Rutting (in)	IRI	Rutting
51.5	38	0.18	0.13	13.50	0.05	0.009	0.002
52.5	46	0.20	0.14	6.50	0.06	0.000	0.002
57.5	47	0.24	0.14	10.50	0.11	0.000	0.000
58	44.5	0.17	0.13	13.50	0.05	0.001	0.001
58	46	0.30	0.12	12.00	0.18	0.001	0.016
59.5	40.5	0.18	0.13	19.00	0.05	0.005	0.002
59.5	55.5	0.25	0.13	4.00	0.12	0.003	0.000
60	40.5	0.26	0.23	19.50	0.03	0.005	0.034
60.5	49.5	0.24	0.17	11.00	0.07	0.000	0.004
61	43.5	0.25	0.23	17.50	0.02	0.002	0.031
61.5	42.5	0.26	0.12	19.00	0.14	0.003	0.002
61.5	49	0.28	0.17	12.50	0.11	0.000	0.002
61.5	49.5	0.16	0.15	12.00	0.01	0.000	0.023
62.5	44.5	0.18	0.14	18.00	0.05	0.001	0.002
62.5	53.5	0.23	0.11	9.00	0.12	0.001	0.002
63.5	43	0.27	0.14	20.50	0.13	0.002	0.000
64	40	0.25	0.12	24.00	0.13	0.005	0.001
64.5	38.5	0.21	0.12	26.00	0.09	0.007	0.000
64.5	42.5	0.28	0.13	22.00	0.15	0.003	0.003
64.5	43.5	0.27	0.25	21.00	0.02	0.002	0.057

191

65	42.5	0.17	0.11	22.50	0.07	0.003	0.000
65.5	50.5	0.17	0.16	15.00	0.01	0.000	0.024
67	34.5	0.22	0.12	32.50	0.10	0.013	0.000
67	42.5	0.25	0.11	24.50	0.14	0.003	0.003
67	46	0.25	0.11	21.00	0.15	0.001	0.006
67	54	0.18	0.10	13.00	0.09	0.001	0.003
67.5	46.5	0.23	0.15	21.00	0.08	0.001	0.001
67.5	55	0.24	0.15	12.50	0.10	0.001	0.000
68	43.5	0.20	0.14	24.50	0.06	0.002	0.002
68	48.5	0.21	0.18	19.50	0.03	0.000	0.013
68.5	45	0.25	0.17	23.50	0.08	0.001	0.004
69	55	0.19	0.12	14.00	0.07	0.001	0.000
69.5	51	0.19	0.09	18.50	0.10	0.000	0.004
69.5	56	0.15	0.12	13.50	0.04	0.002	0.002
69.5	57	0.34	0.12	12.50	0.22	0.002	0.066
69.5	61	0.24	0.12	8.50	0.12	0.006	0.001
70	47.5	0.28	0.24	22.50	0.04	0.000	0.052
70	51	0.21	0.14	19.00	0.07	0.000	0.001
70	66.5	0.38	0.16	3.50	0.22	0.013	0.041
70.5	55	0.29	0.20	15.50	0.09	0.001	0.016
71	49.5	0.18	0.13	21.50	0.06	0.000	0.001
72	50	0.26	0.15	22.00	0.11	0.000	0.000
73	43.5	0.23	0.14	29.50	0.10	0.002	0.000
73	65	0.17	0.10	8.00	0.07	0.010	0.000
74.5	44.5	0.22	0.11	30.00	0.11	0.002	0.001
74.5	49.5	0.25	0.20	25.00	0.05	0.000	0.014
75	51	0.25	0.15	24.00	0.10	0.000	0.000
75.5	47.5	0.20	0.17	28.00	0.03	0.001	0.012
75.5	56.5	0.18	0.11	19.00	0.07	0.001	0.000
76	59.5	0.18	0.09	16.50	0.09	0.003	0.003
77	45.5	0.31	0.28	31.50	0.03	0.001	0.166
77	70	0.14	0.12	7.00	0.03	0.016	0.004
77.5	42.5	0.22	0.13	35.00	0.10	0.003	0.000
78	51	0.26	0.22	27.00	0.04	0.000	0.026
78	52.5	0.28	0.26	25.50	0.02	0.000	0.079
78	63.5	0.16	0.11	14.50	0.06	0.007	0.000
78.5	47.5	0.21	0.12	31.00	0.10	0.001	0.001
78.5	53	0.24	0.15	25.50	0.09	0.000	0.001
79	36	0.22	0.14	43.00	0.09	0.010	0.000
79	44	0.34	0.20	35.00	0.14	0.002	0.012
79.5	43.5	0.27	0.12	36.00	0.15	0.003	0.004
79.5	51	0.29	0.11	28.50	0.19	0.000	0.026
80	52	0.21	0.12	28.00	0.10	0.000	0.001
80.5	55	0.26	0.14	25.50	0.12	0.001	0.000

81	51.5	0.18	0.12	29.50	0.06	0.000	0.001
81	55	0.27	0.11	26.00	0.16	0.001	0.008
81.5	38.5	0.22	0.16	43.00	0.07	0.007	0.002
81.5	58.5	0.20	0.12	23.00	0.08	0.002	0.000
82	42.5	0.27	0.14	39.50	0.13	0.004	0.000
82	46.5	0.21	0.10	35.50	0.11	0.001	0.002
82	55.5	0.24	0.10	26.50	0.14	0.001	0.004
82	81	0.15	0.13	1.00	0.03	0.037	0.006
82.5	52	0.23	0.12	30.50	0.11	0.000	0.000
83.5	55.5	0.22	0.11	28.00	0.11	0.001	0.001
84	46	0.22	0.09	38.00	0.13	0.002	0.005
84.5	51	0.19	0.10	33.50	0.09	0.000	0.001
85	53	0.22	0.09	32.00	0.13	0.000	0.005
85	54.5	0.18	0.13	30.50	0.05	0.000	0.002
86	45	0.23	0.12	41.00	0.11	0.002	0.000
86	56	0.27	0.18	30.00	0.09	0.001	0.006
87	55	0.27	0.11	32.00	0.16	0.000	0.008
87.5	46	0.29	0.15	41.50	0.14	0.002	0.000
88	48	0.21	0.11	40.00	0.10	0.001	0.001
88.5	41.5	0.27	0.17	47.00	0.10	0.005	0.003
88.5	45	0.23	0.11	43.50	0.13	0.003	0.003
89	43	0.23	0.13	46.00	0.10	0.004	0.000
89.5	44	0.26	0.14	45.50	0.13	0.003	0.001
92	66	0.17	0.12	26.00	0.06	0.009	0.000
93	78	0.15	0.13	15.00	0.03	0.032	0.006
93.5	46	0.30	0.16	47.50	0.14	0.003	0.000
97	63	0.20	0.15	34.00	0.05	0.005	0.004
100	54	0.25	0.14	46.00	0.11	0.000	0.000
100.5	74	0.14	0.13	26.50	0.02	0.026	0.010
102	53.5	0.29	0.15	48.50	0.14	0.000	0.000
103.5	64	0.28	0.14	39.50	0.14	0.007	0.001
107.5	45.5	0.28	0.14	62.00	0.14	0.007	0.001
109	59.5	0.32	0.21	49.50	0.11	0.002	0.026
109.5	72.5	0.16	0.10	37.00	0.06	0.028	0.000
110	59	0.24	0.10	51.00	0.14	0.001	0.004
114.5	49	0.36	0.12	65.50	0.24	0.005	0.120
123	45	0.27	0.15	78.00	0.12	0.020	0.000
124	95	0.29	0.15	29.00	0.15	0.225	0.002
52	37.5	0.19	0.08	14.50	0.12	0.010	0.011
60.5	42	0.20	0.07	18.50	0.14	0.003	0.016
65	51.5	0.21	0.09	13.50	0.13	0.000	0.007
68	45	0.16	0.05	23.00	0.11	0.001	0.029
68	50	0.22	0.09	18.00	0.14	0.000	0.008
76.5	46.5	0.16	0.05	30.00	0.11	0.001	0.029

83	41.5	0.18	0.05	41.50	0.13	0.005	0.026
90.5	62	0.17	0.10	28.50	0.08	0.004	0.002
98.5	54.5	0.27	0.12	44.00	0.15	0.000	0.004
105	68	0.20	0.11	37.00	0.10	0.014	0.002
105.5	58	0.18	0.09	47.50	0.09	0.001	0.003
151.5	100	0.27	0.11	51.50	0.16	0.578	0.008
319.5	47.5	0.32	0.12	272.00	0.20	27.178	0.034

Table A-26 Selected data for regression analysis of immediate maintenance effects models (Op2)

IRI before intervention (in/mi)	IRI after intervention (in/mi)	Rut before intervention (in)	Rut after intervention (in)	Improvement in:		Cook's D	
				IRI (in/mi)	Rutting (in)	IRI (in/mi)	Rutting (in)
54.5	39	0.215	0.07	15.5	0.145	0.03	0.01
54.5	44	0.205	0.07	10.5	0.135	0.07	0.01
55.5	35.5	0.3	0.2	20	0.1	0.01	0.02
56	37.5	0.32	0.085	18.5	0.235	0.01	0.03
58.5	34	0.285	0.095	24.5	0.19	0.00	0.00
62.5	37.5	0.255	0.08	25	0.175	0.00	0.01
63	46	0.2	0.1	17	0.1	0.02	0.00
65.5	40.5	0.265	0.175	25	0.09	0.00	0.01
67	36	0.35	0.09	31	0.26	0.00	0.04
67	37	0.225	0.07	30	0.155	0.00	0.01
67.5	37.5	0.285	0.105	30	0.18	0.00	0.00
68.5	41	0.38	0.1	27.5	0.28	0.00	0.07
69	33.5	0.215	0.065	35.5	0.15	0.01	0.01
69	36	0.26	0.195	33	0.065	0.00	0.02
69	38	0.2	0.095	31	0.105	0.00	0.00
70.5	36	0.235	0.105	34.5	0.13	0.00	0.00
70.5	39.5	0.195	0.075	31	0.12	0.00	0.00
70.5	46.5	0.51	0.23	24	0.28	0.00	0.01
71	40	0.28	0.21	31	0.07	0.00	0.03
71.5	50	0.34	0.095	21.5	0.245	0.01	0.03
72	42.5	0.145	0.07	29.5	0.075	0.00	0.00
72	52	0.31	0.18	20	0.13	0.01	0.01
72.5	38	0.185	0.08	34.5	0.105	0.00	0.00
72.5	41.5	0.175	0.06	31	0.115	0.00	0.01
74.5	48.5	0.245	0.075	26	0.17	0.00	0.01
75	47.5	0.425	0.175	27.5	0.25	0.00	0.00
76.5	44	0.26	0.23	32.5	0.03	0.00	0.06
77	48.5	0.205	0.08	28.5	0.125	0.00	0.00
77.5	44.5	0.27	0.215	33	0.055	0.00	0.03

77.5	49	0.35	0.22	28.5	0.13	0.00	0.04
77.5	50	0.205	0.07	27.5	0.135	0.00	0.01
79.5	54.5	0.305	0.215	25	0.09	0.01	0.04
80	46.5	0.325	0.18	33.5	0.145	0.00	0.01
80.5	35	0.32	0.095	45.5	0.225	0.02	0.02
80.5	40.5	0.275	0.105	40	0.17	0.01	0.00
81.5	36	0.23	0.06	45.5	0.17	0.02	0.01
82	36.5	0.29	0.085	45.5	0.205	0.02	0.01
82.5	34.5	0.33	0.1	48	0.23	0.03	0.02
84	51.5	0.46	0.2	32.5	0.26	0.00	0.00
88.5	43.5	0.185	0.085	45	0.1	0.02	0.00
89	38.5	0.275	0.1	50.5	0.175	0.05	0.00
89.5	54	0.375	0.215	35.5	0.16	0.00	0.04
98	62	0.23	0.215	36	0.015	0.00	0.06
102.5	77	0.13	0.1	25.5	0.03	0.10	0.03
105.5	59.5	0.22	0.06	46	0.16	0.01	0.01
121.5	50	0.325	0.16	71.5	0.165	0.94	0.00
148.5	124.5	0.22	0.16	24	0.06	6.72	0.02

Table A-27 Selected data for regression analysis of immediate maintenance effects models (Op3)

IRI before intervention (in/mi)	IRI after intervention (in/mi)	Rut before intervention (in)	Rut after intervention (in)	Improvement in:		Cook's D	
				IRI (in/mi)	Rutting (in)	IRI (in/mi)	Rutting (in)
48.5	44.5	0.115	0.065	4	0.05	0.004	0.002
50.5	43.5	0.12	0.06	7	0.06	0.006	0.005
52	37	0.1	0.07	15	0.03	0.027	0.000
53.5	44.5	0.11	0.085	9	0.025	0.005	0.000
53.5	52.5	0.125	0.12	1	0.005	0.001	0.007
54.5	51.5	0.225	0.155	3	0.07	0.000	0.001
55	41.5	0.12	0.065	13.5	0.055	0.011	0.005
56.5	40.5	0.11	0.075	16	0.035	0.014	0.001
58	53.5	0.115	0.1	4.5	0.015	0.001	0.002
59	55.5	0.18	0.105	3.5	0.075	0.003	0.001
60.5	50	0.135	0.085	10.5	0.05	0.000	0.000
61.5	48	0.165	0.075	13.5	0.09	0.001	0.004
62	49	0.28	0.105	13	0.175	0.001	0.045
62	56.5	0.235	0.165	5.5	0.07	0.003	0.002
63	42	0.11	0.085	21	0.025	0.010	0.000
63	53.5	0.125	0.1	9.5	0.025	0.000	0.001
63	54.5	0.12	0.07	8.5	0.05	0.001	0.002
63.5	49	0.195	0.1	14.5	0.095	0.001	0.002
64	48.5	0.155	0.08	15.5	0.075	0.001	0.003

65.5	52	0.145	0.085	13.5	0.06	0.000	0.001
68	47	0.23	0.155	21	0.075	0.003	0.000
68	47.5	0.185	0.06	20.5	0.125	0.002	0.012
68	50.5	0.16	0.07	17.5	0.09	0.000	0.006
69	47.5	0.115	0.105	21.5	0.01	0.002	0.006
69	54.5	0.24	0.105	14.5	0.135	0.000	0.011
69.5	46.5	0.11	0.06	23	0.05	0.003	0.004
70	58.5	0.125	0.085	11.5	0.04	0.002	0.000
72	46.5	0.21	0.14	25.5	0.07	0.003	0.000
72	57	0.235	0.15	15	0.085	0.001	0.000
72.5	51.5	0.185	0.09	21	0.095	0.000	0.003
72.5	55	0.25	0.1	17.5	0.15	0.000	0.016
72.5	57	0.26	0.235	15.5	0.025	0.001	0.033
72.5	66	0.245	0.215	6.5	0.03	0.011	0.024
73	54	0.155	0.095	19	0.06	0.000	0.000
73	55.5	0.235	0.115	17.5	0.12	0.000	0.004
74	47	0.155	0.07	27	0.085	0.003	0.006
74	50	0.205	0.115	24	0.09	0.001	0.000
74	60.5	0.215	0.175	13.5	0.04	0.003	0.006
74.5	55.5	0.26	0.22	19	0.04	0.000	0.024
75	43	0.1	0.085	32	0.015	0.008	0.001
75	58	0.135	0.11	17	0.025	0.001	0.001
75	68	0.275	0.14	7	0.135	0.013	0.008
75.5	52	0.215	0.185	23.5	0.03	0.000	0.010
76	59.5	0.23	0.17	16.5	0.06	0.002	0.003
76	64.5	0.14	0.12	11.5	0.02	0.007	0.004
76.5	54	0.2	0.15	22.5	0.05	0.000	0.002
76.5	58	0.265	0.205	18.5	0.06	0.001	0.016
76.5	58.5	0.285	0.19	18	0.095	0.001	0.002
77	52.5	0.255	0.09	24.5	0.165	0.000	0.031
77	54.5	0.245	0.11	22.5	0.135	0.000	0.011
77	60.5	0.25	0.1	16.5	0.15	0.002	0.016
77.5	50.5	0.2	0.165	27	0.035	0.001	0.003
77.5	54.5	0.27	0.15	23	0.12	0.000	0.002
77.5	55.5	0.225	0.12	22	0.105	0.000	0.002
78	67	0.32	0.12	11	0.2	0.010	0.089
78.5	50	0.155	0.095	28.5	0.06	0.001	0.000
79	55	0.145	0.12	24	0.025	0.000	0.002
79	59	0.12	0.11	20	0.01	0.001	0.006
80	52	0.19	0.08	28	0.11	0.000	0.005
80.5	48.5	0.145	0.13	32	0.015	0.002	0.005
81	48.5	0.145	0.13	32.5	0.015	0.002	0.005
81	57.5	0.125	0.08	23.5	0.045	0.000	0.001
81.5	60	0.18	0.155	21.5	0.025	0.001	0.004

82.5	55	0.16	0.155	27.5	0.005	0.000	0.009
82.5	55.5	0.23	0.16	27	0.07	0.000	0.001
82.5	62.5	0.18	0.175	20	0.005	0.003	0.010
83	51	0.17	0.085	32	0.085	0.001	0.004
83.5	60.5	0.29	0.155	23	0.135	0.001	0.007
83.5	65.5	0.145	0.135	18	0.01	0.006	0.008
84	49.5	0.18	0.055	34.5	0.125	0.002	0.015
85	48.5	0.14	0.135	36.5	0.005	0.003	0.008
85	52	0.3	0.16	33	0.14	0.001	0.005
86.5	57.5	0.16	0.075	29	0.085	0.000	0.006
86.5	63.5	0.19	0.145	23	0.045	0.003	0.001
86.5	64	0.235	0.2	22.5	0.035	0.003	0.012
87	61.5	0.265	0.185	25.5	0.08	0.002	0.005
87.5	60	0.22	0.08	27.5	0.14	0.001	0.012
88	58	0.22	0.155	30	0.065	0.000	0.001
88.5	56	0.16	0.075	32.5	0.085	0.000	0.006
89.5	57	0.325	0.23	32.5	0.095	0.000	0.023
90.5	55	0.205	0.165	35.5	0.04	0.000	0.005
91	63.5	0.165	0.095	27.5	0.07	0.002	0.000
91.5	46.5	0.185	0.15	45	0.035	0.006	0.003
91.5	50.5	0.305	0.22	41	0.085	0.002	0.018
91.5	59	0.27	0.22	32.5	0.05	0.000	0.024
91.5	60.5	0.125	0.11	31	0.015	0.001	0.003
92	50.5	0.29	0.16	41.5	0.13	0.003	0.003
92	52.5	0.165	0.085	39.5	0.08	0.001	0.002
94	44.5	0.11	0.085	49.5	0.025	0.010	0.000
96	55	0.175	0.1	41	0.075	0.001	0.001
97	67	0.24	0.205	30	0.035	0.005	0.012
97.5	57.5	0.21	0.115	40	0.095	0.000	0.002
98	54	0.135	0.1	44	0.035	0.001	0.000
98.5	53.5	0.23	0.12	45	0.11	0.002	0.002
99.5	57.5	0.215	0.21	42	0.005	0.000	0.018
100.5	72.5	0.15	0.095	28	0.055	0.014	0.001
102	58	0.21	0.195	44	0.015	0.000	0.011
102.5	47	0.205	0.06	55.5	0.145	0.012	0.017
102.5	54.5	0.285	0.175	48	0.11	0.002	0.000
102.5	66.5	0.185	0.075	36	0.11	0.004	0.005
103	56	0.14	0.075	47	0.065	0.001	0.004
105	76	0.255	0.22	29	0.035	0.024	0.024
106	49.5	0.205	0.18	56.5	0.025	0.010	0.007
108.5	62.5	0.245	0.145	46	0.1	0.001	0.000
109	73.5	0.245	0.205	35.5	0.04	0.018	0.018
110.5	54.5	0.215	0.075	56	0.14	0.004	0.012
110.5	87.5	0.085	0.08	23	0.005	0.080	0.002

111	104	0.21	0.12	7	0.09	0.212	0.000
112.5	57	0.285	0.155	55.5	0.13	0.002	0.003
115.5	50	0.275	0.105	65.5	0.17	0.018	0.033
115.5	56	0.15	0.14	59.5	0.01	0.004	0.008
116	42.5	0.13	0.075	73.5	0.055	0.052	0.003
116.5	63	0.23	0.125	53.5	0.105	0.000	0.002
120.5	47.5	0.18	0.145	73	0.035	0.038	0.002
121	73.5	0.14	0.105	47.5	0.035	0.020	0.000
129.5	61.5	0.2	0.165	68	0.035	0.002	0.003
135.5	56	0.245	0.085	79.5	0.16	0.026	0.022
136.5	78.5	0.28	0.25	58	0.03	0.052	0.060
141	60.5	0.33	0.22	80.5	0.11	0.013	0.011
165.5	95.5	0.255	0.115	70	0.14	0.461	0.010
171.5	48.5	0.22	0.14	123	0.08	0.508	0.000
201	65.5	0.21	0.07	135.5	0.14	0.289	0.012

Regression analysis results
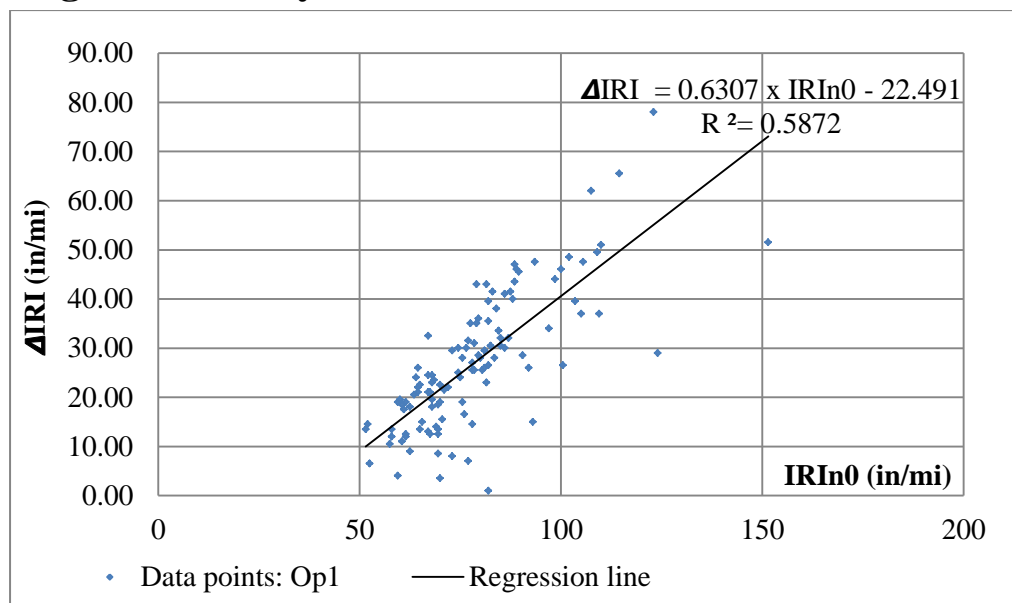
Figure A-47 Regression analysis: maintenance effect of Op1 on IRI
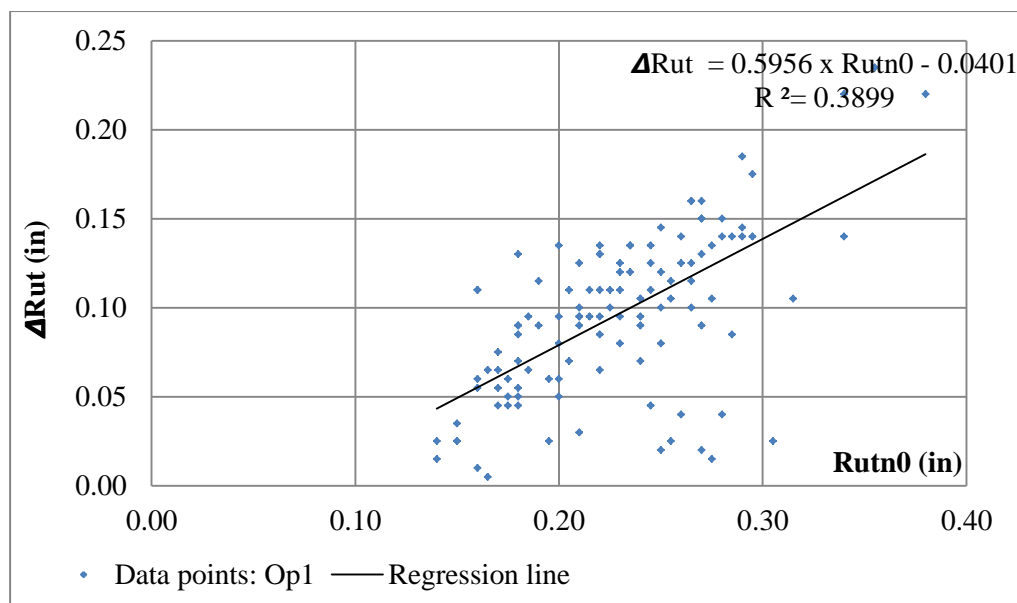
Figure A-48 Regression analysis: maintenance effect of Op1 on rutting
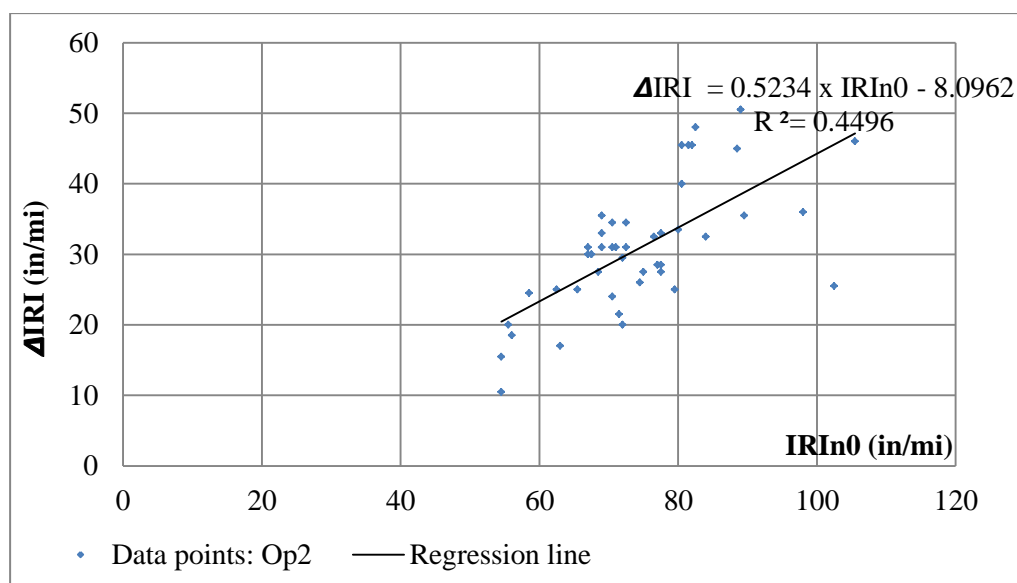
Figure A-49 Regression analysis: maintenance effect of Op2 on IRI
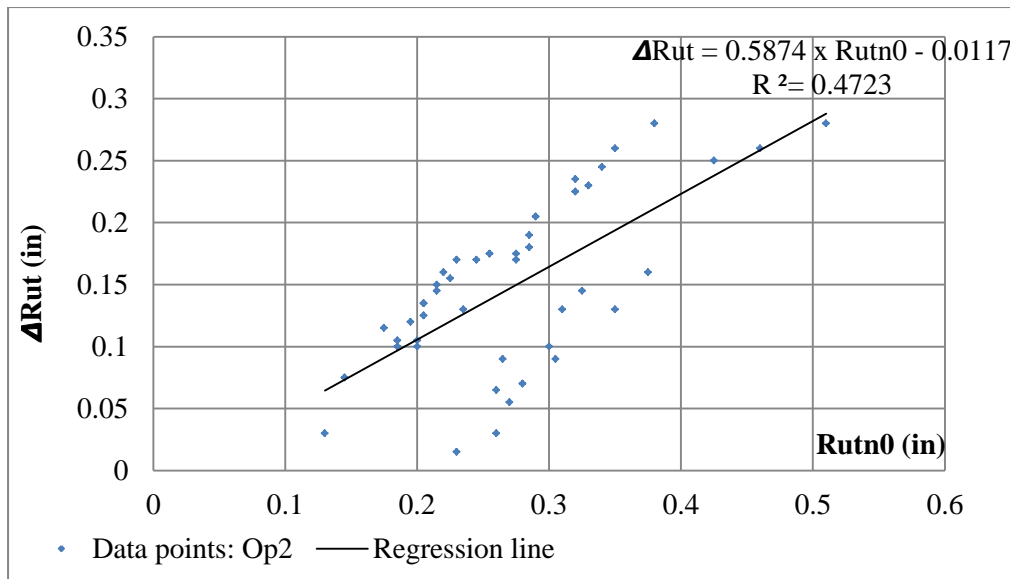
Figure A-50 Regression analysis: maintenance effect of Op2 on rutting
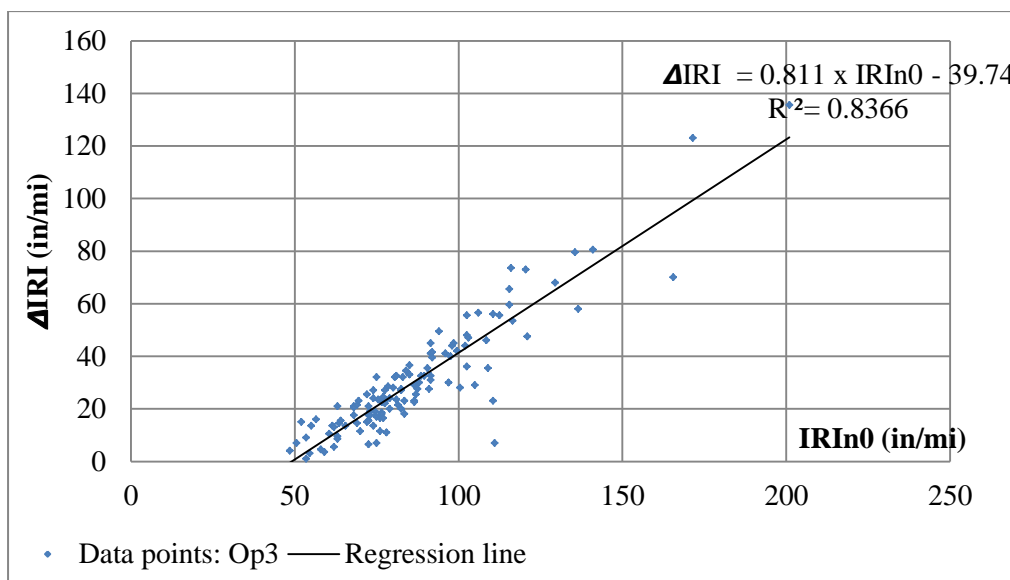
Figure A-51 Regression analysis: maintenance effect of Op3 on IRI
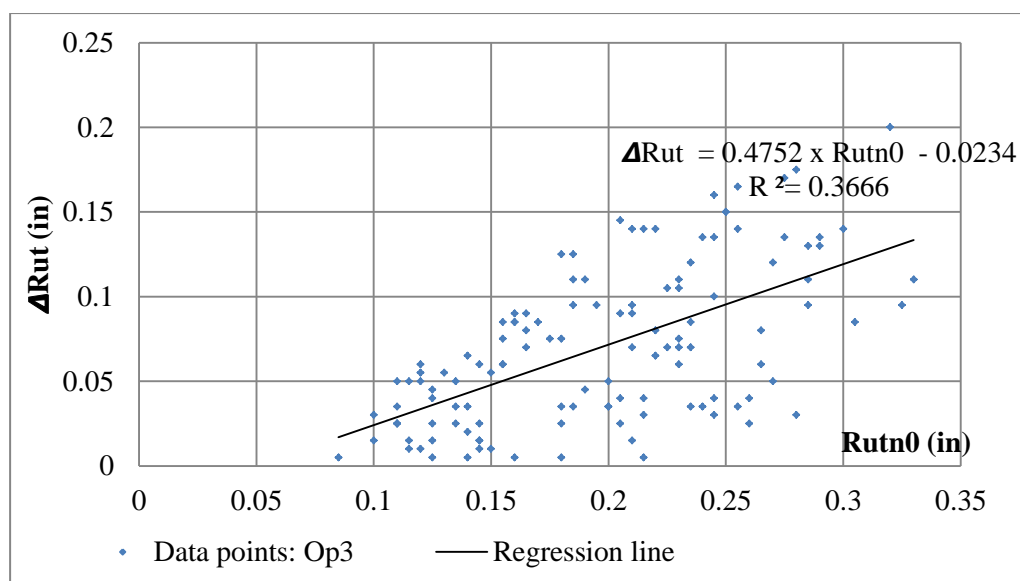
Figure A-52 Regression analysis: maintenance effect of Op3 on rutting

Maintenance effects and thickness
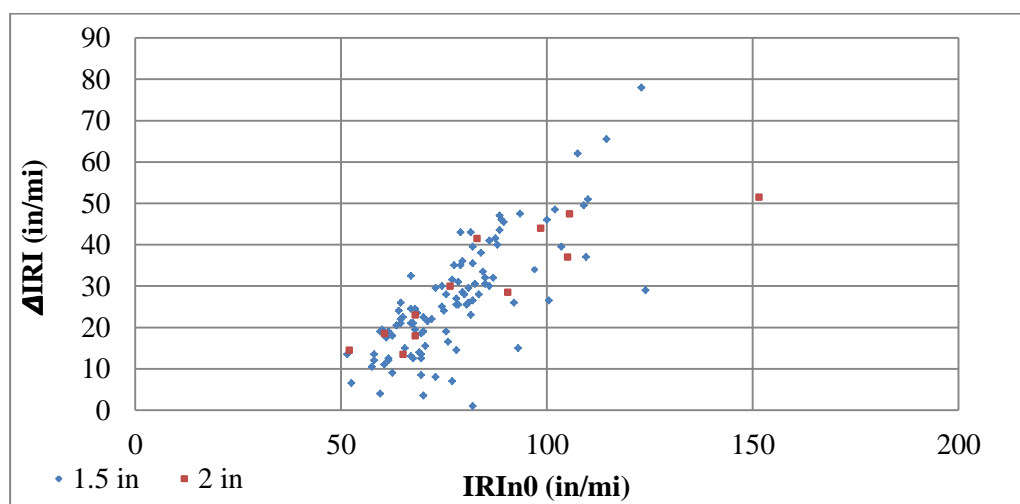
Figure A-53 Op1: Immediate maintenance effect on IRI by overlay thickness
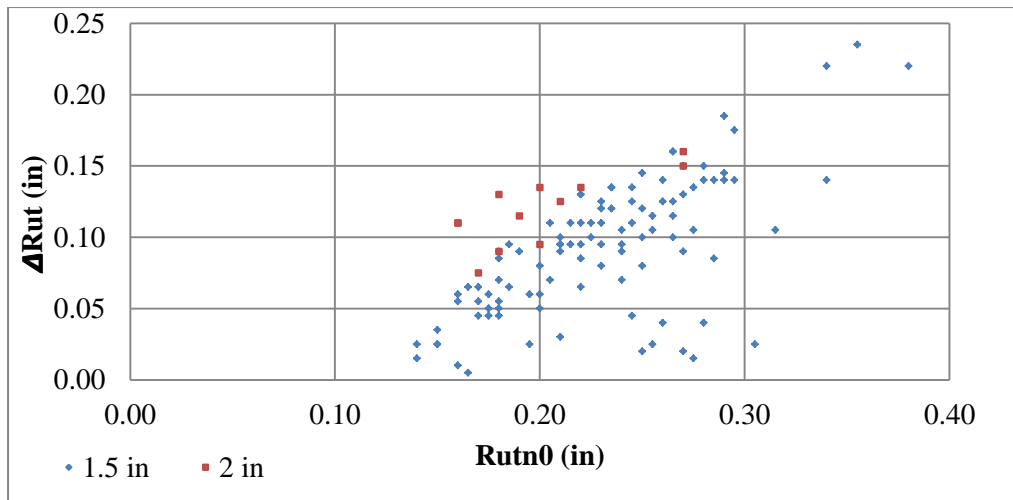
Figure A-54 Op1: Immediate maintenance effect on rutting by overlay thickness
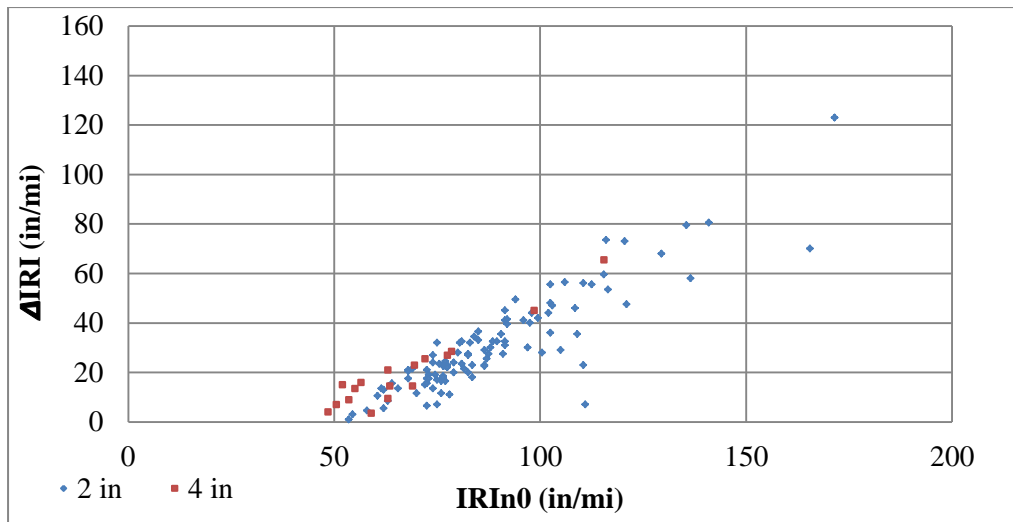
Figure A-55 Op3: Immediate maintenance effect on IRI by filling thickness
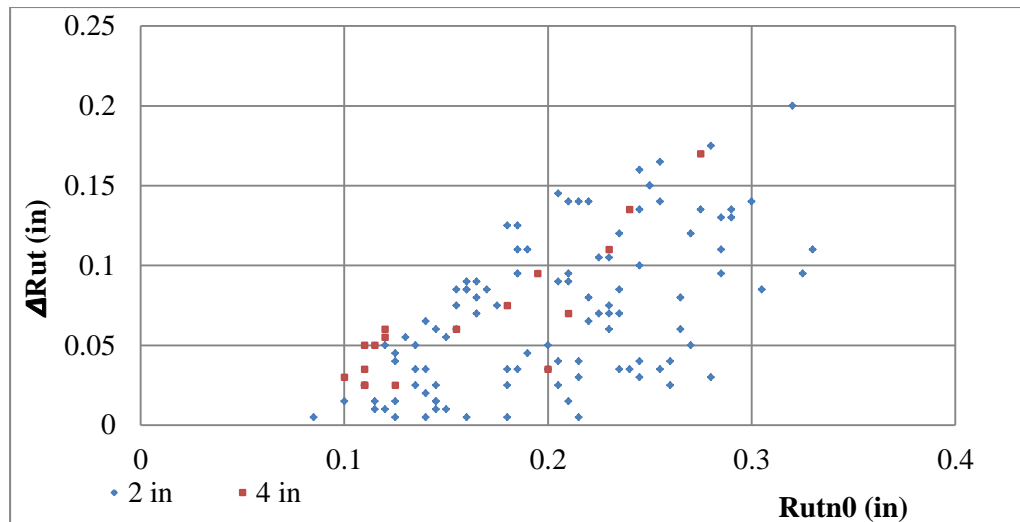
Figure A-56 Op3: Immediate maintenance effect on rutting by filling thickness

Notice: Op2 was not presented because there was only two valid data points of 3.5 inch (≈ 89 mm) in thickness.

Maintenance optimisation and LCCA

An Example of estimations on freeway capacity, WZ capacity, and WZ costs

This appendix gave details of calculation process in determining freeway capacity, WZ capacity, and WZ costs. The freeway capacity was calculated according to FHWA's Highway Capacity Manual (2000). The WZ capacity was computed using Memmott and Dudek's model (1982). The WZ costs were calculated using selected models (see a description in section 2.4.3 and 3.7.2). Excel spreadsheets were developed to calculate these parameters for the three sections.

Freeway capacity

The freeway capacity was calculated in three steps including (TRB, 2000):

Step 1: Calculate Free Flow Speed (FFS)

Step 2: Calculate Base Capacity (BaseCap)

Step 3: Determine Peak Capacity (PeakCap)

Step 1

The free flow speed was calculated using the equation as follows (TRB, 2000) :

$$FFS = BFFS - f_{LW} - f_{LC} - f_N - f_{ID}$$

203

where,

$BFFS$ = base free flow speed

f_{LW} = adjustment factor for land width

f_{LC} = adjustment factor for right shoulder lateral clearance

f_N = adjustment factor number of lanes

f_{ID} = adjustment factor for interchange density

Table A-28 Free flow speed adjustment factor f_{LW} (TRB, 2000)

Lane Width	Reduction in FFS (mph; f_{LW})
12 ft.	0.0
11 ft.	1.9
<=10 ft.	6.6

Table A-29 Free flow speed adjustment factor f_{LC} (TRB, 2000)

Right Shoulder Width	Reduction in FFS (mph; f_{LC})			
	Lanes in One Direction			
	2	3	4	>=5
>=6	0.0	0.0	0.0	0.0
5	0.6	0.4	0.2	0.1
4	1.2	0.8	0.4	0.2
3	1.8	1.2	0.6	0.3
2	2.4	1.6	0.8	0.4
1	3.0	2.0	1.0	0.5
0	3.6	2.4	1.2	0.6

Table A-30 Free flow speed adjustment factor f_N (TRB, 2000)

No. Lanes (One Direction; Urban Only)	Reduction in FFS (mph; f_N)
>= 5	0.0
4	1.5
3	3.0
2	4.5

Table A-31 Free flow speed adjustment factor f_{ID} (TRB, 2000)

Functional Class	Area Size	Interchange Density	Interchange Adj. Factor, (f_{ID})
Urban Interstates	Small Urban	0.70	1.0
	Small Urbanized	0.76	1.3
	Large Urbanized	0.83	1.7
Other Urban Highways Qualifying as Freeways	Small Urban	0.83	1.7
	Small Urbanized	0.88	1.9
	Large Urbanized	0.91	2.1

The base free flow speed equalled to the design speed of the highways, which was assumed to be 65 mph ($\approx$ 105 km/h) for all the three sections. The shoulder length was not recorded from the PMS and f_{LC} was assumed to be 1.8 as a medium value for two lanes highways in one direction. Sec01, Sec02, and Sec03 were all considered to locate in small urban and thus f_N and f_{ID} can be chosen. *FFS* was calculated for the three sections and the results were resented in Table A-32.

Table A-32 Calculation results of FFS (TRB, 2000)

	$BFFS$ (mph)	f_{LW}	f_{LC}	f_N	f_{ID}	FFS (mph)
Sec01	65	6.6	1.8	4.5	1	51.1
Sec02	65	1.9	1.8	4.5	1	55.8
Sec03	65	1.9	1.8	4.5	1	55.8

Step 2

Basecap was calculated with the following equation (TRB, 2000):

$Basecap = 1700 + 10 FFS; for FFS \leq 70$

$Basecap = 2400; for FFS > 70$

Basecap was calculated and presented later in Table A-33.

Step 3

Peakcap was calculated using equation (TRB, 2000):

$Peakcap = Basecap * PHF * N * f_{HV} * f_p$

where,

PHF =peak hour factor

N = number of lanes in one direction

f_{HV} = adjustment factor for heavy vehicles

f_p = adjustment factor for driver population

$$f_{HV} = \frac{1}{1 + P_T(E_T - 1)}$$

where,

P_T = truck percentage as decimal

E_T = passenger-car equivalents

      The value of PHF was assumed to be 0.92 for all the three sections, which accounted for a medium value for urban highways. E_T was assumed to be 1.5 which is for urban. It was assumed that drivers are familiar with the road and traffic conditions and f_p =1. Eventually, $Peakcap$ calculation results were presented in Table A-33.

Table A-33 Calculation results of Peakcap

	Basecap	PHF	N	f_{HV}	f_p	Peakcap
Sec01	2211	0.92	2	0.98	1	3969
Sec02	2258	0.92	2	0.95	1	3957
Sec03	2258	0.92	2	0.92	1	3838

WZ capacity

The WZ capacity was estimated using Equation 2-61. Below is a table to choose the intercept and slope for the equation. The risk factor ($CERF$) represented the probability that the estimated capacity will be less or equal to the actual capacity. To avoid underestimation on the WZ capacity, $CERF$ was chosen to be 0.05, indicating that there was only 5% probability for the actual capacity to be greater than the estimated one.

Table A-34 Coefficients for WZ capacity (Memmott and Dudek, 1982)

Intercept term (a)					
	Open lanes through work zone in one direction				
Number of open lands in one direction	1	2	3	4	5
2	1460				
3	1370	1600			
4	1200	1580	1560		
5	1200	1460	1500	1550	

6	1200	1400	1500	1550	1580
Slope term (b)					
Number of open lands in one direction	1	2	3	4	5
2	2.13				
3	4.05	1.81			
4	0	1.6	0.57		
5	0	1.46	0	0	
6	0	0	0	0	0

WZ delays calculation

The WZ delays were calculated using an Excel spreadsheet. The spreadsheet linked the calculations of the free flow capacity, WZ capacity, and the average IRI of the pavement over the design life (40 years), which were inputs for computing WZ costs. The following case is used as an example to demonstrate the calculation process. The case was for Op3 in Sec03 under baseline scenario with IRI_{min} = 50 in/mi. The inputs for WZ costs are presented as follows:

Table A-35 WZ costs inputs, Op3, Sec03

Input Index		
1	Value of time for car drivers	8 USD/hour
2	Value of time for truck drivers	15 USD/hour
3	WZ start time	00:00
4	WZ end time	08:00
5	Free flow speed	65 mph
6	WZ speed	35 mph
7	Maintenance duration	10 days
8	AADT	43145
9	Truck percentage	16.5%
10	WZ length	0.77 mile (≈1.24 km)
11	Lane width	9.8 feet
12	Free flow capacity	3838
13	WZ capacity	1460
14	Average IRI	variable, = 67.8 in/mi when optimisation completed

To calculate the WZ costs of Op1 and Op2, maintenance duration needs to be changed (see Table 3-6). WZ costs calculations and results for the example can be found in Table A-36. To perform the same calculations for

Sec01 and Sec02, inputs 1-6 were same as Sec03 (see Table A-35) and inputs 7-11 were replaced by section-specific values (see Table 3-3 and Table 3-6). Section-specific parameters were applied to obtain inputs 12-14.

Table A-36 An example of WZ costs calculation

	Demand (veh/h)	Road capacity	Outgoing vehicles	Accumulative incoming vehicles	Accumulative outgoing vehicles	Queue length (Vehicles)	Queueing Delay (vehicle-hours)	Moving delay (vehicle-hours)	Fuel Consumption costs (USD)	Oil consumption (USD)	Tire wear (USD)
Midnight	992	1460	992	992	992	0	0.0	10.1	73.0	13.9	0.0
1:00 am	992	1460	992	1985	1985	0	0.0	10.1	73.0	13.9	0.0
2:00 am	992	1460	992	2977	2977	0	0.0	10.1	73.0	13.9	0.0
3:00 am	992	1460	992	3969	3969	0	0.0	10.1	73.0	13.9	0.0
4:00 am	992	1460	992	4962	4962	0	0.0	10.1	73.0	13.9	0.0
5:00 am	992	1460	992	5954	5954	0	0.0	10.1	73.0	13.9	0.0
6:00 am	2157	1460	1460	8111	7414	697	348.6	14.8	158.6	30.2	0.1
7:00 am	2157	1460	1460	10269	8874	1395	1045.9	14.8	158.6	30.2	0.1
8:00 am	2157	3838	3552	12426	12426	0	697.3	0.0	185.6	30.2	0.1
9:00	2157	3838	2157	14583	14583	0	0.0	0.0	185.6	30.2	0.1

am											
10:00 am	2546	3838	2546	17129	17129	0	0.0	0.0	219.0	35.6	0.1
11:00 am	2546	3838	2546	19674	19674	0	0.0	0.0	219.0	35.6	0.1
Noon	2546	3838	2546	22220	22220	0	0.0	0.0	219.0	35.6	0.1
1:00 pm	2546	3838	2546	24765	24765	0	0.0	0.0	219.0	35.6	0.1
2:00 pm	2546	3838	2546	27311	27311	0	0.0	0.0	219.0	35.6	0.1
3:00 pm	2546	3838	2546	29856	29856	0	0.0	0.0	219.0	35.6	0.1
4:00 pm	1985	3838	1985	31841	31841	0	0.0	0.0	170.7	27.7	0.1
5:00 pm	1985	3838	1985	33826	33826	0	0.0	0.0	170.7	27.7	0.1
6:00 pm	1985	3838	1985	35810	35810	0	0.0	0.0	170.7	27.7	0.1
7:00 pm	1985	3838	1985	37795	37795	0	0.0	0.0	170.7	27.7	0.1
8:00 pm	1337	3838	1337	39133	39133	0	0.0	0.0	115.1	18.7	0.0
9:00 pm	1337	3838	1337	40470	40470	0	0.0	0.0	115.1	18.7	0.0

10:00 pm	1337	3838	1337	41808	41808	0	0.0	0.0	115.1	18.7	0.0
11:00 pm	1337	3838	1337	43145	43145	0	0.0	0.0	115.1	18.7	0.0
Daily costs (USD)							19,150.0	823.6	3,583.5	603.2	1.5
Total costs (USD)							191,499.7	8,235.752	35,834.6	6,032.4	14.7
						Total WZ delay costs (USD)	199,736		Total WZ VOC (USD)	41,882	
						Total WZ costs (USD)	241,617				

An example of LCCA results

Following the same example (Alternative 2, BL, IRI_{min} = 50 in/mi, weighting factor = 1, Sec03), the LCCA results can be shown in

Table A-37.

Table A-37 An example of LCCA results

Years	Maintenance decision-making			Pavement performance		LCC components in NPV (USD)					
	Op1	Op2	Op3	IRI (in/mi)	Rutting (in)	Op1 costs	Op2 costs	Op3 costs	Agency costs	WZ costs	VOC
1	0	0	0	70.6	0.182	0	0	0	0	0	5,754,750
2	0	0	0	73.2	0.234	0	0	0	0	0	5,766,072
3	0	0	0	75.1	0.264	0	0	0	0	0	5,769,182
4	0	0	0	76.5	0.281	0	0	0	0	0	5,766,459
5	1	0	0	51.1	0.171	49,367	0	0	49,367	119,239	5,456,455
6	0	0	0	52.8	0.190	0	0	0	0	0	5,458,076
7	0	0	0	54.4	0.202	0	0	0	0	0	5,458,489
8	0	0	0	56.0	0.214	0	0	0	0	0	5,458,841
9	0	0	0	57.7	0.225	0	0	0	0	0	5,460,264
10	0	0	0	59.6	0.239	0	0	0	0	0	5,463,876

11	0	0	0	61.6	0.257	0	0	0	0	0	5,468,530
12	0	0	0	63.6	0.270	0	0	0	0	0	5,473,095
13	0	0	0	65.4	0.278	0	0	0	0	0	5,475,339
14	0	0	0	67.3	0.287	0	0	0	0	0	5,478,623
15	0	0	0	69.4	0.298	0	0	0	0	0	5,484,046
16	0	0	0	71.3	0.305	0	0	0	0	0	5,487,164
17	0	0	0	73.3	0.313	0	0	0	0	0	5,491,305
18	0	0	0	75.4	0.321	0	0	0	0	0	5,496,460
19	0	0	0	77.6	0.330	0	0	0	0	0	5,502,617
20	0	0	0	79.9	0.342	0	0	0	0	0	5,509,768
21	0	0	0	82.2	0.352	0	0	0	0	0	5,516,813
22	0	0	0	84.4	0.358	0	0	0	0	0	5,522,669
23	0	0	0	86.7	0.365	0	0	0	0	0	5,529,509
24	0	0	0	89.1	0.373	0	0	0	0	0	5,537,323
25	0	1	0	52.9	0.170	0	55,491	0	55,491	266,081	5,130,100
26	0	0	0	55.2	0.176	0	0	0	0	0	5,137,978
27	0	0	0	57.6	0.182	0	0	0	0	0	5,146,817
28	0	0	0	60.1	0.190	0	0	0	0	0	5,156,608
29	0	0	0	62.8	0.200	0	0	0	0	0	5,168,399
30	0	0	0	65.4	0.208	0	0	0	0	0	5,179,002

31	0	0	0	67.9	0.213	0	0	0	0	0	5,188,428
32	0	0	0	70.5	0.218	0	0	0	0	0	5,198,787
33	0	0	0	73.2	0.225	0	0	0	0	0	5,210,069
34	0	0	0	75.8	0.230	0	0	0	0	0	5,220,180
35	0	0	0	78.5	0.235	0	0	0	0	0	5,231,208
36	0	0	0	81.2	0.240	0	0	0	0	0	5,242,109
37	1	0	0	55.3	0.143	44,464	0	0	44,464	107,398	4,957,596
38	0	0	0	58.2	0.151	0	0	0	0	0	4,971,266
39	0	0	0	61.1	0.158	0	0	0	0	0	4,984,794
40	0	0	0	63.9	0.162	0	0	0	0	0	4,997,158
			Average	67.8	0.244	Agency weighting factor	1	Total	149,322	492,719	214,906,220
			Max	89.1	0.373			LCC NPV (USD)			215,548,262
			Min	51.1	0.143						

Notice: The original MEPDG results were presented in months rather than years. The LCCA used years to reduce the size of the optimisation and the values of rutting and IRI at the last month of a year was used to represent annual values.
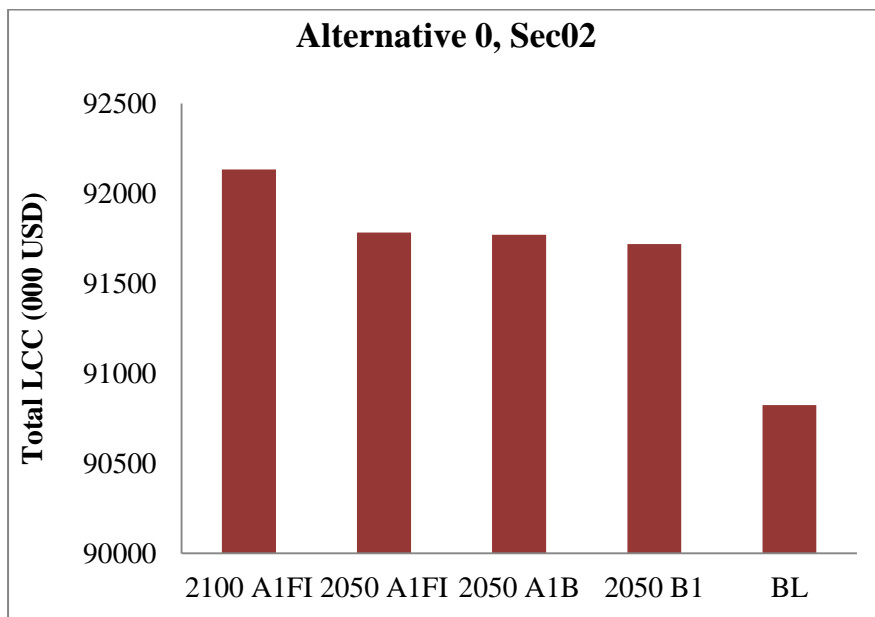
Alternative 0
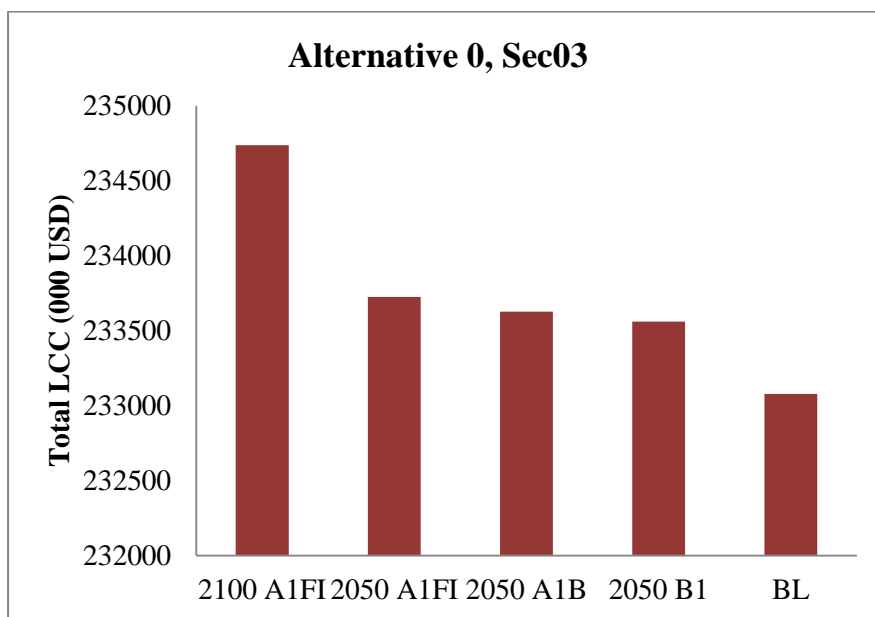

Figure A-57 Sec02: Alternative 0 total LCC

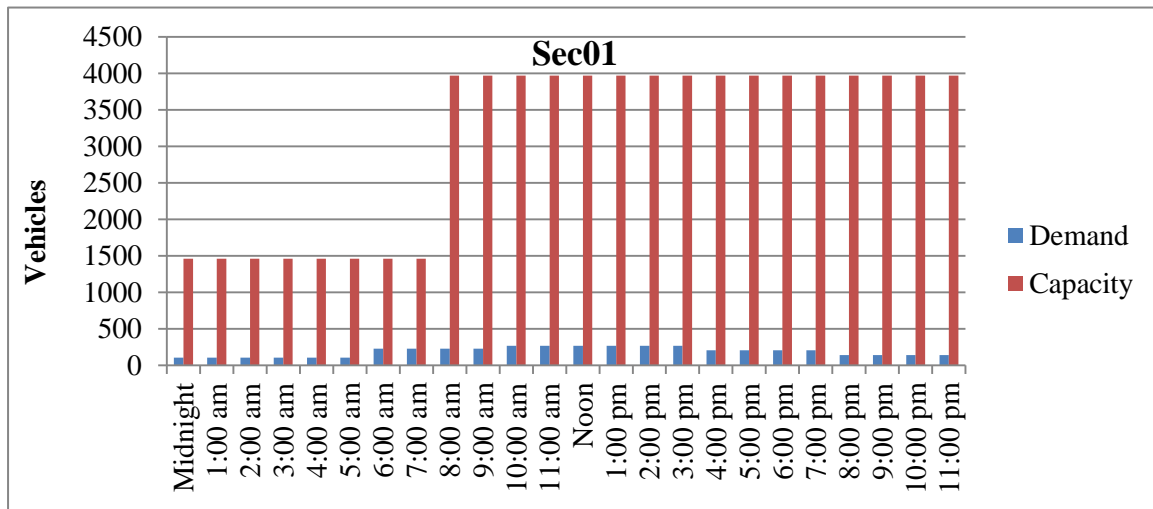Figure A-58 Sec03: Alternative 0 total LCC

Alternative 1

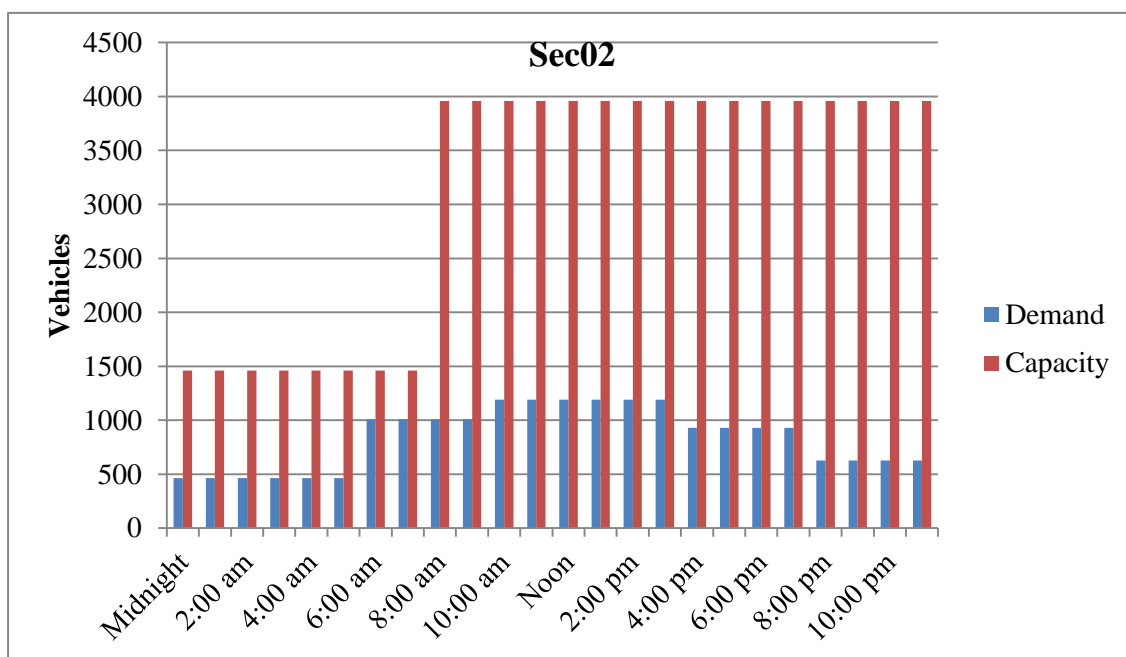Figure A-59 Capacity, WZ capacity, and traffic demand, Sec01

Figure A-60 Capacity, WZ capacity, and traffic demand, Sec02
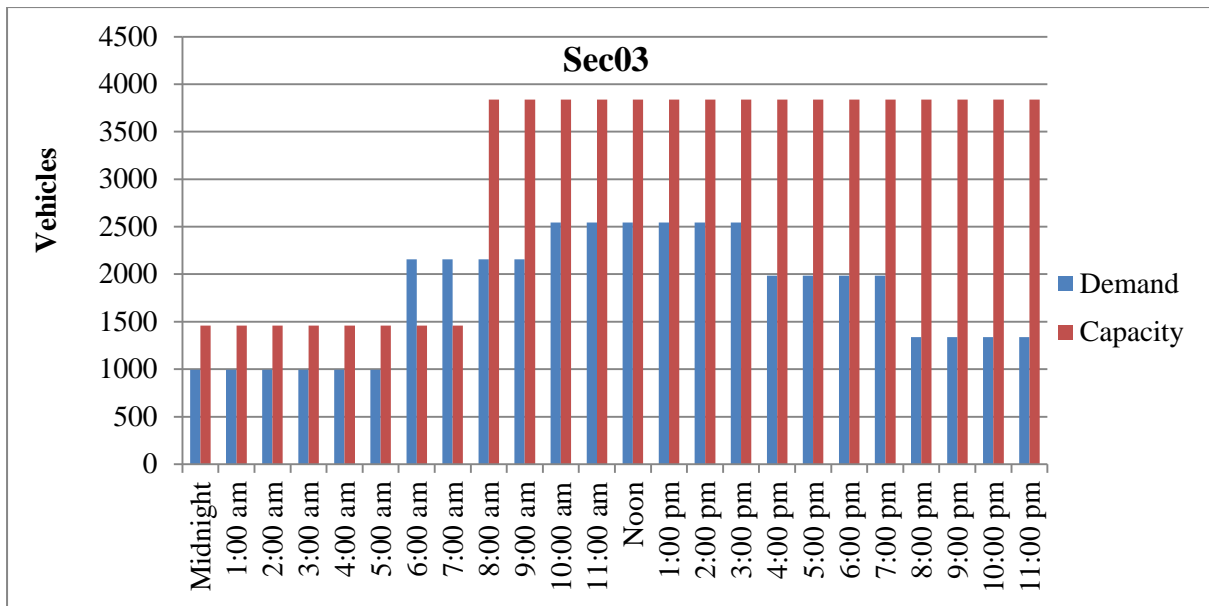
Figure A-61 Capacity, WZ capacity, and traffic demand, Sec03

Performance predictions
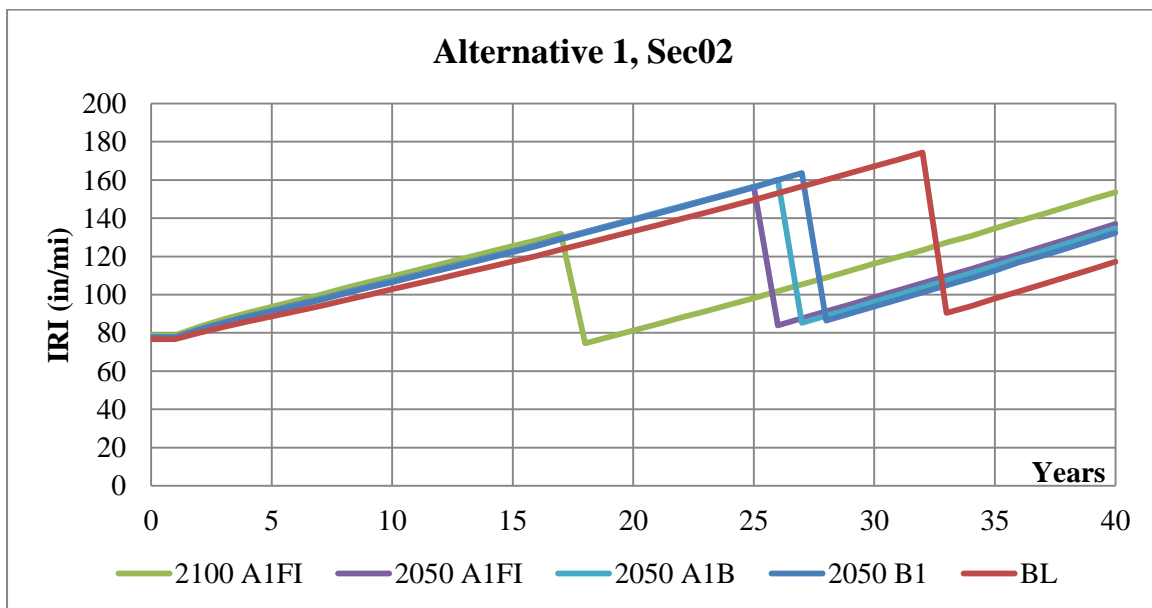
Figure A-62 IRI curve, Alternative 1, Sec02
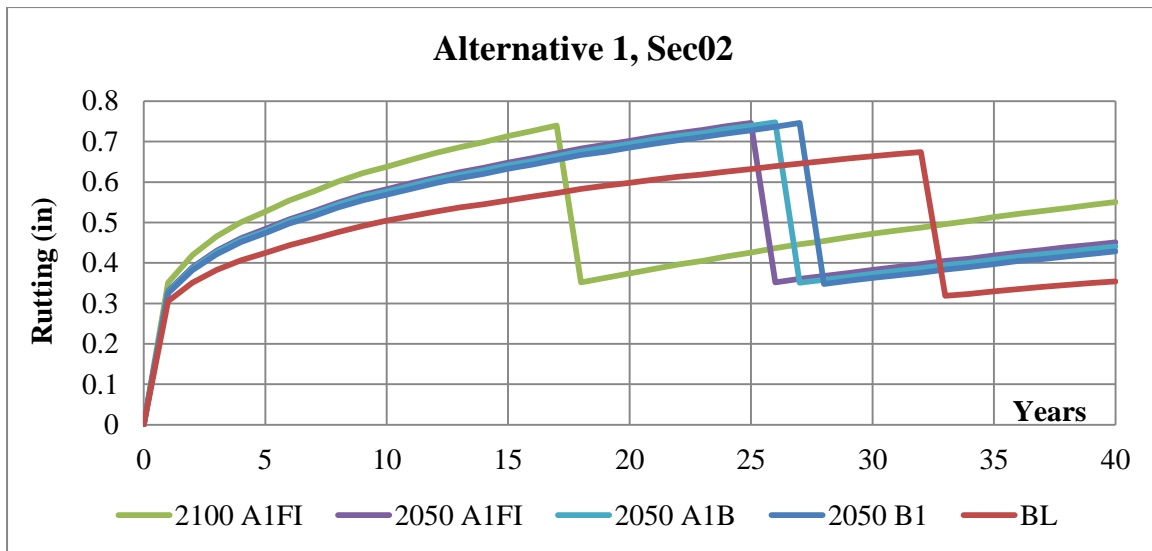
Figure A-63 Rutting curve, Alternative 1, Sec02
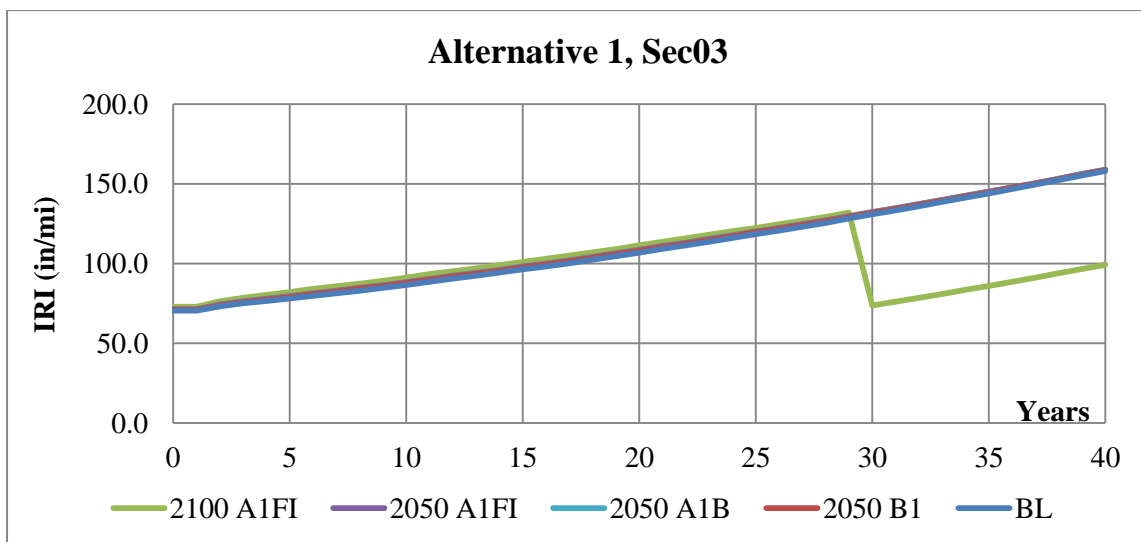
Figure A-64 IRI curve, Alternative 1, Sec03

218
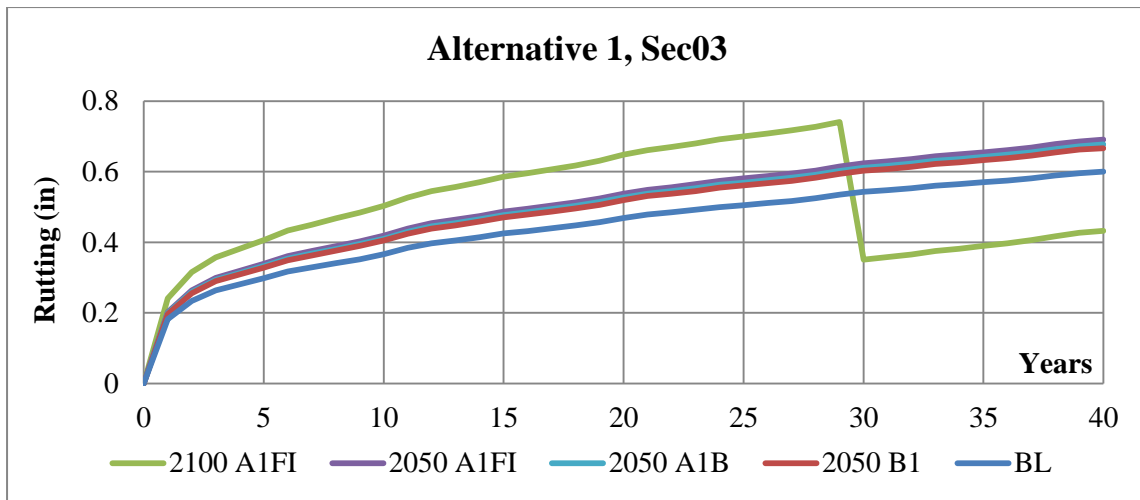
Figure A-65 Rutting curve, Alternative 1, Sec03

Costs summary
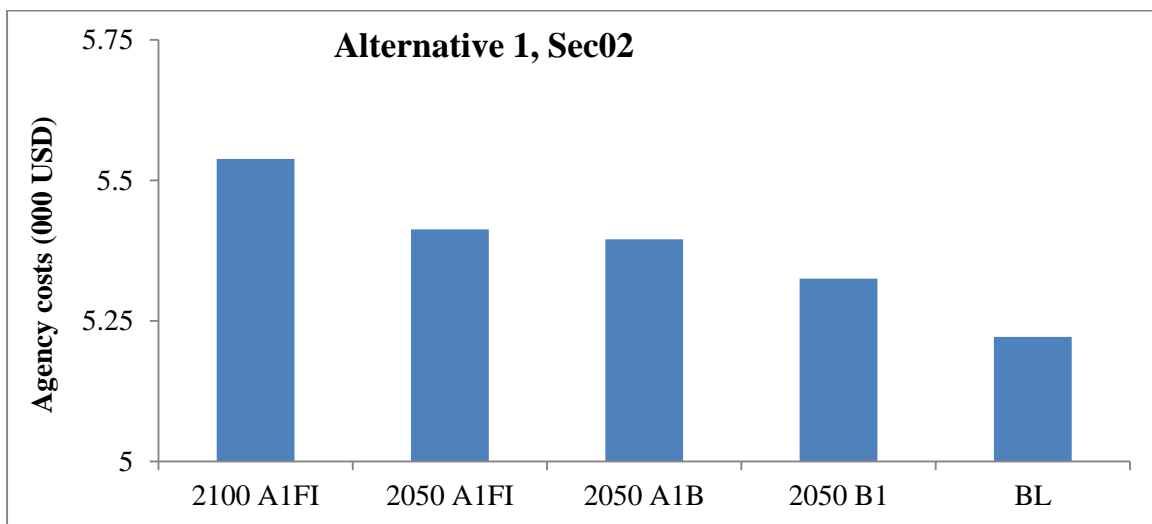
Figure A-66 Agency costs for Alternative 1 Sec02 increased due to climate change
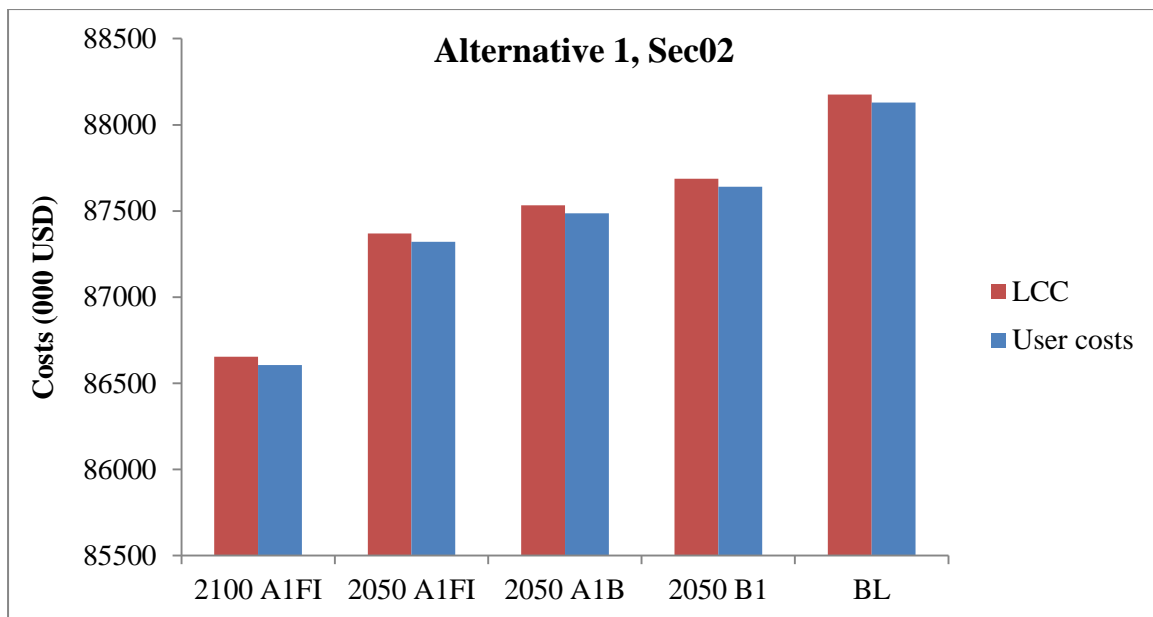
Figure A-67 User costs and LCC for Alternative 1 Sec02 decreased due to climate change
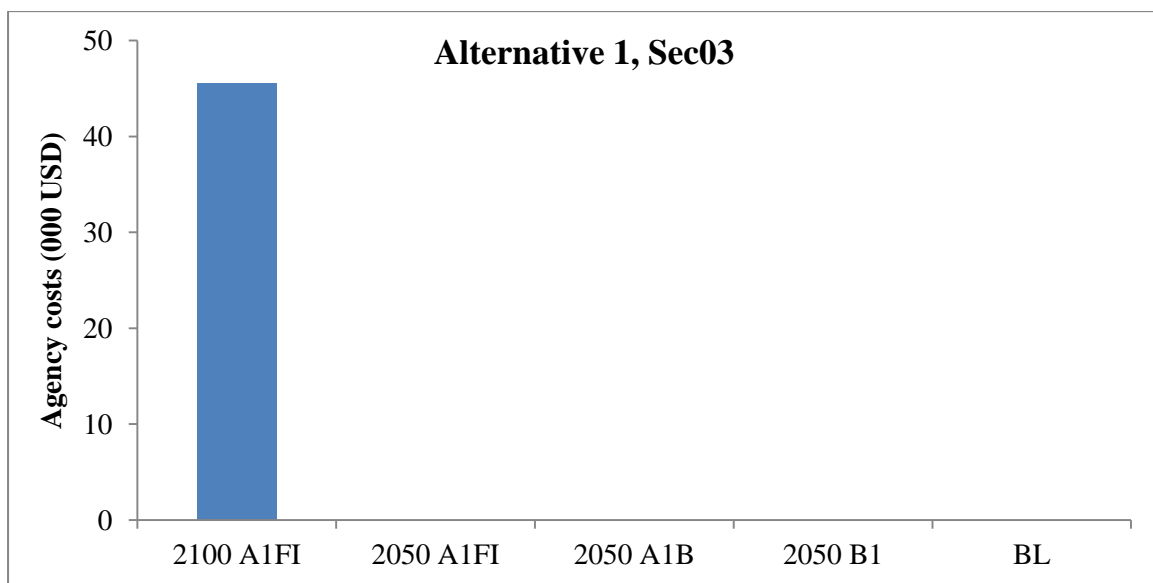
Figure A-68 Agency costs for Alternative 1 Sec03 increased due to climate change
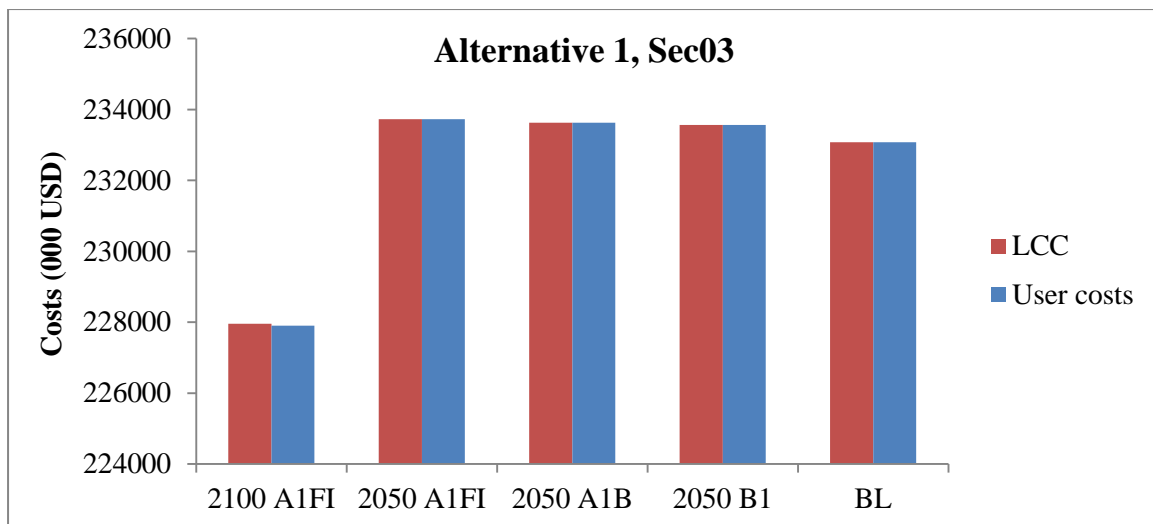
Figure A-69 User costs and LCC for Alternative 1 Sec03 decreased due to climate change

Alternative 2

Sensitivity of LCC to weighting factors
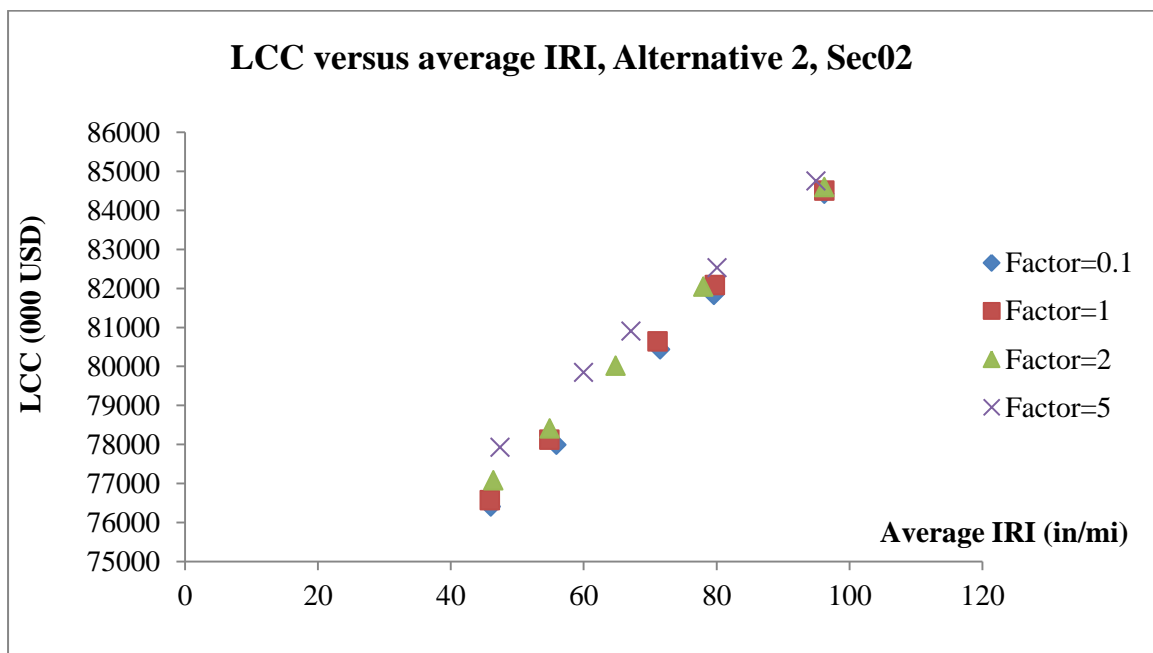
Figure A-70 Influence of agency costs weighting factors on the LCC, Alternative 2, Sec02
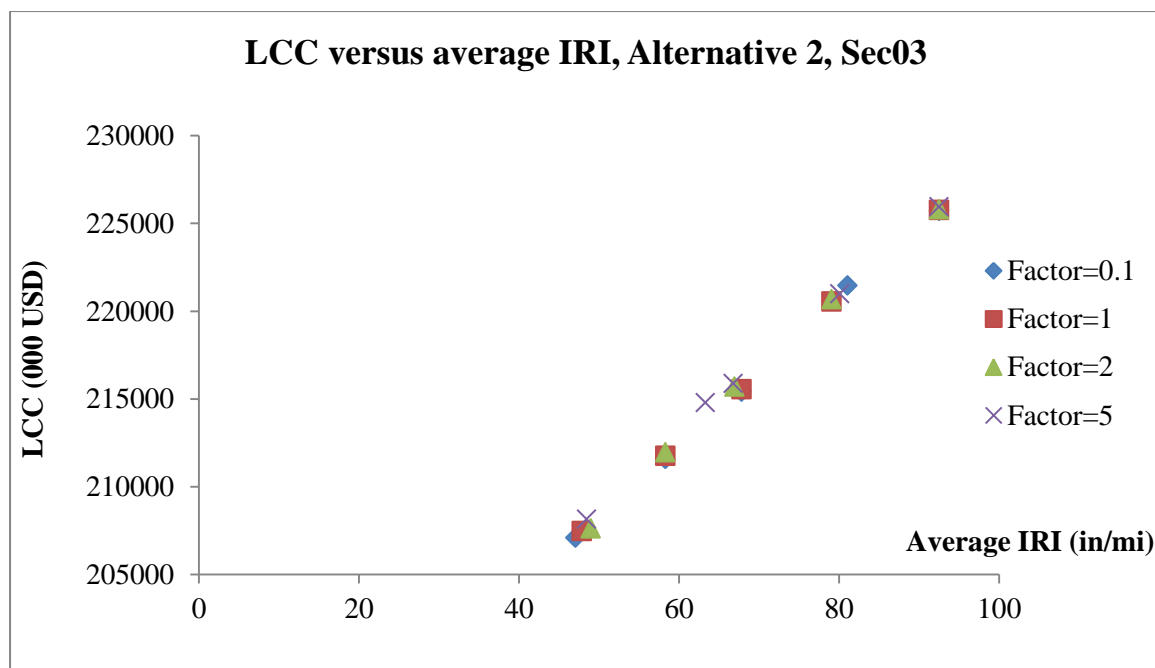
Figure A-71 Influence of agency costs weighting factors on the LCC, Alternative 2, Sec03

Results

Table A-38 An example of decision optimisation result for 2100 A1FI scenario, Alternative 2, Sec01

| IRI_{min} (in/mi)	30			40			50			60			70		
Year	Op 1	Op 2	Op 3	Op 1	Op 2	Op 3	Op 1	Op 2	Op 3	Op 1	Op 2	Op 3	Op 1	Op 2	Op 3
1	0	0	0	0	0	0	0	0	0	0	0	0	0	0	0
2	1	0	0	0	0	0	1	0	0	0	0	0	0	0	0
3	1	0	0	1	0	0	0	0	0	0	0	0	0	0	0
4	0	0	0	0	0	0	0	0	0	0	0	0	0	0	0
5	0	0	0	0	0	0	0	0	0	0	0	0	0	0	0
6	0	0	0	0	0	0	0	0	0	0	0	0	0	0	0
7	0	0	0	0	0	0	0	0	0	0	0	0	0	0	0
8	0	0	0	0	0	0	0	0	0	0	0	0	0	0	0
9	0	0	0	0	0	0	0	0	0	1	0	0	0	0	0
10	0	0	0	1	0	0	0	0	0	0	0	0	0	0	0
11	0	0	0	0	0	0	0	0	0	0	0	0	0	0	0
12	0	0	0	0	0	0	0	0	0	0	0	0	0	0	0
13	0	0	0	0	0	0	0	0	0	0	0	0	0	0	0
14	0	0	0	0	0	0	0	0	0	0	0	0	0	0	0
15	0	0	0	0	0	0	0	0	0	0	0	0	0	0	0
16	1	0	0	0	0	0	0	0	0	0	0	0	0	0	0
17	0	0	0	0	0	0	0	0	0	0	0	0	0	0	0

18	0	0	0	0	0	0	0	0	0	0	0	0	0	0	0
19	0	0	0	0	0	0	0	0	0	0	0	0	0	0	0
20	0	0	0	0	0	0	0	0	0	0	0	0	0	0	0
21	0	0	0	0	0	0	0	1	0	0	0	0	0	0	0
22	0	0	0	1	0	0	0	0	0	0	0	0	1	0	0
23	0	0	0	0	0	0	0	0	0	0	0	0	0	0	0
24	0	0	0	0	0	0	0	0	0	0	0	0	0	0	0
25	0	0	0	0	0	0	0	0	0	0	0	0	0	0	0
26	0	0	0	0	0	0	0	0	0	0	0	0	0	0	0
27	0	0	0	0	0	0	0	0	0	1	0	0	0	0	0
28	0	0	0	0	0	0	0	0	0	0	0	0	0	0	0
29	0	0	0	0	0	0	0	0	0	0	0	0	0	0	0
30	0	1	0	0	0	0	0	0	0	0	0	0	0	0	0
31	0	0	0	0	0	0	0	0	0	0	0	0	0	0	0
32	0	0	0	0	0	0	0	0	1	0	0	0	0	0	0
33	0	0	0	1	0	0	0	0	0	0	0	0	0	0	0
34	0	0	0	0	0	0	0	0	0	0	0	0	0	0	0
35	0	0	0	0	0	0	0	0	0	0	0	0	0	0	0
36	0	0	0	0	0	0	0	0	0	0	0	0	0	0	0
37	0	0	0	0	0	0	0	0	0	0	0	0	0	0	0
38	0	0	0	0	0	0	0	0	0	0	0	0	0	0	0
39	0	0	0	0	0	0	0	0	0	0	0	0	0	0	0
40	0	0	0	0	0	0	0	0	0	0	0	0	0	0	0

Sec01

2100 A1FI

2100 A1FI , Alternative 2, *IRImin* = 30 in/mi , Sec01

2100 A1FI , Alternative 2, *IRImin* = 40 in/mi , Sec01

2100 A1FI , Alternative 2, _IRImin_ = 50 in/mi , Sec01

1 4 7 10 13 16 19 22 25 28 31 34 37 40

■Op1 ■Op2 ■Op3

Year

2100 A1FI , Alternative 2, _IRImin_ = 60 in/mi , Sec01

1 4 7 10 13 16 19 22 25 28 31 34 37 40

■Op1 ■Op2 ■Op3

Year

2100 A1FI , Alternative 2, _IRImin_ = 70 in/mi , Sec01

1 4 7 10 13 16 19 22 25 28 31 34 37 40

■Op1 ■Op2 ■Op3

Year

2050 A1FI

2050 A1FI, Alternative 2, _IRImin_ = 30 in/mi , Sec01

1 4 7 10 13 16 19 22 25 28 31 34 37 40

■Op1 ■Op2 ■Op3

Year

2050 A1FI, Alternative 2, _IRImin_ = 40 in/mi , Sec01

1 4 7 10 13 16 19 22 25 28 31 34 37 40

■Op1 ■Op2 ■Op3

Year

224

2050A1FI, Alternative 2, *IRImin* = 50 in/mi , Sec01

1 4 7 10 13 16 19 22 25 28 31 34 37 40

■Op1 ■Op2 ■Op3

Year

2050A1FI, Alternative 2, *IRImin* = 60 in/mi , Sec01

1 4 7 10 13 16 19 22 25 28 31 34 37 40

■Op1 ■Op2 ■Op3

Year

2050A1FI, Alternative 2, *IRImin* = 70 in/mi , Sec01

1 4 7 10 13 16 19 22 25 28 31 34 37 40

■Op1 ■Op2 ■Op3

Year

2050 A1B

2050 A1B, Alternative 2, *IRImin* = 30 in/mi , Sec01

1 4 7 10 13 16 19 22 25 28 31 34 37 40

■Op1 ■Op2 ■Op3

Year

2050 A1B, Alternative 2, *IRImin* = 40 in/mi , Sec01

1 4 7 10 13 16 19 22 25 28 31 34 37 40

■Op1 ■Op2 ■Op3

Year

225

2050 A1B, Alternative 2, $IRImin = 50$ in/mi , Sec01

1 4 7 10 13 16 19 22 25 28 31 34 37 40

■ Op1 ■ Op2 ■ Op3

Year

2050 A1B, Alternative 2, $IRImin = 60$ in/mi , Sec01

1 4 7 10 13 16 19 22 25 28 31 34 37 40

■ Op1 ■ Op2 ■ Op3

Year

2050 A1B, Alternative 2, $IRImin = 70$ in/mi , Sec01

1 4 7 10 13 16 19 22 25 28 31 34 37 40

■ Op1 ■ Op2 ■ Op3

Year

2050 B1

2050 B1, Alternative 2, $IRImin = 30$ in/mi , Sec01

1 4 7 10 13 16 19 22 25 28 31 34 37 40

■ Op1 ■ Op2 ■ Op3

Year

2050 B1, Alternative 2, $IRImin = 40$ in/mi , Sec01

1 4 7 10 13 16 19 22 25 28 31 34 37 40

■ Op1 ■ Op2 ■ Op3

Year

226

2050 B1, Alternative 2, $IRImin = 50$ in/mi , Sec01

1 4 7 10 13 16 19 22 25 28 31 34 37 40

■ Op1 ■ Op2 ■ Op3

Year

2050 B1, Alternative 2, $IRImin = 60$ in/mi , Sec01

1 4 7 10 13 16 19 22 25 28 31 34 37 40

■ Op1 ■ Op2 ■ Op3

Year

2050 B1, Alternative 2, $IRImin = 70$ in/mi , Sec01

1 4 7 10 13 16 19 22 25 28 31 34 37 40

■ Op1 ■ Op2 ■ Op3

Year

BL

BL, Alternative 2, $IRImin = 30$ in/mi , Sec01

1 4 7 10 13 16 19 22 25 28 31 34 37 40

■ Op1 ■ Op2 ■ Op3

Year

BL, Alternative 2, $IRImin = 40$ in/mi , Sec01

1 4 7 10 13 16 19 22 25 28 31 34 37 40

■ Op1 ■ Op2 ■ Op3

Year

227

BL, Alternative 2, $IRImin$ = 50 in/mi , Sec01


```
1   4   7   10  13  16  19  22  25  28  31  34  37  40
```
■ Op1 ■ Op2 ■ Op3

Year

BL, Alternative 2, $IRImin$ = 60 in/mi , Sec01


```
1   4   7   10  13  16  19  22  25  28  31  34  37  40
```
■ Op1 ■ Op2 ■ Op3

Year

BL, Alternative 2, $IRImin$ = 70 in/mi , Sec01


```
1   4   7   10  13  16  19  22  25  28  31  34  37  40
```
■ Op1 ■ Op2 ■ Op3

Year

Sec02

2100 A1FI

2100 A1FI, Alternative 2, $IRImin$ = 30 in/mi , Sec02


```
1   4   7   10  13  16  19  22  25  28  31  34  37  40
```
■ Op1 ■ Op2 ■ Op3

Year

2100 A1FI, Alternative 2, $IRImin$ = 40 in/mi , Sec02


```
1   4   7   10  13  16  19  22  25  28  31  34  37  40
```
■ Op1 ■ Op2 ■ Op3

Year

228

2100 A1FI, Alternative 2, *IRImin* = 50 in/mi , Sec02

| 1 | 4 | 7 | 10 | 13 | 16 | 19 | 22 | 25 | 28 | 31 | 34 | 37 | 40 |

■ Op1   ■ Op2   ■ Op3

Year

2100 A1FI, Alternative 2, *IRImin* = 60 in/mi , Sec02

| 1 | 4 | 7 | 10 | 13 | 16 | 19 | 22 | 25 | 28 | 31 | 34 | 37 | 40 |

■ Op1   ■ Op2   ■ Op3

Year

2100 A1FI, Alternative 2, *IRImin* = 70 in/mi , Sec02

| 1 | 4 | 7 | 10 | 13 | 16 | 19 | 22 | 25 | 28 | 31 | 34 | 37 | 40 |

■ Op1   ■ Op2   ■ Op3

Year

2050 A1FI

2050 A1FI, Alternative 2, *IRImin* = 30 in/mi , Sec02

| 1 | 4 | 7 | 10 | 13 | 16 | 19 | 22 | 25 | 28 | 31 | 34 | 37 | 40 |

■ Op1   ■ Op2   ■ Op3

Year

2050 A1FI, Alternative 2, *IRImin* = 40 in/mi , Sec02

| 1 | 4 | 7 | 10 | 13 | 16 | 19 | 22 | 25 | 28 | 31 | 34 | 37 | 40 |

■ Op1   ■ Op2   ■ Op3

Year

229

2050 A1FI, Alternative 2, *IRImin* = 50 in/mi , Sec02

1   4   7   10   13   16   19   22   25   28   31   34   37   40
■ Op1   ■ Op2   ■ Op3

Year

2050 A1FI, Alternative 2, *IRImin* = 60 in/mi , Sec02

1   4   7   10   13   16   19   22   25   28   31   34   37   40
■ Op1   ■ Op2   ■ Op3

Year

2050 A1FI, Alternative 2, *IRImin* = 70 in/mi , Sec02

1   4   7   10   13   16   19   22   25   28   31   34   37   40
■ Op1   ■ Op2   ■ Op3

Year

2050 A1B

2050 A1FI, Alternative 2, *IRImin* = 30 in/mi , Sec02

1   4   7   10   13   16   19   22   25   28   31   34   37   40
■ Op1   ■ Op2   ■ Op3

Year

2050 A1FI, Alternative 2, *IRImin* = 40 in/mi , Sec02

1   4   7   10   13   16   19   22   25   28   31   34   37   40
■ Op1   ■ Op2   ■ Op3

Year

2050 A1FI, Alternative 2, *IRImin* = 50 in/mi , Sec02

1   4   7   10   13   16   19   22   25   28   31   34   37   40
■ Op1   ■ Op2   ■ Op3

Year

230

2050 A1FI, Alternative 2, *IRImin* = 60 in/mi , Sec02

1 4 7 10 13 16 19 22 25 28 31 34 37 40
■ Op1 ■ Op2 ■ Op3

Year

2050 A1FI, Alternative 2, *IRImin* = 70 in/mi , Sec02

1 4 7 10 13 16 19 22 25 28 31 34 37 40
■ Op1 ■ Op2 ■ Op3

Year

2050 A1B, Alternative 2, *IRImin* = 30 in/mi , Sec02

1 4 7 10 13 16 19 22 25 28 31 34 37 40
■ Op1 ■ Op2 ■ Op3

Year

2050 A1B, Alternative 2, *IRImin* = 40 in/mi , Sec02

1 4 7 10 13 16 19 22 25 28 31 34 37 40
■ Op1 ■ Op2 ■ Op3

Year

2050 A1B, Alternative 2, *IRImin* = 50 in/mi , Sec02

1 4 7 10 13 16 19 22 25 28 31 34 37 40
■ Op1 ■ Op2 ■ Op3

Year

231

2050 A1B, Alternative 2, $IRImin = 60$ in/mi , Sec02

1 4 7 10 13 16 19 22 25 28 31 34 37 40

■Op1 ■Op2 ■Op3

Year

2050 A1B, Alternative 2, $IRImin = 70$ in/mi , Sec02

1 4 7 10 13 16 19 22 25 28 31 34 37 40

■Op1 ■Op2 ■Op3

Year

2050 B1

2050 B1, Alternative 2, $IRImin = 30$ in/mi , Sec02

1 4 7 10 13 16 19 22 25 28 31 34 37 40

■Op1 ■Op2 ■Op3

Year

2050 B1, Alternative 2, $IRImin = 40$ in/mi , Sec02

1 4 7 10 13 16 19 22 25 28 31 34 37 40

■Op1 ■Op2 ■Op3

Year

2050 B1, Alternative 2, $IRImin = 50$ in/mi , Sec02

1 4 7 10 13 16 19 22 25 28 31 34 37 40

■Op1 ■Op2 ■Op3

Year

232

2050 B1, Alternative 2, _IRImin_ = 60 in/mi , Sec02


```
1   4   7   10  13  16  19  22  25  28  31  34  37  40
```
■ Op1 ■ Op2 ■ Op3

Year

2050 B1, Alternative 2, _IRImin_ = 70 in/mi , Sec02


```
1   4   7   10  13  16  19  22  25  28  31  34  37  40
```
■ Op1 ■ Op2 ■ Op3

Year

_BL_

BL, Alternative 2, _IRImin_ = 30 in/mi , Sec02


```
1   4   7   10  13  16  19  22  25  28  31  34  37  40
```
■ Op1 ■ Op2 ■ Op3

Year

BL, Alternative 2, _IRImin_ = 40 in/mi , Sec02


```
1   4   7   10  13  16  19  22  25  28  31  34  37  40
```
■ Op1 ■ Op2 ■ Op3

Year

BL, Alternative 2, _IRImin_ = 50 in/mi , Sec02


```
1   4   7   10  13  16  19  22  25  28  31  34  37  40
```
■ Op1 ■ Op2 ■ Op3

Year

233

BL, Alternative 2, $IRImin = 60$ in/mi , Sec02

Op1   Op2   Op3

Year

BL, Alternative 2, $IRImin = 70$ in/mi , Sec02

Op1   Op2   Op3

Year

Sec03

2100 A1FI

2100 A1FI, Alternative 2, $IRImin = 30$ in/mi , Sec03

Op1   Op2   Op3

Year

2100 A1FI, Alternative 2, $IRImin = 40$ in/mi , Sec03

Op1   Op2   Op3

Year

2100 A1FI, Alternative 2, $IRImin = 50$ in/mi , Sec03

Op1   Op2   Op3

Year

2100 A1FI, Alternative 2, *IRImin* = 60 in/mi , Sec03

1 4 7 10 13 16 19 22 25 28 31 34 37 40
■ Op1 ■ Op2 ■ Op3
Year

2100 A1FI, Alternative 2, *IRImin* = 70 in/mi , Sec03

1 4 7 10 13 16 19 22 25 28 31 34 37 40
■ Op1 ■ Op2 ■ Op3
Year

2050 A1FI

2050 A1FI, Alternative 2, *IRImin* = 30 in/mi , Sec03

1 4 7 10 13 16 19 22 25 28 31 34 37 40
■ Op1 ■ Op2 ■ Op3
Year

2050 A1FI, Alternative 2, *IRImin* = 40 in/mi , Sec03

1 4 7 10 13 16 19 22 25 28 31 34 37 40
■ Op1 ■ Op2 ■ Op3
Year

2050 A1FI, Alternative 2, *IRImin* = 50 in/mi , Sec03

1 4 7 10 13 16 19 22 25 28 31 34 37 40
■ Op1 ■ Op2 ■ Op3
Year

235

2050 A1FI, Alternative 2, *IRImin* = 60 in/mi , Sec03

1   4   7   10 13 16 19 22 25 28 31 34 37 40

■ Op1   ■ Op2   ■ Op3

Year

2050 A1FI, Alternative 2, *IRImin* = 70 in/mi , Sec03

1   4   7   10 13 16 19 22 25 28 31 34 37 40

■ Op1   ■ Op2   ■ Op3

Year

2050 A1B

2050 A1B, Alternative 2, *IRImin* = 30 in/mi , Sec03

1   4   7   10 13 16 19 22 25 28 31 34 37 40

■ Op1 ■ Op2 ■ Op3

Year

2050 A1B, Alternative 2, *IRImin* = 40 in/mi , Sec03

1   4   7   10 13 16 19 22 25 28 31 34 37 40

■ Op1   ■ Op2   ■ Op3

Year

2050 A1B, Alternative 2, *IRImin* = 50 in/mi , Sec03

1   4   7   10 13 16 19 22 25 28 31 34 37 40

■ Op1   ■ Op2   ■ Op3

Year

2050 A1B, Alternative 2, $IRImin = 60$ in/mi , Sec03

1   4   7   10 13 16 19 22 25 28 31 34 37 40
■ Op1 ■ Op2 ■ Op3

Year

2050 A1B, Alternative 2, $IRImin = 70$ in/mi , Sec03

1   4   7   10 13 16 19 22 25 28 31 34 37 40
■ Op1 ■ Op2 ■ Op3

Year

2050 B1

2050 B1, Alternative 2, $IRImin = 30$ in/mi , Sec03

1   4   7   10 13 16 19 22 25 28 31 34 37 40
■ Op1 ■ Op2 ■ Op3

Year

2050 B1, Alternative 2, $IRImin = 40$ in/mi , Sec03

1   4   7   10 13 16 19 22 25 28 31 34 37 40
■ Op1 ■ Op2 ■ Op3

Year

2050 B1, Alternative 2, $IRImin = 50$ in/mi , Sec03

1   4   7   10 13 16 19 22 25 28 31 34 37 40
■ Op1 ■ Op2 ■ Op3

Year

237

2050 B1, Alternative 2, $IRImin = 60$ in/mi , Sec03

1 4 7 10 13 16 19 22 25 28 31 34 37 40

■ Op1 ■ Op2 ■ Op3

Year

2050 B1, Alternative 2, $IRImin = 70$ in/mi , Sec03

1 4 7 10 13 16 19 22 25 28 31 34 37 40

■ Op1 ■ Op2 ■ Op3

Year

BL

BL, Alternative 2, $IRImin = 30$ in/mi , Sec03

1 4 7 10 13 16 19 22 25 28 31 34 37 40

■ Op1 ■ Op2 ■ Op3

Year

BL, Alternative 2, $IRImin = 40$ in/mi , Sec03

1 4 7 10 13 16 19 22 25 28 31 34 37 40

■ Op1 ■ Op2 ■ Op3

Year

BL, Alternative 2, $IRImin = 50$ in/mi , Sec03

1 4 7 10 13 16 19 22 25 28 31 34 37 40

■ Op1 ■ Op2 ■ Op3

Year

238

BL, Alternative 2, *IRImin* =60 in/mi , Sec03

1   4   7   10 13 16 19 22 25 28 31 34 37 40

■ Op1 ■ Op2 ■ Op3

Year

BL, Alternative 2, *IRImin* = 70 in/mi , Sec03

1   4   7   10 13 16 19 22 25 28 31 34 37 40

■ Op1 ■ Op2 ■ Op3

Year

239